EXPERIMENTAL INVESTIGATION OF SMALL-SCALE GASIFICATION OF WOODY BIOMASS

by

Maria Barrio

A thesis submitted to

The Norwegian University of Science and Technology

for the degree of

Doktor Ingeniør

May 2002
The Norwegian University of Science and Technology
Faculty of Engineering Science and Technology
Department of Thermal Energy and Hydropower
7491 Trondheim, Norway

URN:NBN:no-2340

URN:NBN:no-2340

NTNU
Norges teknisk-naturvitenskapelige universitet

The Norwegian University of Science and Technology

Report no:
2002:05

Classification
Open

POSTADRESSE
NTNU
INSTITUTT FOR TERMISK ENERGI OG VANNKRAFT
Kolbjørn Hejes vei 1A
N-7491 Trondheim - NTNU

TELEFONER
Sentralbord NTNU: 73 59 40 00
Instituttkontor: 73 59 27 00
Vannkraftlaboratoriet: 73 59 38 57

TELEFAX
Instituttkontor: 73 59 83 90
Vannkraftlaboratoriet: 73 59 38 54

Title of report	Date
EXPERIMENTAL INVESTIGATION OF SMALL-SCALE GASIFICATION OF WOODY BIOMASS	May 2002
	No. of pages/appendixes 204/32
Author s) Maria Barrio	Project manager (sign.) Johan E. Hustad
Division Faculty of Engineering Science and Technology Department of Thermal Energy and Hydropower	Project no.
ISBN no. 82-471-5435-8	Price group

Abstract

A small-scale stratified downdraft gasifier has been built and operated under stable conditions using wood pellets as fuel and air as gasification agent. The problems observed during the preliminary experiments have been described and explained; they are mainly related to the stability of the process. The stable operation of the gasifier has been characterised by the gas composition and the product gas tar and particle content. The biomass feeding rate has varied between 4,5 and 6,5 kg/h. The CO content of the product gas (23-26 % vol.) is higher than in similar gasifiers and the H_2 content has been found to vary between 14 and 16 % vol. The tar content in the product gas (ca. 3 g/Nm^3) is rather high compared with similar gasifiers. The temperature profile, together with other relevant parameters like the air-excess ratio, the air to fuel ratio and gas to fuel ratio have been calculated. The experiments show that the air excess ratio is rather constant, varying between 0,25 and 0,3. Experiments have been conducted with a gas engine using mixtures of CH_4, CO, H_2, CO_2 and N_2 as a fuel. NO_x and CO emissions are analysed.
The char gasification process has been studied in detail by means of Thermogravimetric Analysis. The study comprises the chemical kinetics of the gasification reactions of wood char in CO_2 and H_2O, including the inhibition effect of CO and H_2. A kinetic model based on Langmuir-Hinshelwood kinetics has been found which relates the mass loss rate to the temperature, gas composition and degree of conversion for each reaction. The ratio CO/CO_2 has been found to be a relevant parameter for reactivity. The gasification experiments in mixtures of CO_2 and H_2O give reasons to believe that the rate of desorption for the complex C(O) varies depending on the gas mixture surrounding the char. It has been found that if the experimental data are obtained from separate H_2O/N_2 and CO_2/N_2 experiments, the reactivity of the char in mixtures of CO_2 and H_2O can be fairly predicted.

	Indexing Terms English	Indexing Terms Norwegian
Group 1	Heat Engineering	Varmeteknikk
Group 2 Selected by author	Solid Fuels	Faste brensler
	Biomass	Biomasse
	Gasification	Gassifisering
	Reactivity	Reaktivitet

URN:NBN:no-2340

URN:NBN:no-2340

ACKNOWLEDGMENTS

This document is the result of four years of work. There have been many good and bad moments during these years. I specially want to thank my supervisor, Prof. Johan Hustad, for helping me through the dark days. He has also given me many suggestions and helpful comments.

Most of my motivation has come from the time I spent working together with others. Silke Hübner, Uk Chantaka, Torsten Goehler, Lena Berg, Christian Sømme, Jose M. Granados and Mathias Olschar deserve to be mentioned here. I tried to help them during their projects as undergraduate students and in return I got their enthusiasm and encouragement to continue with my work.

During this Ph.D. adventure I have shared the boat with other Ph.D. students: Håvar Risnes, Benny Gøbel, Mette Stenseng, Klaus Zepter and Morten Fossum. I thank them for the fruitful technical discussions, for their helping hand, and mainly for their friendship.

Thanks to Lasse H. Sørensen and his research group. He received me with great hospitality in Denmark during my experimental work. He has always been available for discussions, questions and comments. I received also a very warm welcome at the Denmark Technical University. I thank Ulrik Henriksen and his group for this.

The experimental work also required an effort from the workshop personal. I thank them, especially Oddmund Rydningen and Halvor Flatberg. Most of what I have learnt from them is not written in this thesis but is equally important.

The Norwegian Research Council and, during the last period, the Nordic Energy Research Programme are acknowledged for their financial support.

My family has encouraged me during these years despite being difficult to understand what I was doing due to the distance.

Daniel, my husband, has been by my side all this time. He knew when to listen, when to question and when to encourage. Without his support I would not have come to the end of this challenge. Thanks.

URN:NBN:no-2340

URN:NBN:no-2340

TABLE OF CONTENTS

URN:NBN:no-2340

URN:NBN:no-2340

LIST OF FIGURES

URN:NBN:no-2340

URN:NBN:no-2340

LIST OF TABLES

URN:NBN:no-2340

URN:NBN:no-2340

SUMMARY

This experimental investigation focuses on woody biomass gasification. A small-scale stratified downdraft gasifier has been built and operated under stable conditions using wood pellets as fuel and air as gasification agent. The problems observed during the preliminary experiments have been described and explained; they are mainly related to the stability of the process. The stable operation of the gasifier has been characterised by the gas composition and the product gas tar and particle content. The biomass feeding rate has varied between 4,5 and 6,5 kg/h. The CO content of the product gas (23-26 % vol.) is higher than in similar gasifiers and the H_2 content has been found to vary between 14 and 16 % vol. The tar content in the product gas (ca. 3 g/Nm^3) is rather high compared with similar gasifiers. The temperature profile, together with other relevant parameters like the air-excess ratio, the air to fuel ratio and gas to fuel ratio have been calculated for each experiment to allow for comparison with other investigations. The experiments show that the air excess ratio is rather constant, varying between 0,25 and 0,3.

Experiments have been conducted with a gas engine using mixtures of CH_4, CO, H_2, CO_2 and N_2 as a fuel. NO_x and CO emissions are analysed. The results show that NO_x emissions are low for LCV gases but increase as the content of methane in the mixture increases. On the other hand, the CO emissions for the LCV gas are very high and decrease as CH_4 is added to the fuel mixture.

The char gasification process has been studied in detail by means of Thermogravimetric Analysis. The study comprises the chemical kinetics of the gasification reactions of wood char in CO_2 and H_2O, including the inhibition effect of CO and H_2. A kinetic model based on Langmuir-Hinshelwood kinetics has been found which relates the mass loss rate to the temperature, gas composition and degree of conversion for each reaction.
Kinetic parameters have been obtained for the steam gasification of birch and beech char. Langmuir-Hinshelwood kinetics predict fairly the inhibition effect of H_2. Birch and beech present very similar kinetic parameters, although they differ in the reactivity profiles. The gasification of birch in CO_2 has been studied in a similar manner, also including the inhibition effect of CO. Again, Langmuir-Hinshelwood kinetics predict very well the experimental data. The ratio CO/CO_2 has been found to be a relevant parameter for reactivity. Temperature seems to have a small effect on the shape of the reactivity profile while reactant's partial pressure and the ratio CO/CO_2 show no influence. The gasification experiments in mixtures of CO_2 and H_2O give reasons to believe that the rate of desorption for the complex C(O) varies depending on the gas mixture surrounding the char. It has been found that if the experimental data are obtained from separate H_2O/N_2

URN:NBN:no-2340

and CO_2/N_2 experiments, the reactivity of the char in mixtures of CO_2 and H_2O can be fairly predicted. Nevertheless, the optimum prediction of reactivity for mixtures of H_2O/CO_2 should be obtained from experiments conducted with $H_2O/CO_2/N_2$ mixtures only.

URN:NBN:no-2340

1 INTRODUCTION AND BACKGROUND

1.1 OBJECTIVES OF THE WORK

This experimental investigation focuses on biomass gasification. The main objectives have been:

- Build and operate a small-scale downdraft gasifier using wood pellets as fuel.
- Test and evaluate the more recent stratified downdraft gasifier (also known as "open core") as an alternative design to the more traditional downdraft gasifier known as the Imbert gasifier.
- Study the char gasification process, both inside the gasifier but also using other experimental techniques as Thermogravimetric Analysis. The study comprises the chemical kinetics of the gasification reactions and the influence of other gases present in the gas mixture surrounding the char.

This Ph.D. work has clearly an experimental character. Time and energy have been spent in the laboratory and a lot of knowledge has been acquired during these hours. This type of experimental knowledge is hardly reflected in a written document.

1.2 THESIS OVERVIEW

The work is presented in four chapters. The first chapter is an introduction to biomass gasification with special emphasis on char gasification and energy production from biomass gasification. The second chapter is devoted to the experimental work conducted in the small-scale downdraft gasifier and the gas engine coupled to the gasifier. Papers I, II and III are included in this chapter.

The third chapter concentrates on the char gasification reactions. The experimental work of this chapter has been conducted using Thermogravimetric Analysis. Most of the experiments have been conducted at Reatech in Denmark, and in close cooperation with the Technical University of Denmark. The results are presented in Papers IV, V and VI.

Finally, Chapter 4 presents the conclusions from this Ph. D. study. Although Chapter 2 and 3 refer to different equipment and different experimental techniques, they complement each other. The detailed analysis of the reactions that take place inside a gasifier needs other type of equipment depending on the subject of study. In this case, the chemical reaction of the char has been isolated from the other many processes and factors that interact in the gasifier.

URN:NBN:no-2340

1.3 BIOMASS AS AN ENERGY SOURCE

Biomass can be defined as "all the matter that can be derived directly or indirectly from plant photosynthesis, vegetal and animal". It is therefore a renewable energy source. Biomass, as a source of energy, increases the possibilities for local, regional or national self-supply, relatively independent from international market fluctuations and fossil fuels availability. Moreover, renewable energies do not contribute as much as fossil fuels to environmental pollution and are not as risky as nuclear power. (Grønli, 1996)

If biomass was grown at the same rate as it was consumed, the net contribution to atmospheric CO_2 would be zero. In addition, most types of biomass contain negligible amounts of sulphur and therefore offer benefits by reducing SO_2 emissions. However, some biomass fuels like straw present higher sulphur content and can produce emissions, as recently studied by Knudsen et al. (2001) among others. Biomass utilisation can also result in nitrogen related emissions; however, as Easterly and Burnham (1996) mention, the fuel-bound nitrogen in biomass is much lower than in coal resulting in lower NO_x emissions.

Regarding the large scale utilisation of biomass, the industrial structure should be different in the opinion of Williams and Larson (1996) since biomass is an unusual fuel and often is not readily available for long-term contracts, as coal or natural gas. They also comment that power producers from biomass may sometimes produce biomass themselves, in order to secure fuel supplies for the life plant investment or form joint ventures with forest product agricultural industries to increase security on the biomass supply.

1.3.1 BIOMASS COMPOSITION AND TYPES

The main chemical constituents of biomass are:

- cellulose,
- hemicellulose, and
- lignin.

The two former comprise the cell walls in biomass fibers and are characterised chemically as high molecular weight glucose molecules. The third component, lignin, acts as a "glue", keeping the fiber cells together. Lignin is a polymer that can form polyaromatic compounds in the conversion products. The proportion between lignin and cellulose content in biomass is 40/60. Biomass is also characterised by a high content of oxygen, what justifies its high thermal instability (Hallgren, 1996).

URN:NBN:no-2340

Three main types of biomass can be distinguished, regarding the origin and previous use:

- crops,
- residues, and
- solid wastes.

Table 1.1 presents several types of crops with some examples and characteristics.

Crop type	Examples	Comments
Woody species -long term rotation(15-50 years) -short term rotation (3-5 years).	Poplar, willow, eucalyptus, etc.	Negligible sulphur content, low ash, high volatile content and high char reactivity.
Herbaceous annual crops	Miscanthus, sweet sorghum, etc.	
High sugar/starch crops	Sugar-cane, maize and sugar beet, wheat, etc.	Already used for ethanol production.
Oil containing crops	Oil seed rape, sunflower, etc.	Used to extract vegetable oils (bio-diesel).

Table 1.1: Types of crops.

As the use of biomass increases, dedicated energy crops will become necessary. The short rotation woody crops will be preferred for dedicated energy crops in the future of biomass sources. These species are generally hardwood trees that would be harvested every 5-10 years and regrown from the tree stump reducing then annual costs for establishing and managing crops. The production of energy crops requires less intensive management than other agricultural crops because of the low need for fertilizers and pesticides. Furthermore, as pointed out by Easterly and Burnham (1996), since the roots remain in the soil after harvesting, soil erosion can be reduced.

Biomass residues can have several origines. Table 1.2 summarizes the different sources and presents some examples.

URN:NBN:no-2340

Type of biomass residue	Examples	Comments
Forestry residues	Branches and tops from clear felling, storm-damaged trees and thinnings.	
Agricultural residues	Cereal crops and also food processing wastes like nutshells.	Some wastes have to stay in the field to nourish the soil; the rest has to be removed to avoid pests and diseases.
Manufacturing industry	Bark, sawdust, planner savings and off-cuts from sawmills. Black liquor from pulp and paper production	The manufacturer often uses most of their own residues. Smaller sawmills might not use them.
Construction industry	Construction and demolition wood, broken wood pallets, fruit boxes and other wood packaging.	Construction wood might present some contaminants, if wood has been treated.

Table 1.2: Types of biomass residues.

A common characteristic of residues and wastes is the variable composition, moisture and ash content, concentration of heavy metals and content of nitrogen, sulphur and chlorine, as referred by van Ree et al. (1997). Table 1.3 compares the composition and energy content of different crops and residues.

	Wood and wood residues		Agricultural residues		Construction residues	Energy crops	
	Clean wood	Bark from spruce	Straw from wheat	Grass Red canary	Waste/ demolition wood	Salix	Units
Moisture	50	55-65	55	60	15-20	50	Wt% of wet fuel
Ash	1.3	2.34	4.71	8.85	0.9	1.18	Wt% of dry fuel
Fixed-C	13.2	22.46	17.59	17.65		18.92	Wt% of dry fuel
HHV	19.2	19.83	18.94	18.37	15.4	19.75	MJ/kg
LHV	15.4	18.54	17.65	17.13	13.9	18.42	MJ/kg
Composition							wt% (daf)
C	49.1	51.1	49.6	49.4	48.8	50.3	
H	6.00	6.04	6.16	6.25	5.25	6.17	
O	44.3	42.4	43.5	42.7	45.6	43.1	
N	0.48	0.41	0.61	1.54	0.15	0.40	
S	0.01	0.03	0.07	0.15	0.03	0.03	
Cl	0.10	0.03	0.18	0.07	0.08	0.004	

Table 1.3: Comparison of biomass crops and residues.

Finally, municipal and industrial solid waste is an important biomass source. All organic and paper wastes are combustible material, representing in general a 90% of Municipal

URN:NBN:no-2340

Solid Waste (MSW) (Easterly and Burnham, 1996). In the opinion of van Ree et al. (1997), it is important to note that as a waste treatment option, any biomass technology will have to meet the emission standards for waste treatment in the country. Furthermore, the system should be flexible enough to admit some variety in biomass fuels.

1.3.2 COMPARISON WITH OTHER FUELS

The most similar solid fuel to biomass is coal. Both require fuel storage and systems to transport the fuel from the storage to the boilers (Easterly and Burnham, 1996). However, the energy content is very different: bituminous coal has 30,2 MJ/kg, where hardwoods have 19,8 MJ/kg (dry), and agricultural residues average about 18 MJ/kg (dry). The variation in energy content is clearly explained by the fuel H/C ratio and the O/C ratio, as shown in the Van Krevelen diagram (Figure 1.1).

As the carbon content of the fuel increases, the energy content also increases. However, biomass feedstocks have unique properties that offer potential advantages in gasification processes. Biomass has higher oxygen content what results in higher reactivity and contains high amounts of volatile matter compared with coal (Hallgren, 1996).

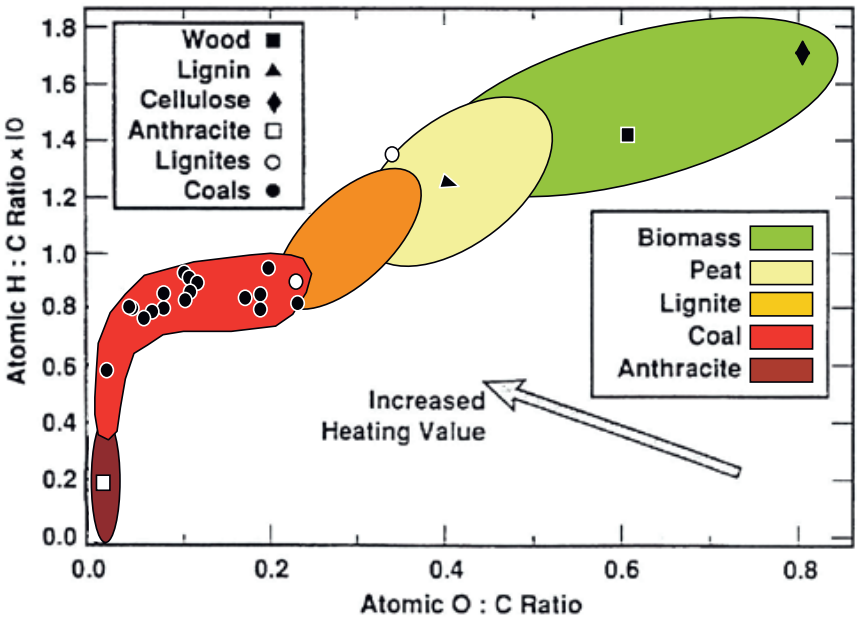

Figure 1.1: Van Krevelen diagram.

In addition, coal contains a considerable amount of sulphur, as commented by Consonni and Larson (1994), whose removal at high temperature is one of the key obstacles in the

URN:NBN:no-2340

commercialization of coal gasification. On the contrary, biomass contains little or any sulphur.

The recent overview of Maniatis (2000) compares several feedstocks in terms of market potential and overall technology reliability, as shown in Figure 1.2.

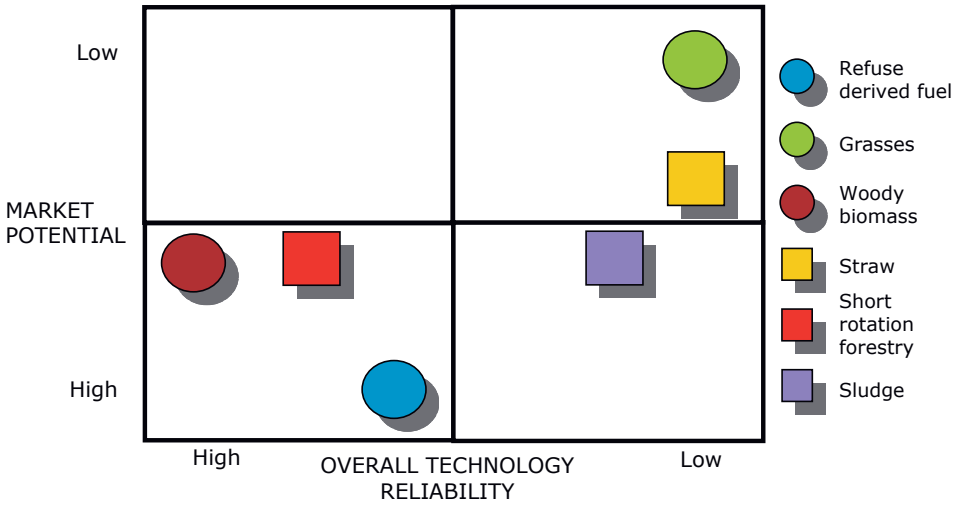

Figure 1.2: Market potential and technology reliability for several feedstocks (Maniatis, 2000).

The physical form of biomass is heterogeneous and the moisture content when harvested is often very high (40-50% moisture content) what reduces the energy content to 9,9 MJ/kg and 9,3-9,8 MJ/kg for hardwood and agricultural residues respectively. It is also difficult to handle solid form biomass so some modifications are usually needed (comminution, drying, storage and feeding systems) (Grønli, 1996). When biomass is densified by processing and compactation, its bulk volume is much closer to the coal one (Easterly and Burnham, 1996).

Table 1.4 compares the bulk volumes of several biomass types and coal.

URN:NBN:no-2340

Type of fuel	Bulk volume (m^3/ton)
Woodchips	4,4-5,6
Wood pellets	1,6-1,8
Loose straw	24,7-49,5
Baled straw	4,9-9,0
Waste pellets	1,7-2,3
Coal	1,1-1,5

Table 1.4: Typical bulk volume of biomass and coal (Easterly and Burnham, 1996).

The ash content of biomass is also lower than in coal, although the amount of ash depends highly on the type of biomass. Some types of biomass can also present high contents of alkaline metal (Na, K), that lower ash melting temperatures that yield to an increase in ash deposition and fouling (obstruction) of boiler equipment (Easterly and Burnham, 1996). The potential erosion and fouling for several types of biomass and coal is presented in Table 1.5.

		Acids				Bases					
	Ash(%)	Fe_2O_3	Al_2O_3	P_2O_5	TiO_2	CaO	MgO	Na_2O	K_2O	SiO_2	Ratio [a]
Potential erosion [a]											
Rice husk	23.4	0.10	2.00			0.20	0.20	0.10	1.20	95.60	0.01
Bagasse, Hawaii	3.5	14.80	15.30		3.50	1.92	2.21	0.86	3.52	54.00	0.08
Construction wood	3.4	4.23	12.55	1.35	0.59	10.87	2.69	4.71	5.55	53.56	0.09
Wheat straw	8.9	1.50	2.00			5.00	3.60	0.30	6.60	78.20	0.09
Rice straw	13.4	0.30	3.30			2.00	2.80	1.10	8.00	79.80	0.11
Pine bark	3.0	3.00	14.00			25.50	6.50	1.30	6.00	39.00	0.19
Demolition wood	4.9	6.22	6.03	0.88		15.96	3.76	3.87	2.41	41.21	0.23
Whole tree average	1.3	3.99	8.87	3.03		23.43	4.59	1.62	10.48	34.81	0.35
Manure	34.9	1.88	6.06	5.52	0.25	13.05	4.45	4.85	12.29	41.99	0.41
Western hog fuel	0.5	4.41	2.31		0.01	25.37	7.62	5.64	9.26	35.18	0.42
Softwood bark	2.0	5.00	6.30			57.00	5.50	3.10	4.10	16.00	0.45
Jack pine	2.1	5.00	6.30		0.20	51.60	5.50	3.10	4.10	16.00	0.45
Eastern hemlock	2.5	1.30	2.10			53.60	13.10	1.10	4.60	10.00	0.57
Almond shells	4.8	3.77				12.27	2.49	5.08	14.14	22.60	0.85
Oat straw	4.0	0.50	0.80			12.30	3.00	0.30	40.30	37.30	1.09
Tree prunings	2.0	1.94				19.90	8.30	1.48	12.66	9.95	1.42
Walnut shells	0.6	2.40				7.00	6.65	1.08	21.50	13.60	1.66
Potential fouling [a]											
Cotton stalks	4.6	0.50	0.80			16.40	5.20	2.00	30.00	8.40	3.81
Hardwood bark	3.4	0.60	0.50			77.00	1.90	3.90	7.20	1.50	7.40
Oak	1.6	3.40				26.00	2.90	1.60	42.00	5.50	7.93
Sunflower seed husks	4.2	0.60	0.10			9.20	7.20	0.40	39.30	1.70	23.35
Cotton gin trash [b]	9.4	3.30	4.30			16.10	8.00		11.30	40.70	
Annual ryegrass [b]	5.0	0.20				3.80	1.90	4.10	14.00		
Bituminous coal	5-13	5-35	10-35			1-20	0.3-4	1-4			20-60

[a] Fuel types with a ratio $[(Na_2O+K_2O)/SiO_2]$ above 2 require special precautions to avoid fouling problems. If the ratio is below 0.2, then erosion may occur unless precautions are taken.
[b] Insufficient information to calculate the ratio.

Table 1.5: Potential erosion and fouling for several biomass types and coal (Easterly and Burnham, 1996).

Easterly and Burnham (1996) also compare the power plant size for coal and biomass. The typical size of a biomass power plant is 15-50 MW, around ten times smaller range than coal (150-500 MW). In their opinion, biomass plants can not benefit from large-scale economies and usually present a net electrical efficiency of 18-25%. The difference in size between coal and biomass plants is due to fuel supply considerations (Palmer et

URN:NBN:no-2340

al., 1993). A power plant centrally located can collect wood residues from an area of 120 km radius. If transportation is low cost, like barge (boat) or rail, the distance can increase, according to Easterly and Burnham (1996). Close to source, the cost of useful energy in the form of lignocellulose is often competitive with fossil fuels.

1.3.3 BIOMASS PRODUCTION AND COSTS

According to Holt and van der Burgt (1998), the biomass contribution to primary energy consumption is worldwide between 15% and 20%. Recent numbers from the International Energy Agency show that biomass energy represents approximately 14% of the world final energy consumption (Figure 1.3).

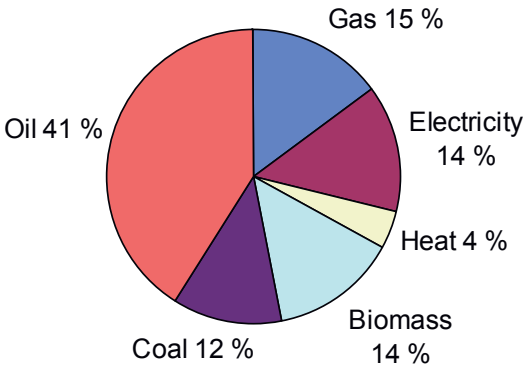

Figure 1.3: World final energy consumption, 1995. Source: IEA. (D'Apote, 1998)

However, this proportion varies enormously between the industrialized and the developing countries as shown in Figure 1.4.

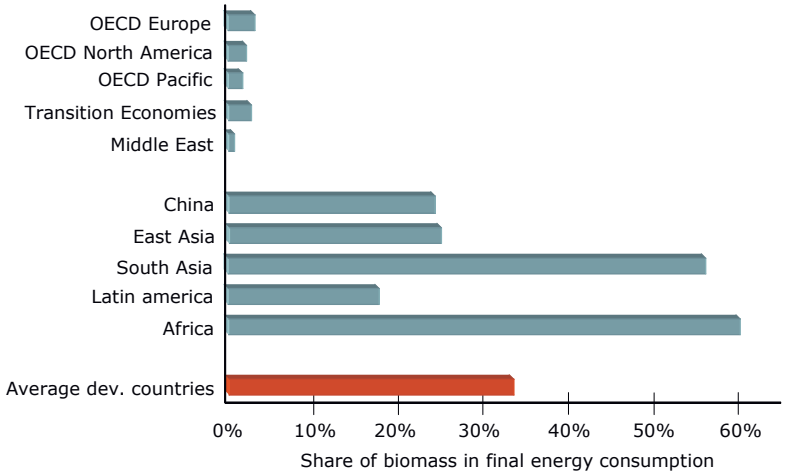

Figure 1.4: Importance of biomass in different world regions, 1995. Source: IEA. (D'Apote, 1996)

URN:NBN:no-2340

Most of the present biomass activity is unsustainable because of the environmental damage (soil erosion, loss of biological diversity) caused by an increase in fuelwood gathering and charcoal making in many regions in Africa, Latin and South-America and Asia (Grønli, 1996). It is also an inefficiently utilised resource in many cases (biomass for domestic cooking, for example). The resource ownership is not always well defined, the price of fuelwood is not defined or there is no organised mechanism to channel resources into replanting (Booth and Elliott, 1993).

Renewable energy sources (RES) covered 5,3 % of the total energy demand in the European Union in 1995, where biomass represented 63 % of the total RES, i.e. 515,6 TWh. It is mainly used in form of heat, being only 22,3 TWh used for electricity generation. Figure 1.5 shows the percentage of each renewable energy in Europe in 1995 and the use of biomass and waste.

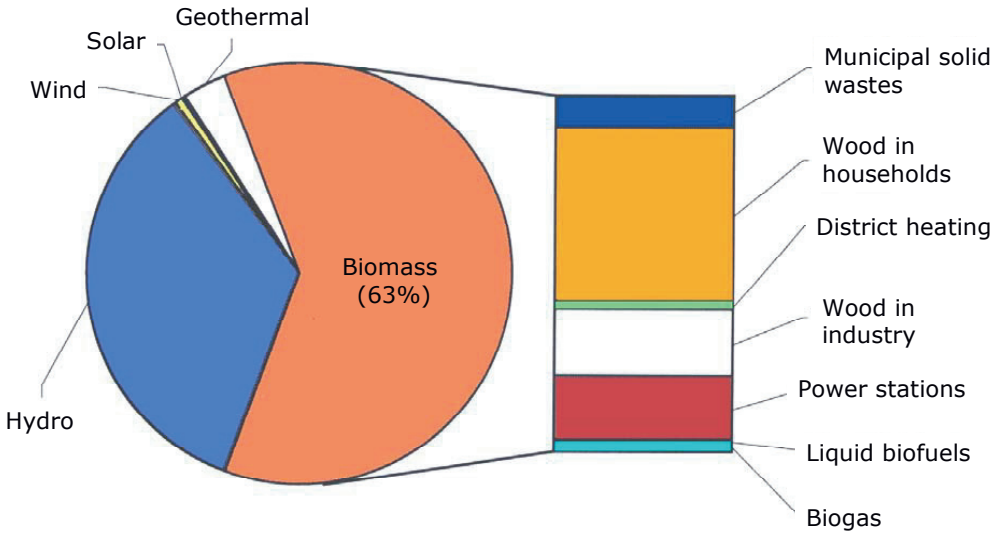

Figure 1.5: Percentage share of RES in Europe in 1995. Source:IEA. (Roubanis, 1998)

In Norway, biomass accounts for approximately 5,5% of the total energy use, i.e. 12,6 TWh/year. Figure 1.6 shows the actual use of bioenergy in the Nordic countries. In Finland and Sweden, the major consumers of biofuels are the pulp and paper industry using bark, peat and black liquor. In Denmark, it is essential the combustion of straw bales in small boilers for district heating. In Norway, the use of wood stoves is very common. These units (<20kW) represent, according to Grønli (1996), about the 50% of biomass consumption in Norway.

URN:NBN:no-2340

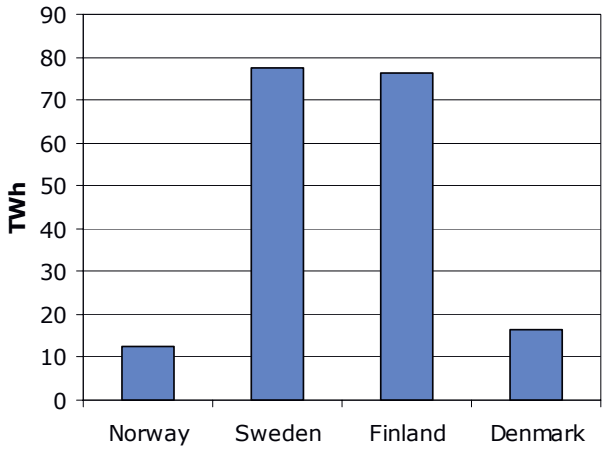

Figure 1.6: Actual use of bioenergy in Norway, Sweden, Finland and Denmark (Vaa Beyer and Skreiberg, 2000).

According to Easterly and Burnham (1996), all forms of biomass energy represented a 3,6% of the total supply of energy in the US in 1991. And, as a contribution to the electric power production, biomass contributed 2,4%, compared to the 3,8% of hydroelectric. Among biomass, wood is by far the largest source, followed by municipal solid waste. In their opinion, the biggest source of biomass will be in the far future the dedicated energy crops.

Walsh et al. (1999) present the potential annual biomass available in the US for three price scenarios. Figure 1.7 summarizes the data.

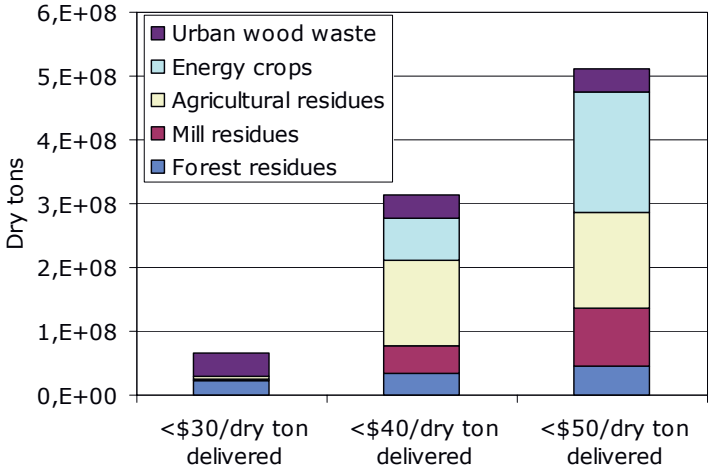

Figure 1.7: Estimated annual feedstock quantities in the US, 1995. (Walsh et al., 1999)

URN:NBN:no-2340

Looking at the future use of biomass, D'Apote (1998) presents an energy projection for biomass and also conventional energy (Table 1.6). The consumption of biomass in developing countries is expected to increase but at a lower rate than the use of conventional energy. As the Gross Domestic Product (GDP) is also expected to increase, people in urban areas will gradually switch to conventional fuels.

	1995				2020				Average annual Growth rate (1995-2020)		
	Biomass	Conv. energy	Total	Share of biomass	Biomass	Conv. energy	Total	Share of biomass	Biomass	Conv. energy	Total
China	206	649	855	24%	224	1524	1748	13%	0.3	3.5	2.9
East Asia	106	316	422	25%	118	813	931	13%	0.4	3.8	3.2
South Asia	235	188	423	56%	276	523	799	35%	0.6	4.2	2.6
Latin America	73	342	416	18%	81	706	787	10%	0.4	2.9	2.6
Africa	205	136	341	60%	371	260	631	59%	2.4	2.6	2.5
Total developing countries	**825**	**1632**	**2456**	**34%**	**1071**	**3825**	**4897**	**22%**	**1.0**	**3.5**	**2.8**
Other non-OECD countries	24	1037	1061	1%	26	1669	1695	1%	0.3	1.9	2.8
Total non-OECD countries	**849**	**2669**	**3518**	**24%**	**1097**	**5494**	**6591**	**17%**	**1.0**	**2.9**	**2.5**
OECD countries	81	3044	3125	3%	96	3872	3968	2%	0.7	1.0	1.0
World	**930**	**5713**	**6643**	**14%**	**1193**	**9365**	**10558**	**11%**	**1.0**	**2.0**	**1.9**

Table 1.6: Final energy projections including biomass (Mtoe).
Source: IEA. (D'Apote, 1998)

Roos et al. (1999) has identified recently the critical factors to bioenergy implementation as being:

- Integration and infrastructure,
- Scale effects,
- Competition in bioenergy sector,
- Competition with other business,
- National policy and policy influence, and
- Local policy and opinion.

In the opinion of de Tourris (1997), and referring to biomass gasification systems in particular, four key success factors are needed to ensure economic viability:

- The site must be remote and difficult to reach in terms of delivering conventional fuels;
- Biomass supply must be as regular as possible in terms of quality and quantity;
- Unskilled workers with a high degree of motivation must be employed to operate and maintain the gasifiers and

URN:NBN:no-2340

- The system must operate at a stable load for not less than 2000 to 8000 hours/year.

Although it is expected that natural gas is to become the cheapest energy in the future, biomass could become the low cost option for countries where natural gas is not available (Booth and Elliott, 1993). Some recent studies reported by Craig et al. (1995) demonstrate that biomass system's costs and performance can become competitive or attractive in existing niche markets like: areas with non-fossil mandates, with high fossil fuel costs, with rural development concerns, with waste or residue disposal concerns or with very low biomass costs. The production of attractive co-products will also be of interest.

Finally, the price of biomass power plants will only decrease if replication is done (5-10 times). Booth and Elliott (1993) refer that for a 25 MW_e plant, the cost could go from US$3000/kW (1 unit) to US$1300-1500/kW (5-10 units), considering economies of scale.

1.4 THERMOCHEMICAL CONVERSION PROCESSES

In order to benefit from the chemical energy contained in biomass, this energy has to be transformed into more convenient energy forms like heat or electricity. Some processes involve an intermediate transformation from the solid fuel into another energy carrier (gas or liquid fuel).
As referred by Grønli (1996), there are, in principle, three types of conversion processes:

- Biochemical -via microbiological action-
- Thermochemical -via heat treatment-
- Physical/chemical processing

This Ph.D. work concentrates only on the thermochemical conversion processes.

Four thermochemical processes can be distinguished:

- Pyrolysis
- Gasification
- Combustion
- Liquefaction

Some of them are endothermic and others exothermic and often they take place simultaneously inside the same reactor. Figure 1.8 presents the thermochemical conversion process and the paths for energy utilisation.

URN:NBN:no-2340

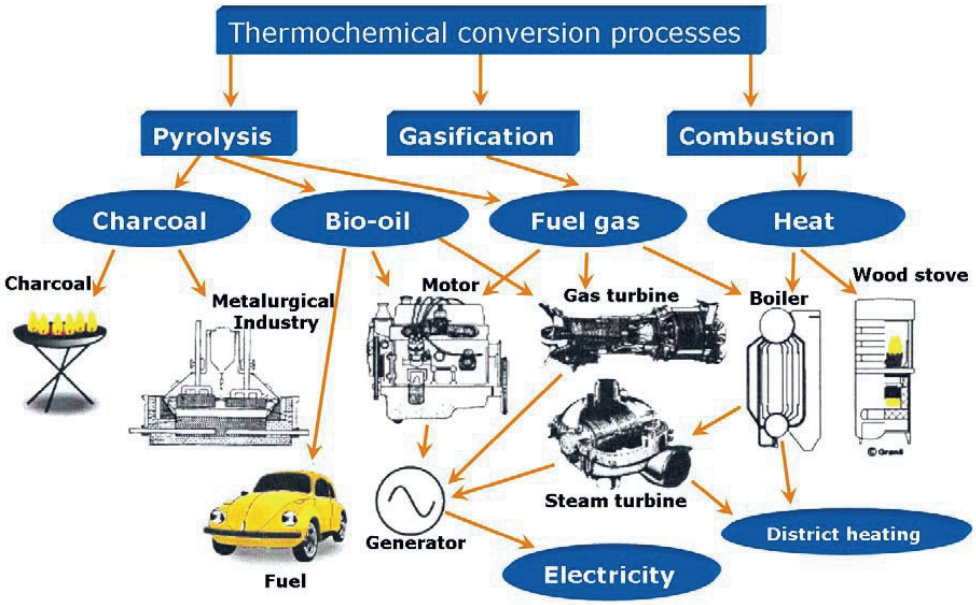

Figure 1.8: Thermochemical conversion processes and energy utilisation. (Grønli, 1996)

The products from any thermochemical process are:

- a solid residue, called char
- a gas product
- a tarry liquid of complex composition, known as "tar", often present in vapour phase at process temperature

As commented by Hallgren (1996), the characteristics of the products (gas, liquids and solid) depend on a broad range of factors such as the chemical and physical characteristics of the feedstock, the heating rate, the initial and final process temperature, pressure and type of reactor.

The next sections describe each thermochemical process.

1.4.1 PYROLYSIS OR DEVOLATILIZATION

Pyrolysis is the thermal degradation of biomass in the absence of an oxidising agent at 200-500 °C. The term devolatilization is also used as equivalent to pyrolysis but it is usually understood that devolatilization implies the presence of an oxidizing agent.

Nevertheless, the surrounding atmosphere is of little importance to the thermal degradation of the solid fuel although it might affect the subsequent reactions of the volatile matter released. Depending on the method used, the process leads to a mixture

URN:NBN:no-2340

of tar vapours (usually with a high heating value of 20-25 MJ/kg), gases and highly reactive carbonaceous char of different proportions. As mentioned before, the factors that affect these proportions are temperature, pressure, gas atmosphere, residence time, heating rate, type of reactor and reaction time. The pyrolysis process is sketched in Figure 1.9.

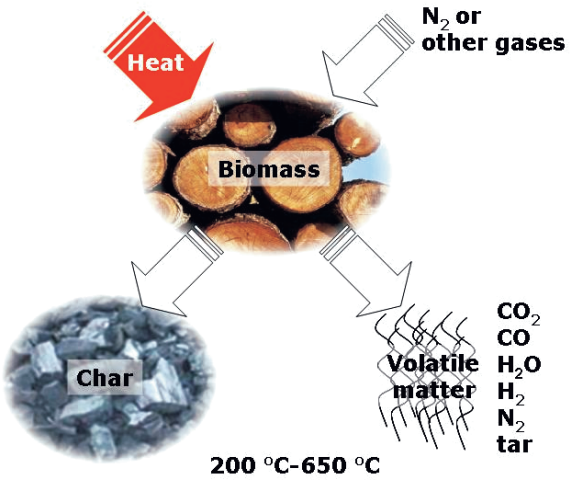

Figure 1.9: Sketch of the pyrolysis process.

Each biomass contains different yields of volatile matter, char and ash, but generally more than 80% of dry biomass is converted into volatiles during pyrolysis. The volatile matter is mainly composed of monomers of the cellulose, hemicellulose and lignin polymer that form the biomass (Reed and Das, 1988).

The pyrolysis gas contains mainly hydrogen, carbon dioxide, carbon monoxide, methane and light saturated and unsaturated hydrocarbons (Hallgren, 1996). The gas can be used for power generation or heat production; it can alternatively be synthesised to methanol or ammonia (Grønli, 1996). In the opinion of Booth and Elliott (1993), power generation appears to be superior to ethanol production because electricity from biomass could be cost competitive compared with coal based power, while ethanol prices are far way from oil prices in the transport market.

The liquid product from pyrolysis consists mainly of polyaromatic hydrocarbons (PAH), oxygenated aromatic compounds such as phenol and water (due to the moisture content of the fuel) (Hallgren, 1996). It is also called pyrolysis oil or bio-oil and can be upgraded to hydrocarbon liquid fuels for combustion engines, or directly used for power generation

URN:NBN:no-2340

or heat (Grønli, 1996). Hallgren (1996) refers that the calorific value of the pyrolysis oils varies between 5-30 MJ/kg although they are physically and chemically unstable products.

The char produced during pyrolysis can be upgraded to activated carbon (metallurgical industry use), domestic cooking fuel or barbecuing (Grønli, 1996). This solid product is more thermally instable than peat or coal, especially from grass biomass. Low heating rates and long residence times will decrease the reactivity of the char. On the contrary, high heating rates contribute to increase the reactivity of the resulting char, making it more suitable for further thermal treatment like gasification or combustion (Hallgren, 1996). The characteristics of the remaining char depend enormously on the pyrolysis conditions, namely heating rate and final pyrolysis temperature. Therefore, the pyrolysis conditions are one of the most important parameters when studying char reactivity and char pore structure.

The pyrolysis process is rather complex and its reaction mechanisms vary depending on the temperature, heating rate and pressure, as shown in Figure 1.10.

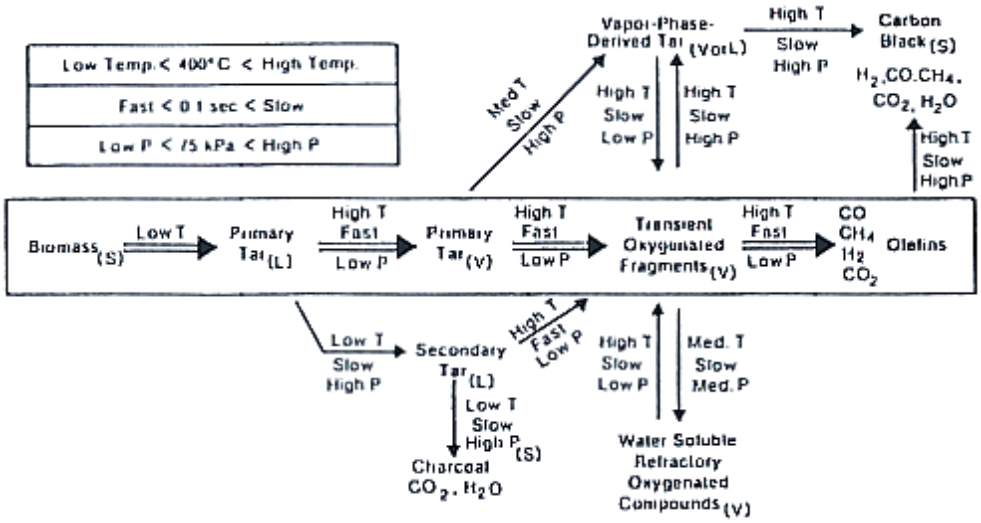

Figure 1.10: Pathways for biomass pyrolysis (Antal, 1982).

At high temperatures tar cracking takes place and lighter hydrocarbons are produced. The gas production can also be improved by increasing final temperature of the process. Low final pyrolysis temperatures and slow heating rates maximise char formation (20-30 MJ/kg). Finally, at increasing pressure, the gas/solid reactions are enhanced and can also result in higher yields of gaseous and liquid products (Hallgren, 1996).

URN:NBN:no-2340

1.4.2 GASIFICATION

Char gasification is the endothermic process where the char, solid residue from a pyrolysis process, is transformed into a gaseous mixture of CO, CO_2, CH_4, H_2 and H_2O in a reducing atmosphere usually composed of CO_2 and H_2O.

Being char gasification an endothermic process, some source of heat is required. The common heat source is the combustion of the volatile matter released during pyrolysis. The addition of an oxidation agent is necessary for this combustion process. As already mentioned previously, the thermal degradation of biomass in the presence of an oxidation agent should rather be referred as devolatilization and not pyrolysis. Figure 1.11 shows schematically the char gasification process.

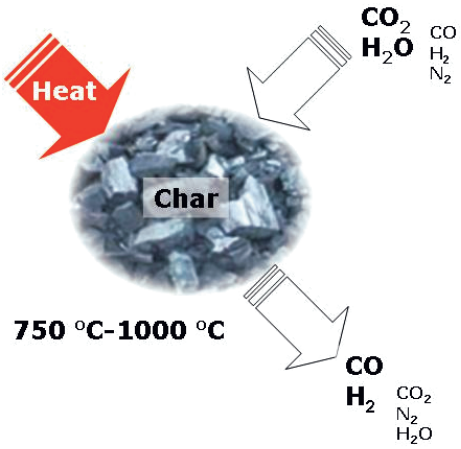

Figure 1.11: Sketch of the char gasification process.

It is however common to denote as "biomass gasification" the overall process where not only the char is transformed into gas but where all drying, devolatilization, volatile matter combustion and char gasification take place.

The biomass gasification process is also referred as "pyrolysis by partial oxidation". It intends to maximize the gaseous product, and generally takes place between 800 and 1100 °C. The product gas contains CO, CO_2, H_2, H_2O, CH_4, N_2 (if air is used), apart from contaminants like small char particles, small amounts of ash and tar.

The oxidizing agent can be air, oxygen, steam or a mixture of them. Air gasification produces a low calorific value gas (LCV) of 4-7 MJ/Nm^3 (HHV) while oxygen gasification yields to a medium calorific value gas (MCV) of 10-18 MJ/Nm^3 (HHV). However, oxygen gasification is a very expensive procedure. Some researchers have also experimented gasification with an oxygen-enriched atmosphere what could be more reasonable. Pure

URN:NBN:no-2340

steam gasification can also produce a MCV gas. Both oxygen and steam gasification produce a nitrogen free gas. The biomass gasification process is shown in Figure 1.12.

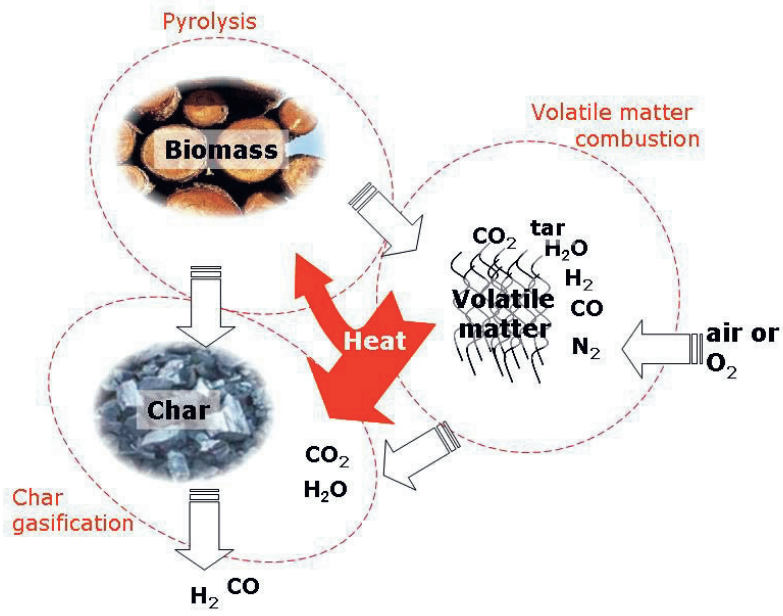

Figure 1.12: Scheme of the biomass gasification process.

The product gas from a gasification process, also called producer gas, has several uses:

- It can be upgraded to methanol by synthesis,
- burned for production of hot water or steam in a boiler, or
- burned for electricity production either in a gas turbine or in an internal combustion engine.

Chemical synthesis generally requires the use of a medium calorific value gas (MCV) (non-nitrogen diluted) with minimum contaminants for optimal conversion to chemicals (Paisley et al., 1994).
If the product gas is to be used for electricity production, the gas needs to be clean from char-particles, tar and ash before entering a gas turbine or a combustion engine. Still, the hot outlet gas from the gas turbine can be used to produce steam for a steam turbine, being the process an Integrate Gasification Combined Cycle (IGCC). Section 1.6 gives more details about power production from biomass gasification.

Compared to coal, biomass is more reactive. This can result in higher gasification efficiencies and lower gasification temperatures. However, the research conducted on

URN:NBN:no-2340

coal gasification is in some respects very relevant for biomass gasification, for instance the design of a biomass integrated gasifier/gas turbine (BIG/GT) (Consonni and Larson, 1994).

Section 1.5 contains more detailed information about the different gasification processes, reactions involved and other relevant aspects.

1.4.3 COMBUSTION

Combustion means the complete oxidation of the biomass feedstock. The process provides very hot gases that can be used to raise steam or to provide a heat space for a Stirling engine. The combustion process of biomass is far better known than the other thermochemical processes and it is one of the oldest heat production technologies although most of the traditional processes are not sustainable. Figure 1.13 shows the process in a simplified diagram.

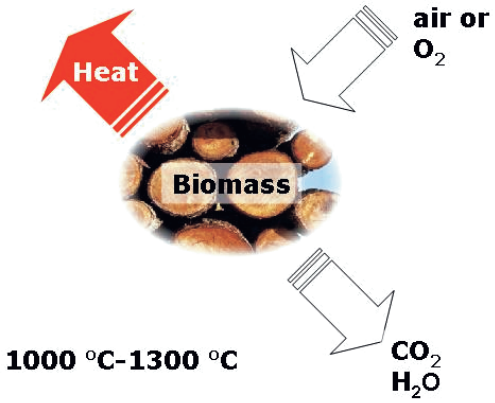

Figure 1.13: Sketch of the combustion process.

Examples of biomass combustion are numerous, going from traditional wood stove combustion to pressurized fluidized bed combustion of straw or olive residues. The research in biomass combustion is focused nowadays on the NO_x emissions (and SO_x emissions in some biomass types) and on synergies from co-combustion of biomass with waste or coal.

As in the case of biomass gasification, drying and pyrolysis will be always a previous step in any combustion process.

URN:NBN:no-2340

1.4.4 LIQUEFACTION

The process takes place at low temperatures (250-350 °C) and high pressures (100-200 bar). The objective is to maximise the liquid product as well as its quality (35-40 MJ/kg) and lower the oxygen content. With less oxygen content, comments Grønli (1996), the liquid is more stable and needs less upgrading to a hydrocarbon product. High hydrogen, partial pressure and a catalyst can improve the selectivity of the process and accelerate the reaction.

1.4.5 COMPARISON AND INTERACTION BETWEEN THE DIFFERENT CONVERSION PROCESSES

Pyrolysis, gasification and combustion can be distinguished by the air excess ratio. Table 1.7 compares the conversion processes. Liquefaction is not considered in this comparison because the high operational pressure makes the process very different from the others.

Air excess ratio	Process	Reaction	Product favoured	Product application
0	Pyrolysis	Endothermic	Liquid hydrocarbons	Chemical energy
0<ER<1	Gasification	Endo/exothermic	Product gas (CO, H2)	Chemical energy/sensible energy
ER>1	Combustion	Exothermic	Heat	Sensible energy

Table 1.7: Comparison of thermochemical conversion processes.

Gasification can give a higher efficiency in electricity production technology compared to combustion. Other differences concerning emissions and cleaning costs have been studied by Hashler et al. (Babu, 1995). Larson and Williams (1988) present a comparison between several combustion and gasification processes from a power generation point of view, favourable to the gasification option. Di Blasi et al. (1999) refer that the advantages of gasification over combustion are related to the fact that gasification implies gas phase combustion while combustion is a solid-phase combustion.

Gas phase combustion presents the following advantages:

- Higher rates of heat release
- Higher burning efficiencies
- Easily controlled and adjustable energy output
- Simpler burner construction
- No particle emissions
- Reduced NO_x emissions
- Less fouling in heat exchanger equipment
- Direct gas burning in internal combustion engines

URN:NBN:no-2340

- Application in combined cycles
- Easy distribution of gases over short distances

In addition, gasification allows for the utilisation of fuel cells. Fuel cell applications have by definition higher electrical efficiency because the chemical energy contained in the fuel is directly transformed into electricity without the intermediate transformation into thermal energy.

As previously referred, biomass gasification generally involves a pyrolysis and a combustion process. This close interaction between the diverse thermochemical conversion processes implies that despite this research being focused on gasification, the devolatilization and combustion mechanisms should be well known or at least not ignored if reliable results are to be expected.

The devolatilization conditions dictate the volatile matter composition and properties. The volatile matter characteristics and the amount and quality of the oxidation agent determine the combustion process, namely combustion products and heat released.
Finally, the gasification process is entirely governed by the heat available for reaction, gasification agent and char amount and properties; the latter are dictated by the devolatilization process.

1.5 BIOMASS GASIFICATION

This section focuses on the chemical and thermal processes occurring during biomass gasification. Other aspects like the influence of oxidizing agent, type of reactor and gas quality are also mentioned. Regarding gas quality, tar formation and destruction is of great importance and has therefore been commented with more detail.

1.5.1 GASIFICATION REACTIONS

As previously referred, biomass gasification can be considered as a three-step process: devolatilization -producing volatile matter and char-, secondary reactions of the volatile matter and char gasification.

The main chemical reactions involved in char gasification are:

Boudouard reaction: $C + CO_2 + \text{heat} \Rightarrow 2\ CO$
Water-gas reaction: $C + H_2O + \text{heat} \Rightarrow CO + H_2$

These reactions are endothermic and very slow at temperatures below 800 °C. This Ph.D. investigation has studied the two reactions in detail. The results are presented in Chapter 3.

URN:NBN:no-2340

The heat required by the char gasification reactions is provided by the following exothermic reactions:

Volatile matter combustion: $[C_xH_y+CO+H_2+CH_4] + O_2 \Rightarrow CO_2 + H_2O + heat$
Char combustion: $C + O_2 \Rightarrow CO_2 + heat$

Usually there is some methane formed as well, following the reaction:

$CO + 3H_2 \Rightarrow CH_4 + H_2O$

Although the reaction is slow unless a catalyst is present, it is quite exothermic and can provide heat to the system (Reed and Das, 1988). Methane formation is quite low in biomass gasification, unless the pressure is high.

Finally, the interaction of the gaseous species formed during pyrolysis and gasification is governed by the following reaction:

Water-gas shift reaction: $CO_2 + H_2 \Leftrightarrow CO + H_2O$

Alternatively, biomass gasification could be expressed as a single reaction, as suggested by Reed and Das (1988). Ideally, biomass, expressed as $CH_{1.4}O_{0.6}$, will react with the minimum amount of oxygen required in order to obtain a mixture of CO and H_2, according to the formula:

$CH_{1.4}O_{0.6} + 0.2\ O_2 \Rightarrow CO + 0.7\ H_2$

But, in practice, some extra oxygen is needed and the reaction becomes:

$CH_{1.4}O_{0.6} + 0.4\ O_2 \Rightarrow 0.7CO + 0.3CO_2 + 0.6\ H_2 + 0.1\ H_2O$

1.5.2 GASIFICATION PROCESSES

This section focuses on the gasification agent and on how to provide heat for the gasification process. Table 1.8 summarizes the advantages and disadvantages of the different gasification agents.

URN:NBN:no-2340

Gasification agent	Advantages	Disadvantages	Heating value of product gas (MJ/Nm^3)
Air	Inexpensive	Low heating value	4-7
Oxygen	N_2 free product gas Medium heating value	Expensive	10-18
Steam	N_2 free product gas Medium heating value Enhanced H_2 content	Very endothermic process	10-18

Table 1.8: Comparison of gasification agents.

1.5.2.1 AIR GASIFICATION

Gasification takes place usually at 700-1000 °C. Fredriksson and Kjellström (1996) experimented in their cyclone gasifier with the gasification temperature and found that a minimum temperature of 800 °C was required for stable gasification (wall temperature above 600°C). The yield of products and operating temperature depends on the amount of oxidant added to the system.

Values of the air excess ratio for gasification are usually between 0,2 and 0,4, being the optimum value about 0,25. If the air excess ratio is lower, the char will not be gasified and some energy will be retain in the wood as charcoal; if the air excess ratio is higher, then some of the gas will be burned and temperature will rise rapidly. Reed and Das (1988) and other investigators have observed that in a fixed bed, the equivalence ratio is self-controlled by having a constant bed height. This phenomenon has been experienced in this investigation as well; it is commented in detail in Chapter 2.

The ratio CO/CO_2 (or H_2/H_2O) is a measure of the producer gas quality. About the 30% of the biomass is burned to provide energy for gasification of the rest. The amount of excess oxygen depends on the efficiency of the process that can be improved by insulation, drying of the biomass or air preheating (Reed and Das, 1988).

Wang and Kinoshita (1992) performed parametric tests for atmospheric nitrogen/oxygen gasification. They examined the effect of residence time, equivalence ratio, gasification temperature and steam injection on the gas yield, composition and heating value. Among their conclusions it is interesting to point that the concentrations of CO and H_2 were found smaller than theoretically predicted and still CO_2 and CH_4 yields were higher than predicted.

URN:NBN:no-2340

1.5.2.2 STEAM GASIFICATION

The gasification process referred as "steam gasification" can use as a gasifying agent either only steam, a mixture air/steam, a mixture oxygen/steam, or others. A higher steam content of the gasifying agent results in an enhanced H_2 content of the product gas.

Pure steam gasification produces synthesis gas (syngas), that mainly contains hydrogen and carbon monoxide and that can be used for methanol production among other applications. However, the raw syngas also contains unwanted components like methane and tar that have to be removed in a conditioning process. For methanol production as well as for some fuel cell applications, the H_2/CO has to be adjusted to a certain value. These processes do always involve catalytic reactions and are slightly out of the scope of this work.

The steam atmosphere enhances the reforming reactions and the char gasification reactions producing then lighter gases such as H_2, CO and CO_2 (Rapagnà and Foscolo, 1996; Rapagnà and Latif, 1997). On the other hand, since the steam gasification reactions are very endothermic, the heating rate diminishes and consequently, the formation of methane also decreases (Fredriksson and Kjellström, 1996).

1.5.2.3 SUPERCRITICAL WATER GASIFICATION

This quite new process is somewhat similar to steam gasification but initially the water is in the liquid phase at 350-600 °C and at pressures about 17-35 MPa (Minowa et al., 1997). A nickel catalyst promotes the reaction between the water and the biomass. The process gives large yields of hydrogen and carbon dioxide and a very low yield of methane.

1.5.2.4 OXYGEN GASIFICATION

The main consequence of having a nitrogen free gasification agent, and consequently also a nitrogen free product gas, is the considerable increase in the heating value (11,5 MJ/Nm^3). However, oxygen gasification is economically unattractive in the opinion of many. A possible alternative could be to use oxygen-enriched air, what could be less expensive and improve considerably the syngas quality.

In some cases, oxygen is added in the steam gasification process to provide some energy for the endothermic reactions so the process is auto-thermal. However, in the opinion of Aznar et al. (1993), this procedure is not recommended because the heating value of the product gas will diminish with oxygen addition.

URN:NBN:no-2340

1.5.2.5 INDIRECTLY HEATED BIOMASS GASIFICATION

As already mentioned, the most relevant reactions for biomass gasification are endothermic. So far, we have considered processes where part of the biomass (part of the volatiles) burn inside the gasification reactor, providing thus heat for the process.

Alternatively, one can provide heat indirectly, i.e., by other means without making use of the produced fuel gas. This process can produce medium heating value gas without requiring oxygen. There are several gasifier designs working with this principle, as shown in Table 1.9, and some of them will be presented in detail in this section.

Design principle	Examples	References
In-bed heat exchanger	MTCI process	Black, 1991; Kandaswamy et al. 1991
Combustion of by-product char in a second reactor where heat is carried by the circulating sand.	Battelle process	Consonni and Larson, 1994; Paisley et al. 1994; Farris and Weeks, 1996
	Twin fluidized bed system	Bridgwater, 1995; Cen et al. 1993; Herguido et al. 1992
Combustion of the char and heat transferred through sand recirculation but in a sole reactor	Fast internally circulating fluidized bed	Hofbauer et al. 1997a, 1997b; Fercher et al. 1998
	AVSA process	Platiau and Faniel, 1989
Electrical heated bed surface	Spouted bed	Janarthanan and Clements, 1997
The gasifying agent itself carries the sensible heat	Allothermal gasification	Kubiak and Mühlen, 1998; Chughtai and Kubiak, 1998

Table 1.9: Indirectly heated biomass gasification processes.

THE MTCI PROCESS

Manufacturing and Technology Conversion International (MTCI) is a company developing an advanced gasification system for paper mill residues and black liquor (Figure 1.14).

The heat required for the gasification reactions is provided by a heat exchanger inserted into the gasifier. The heat exchanger is based on the pulse combustion theory, what provides enhanced heat transfer properties. The intention is to burn part of the product gas in the combustion chamber, although as a first approach they use natural gas. The gasifying agent is steam and/or recirculated product gas.

The bed material is sodium carbonate (limestone) and acts as a catalyst for the steam-char reactions. The gasifier temperatures are about 600-650 °C, what promotes a very high thermal efficiency of the system. As the other indirect heated systems, the gasification produces a medium heating value gas, in this case of about 14 MJ/Nm^3.

URN:NBN:no-2340

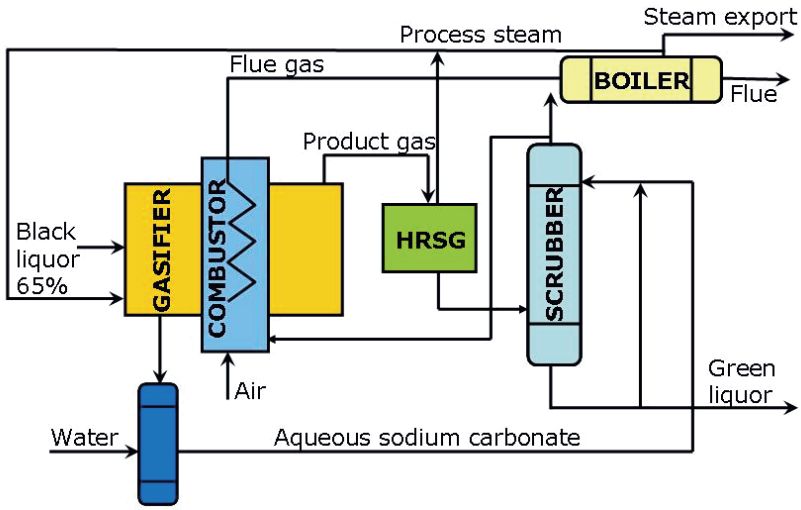

Figure 1.14: MTCI process for black liquor (Black, 1991).

THE BATTELLE PROCESS

The Battelle Process consists of two interconnected fluidized circulating beds (Paisley et al. 1994); it is classified by Bridgwater (1995) as a Fast Fluid Bed (Figure 1.15).

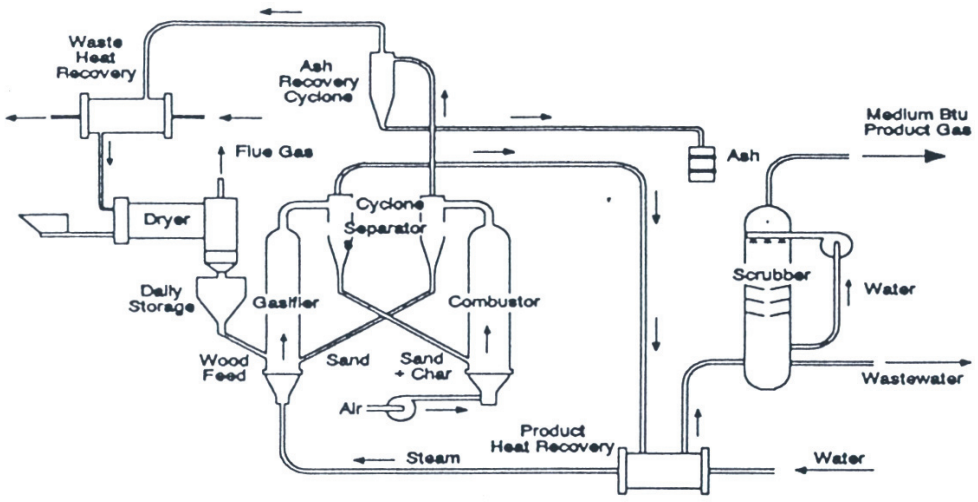

Figure 1.15: The Battelle process (Paisley et al. 1994).

The first circulating bed acts as a gasifier – mainly of the volatile yield- and the second as a char combustor. The sand heated by the combustion process is recirculated into the gasifier, providing then the heat required for the gasification reaction. The sand from the gasifier, together with the char is again recirculated into the combustor. The gas

URN:NBN:no-2340

produced in the gasifier is removed so it does not enter the combustion reactor. The gasification agent is a mixture of steam and recirculated product gas[1]. This means that the produced gas does not contain nitrogen but mainly hydrogen and carbon monoxide and it has a higher heating value (17-19 MJ/m^3), i.e. has the advantages of the steam gasification. For the char combustion, the necessary air is added into the second reactor.

The advantages of the process are:

- High biomass throughputs that reduce investment costs, allow modular fabrication and simplify operability
- The process does not require much fuel preparation
- It produces a medium heating value gas without using oxygen
- It does not produce char or tar as by-products
- Low influence of the biomass moisture regarding the heating value of the product gas, what is desirable for power generation
- Economically more interesting than direct biomass combustion

However, Consonni and Larson (1994) comment that the thermal losses of this indirectly heated gasifier appear to be relatively higher (2%) compared with other gasifiers (0,6% for pressurized systems and 1% for atmospheric). This statement should be verified since the differences could be due to the larger volumes of both gasifier and combustor.

The flue gas from the combustion reactor can be used for preheating the air supply or for fuel drying. The high heating rates and short residence times in the gasification reduce the tendency to form tars but still some secondary and tertiary tar are formed (Paisley, 1997). The system includes a scrubber for the product gas cleaning. The condensed organic phase retained in the scrubber, once separated from the water, can be re-injected into the combustor[2].

An alternative design is the twin fluid bed system. Such system is characterized by Bridgwater (1995) as a complex and costly design that requires large capacities for viability and has low efficiency but high specific capacity. The twin fluid bed provides good gas-solid mixing and it allows direct catalyst addition in the reactor. Examples of

[1] Actually, most of the gasifying agent is recirculated product gas with a short steam addition (Consonni and Larson, 1994), and according to Rohrer and Paisley (1995) very little fluidizing agent is required because most fluidizing gas is the volatile matter and water released from the biomass as soon as it enters the reactor and contacts the hot sand.

[2] According to Gebhard et al. (1994), the scrubbing process is economically unattractive and they study an alternative catalytic conditioning system for the raw syngas from the Battelle Columbus Laboratory gasifier.

URN:NBN:no-2340

twin fluid bed are Ebara (Japan), Tsukishima (Japan), the Multisolid and Catalytic Double Fluidized Bed Circulating System (Herguido et al., 1992[3]).

A similar arrangement is presented by Cen et al. (1993) for rice hulls gasification as an "Outer Circulating Fluidized Bed". The gasifying agent is also a mixture of steam and recirculated product gas. The gasifier operates at 750-800 °C in a bubbling fluidized bed while the combustor is a fast fluidized bed and operates at 900-950 °C. They tested a cold flow model and according to their analysis, an air leakage into the gasifier can produce considerable losses of heating value. For example, an air leakage ratio of 2,5 % will decrease the gas heating value by 7 %, and a gas leakage of 5 % will produce a 13% decrease. They also run some gasification tests and point that an increase in gasification temperature will require a higher solid recirculation and this will lead to higher heat losses.

THE FAST INTERNALLY CIRCULATING FLUIDIZED BED

The **F**ast **I**nternally **C**irculating **F**luidized **B**ed (FICFB) developed by Hofbauer et al. (1997a; 1997b) and Fercher et al. (1998) is based on the same principle although it improves the thermal efficiency of the system by its compact design. The system is shown in Figure 1.16.

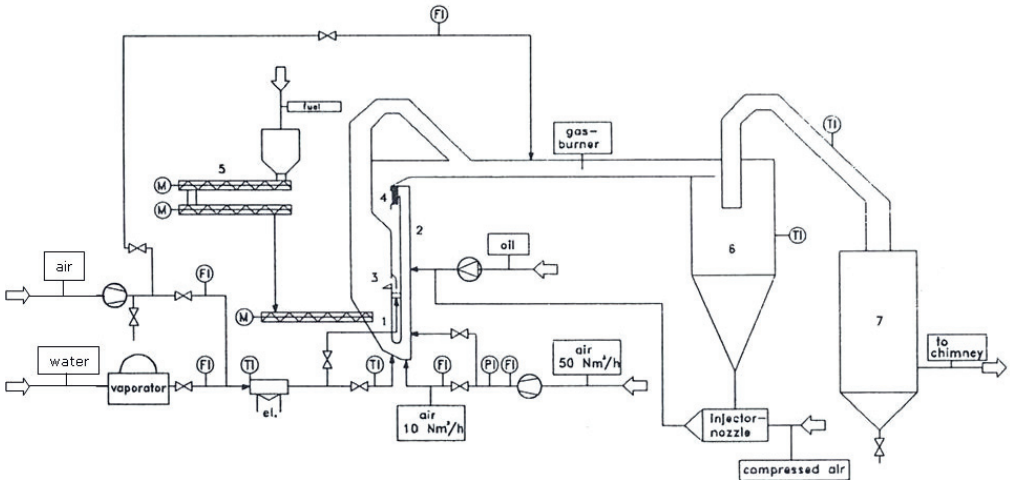

Figure 1.16: The Fast Internally Circulating Fluidized Bed (Hofbauer et al., 1997a).

Instead of two fluidized bed reactors, there is only one reactor divided in two zones. The bed material recirculation takes place between the zones and the product gas is extracted from the system by means of a siphon. The design of the reactor is simpler and

[3] The system described by Herguido et al. (1992) was dismantled some years later because it was found expensive and complex compared to a more conventional gasifier, as explained by Gil et al. (1997).

URN:NBN:no-2340

the investment costs lower. Their results show hydrogen concentrations in the product gas of about 35 % and a calorific value above 13 MJ/Nm^3. In the pilot plant the group is operating, an electrical steam generator produces the steam for the gasification.

The results presented in 1998 after two years of experience (Fercher et al. 1998) are:

- The composition of the product gas depends on the gasification temperature, the residence time and the elementary analysis of the fuel, especially the C, H and O content. The higher the C content, the higher hydrogen yield in the product gas. Increasing temperature also produces higher amounts of hydrogen.
- The tar content is quite low compared to air gasification. This can be due to the steam atmosphere that enhances the reforming reactions that produce lighter gas (Rapagnà and Latif, 1997). The tar content depends on the gasification temperature and the fuel itself. However, the amount of steam required for fluidization is quite larger than the steam required for the reactions.
- The fuel moisture content influences largely the chemical efficiency of the process but not the product gas composition.
- The gasification temperature does not influence the chemical efficiency but the tar content. It should be as high as possible.
- The upper limit of the combustion temperature is the ash melting temperature.

The AVSA process uses steam together with recirculated product gas as gasification agent. Platiau and Faniel (1989) present some results from the cold and hot matematical model regarding gas leakage between the gasifier and the combustor.

THE SPOUTED BED

Another arrangement for indirect heating is the pilot scale spouted bed gasifier presented by Janarthanan and Clements (1997) that is shown in Figure 1.17.

The bed consists of two concentric zones where the inner one is a fluidized column for the steam gasification and the outer collects particles. The system is electrically heated and the radiant heat represents a very large contribution to the heating rate. Catalyst addition is also allowed in the reactor.

URN:NBN:no-2340

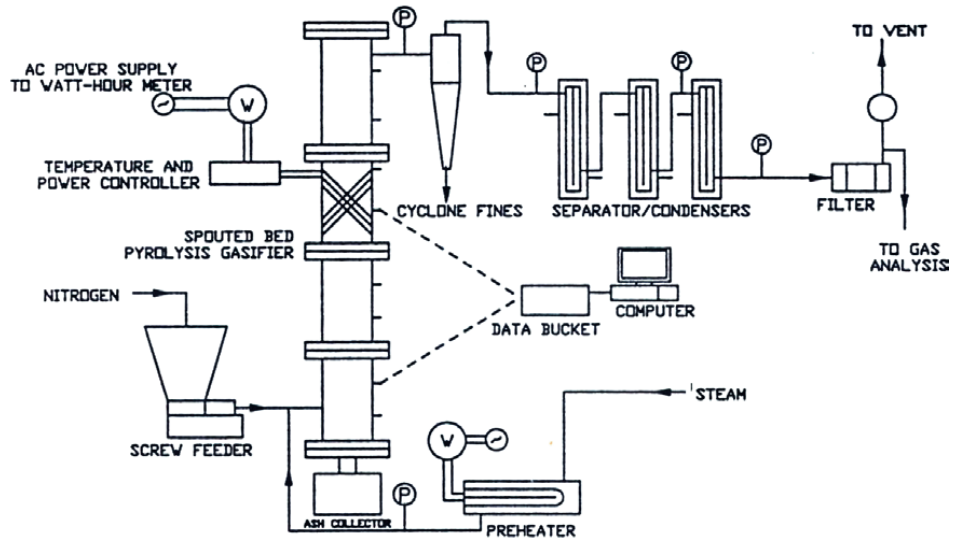

Figure 1.17: Indirectly heated gasification in a spouted bed gasifier (Janarthanan and Clements 1997).

THE ALLOTHERMAL GASIFICATION

The gasification agent itself, essentially steam, carbon dioxide or/and nitrogen, provides the heat required for the endothermic gasification reactions. The gasifying agent is heated (or generated, if steam) by combustion of part of the product gas (approx. 25%), after dust removal, with air or oxygen. The allothermal gasification process presented by Kubiak and Mühlen (1998) is shown in Figure 1.18.

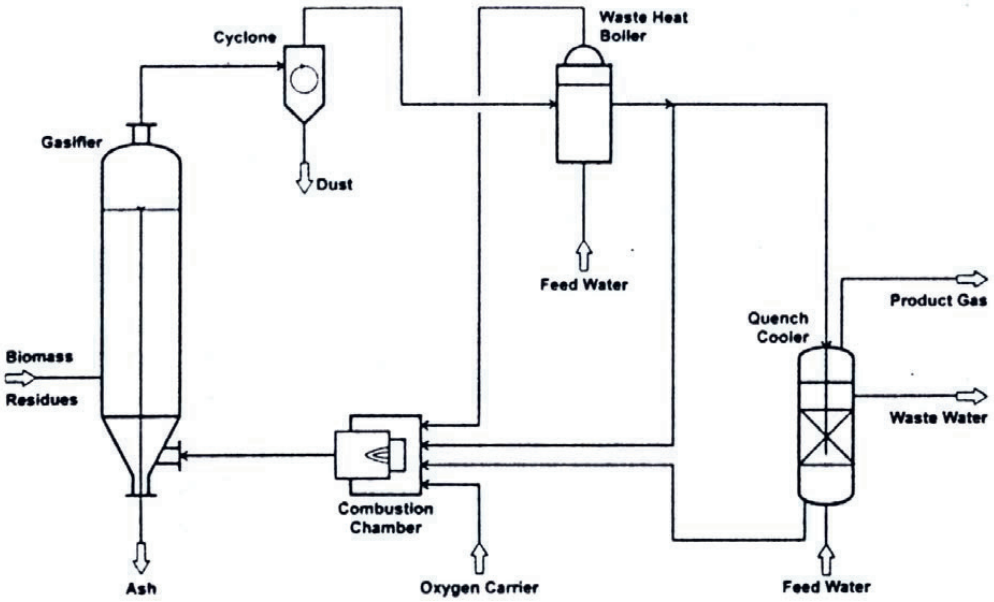

Figure 1.18: Allothermal gasification for waste and biomass
(Chughtai and Kubiak, 1998).

URN:NBN:no-2340

The process has already being tested in a pilot plant for coal gasification. The prototype installation for biomass includes a pressurized fluidized bed gasifier but experimental results are not available yet.

1.5.2.6 CHAR GASIFICATION

Some researchers have investigated the gasification of the char, what implies that a previous process (slow or fast pyrolysis or devolatilization) has taken place. The pyrolysis conditions influence greatly the reactivity characteristics of the char. However, the gases produced during devolatilization or pyrolysis will be still present in a real case, but might have been removed in experimental installations.

The presence of the product gases has to be taken into consideration. For peat and coal, the product gases significantly reduce the gasification rate. However, for biomass-derived fuels, the high yield of volatile substances and the different types of ash-forming materials can even catalyze the gasification reactions (Moilanen and Saviharju, 1997).

In Espenäs opinion (1993), the presence of freshly formed pyrolysis gases reduces the reactivity of highly reactive char. Furthermore, he shows in his experiments that the moisture content of the fuel in fast pyrolysis increases the reactivity.

1.5.3 THE WATER-GAS SHIFT REACTION

As already mentioned, the reaction:

$CO + H_2O \Leftrightarrow CO_2 + H_2$

is of great importance in gasification. Among researchers, there is a certain disagreement about whether the water-gas shift reaction is in equilibrium or not during gasification.

Assuming equilibrium in the reactions simplifies the analysis and, for instance, allows parametric study as that presented by Nordin et al. (1997). The experiments of Herguido et al. (1992) with pure steam gasification show that the gas composition approaches the shift reaction equilibrium composition for temperatures above 750 °C. They mention other authors work, for further information.

However Fredriksson and Kjellström (1996), in their experiments with air and air/steam gasification at 800-940 °C found that the gas composition could not be predicted with equilibrium calculations. Also Paisley (1997) calculated the equilibrium compositions for

URN:NBN:no-2340

the tar and methane reforming reactions and for the water-gas shift reaction between 700 and 1000 °C. The experimental compositions were far from equilibrium both for methane concentration and for the H_2/CO ratio.

1.5.4 TYPES OF REACTOR

1.5.4.1 FIXED-BED GASIFIERS

These reactors are rather easy to construct and operate and are widely available, especially in developing countries. They are suitable for small scale applications but have in general limited scale-up properties. The size of fixed bed gasifiers is in most cases below 1 MW. The reason for its limited size is that a high temperature zone is required to reduce the tar content of the product gas; as the gasifier diameter increases, it is more difficult to create such a high temperature zone.

An advantage of fixed bed gasifiers is the low particle content of the product gas, since the bed of char itself acts as a filter.

There are mainly two types of fixed bed gasifiers, depending on whether the gasification agent is feed from the top of the reactor, as the biomass, or from the bottom and therefore counter-current to the biomass flow.

The latter design is called "updraft" gasifier and is not very much in use. It produces a lot of tars because the products from devolatilization do not cross the high temperature zone of the reactor. The updraft gasifier is only suitable for heat production applications, where the tar content of the product gas is irrelevant.

When both biomass and gasification agent flow downwards, the gasifier is called a "downdraft" gasifier. The most popular design is known as the Imbert gasifier and it is characterised by a reduction in diameter just below the air supply. The reduction, or throat, helps creating a high temperature zone for tar cracking. An alternative design is the Stratified downdraft gasifier, or open core. This design has no throat and both biomass and gasification agent are fed from the top of the reactor. The stratified downdraft gasifier is easier to construct but presents other disadvantages like operation instability. Figure 1.19 shows the three fixed bed designs mentioned.

URN:NBN:no-2340

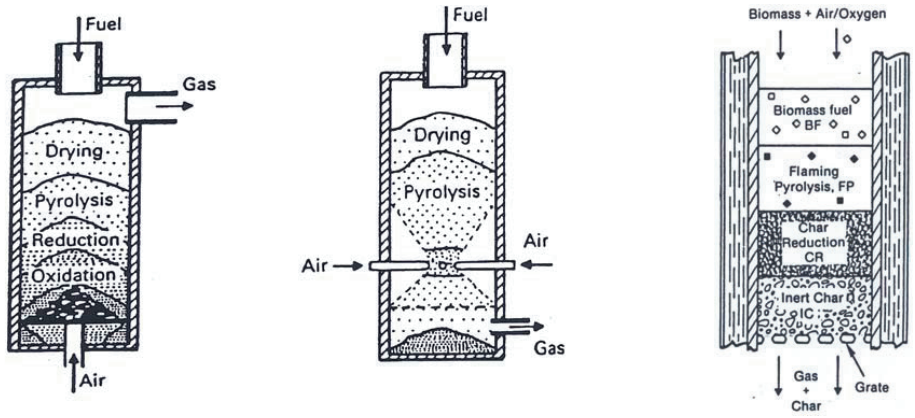

Figure 1.19: Fixed-bed reactors. a) Updraft, b) Imbert downdraft, c) Stratified downdraft (Reed and Das, 1988).

As mentioned earlier in the introduction, this Ph. D. work has concentrated on the operation of a stratified downdraft gasifier, built in our laboratories. The complete description of the reactor and the results achieved are presented in Chapter 2.

1.5.4.2 FLUIDIZED-BED GASIFIERS

In the opinion of Consonni and Larson (1994), the fluidized bed reactors represent the most promising gasifier design for directly heated biomass gasification. They present higher throughput capabilities and greater fuel flexibility than fixed beds and can accept low-density feedstock. They required minimal pre-processing of feedstock. However, as referred by Williams and Larson (1996), they present more problems regarding gas quality control because of the higher temperature outlet (800-1000 °C) at which alkali metals will not condense and because much more particulate is carried over. Ceramic or sintered-metal filters are required.

Still, circulating fluidized beds (CFB) allow for more complete fuel conversion and higher specific throughputs than bubbling beds.

Figure 1.20 shows both gasifier designs.

Examples of commercial biomass-fired atmospheric CFB's are: Ahlstrom (Finland), Lurgi (Germany) and TPS/Studsvik (Sweden) (Williams and Larson, 1996).

URN:NBN:no-2340

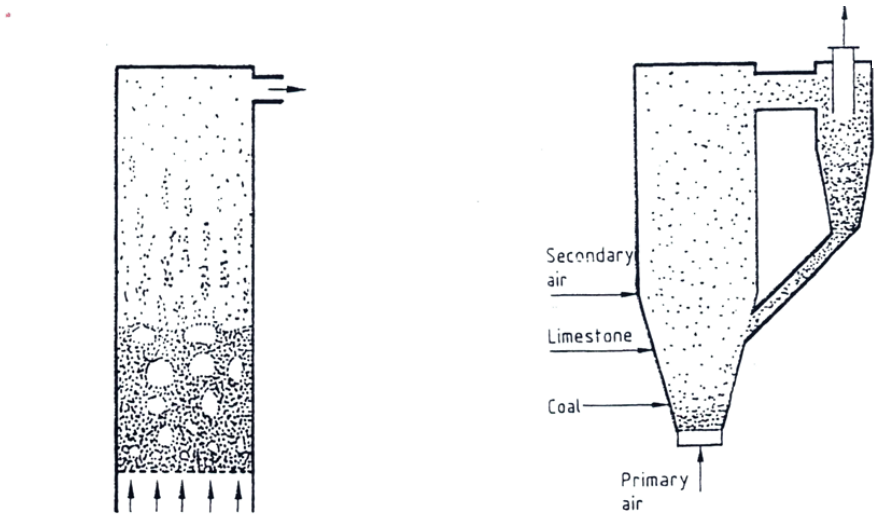

Figure 1.20: Fluidized bed reactors: a) Bubbling bed, b) Circulating bed.

1.5.4.3 COMPARISON BETWEEN REACTOR DESIGNS

Warnecke (2000) has recently presented a thorough comparison between fixed bed and fluidized bed gasifiers. Table 1.10 summarizes the conclusions.

Reactor type	Fixed bed	Fluidized bed
Criteria		
Technology	(-) Hot spots with exothermic reaction (-) Possible ash fusion on grate (-) Channelling possible (-) Low specific capacity (-) Long heat-up periods	(+) Best temperature distribution (-) Conflicting temperature requirement (+) Good gas solid contact and mixing (+) High specific capacity (+) Easily start and shut down, fast heat-up[4]
Use of material	(+) High ash content feedstock possible (-) Large and uniform pellets needed (+) Relatively clean gas is produced[5]	(+) Tolerates fuel quality variations (+) Broad particle-size distribution (-) High dust content in gas phase
Use of energy	(+) High carbon conversion efficiency	(+) High carbon conversion efficiency
Environmental	(+) Molten slag possible	(-) Ash not molten
Economy	(-) High investment for high loads	(+) Low investment

Table 1.10: Comparison of fixed and fluidized bed reactors. (+): advantages, (-): disadvantages.

Finally, the recent overview of Maniatis (2000) presents the status for several gasification reactors regarding its technology strength and market attractiveness. Figure 1.21 shows the conclusions.

[4] In circulating fluidized bed the heat-up is even faster.
[5] This is not the case for updraft gasifiers.

URN:NBN:no-2340

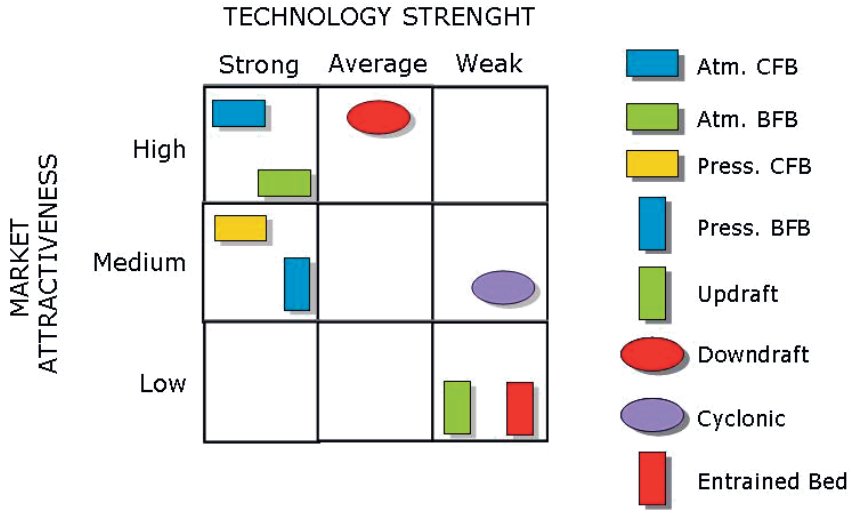

Figure 1.21: Status of gasification technologies (Modified from Maniatis, 2000).

Atmospheric circulating fluidized bed gasifiers have been proven reliable with various feedstocks and relatively easy to scale up (up to 100 MW_{th}). Also atmospheric bubbling fluidized bed gasifiers are reliable at small-medium scale (up to 25 MW_{th}) but are somewhat limited in their capacity size. Pressurized fluidized systems are less attractive because of the increased costs related to the construction. They present however other advantages like their suitability for integrated combined cycle applications because the product gas does not need to be pressurized after gasification.

Downdraft gasifiers are attractive for small applications (<1,5 MW_{th}) and the market is large in all world regions. The problem of tar removal and more automated operation is still present. Updraft gasifiers are not attractive for power generation because of the high tar content.

1.5.5 GAS CONDITIONING

The gas leaving the gasifier has to be somewhat modified for the different applications available. This process can be complex and include many sub-processes, depending on the final use of the product gas. A gas conditioning process can include the following tasks:

- Particle removal at high temperatures through metallic or ceramic filters
- Modification of the H_2/CO ratio by means of catalytic reactors
- Methane reforming
- Tar reforming
- Product gas cooling to moderate temperatures in order to condense alkali

URN:NBN:no-2340

- Alkali removal after cooling with filters
- Product gas cooling to ambient temperatures by means of wet scrubbing in order to condense tar
- Compression

Hot-gas conditioning, as defined by Paisley (1997), is done by passing the raw product gas through a catalytic reactor (either a fixed or a fluidized bed) under temperature and pressure nearly similar to those of the gasifier. At the catalyst surface, tar compounds undergo reforming reactions with the steam in excess from the gasification reactions. The absence of cooling or heating operations increases considerably the overall thermal efficiency of the system.

1.5.5.1 TAR

According to Maniatis (2000), the efficient and economic removal of tar is still the main technical barrier for commercialization of power generation from biomass gasification. Ståhlberg et al. (1998) define tar as "a complex mixture of organic compounds ranging from light compounds like benzene to heavy aromatic hydrocarbons". These liquid products from biomass gasification appear generally in the gas phase at gasification temperatures. They could seriously damage industrial equipment such as gas turbines and gas engines if they condense.

There is still lack of agreement about how to define tars and how to classify them. There are however some general groups like light tars and heavy tars.

A critical aspect among gasification researchers is the measurement system that is complicated if it is not to interfere with the system, but obtain an accurate measurement.

It is becoming crucial an agreement regarding a measurement method so different gasifiers can be compared regarding tar production. An important effort is being made by the working group of the Biomass Gasification Task of the IEA Bioenergy Agreement (Neeft et al., 2000; Abatzoglou et al., 2000).

Another area of study concerning tars is the analysis of its formation during pyrolysis and the dependence on temperature, heating rate and other pyrolysis conditions. Other research work is concentrated in the tar further reactions (thermal cracking and partial oxidation), its interaction with the char or the effect of catalytic reactions.

One of the most promising gasifier designs regarding tar content is the two-stage gasifier (Figure 1.22). The pyrolysis and char gasification take place in two independent reactors

URN:NBN:no-2340

that are interconnected. The pyrolysis gas is burnt before it enters the char gasification reactor. Bentzen and Henriksen (2000) report tar contents of 5-24 mg/Nm^3. Low tar contents (40-100 mg/Nm^3) are also reported by Mukunda (Milne et al., 1998).

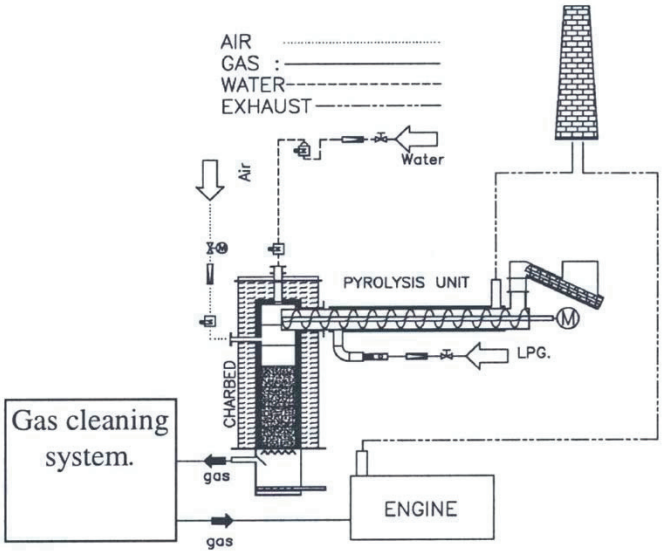

Figure 1.22: The 100 kW two-stage gasifier at the Technical University of Denmark (Bentzen et al., 1999).

1.5.5.2 TAR FORMATION

Different tar compounds are formed at the different pyrolysis conditions. Evans and Milne (1997) classify the tar in three categories:

- Primary pyrolysis products, produced at low temperature operation and characterized by cellulose, hemi-cellulose and ligning-derived products.
- Secondary pyrolysis products, characterized by phenolic peaks.
- Tertiary products that include methyl derivatives of aromatics (alkyl products) and condensed tertiary products that include benzene, toluene, naphtalene, etc. These compounds have a higher molecular weight, are usually produced at higher reaction severity and are the precursors of particulate matter.

In their opinion, the assumption of tar cracking to CO, H_2 and other light gases at higher temperatures is only valid for the primary pyrolysis products. Tertiary condensed products will rather increase their molecular weight with temperature. Brandt and Henriksen (1998) present the influence of temperature and available oxygen on tar composition.

URN:NBN:no-2340

Paisley (1997) refers that shorter reactor residence times and higher heating rates generally produce tar with lower molecular weight than tar produced with longer residence time and lower heating rates.

The different tar compounds described above also perform differently in a catalytic process. For example, tar formed at lower temperatures (primary and secondary products) is more satisfactory removed even in a larger amount than tar formed at high temperatures (tertiary products) in a catalytic process (Bilbao et al., 1998; Evans and Milne, 1997).

Naphthalene is considered by Lammers et al. (1997) as one of the major compounds in high temperature fluidized bed gasification and it is also considered one of the most problematic.

1.5.5.3 TAR DESTRUCTION

A possible solution to avoid tar in the product gas is to cool the gas so the tar condenses. The temperature at which condensation takes place depends on the type of tar. A simple approach taken by Evans and Milne (1997) is to insert an aluminium foil in the secondary gas-phase reactor so the tar condenses in the metal. Beck et al. (1981) use tar impingers to retain only tar[6] keeping the water as steam. Another way of removing tar is by wet scrubbing. This process cools the gas until ambient temperature with the consequent loss of sensible energy and the production of waste water.

In many cases, a catalyst (like dolomite, for instance) can be added in-bed in the gasifier, considerably decreasing the tar production[7]. There is an extensive amount of literature about catalytic conditioning of the synthesis gas. However, some authors like Rapagnà et al. (1998) and Aznar et al. (1993) mention that the tar content of the product gas before catalytic conditioning should be low in order to preserve the lifetime of the catalyst.

An alternative solution is to decompose the tar in lighter compounds (H_2, CO, CO_2, CH_4) that contribute to the heating value of the gas. There are at least two methods to decompose the tar: Thermal cracking and partial oxidation. The former process takes

[6] The tar impingers operate at about 110-140 °C.

[7] Caballero et al. (1998) mention that with in-bed use of dolomite, the tar content can be reduced down to 1-2 g/Nm^3 in the raw gas. Rapagnà et al. (1998) rather recommend olivine, a mineral substance catalytically active, harder and mechanically more resistant than dolomite, although not as effective as dolomite for tar destruction. Dolomite becomes powder after certain time and leaves the bed together with the ash (Olivares et al., 1997); therefore dolomite has to be supplied at a constant rate.

URN:NBN:no-2340

place in the absence of air and is due to a temperature effect while the partial oxidation process takes place with a certain air ratio.
Thermal cracking and partial oxidation of the pyrolysis gas has been studied by Brandt and Henriksen (1998) among others. They investigated the reactions at 800, 900 and 1000 °C and at different air ratios (from 0 -thermal cracking- to 0,7 -several degrees of partial oxidation-). The pyrolysis gas is generated by slow pyrolysis at 600 °C. Tar is significantly reduced by partial oxidation and at excess air ratio above 0,2, temperature does not seem to have influence on the tar content. Furthermore, their work shows that it is possible to reduce tar content without affecting the hydrogen or the CO yield in the produced gas. The thermal cracking experiments show that the tar content diminishes with increasing temperature, being though considerably higher than the content with partial oxidation.

Aznar et al. (1993) suggest that feeding the biomass from the top of a fluidized bed gasifier increases the tar content because the biomass does not reach the reaction zone that fast. It would be better to feed the biomass at the bottom of the bed, so it goes along with the gasifying agent and reacts completely.

There is also a lot of work done with catalysts (mainly Ni, Al) to reduce the tar problem and simultaneously to increase the hydrogen yield in the produced gas. There are two main catalysts used in biomass gasification; dolomite and nickel-based catalyst. Apart from their performance –Nickel-based catalysts are more efficient with tar and methane generally-, they have very different cost. Nickel-based catalysts are very expensive and have a short live what make them unsuitable for large-scale reactors (Lammers et al., 1997). Dolomite is less expensive and can be added as a feedstock to the gasifier or in a secondary catalytic reactor.

Finally, there are some researchers who do not consider the tar content of the product gas a problematic issue. In the opinion of Williams and Larson (1996), tars do not seem to be such a big problem if the temperature of the exit gas from the gasifier is high enough so the tars are in the vapour phase. Tar will be burn in the turbine without further problem. Furthermore, it is even good to have tar so the heating value of the gas increases. According to Faaij et al. (1997), tar can increase the heating value of the gas by 3-6 %, and such increase (6 %) can positively affect the net conversion efficiency by ca. 2 percentage points. Craig (1997) experienced burning product gas after high temperature filtration with no further problems.

URN:NBN:no-2340

1.5.6 PRESSURIZED GASIFICATION

With pressurized gasification, the fluidizing agent is pressurized before entering the gasifier. In case of gas turbines, it is necessary to compress the fuel gas previous to combustion if gasification takes place at atmospheric pressure. This second process has more thermodynamic losses associated and also, compressing the product gas can be problematic due to the tar content. Tar would not be a problem in a pressurized system because it will burn in the combustor (as long as the temperature in the cleaning system does not go below 400 °C and if the residence time inside the combustor is long enough for complete tar burning) (Bridgwater, 1995).

However, the biomass feeding system becomes more complex in a pressurized reactor and inert gas leakage could also take place. Furthermore, a pressurized installation requires successful large-scale demonstration although this does not seem to pose big difficulties (Consonni and Larson, 1994).

The commercial-scale pressurized systems under development in 1994 operated within a pressure range of 20-35 bar. These systems will therefore be able to directly fuel existing small-to-medium power output aeroengines (pressure ratio between 18 and 22), but not the new large engines with pressure ratios around 30 (intercooling included). Preparing the gasifiers for such pressures will involve further development of biomass feeding systems, fluidization characteristics and chemical kinetics. Barbucci and Trebbi (1994) recommend pressurized gasification at high temperatures so the product gas can be directly fed in the combustion chamber and maintain most of the sensible heat. They ensure that the efficiency can increase by 3 points if the design avoids gas cooling. However, the equipment for hot gas cleaning (ceramic filters) still shows poor mechanical resistance and low efficiency in alkali vapors removal at high temperatures.

As already mentioned in Section 1.5.4.3, the capital costs of a pressurized system are much higher than the atmospheric one, mainly due to higher equipment and construction costs. On the other side, pressurized systems have a lower volume and allow higher processing rates (Larson et al., 1989). Finally, given the high reactivity of biomass, a pressurized system does not offer great advantages from the chemical kinetics-point of view. Gas compositions and heating values are nearly the same in both systems (Bridgwater, 1995).

Espenäs (1993) conducted several experiments for steam gasification at different pressures. The reaction rate increases for higher pressures (and higher steam partial pressures) for char formed during pyrolysis at the same pressures. However, his results

URN:NBN:no-2340

also show that peat char formed at high pressure is less reactive than char formed at low pressure, both with slow heating. Finally, he concludes that the pressure influence in the char gasification process can not be generalized and that depend on the type of fuel and the reactor scheme.

According to Wang and Kinoshita (1993), the advantages of high-pressure gasification are the higher reaction rate due to increased partial pressures of the species and longer residence times due to lower volumetric flow. However, increasing the pressure means higher yields of carbon and methane and lower concentrations of hydrogen and carbon monoxide due to a shift in the equilibrium.

Aldén et al. (1997) conducted experiments to analyze the high temperature catalytic gas cleaning for pressurized gasification. Although their analysis is done with nitrogen as the gasifying agent (therefore pyrolysis) some of their result could bring some relevant information:

- Higher operating pressures produce less tar although the residence time also increased at higher pressures.
- Large pressures enhance soot formation and recarbonisation of the dolomite.

1.6 POWER GENERATION FROM BIOMASS GASIFICATION

1.6.1 INTRODUCTION

Power production from biomass combustion is more common nowadays, using the exhaust gas to raise steam and using the steam in a steam turbine. However, this section focuses on power production from biomass gasification: type of cycles and equipment, advantages and problematic. Biomass gasification is in principle better suited for power generation than combustion allowing for higher electrical efficiencies.

1.6.2 TYPES OF CYCLE

There are mainly two types of cycles suitable for biomass gasification power production, depending on the type of engine. If a gas turbine is used, the cycle is originally based on the Brayton cycle; if the product gas is used in a gas engine, internal combustion engine, then the cycle is based on the Otto cycle. Figure 1.23 and Figure 1.24 show the P-V and T-S diagram for each cycle.

URN:NBN:no-2340

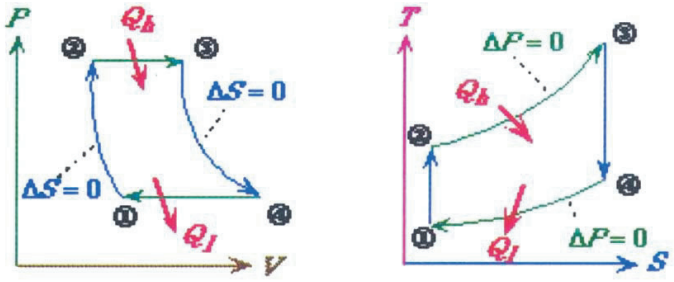

Figure 1.23: P-V and T-S diagram for the Brayton cycle (gas turbine).

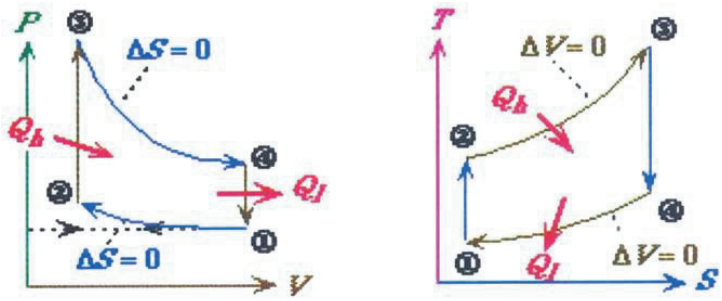

Figure 1.24: P-V and T-S diagram for the Otto cycle (internal combustion engine).

The gas turbine coupled with an air-blown gasifier creates a class of cycles known as Biomass Integrated Gasifier – Gas Turbine (BIG/GT) cycles (Booth and Elliott, 1993). BIG/GT technologies (with fixed bed) can convert a 60% of biomass energy into electricity and steam, being the gas turbine the one contributing the most for the electricity production (Williams and Larson, 1996). In countries where biomass growth has low costs, BIG/GT can compete with coal-fired systems. Such units will be much smaller than conventional central-station power-generating units.

Finally, gas turbines can be used together with steam turbines in Integrated Gasification Combined Cycles (IGCC). Faaij et al. (1997) present a feasibility study of a combined cycle based on a gas turbine, using biomass as a fuel in an atmospheric gasifier with a secondary catalytic reactor and cold gas cleaning. They conclude that Biomass Integrated Gasifier/Combined Cycle (BIGCC) is a feasible process, whose cost is very sensitive to system efficiency but not that much to transport distance. Another problem with Biomass Gasifier Combined Cycle is that it requires certain size (30-50MW_e) to be economical feasible (Wilén and Kurkela, 1997). According to Fredriksson and Kjellström (1996), gas

URN:NBN:no-2340

turbines fired directly with wood power are economically attractive for cogenerating power plants up to 20 MW_e.

1.6.3 GAS TURBINES FOR PRODUCT GAS

A gas turbine can achieve higher thermodynamic efficiency due to the peak cycle temperature of modern gas turbine compared to the steam turbine. Furthermore, gas turbines are being improved every day with new turbine blade materials and cooling technologies, allowing higher inlet temperatures and therefore, increasing efficiency. In addition, the unit capital cost for a gas-turbine system is relatively low and insensitive to scale (Williams and Larson, 1996). Figure 1.25 shows a simplified gas turbine system.

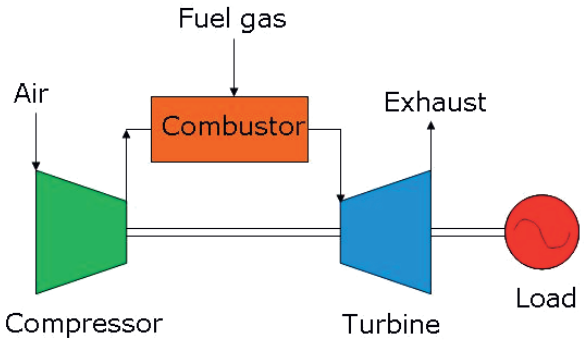

Figure 1.25: Gas turbine power generation system.

1.6.3.1 TYPES OF GAS TURBINE

There are two types of gas turbines: heavy-duty industrial turbines, designed for power generation, and lighter, compact aeroderivative gas turbines. Technological improvements are usually first applied to aeroderivative gas turbines (military interests) and afterwards implemented in the stationary power applications (Williams and Larson, 1996).

Cycles based on the aeroderivative turbines are more adequate to biomass applications, due to their higher efficiency and lower unit cost at modest scale (<100 MW_e), lower maintenance cost due to modular nature and relative small weight (Williams and Larson, 1996). Furthermore, the outlet temperature in an aeroderivative turbine is still high and therefore recommended for combined cycles (Van Ree et al., 1997).

This type of turbine is commonly used with "classic" fuels for power generation up to 50 MW (Camporeale and Fortunato, 1996). For biomass applications, Consonni and Larson (1994) propose a 25-30 MW power output range, and for advanced combined cycles including intercooling 22-75 MW.

URN:NBN:no-2340

Industrial turbines (also known as heavy-duty turbines) can nevertheless easily tolerate larger deviations from their design operation point due to their more robust construction and can also tolerate larger mechanical and thermal stresses, larger particle content, and more corrosive combustion gases (Consonni and Larson, 1994). Finally, industrial turbines are usually designed for optimal performance in combined cycle, i.e. the exhaust gases are still hot enough to raise steam to the required conditions for the steam cycle (Williams and Larson, 1996).

The aeroderivative turbine GE LM2500 is used in many demonstration plants (Figure 1.26). According to Palmer et al. (1993), this turbine is well suited for biomass gasification projects because of its size and its flexible operation, since it is designed for steam injection.

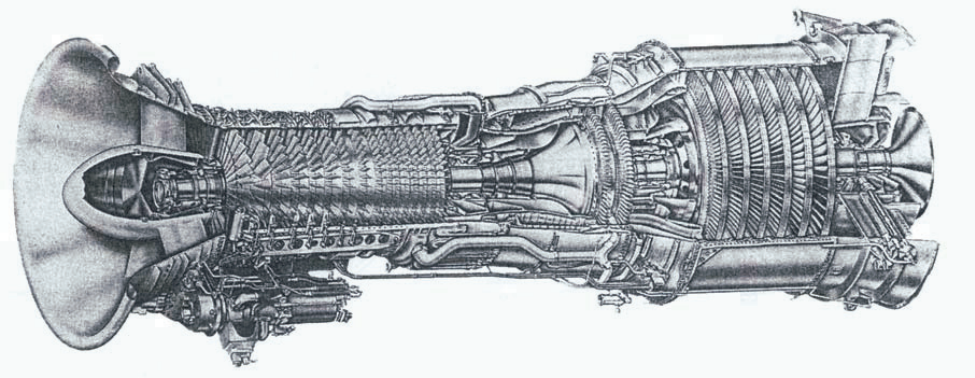

Figure 1.26: LM2500PH gas turbine (Neilson, 1999).

1.6.3.2 GAS TURBINE DEVELOPMENT

Gas turbine technology has already been developed for natural gas and clean liquid fuel applications. A considerable effort has also been directed to the coupling of coal gasification with gas turbines since through gasification the environmental impact of coal burning diminishes considerably and because of the thermodynamic advantages of the gas turbine (Williams and Larson, 1996). A considerable part of the research effort made with coal gasification can be directly applied to biomass gasification like high-temperature gas cleanup, including particulates and alkali removal and gas upgrading (Babu and Whaley, 1992).

The most relevant aspects to evaluate the suitability of certain fuel for a gas turbine are:

- Mass flow limits through the turbine.
- Pressure loss through the fuel injection system.
- Combustion stability.

URN:NBN:no-2340

1.6.3.3 MASS FLOW LIMIT THROUGH THE TURBINE

Gas turbines are usually prepared to work with high calorific value fuels like light and heavy distillate liquid fuels and mainly natural gas. The calorific value of natural gas is about 35 MJ/Nm^3, while this value for a typical biomass-derived fuel is about 4-6 MJ/Nm^3 for directly heated gasification and about 10 MJ/Nm^3 for indirectly heated, according to Consonni and Larson (1994). A direct consequence of this difference in energy density is the need for a 5 to 10 times higher fuel gas flow, compared to natural gas, in order to maintain the same firing temperature. This ratio could even be 20, as pointed out by Hoppesteyn et al. (1997) if a high temperature cleaning system between the gasifier and the gas turbine is to be considered.

One possible solution to accommodate this flow is to decrease the temperature in order to increase fuel density but this will reduce efficiency (Consonni and Larson, 1994). Another possibility is to increase the turbine inlet pressure[8]. This solution increases the pressure in the combustor and the pressure ratio of the compressor. This could lead the compressor to its surge limit resulting in strong vibrations for the same inlet conditions and rotational speed (Hoppesteyn et al., 1997). There are two possible modifications to avoid the compressor reaching its surge limit:

- Modification of the geometry of the high-pressure turbine: increase blade height of nozzle discharge angle.
- Decrease the compressor airflow by adjusting the inlet guide vanes (Consonni and Larson, 1994).

For pressurized systems, the compressor can also supply pressurized air for the gasification process. The mass flow supplied for gasification is almost equal to the fuel flow so both compressor and turbine will process nearly similar mass flows, resulting on a moderate increase in the pressure ratio and therefore, small concern about the compressor limitations (Consonni and Larson, 1994). However, Bridgwater (1995) suggests that this option will require extensive modifications in the compressor and impose problems on the system and therefore the pressurized system will rather require a separate additional compressor.

In the case of indirectly heated gasification, where a medium heating value syngas is produced, the problems associated to large syngas volume flow are less critical and the amount of steam injection allowed might increase.

[8] This is because essentially all turbines operate under choked flow conditions at the expander inlet (Consonni and Larson, 1994).

URN:NBN:no-2340

1.6.3.4 PRESSURE LOSS THROUGH THE FUEL INJECTION SYSTEM

As already mentioned, another important aspect of the gas turbine operation is the pressure loss through the fuel injection. The nozzle is originally designed for a fuel with much higher energy density and with lower temperatures at the combustor inlet; in some cases, the same nozzle can be used but in others, small modifications are required. Consonni and Larson (1994) expect than in the near future, gas turbines could be especially designed for low BTU applications, and then the combustor and the nozzle will be re-designed.

1.6.3.5 COMBUSTION STABILITY

Regarding combustion stability, the type of combustor used in the industrial turbines (can type) provides enough cross-section and volume for complete and stable combustion, as several installations prove it, with a reasonable pressure loss (Consonni and Larson, 1994).

However, the combustor in the aeroderivative turbines is more compact and there is not comparable experience with this type of turbines. There is certain disagreement among researchers about the suitability of the commercial combustor. In the opinion of Consonni and Larson (1994), the experimental work up to 1994 (GE LM500 and LM 2500) suggests that the combustion stability would not be a problem as far as the fuel gas contains some hydrogen. On the other hand, Hoppesteyn et al. (1997) and Craig et al. (1994) assume that the combustor will have to be modified in order to cope with such high gas velocities.

1.6.3.6 GAS TURBINE REQUIREMENTS

Although gas turbines have relatively flexible operating conditions, especially the aeroderivative type, there are certain limits due to compressor surging, overspeed and shaft torque limits (Palmer et al., 1993).

There are still many problems to solve regarding the use of gas turbines for product gas. Among them, the possible erosion caused by particles in the gas and deposition of alkali metals (Na, K, Li) that could also produce severe corrosion in the turbine blades (Hoppesteyn et al., 1997). The levels of particles, alkali metals and condensable tars tolerated by a gas turbine are not very well established due to lack of experience. The limits given by the manufacturers are probably conservative (Consonni and Larson, 1994). For instance, they mention, the level of particles allowed in the GE specifications for the gas turbine will imply a particle concentration in the unburned product gas of 3-5 ppm_w. Particle concentrations in the raw gas from a fluidized bed are about

URN:NBN:no-2340

5000 ppm_w to 10000 ppm_w. This large difference shows the key importance of an efficient gas cleaning system: ceramic filters and/or wet scrubbers.

1.6.3.7 ALKALI METALS

Table 1.11 presents the maximum allowable concentrations of contaminants in the flue gas stream to the LM 2500 turbine, after combustion. The maximum allowable concentration of the same components in the product gas is 5 times the former, being this the usual practice for natural gas calculations.

	Maximum concentration allowed in the gas flow to the turbine. GE specifications for the LM2500 (Consonni and Larson, 1994)		Notional gas turbine fuel specifications (Bridgwater, 1995)		Maximum concentration allowed in the gas at the gasifier exit (Neilson, 1998)	
Solids (Ash, char, etc.)	D<10 microns	600 ppbw	D<10 microns	10 ppmw 50mg/Nm^3 Babu (95)	3000 ppbw	
	10<D<13 microns	6 ppbw	10<D<20 microns	1.0 ppmw	30 ppbw	
	D>13 microns	0.6 ppbw	D>20 microns	0.1 ppmw	3 ppbw	
Lead (Pb)	20 ppbw				100 ppbw	
Vanadium (V)	10 ppbw				50 ppbw	
Alkali	Alkali metals (Na, K, Li)	4 ppbw	Alkali concentration	20-1000 ppbw (0,24mg/Nm^3) (Babu, 1995)	Alkali vapours	100-200 ppbw Williams and Larson, 1996
	Alkali sulphates	12 ppbw	Alkali metals + sulfur	0.1 ppmw		
Total metals			1 ppmw			
Chlorides	500 ppbw		0.5 ppmw			
Calcium (Ca)	40 ppbw					
Tars at delivery temp.			All in vapour form or none (8mg/Nm^3) (Babu, 1995)			
S (H_2S + SO_2, etc.)			1 ppmw			
NH_3/N_2			No limit/ No limit			
Max. delivery temp.			450-600 °C			
Min. LHV			4-6 MJ/Nm^3			
Min. H_2 content			10-20 % vol.			

Table 1.11: Maximal concentration of contaminants allowed in gas turbines.

Heavy metals concentration depends on the gasification temperature and type of fuel. They will evaporate partly in the gasifier probably more than under combustion conditions and will condense when cooling. The rest of heavy metals will stay in the gasifier ash and fly ash. The volatile metals (Pb, Cd, Hg) will concentrate in the fly ash since they will mainly evaporate and condense during gas cooling (Van Ree et al., 1997).

In the opinion of Bridgwater (1995), alkali metals together with sulfur are the major problem in turbine operation. At temperatures over 600 °C, the alkali metals are in the vapour phase[9]. So, in order to remove them from the gas, it is necessary to cool the gas in presence of liquid or solid particles so the alkali metals condense. There are two possible approaches: either cooling only to 350-400 °C and filter (hot gas cleaning) or wet scrubbing, which would imply a further cooling of the syngas (Consonni and Larson, 1994). According to Williams and Larson (1996), in a fixed bed gasifier the alkalis appear

[9] According to Fredriksson and Kjellström (1996), quoting Misra et al. (1993), corrosive metals are only in the vapor phase above 850 °C.

URN:NBN:no-2340

to condense on particulate matter even up to 500-600 °C. Fredriksson and Kjellström (1996) propose a process to overcome the alkali deposition problem by using a two-stage combustion procedure. First a cyclone gasifier/separator where the wood powder is gasified either with air or with steam at temperatures between 800 °C and 900 °C. As explained by the same author in a later work (1997), at enough low gasification temperatures the alkali will also condense in the char particles. In the cyclone the solid char and the ash are separated from the synthesis gas and then, as the second step, the gas enters the modified gas turbine combustor.

1.6.3.8 OTHER REQUIREMENTS

As previously mentioned, tars (condensable organic compounds) could also become a serious problem if they condense in the cool surfaces inside the turbine, causing obstructions, clogging, etc.

A further limitation is imposed in the simulation of Faaij et al. (1997) where in order to meet the gas turbine constrains, the ash content of the fuel should be less than 10-20 % (wt, dry) and the moisture content also lower than ~70% (wt, wet).

According to Larson et al. (1989), gas turbines do not have strict requirements concerning gas composition as far as the fuel is within flammability limits and the heating value of the fuel is above 4 MJ/Nm^3.

Another point of attention in power generation systems for biomass derived fuel is the influence of the fuel moisture. In some cases, generally with air blown gasification, the fuel is previously dried consuming thus part of the energy produced (Faaij et al., 1997). In other, as presented by Hulkkonen et al. (1993), the fuel is dried with high-pressure steam not affecting the efficiency of the cycle. Finally, if steam is used as the gasification agent, the moisture content does not affect the composition of the product gas but it influences considerably the chemical efficiency of the process (Fercher et al., 1998).

1.6.4 GAS ENGINES FOR PRODUCT GAS

Internal combustion engines are in general more suitable for small scale applications because of their size and in principle higher resistance to contaminants than gas turbines. Also looking at investment and operation costs, internal combustion engines are currently the best alternative (Svendsgaard, 2000). As explained by Reed and Das (1988), gasoline engines, natural-gas engines and diesel engines can be used with product gas. Diesel engines have to be adapted by reducing the compression ratio, adding a spark-ignition system and replacing the injectors with spark plugs.

URN:NBN:no-2340

According to Ahrenfeldt et al. (2000), most of the stationary gas engines operating today are modified diesel engines. They also refer the following gas engine characteristics:

- High mean effective pressure, high compression ratio and lean operation, leading to a low fuel consumption
- High exhaust gas temperature, suitable for co-generation or combined heat and power applications
- Low emissions of CO and NO_x
- Longer lifetime when using product gas than using liquid fuels because of fewer particles in the combustion system

Due to the differences in flammability, the ignition timing should be adjusted. A detailed study of the influence of the ignition timing has been conducted by Shashikantha and Parikh (1999).

Finally, two more aspects have to be considered when using an internal combustion engine: the gas intake system and the start-up of the engine. The gas intake system usually consists of a gas mixer where the necessary amount of producer gas is allowed into the mixture. An additional fuel, generally natural gas, is also allowed into the gas mixture for start-up purposes.

1.6.5 EMISSIONS

The emissions of NO_x have two sources: thermal NO_x and combustion of ammonia present in the fuel gas. Regarding the former, emissions are very low in state-of-the-art GE gas turbines (15 ppmv), and even lower because of the lower adiabatic flame temperature of LCV gasses.

Another obstacle for the use of synthesis gas from biomass is the relatively high content of NH_3 and HCN; these species will be transformed into NO_x during the combustion process. Ammonia (NH_3) is produced during gasification. It can be partially removed by adding dolomite and it has been proved that only part of the N contained in the biomass is transformed into NH_3. Other portion of N is transformed into N_2 by not too well known processes. The wet scrubber also helps the ammonia removal (Van Ree et al., 1997).

A secondary measure to reduce emissions is the conventional scrubbing system suggested by Rohrer and Paisley (1995) that also retains the metal aerosols.

A good primary measure to avoid NO_x emissions is to premix the fuel gas with the air before entering the combustion chamber. However, with the synthesis gas this is not possible due to its high content of H_2 that could easily provoke pre-ignition or flashback

URN:NBN:no-2340

of the mixture. Nevertheless, the content of H_2 has a positive effect by stabilising the combustion thanks to its high burning velocity. As mentioned by Maughan et al. (1994), hydrogen will result in higher local flame temperatures, increased reaction rates in the recirculation zone and larger OH concentrations and CO burnout rates. Furthermore, hydrogen will lower the lean flammability limit and enlarge the flame length towards the end of the combustor, what will allow longer residence time for the CO combustion.

Compared with natural gas, CO emissions from a turbine fired with LCV gas will be higher due to the lower combustion temperature, as referred by Van Ree et al. (1997), and also due to the higher CO concentration in the fuel gas. Contrary to H_2, the other main component of the synthesis gas, CO, has a low burning velocity and therefore needs a longer residence time for complete combustion. Usually, steam injection can strongly enhance CO emissions due to the cooling flame. However, as mentioned, the presence of H_2 could positively influence the CO combustion (Maughan et al., 1994).

Sulphur could also be a major problem in turbine operation although it only appears in very small concentrations in biomass-derived fuels. This is one of the advantages of biomass gasification compared to coal gasification (Barbucci and Trebbi, 1994). However, even traces of sulphur could damage the turbine and should be removed (Bridgwater, 1995).

1.7 CHALLENGES AND PROSPECTS FOR BIOMASS GASIFICATION

According to Maniatis (2000), it is a challenge to integrate the gasification technologies into existing or recently developed systems in order to demonstrate the attractiveness of the technology.

Another recent study about biomass conversion technologies (European Commission, 1999) presents the following conclusions:

- Biomass gasification is an interesting option because it allows the use of biomass in several sectors of the energy market.
- The quantities of biomass locally available will limit the capacity of future gasification plants.
- It is expected that the power generation by means of integrated gasification combined cycle plants (IGCC) using gas turbine will reach 45% efficiency.
- Combined heat and power applications will be preferred although the capacity will be limited by the local need of low temperature heat. Industrial heat

URN:NBN:no-2340

receivers will be preferred to district heating because of their longer operation time.

- Biomass gasification for the production of liquid fuels (bio-oil) or synthetic natural gas (SNG) is not expected to become competitive in the near future.
- Future development should concentrate on reducing the cost of the gasification plant itself since it is the gasification plant the main cost factor.
- Gasification of biomass waste alone or co-gasification of biomass with waste and coal is encouraged and expected to improve the economics.

URN:NBN:no-2340

1.8 REFERENCES

1. Abatzoglou, N. et al. (2000). The development of a draft protocol for the sampling and analysis of particulate and organic contaminants in the gas from small biomass gasifiers, Biomass and Bioenergy, Vol 18, pp. 5-17.
2. Ahrenfeldt, J., Henriksen, U. & Schramm, J. (2000). Experimental on wood gas engines, The Technical University of Denmark, Department of Energy Engineering, ET-ES 2000-04,
3. Aldén, H., Hagström, P., Hallgren, A. & Waldheim, L. (1997). Investigations in high temperature catalytic gas cleaning for pressurized gasification processes, Developments in Thermochemical Biomass Conversion, Blackie Academic & Professional, 1997, pp. 1131-1143.
4. Antal, M.J. (1982). Biomass pyrolysis: a review of the literature. Part 1 - Carbohydrate pyrolysis, Advances in Solar Energy, Vol. 1, pp. 61-111.
5. Aznar, M.P., Corella, J., Delgado, J. & Lahoz, J. (1993). Improved steam gasification of lignocellulosic residues in a fluidized bed with commercial steam reforming catalysts, Industrial & Engineering Chemistry Research, Vol. 32, pp. 1-10.
6. Babu, S.P. & Whaley, T.P. (1992). IEA biomass thermal gasification project, Biomass and Bioenergy, Vol. 2, No. 1-6, pp. 299-306.
7. Babu, S.P. (1995). Thermal gasification of biomass technology developments: End of task report for 1992 to 1994, Biomass and Bioenergy, Vol. 9, Nos. 1-5, pp. 271-285.
8. Barbucci, P. & Trebbi, G. (1994). Biomass based systems for the generation or cogeneration of electricity, International Journal of Solar Energy, Vol. 15, pp. 171-178.
9. Beck, S.R. Wang, M.J. & Hightower, J.A. (1981). Gasification of oak sawdust, mesquite, corn stover and cotton gin trash in a countercurrent fluidized bed pilot reactor, Biomass as a Nonfossil Fuel Source, ACS Symposium Series 144, pp. 335-349.
10. Bentzen, J.D. & Henriksen, U. (2000). Condensate from a two-stage gasifier, 1st World Conference on Biomass for Energy and Industry, Sevilla, Spain, 5-9 June 2000.
11. Bentzen, J.D., Henriksen, U. & Hansen, C.H. (1999). Investigations of a two-stage gasifier, 2nd Olle Lindström Symposium on Renewable Energy, Royal Institute of Technology, Stockholm, Sweden, June 1999, pp. 117-120.
12. Bilbao, R., García, L., Salvador, M.L. & Arauzo, J. (1998). Steam gasification of biomass in a fluidized bed, effect of a Ni-Al catalyst, Biomass for Energy and Industry. 10th European Conference and Technology Exhibition, 8-11 June 1998, Würzburg, Germany, pp. 1708-1711.
13. Black, N.P. (1991). Biomass gasification project gets funding to solve black liquor safety and landfill problems, Tappi Journal, Vol. 74, No. 2, pp. 65-68.
14. Booth, R. & Elliott, P. (1993). Biomass energy overview, European Seminar BIOWATT, Innovative Technologies for the Production of Electricity from Biomass, October 4-5, Milan, Italy. (Preprints)
15. Brandt, P. & Henriksen, U. (1998). Decomposition of tar in pyrolysis gas by partial oxidation and thermal craking. Part 2, Biomass for Energy and Industry. 10th European Conference and Technology Exhibition, 8-11 June 1998, Würzburg, Germany.
16. Bridgwater, A.V. (1995). The technical and economic feasibility of biomass gasification for power generation, Fuel, Vol. 74, No. 5, pp. 631-653.
17. Caballero, M.A., Aznar, M.P., Gil, J., Martín, J.A. & Corella, J. (1998). Co-shift catalytic beds after a biomass gasifier and a steam-reforming catalytic reactor to get new and interesting exit gas compositions, Biomass for Energy and

URN:NBN:no-2340

Industry. 10th European Conference and Technology Exhibition, 8-11 June 1998, Würzburg, Germany, pp. 1789-1793.
18. Camporeale, S. & Fortunato, B. (1996). Design and off-design performance of advanced mixed gas-steam cycle power plants, Proceedings of the 31st Intersociety Energy Conversion Engineering Conference, 11-16 August 1996, Washington, DC, USA, Vol. 2, pp. 695-701.
19. Cen, K. et al. (1993). Research on rice hulls gasification gas/steam co-generation system using a circulating fluidized bed, ENERGEX '93 - The 5th International Energy Conference, 18-22 October, 1993. Vol. III, pp. 683-692.
20. Chughtai, M.Y. & Kubiak, H. (1998). Hydrogen from biomass, Biomass for Energy and Industry. 10th European Conference and Technology Exhibition, 8-11 June 1998, Würzburg, Germany, pp. 284-286.
21. Consonni, S. & Larson, E.D. (1994). Biomass-gasifier/aeroderivative gas turbine combined cycles: Part A - Technologies and performance modeling, part B - Performance calculations and economic assessment, ASME Cogen Turbo Power '94. IGTI-Vol. 9, pp. 599-623.
22. Craig, J. (1997). Personal communication.
23. Craig, K.R., Bain, R.L. & Overend, R.P. (1995). Biomass power systems - Where are we, where are we going, and how do we get there? The role of gasification, EPRI Conference on New Power Generation Technology, October 25-27, San Francisco, California, USA.
24. Craig, K.R., Mann, M.K. & Bain, R.L. (1994). Cost and performance potential of advanced integrated biomass gasification combined cycle power systems, ASME cogen Turbo Power '94. IGTI-Vol. 9, pp. 641-654.
25. D'Apote, S.L. (1998). IEA biomass energy analysis and projections, Biomass Energy: Data, Analysis and Trends, Conference proceedings, Paris, France, 23-24 March 1998, IEA.
26. De Tourris, O. N. (1997). Personal communication.
27. Di Blasi, C., Signorelli, G. & Portoricco, G. (1999). Countercurrent fixed-bed gasification of biomass at laboratory scale, Industrial & Engineering Chemistry Research, Vol. 38, pp. 2571-2581.
28. Easterly, J.L. & Burnham, M. (1996). Overview of biomass and waste fuel resources for power production, Biomass and Bioenergy, Vol. 10, No. 2-3, pp. 79-92.
29. Espenäs, B.G. (1993). Reactivity of biomass and peat chars formed and gasified at different conditions, Advances in Thermochemical Biomass Conversion, Blackie Academic & Professional, 1993, pp. 142-159.
30. European Commission, (1999). Biomass Conversion Technologies, Achievements and prospects for heat and power generation, Report number 18029 EN,
31. Evans, R.J. & Milne, T.A. (1997). Chemistry of tar formation and maturation in the thermochemical conversion of biomass, Developments in Thermochemical Biomass Conversion, Blackie Academic & Professional, 1997, pp 803-816.
32. Faaij, A. et al. (1997). Gasification of biomass wastes and residues for electricity production, Biomass and Bioenergy, Vol. 12, Nos. 6, pp. 387-407.
33. Farris, S.G. & Weeks, S.T. (1996). Commercial demonstration of biomass gasification, the Vermont project, Bioenergy'96, Partnerships to Develop and Apply Biomass Technologies, 15-20 September, 1996, pp. 44-51.
34. Fercher, E., Hofbauer, H., Fleck, T., Rauch, R. & Veronik, G. (1998). Two years experience with the FICFB-gasification process, Biomass for Energy and Industry. 10th European Conference and Technology Exhibition, 8-11 June 1998, Würzburg, Germany, pp. 280-283.
35. Fredriksson, C. & Kjellström, B. (1996). Cyclone gasification of steam injected wood powder, Nordic Seminar on Thermochemical Conversion of Solid Fuels, 4-6 December 1996, NTH, Trondheim, Norway.
36. Fredriksson, C. & Kjellström, B. (1997). Alkali separator in steam injected cyclone wood powder gasifier for gas turbine application, Developments in

URN:NBN:no-2340

Thermochemical Biomass Conversion, Blackie Academic & Professional, 1997, pp. 921-931.
37. Gebhard, S.C., Wang, D., Overend, R.P. & Paisley, M.A. (1994). Catalytic conditioning of synthesis gas produced by biomass gasification, Biomass and Bioenergy, Vol. 7, Nos. 1-6, pp. 307-313.
38. Gil, J., Aznar, M.P., Caballero, M.A., Francés, E. & Corella, J. (1997). Biomass gasification in fluidized bed at pilot scale with steam-oxygen mixtures. Product distribution for very different operating conditions, Energy and Fuels, Vol. 11, pp. 1109-1118.
39. Grønli, M. (1996). Theoretical and experimental study of the thermal degradation of biomass, Ph. D. Thesis, Norwegian University of Science and Technology.
40. Hallgren, A. (1996). Theoretical and engineering aspects of the gasification of biomass, Ph.D. Thesis, Lund University, Sweden.
41. Herguido, J., Corella, J. & González-Saiz, J. (1992). Steam gasification of lignocellulosic residues in a fluidized bed at a small pilot scale. Effect of the type of feedstock, Industrial & Engineering Chemistry Research, Vol. 31, pp. 1274-1282.
42. Herguido, J., Corella, J., Artal, G. & Garcia-Bordeje, J.E. (1992). Results with a multisolid circulating fluid bed pilot plant for the improved steam gasification of biomass, Biomass for Energy, Industry and the Environment, pp. 792-796.
43. Hofbauer, H. et al. (1997). The FICFB - gasification process, Developments in Thermochemical Biomass Conversion, Blackie Academic & Professional, 1997, pp 1016-1025.
44. Hofbauer, H. (1997). Hydrogen-rich gas from biomass steam gasification, Project description, JOR3CT970196.
45. Holt, N.A. & van der Burgt, M.J. (1998). Biomass conversion: prospects and context, Power Production from Biomass III, Gasification and Pyrolysis R&D&D for Industry, 14-15 September, Espoo, Finland, pp. 163-177.
46. Hoppesteyn, P.D.J., de Jong, W., Andries, J. & Hein, K.R.G. (1997). Combustion of biomass-derived low calorific value gas, Combustion and Emissions Control III, The Institute of Energy, Pergamon, London 1997.
47. Hulkkonen, S., Äijlälä, M. & Holappa, J, (1993). Integration of a fuel dryer to a gas turbine process, ASME Cogen Turbo Power '93. IGTI-Vol. 8, pp. 61-67.
48. Janarthanan, A.K. & Clements, L.D. (1997). Gasification of wood in a pilot scale spouted bed gasifier, Developments in Thermochemical Biomass Conversion, Blackie Academic & Professional, 1997, pp 945-959.
49. Kandaswamy, D.S., Warren, D.W. & Mansour, M.N. (1991). Indirect steam gasification of paper mill sludge waste, Tappi Journal, Vol. 74, No. 10, pp. 137-143.
50. Knudsen, J.N.et al. (2001). Experimental investigation of sulfur release during thermal conversion of wheat straw and its application to full-scale grate firing, Sixth International Conference on Technologies and Combustion for a Clean Environment, 9-12 July, 2001, Oporto (Portugal), Vol. 3, pp. 1303-1309.
51. Kubiak, H. & Mühlen, H.J. (1998). Gas and electricity production from waste material and biomass via allothermal gasification, Biomass for Energy and Industry.10th European Conference and Technology Exhibition, 8-11 June 1998, Würzburg, Germany, pp. 1693-1695.
52. Lammers, G., Beenackers, A.A.C.M. & Corella, J. (1997). Catalytic tar removal from biomass producer gas with secondary air, Developments in Thermochemical Biomass Conversion, Blackie Academic & Professional, 1997, pp. 1179-1193.
53. Larson, E.D., Svenningsson, P. & Bjerle, I. (1989). Biomass gasification for gas turbine power generation, Johansson, T.B. et al. editors, Electricity, 1989, pp. 697-739.
54. Larson, E.D. & Williams, R.H. (1988). Biomass-fired steam-injected gas turbine cogeneration, ASME Cogen-Turbo II Proceedings, pp. 57-66.

URN:NBN:no-2340

55. Maniatis, K. (2000). Progress in biomass gasification: an overview, Progress in Thermochemical Biomass Conversion, Tyrol, Austria, 17-22 September 2000, Vol. 1, pp. 1-31.
56. Maughan, J.R., Bowen, J.H., Cooke, D.H. & Tuzson, J.J. (1994). Reducing gas turbine emissions through hydrogen-enhanced, steam-injected combustion, ASME Cogen Turbo Power '94. IGTI-Vol. 9, pp. 381-390.
57. Milne, T.A., Abatzoglou, N. & Evans, R.J. (1998). Biomass gasifier "Tars": Their nature, formation, and conversion. NREL/TP-570-25357, ISBN 1-890607-15-6.
58. Minowa, T., Ogi, T. & Yokoyama, S. (1997). Hydrogen production from lignocellulosic materials by steam gasification using a reduced nickel catalyst, Developments in Thermochemical Biomass Conversion, Blackie Academic & Professional, 1997, pp 932-941.
59. Moilanen, A. & Saviharju, K. (1997). Gasification reactivities of biomass fuels in pressurised conditions and product gas mixtures, Developments in Thermochemical Biomass Conversion, Blackie Academic & Professional, 1997, pp 828-837.
60. Neeft, J.P.A. et al. (2000). Guideline for sampling and analysis of "tars" and particles in biomass producer gases, Progress in Thermochemical Biomass Conversion, Tyrol, Austria, 17-22 September 2000.
61. Neilson, C.E. (1998). LM2500 gas turbine modifications for biomass fuel operation, Biomass and Bioenergy, Vol. 15, No. 3, pp. 269-273.
62. Nordin, A., Kallner, P. & Johansson, E. (1997). Gas quality from biomass gasification; an extensive parametric equilibrium study, Developments in Thermochemical Biomass Conversion, Blackie Academic & Professional, 1997, pp. 838-850.
63. Olivares, A., Aznar, M.P., Caballero, M.A., Gil, J., Francés, E. & Corella, J. (1997). Biomass gasification: Produced gas upgrading by in-bed use of dolomite, Industrial & Engineering Chemistry Research, Vol. 36, pp. 5220-5226.
64. Paisley, M.A., Litt, R.D., Overend, R.P. & Bain, R.L. (1994). Gas turbine power generation from biomass gasification, ASME Cogen Turbo Power '94. IGTI-Vol. 9, pp. 625-629.
65. Paisley, M.A. (1997). Catalytic hot gas conditioning of biomass derived product gas, Developments in Thermochemical Biomass Conversion, Blackie Academic & Professional, 1997, pp. 1209-1223.
66. Palmer, C.A., Erbes, M.R. & Pechtl, P.A. (1993). Gatecycle performance analysis of the LM2500 gas turbine utilizing low heating value fuels, ASME Cogen Turbo Power '93. IGTI-Vol. 8, pp. 69-76.
67. Platiau, D. & Faniel, Y. (1989). The AVSA biomass gasification process, Energy from Biomass 4. Proceedings of the 3rd contractors'meeting, Paestum, 25-27 May 1988, pp. 563-579.
68. Rapagnà, S. & Foscolo, P.U. (1996). Gasification of biomass in a fluidised bed reactor: The influence of temperature and biomass particle size, Biomass for Energy and the Environment. Proceedings of the 9th European Bioenergy Conference, June 1996, Copenhagen, Denmark.
69. Rapagnà, S., Jand, N. & Foscolo, P.U. (1998). Utilisation of suitable catalysts for the gasification of biomasses, Biomass for Energy and Industry. 10th European Conference and Technology Exhibition, 8-11 June 1998, Würzburg, Germany, pp. 1720-1723.
70. Rapagnà, S. & Latif, A. (1997). Steam gasification of almond shells in a fluidised bed reactor: The influence of temperature and particle size on product yield and distribution, Biomass and Bioenergy, Vol. 12, No. 4, pp. 281-288.
71. Rapagnà, S., Jand, N. & Foscolo, P.U. (1998). Catalytic gasification of biomass to produce hydrogen rich gas, International Journal of Hydrogen Energy, Vol. 23, No. 7, pp. 551-557.
72. Reed, T.B.& Das, A. (1988). Handbook of biomass downdraft gasifier engine systems, The Biomass Energy Foundation Press, 1810 Smith Rd., Golden, CO. 80401.

URN:NBN:no-2340

73. Rohrer, J.W. & Paisley, M. (1995). Commercial demonstration of atmospheric medium btu fuel gas production from biomass without oxygen - The Burlington, Vermont project, Power-Gen '95. Book IV, pp. 171-186.
74. Roos, A. et al.(1999). Critical factors to bioenergy implementation, Biomass and Bioenergy, Vol. 17, pp. 113-126.
75. Roubanis, N. (1998). Energy from biomass: The EU experience, Biomass Energy: Data, Analysis and Trends, Conference proceedings, Paris, France, 23-24 March 1998, IEA.
76. Shashikantha & Parikh, P.P. (1999). Spark ignition producer gas engine and dedicated compressed natural gas engine - Technology development and experimental performance optimisation, SAE Technical Paper Series, 1999-01-3515,
77. Ståhlberg, P. et al. (1998). Sampling of contaminants from product gases of biomass gasifiers, VTT Research notes 1903, Technical Research Centre of Finland.
78. Svendsgaard, O.B. (2000). Gas engine for a biomass powered small scale heat- and power plant, Diploma report, Institute of Thermal Energy and HydroPower, Norwegian University of Science and Technology (NTNU), Norway.
79. Vaa Beyer, R. & Skreiberg, Ø. (2000). Biomasse ressurser i Norge, Bionett, Norsk Bioenergi Nettverk, 1998-2000, Sluttrapport, Temablader.
80. Van Ree, R. et al. (1997). Chapter III: Gasification of biomass wastes and residues for electricity production, accepted for publication in "Biomass and Bioenergy".
81. Walsh, M.E. et al. (1999). Biomass feedstock availability in the United States: 1999 state level analysis, Bioenergy Information Network, http://bioenergy.ornl.gov/resourcedata
82. Wang, Y. & Kinoshita, C.M. (1992). Experimental analysis of biomass gasification with steam and oxygen, Solar Energy, Vol. 49, No. 3, pp. 153-158.
83. Wang, Y. & Kinoshita, C.M. (1993). Kinetic model of biomass gasification, Solar Energy, Vol. 51, No. 1, pp. 19-25.
84. Warnecke, R. (2000). Gasification of biomass: comparison of fixed bed and fluidized bed gasifier, Biomass and Bioenergy, Vol. 18, pp. 489-497.
85. Wilén, C. & Kurkela, E. (1997). Gasification of biomass for energy production. State of technology in Finland and global market perspectives, Technical Research Centre of Finland, VTT Tiedotteita - Meddelanden - Research Notes 1842.
86. Williams, R.H. & Larson, E.D. (1996). Biomass gasifier gas turbine power generating technology, Biomass and Bioenergy, Vol. 10, No. 2-3, pp. 149-166.

URN:NBN:no-2340

URN:NBN:no-2340

2. THE SMALL-SCALE DOWNDRAFT GASIFIER

2.1 INTRODUCTION AND BACKGROUND

The design and construction of the stratified downdraft gasifier started in 1998. It was in operation for the first time in August 1999. Both the construction and the operation of the reactor have required a large contribution from the workshop personal, the effort of several Ph. D. students and the valuable help of many undergraduate students. The objectives of building the gasifier were:

- To build and operate a small-scale combined heat and power (CHP) plant, based on renewable energy, using low calorific gas (LCV gas) as fuel,
- to study the gasification process, filtration techniques and heat and power generation from renewable energy sources in detail but from an experimental point of view, and
- to test the innovative and promising design of stratified downdraft gasifier.

The small-scale CHP plant is shown in a simple diagram in Figure 2.1. It consists of:

- a gasification reactor where the oxidant (air, initially) reacts with the solid fuel (pellets, initially) and produces the fuel gas,
- a gas upgrading system, where the gas is dried, cleaned, i.e. prepared for its further use
- a gas engine where the gas is burnt, producing mechanical energy
- and a water brake where the mechanical energy is measured and absorbed. This water brake substitutes the electrical generator that is not of interest in this laboratory application.

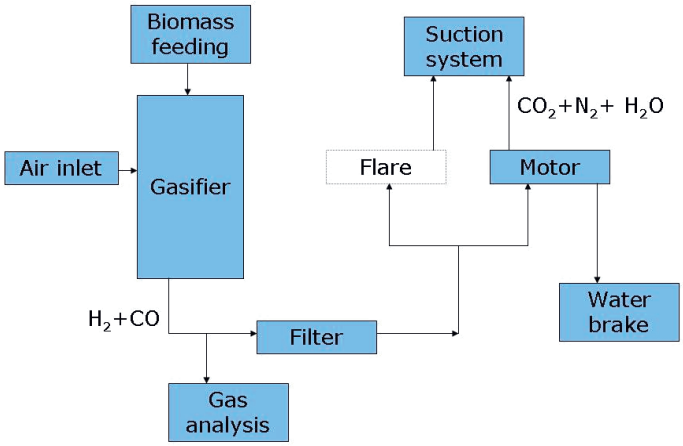

Figure 2.1: Scheme of the combined heat and power demonstration plant.

URN:NBN:no-2340

The gasification reactor is a stratified downdraft gasifier, also known as throatless gasifier or as open core gasifier and works at a pressure slightly higher than atmospheric (1 bar). Figure 2.2 shows the reactor; a thorough description of the gasifier is given in Paper I.

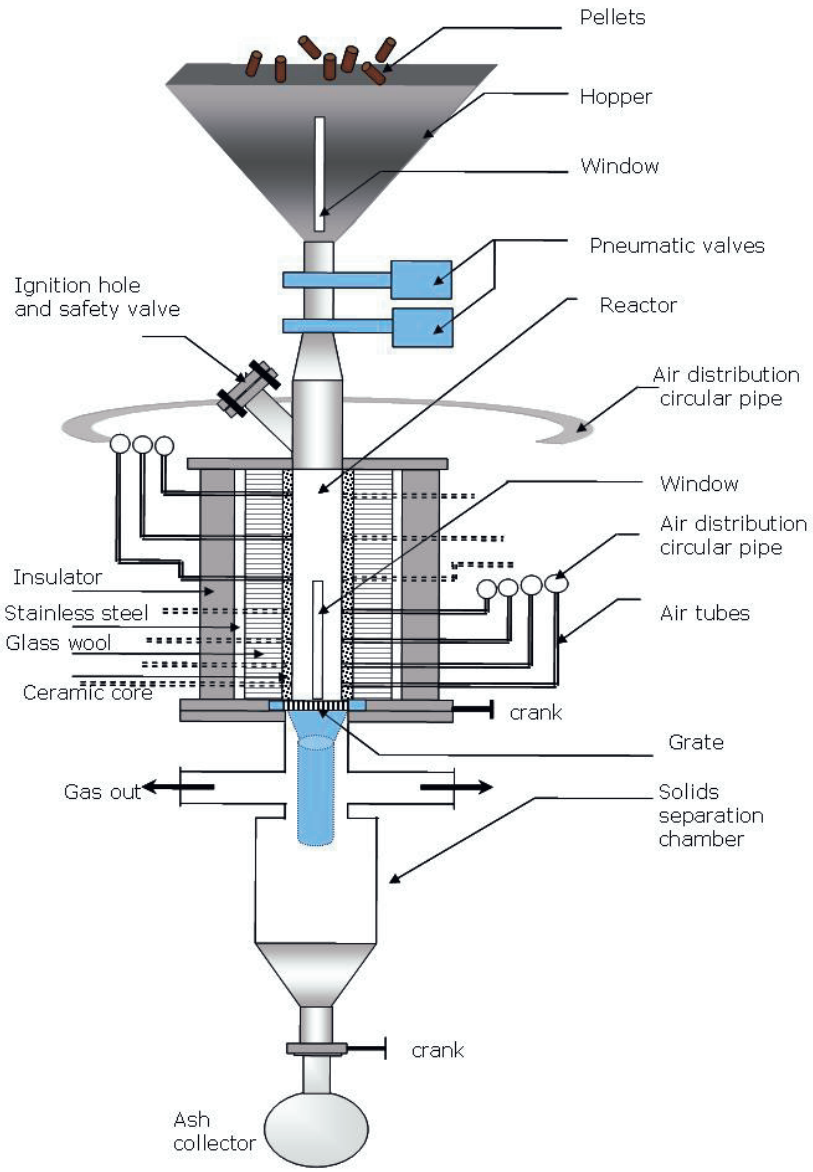

Figure 2.2: The stratified downdraft gasifier at the Norwegian University of Science and Technology.

The first stratified downdraft gasifier was probably built by T. Reed (Reed and Das, 1988). The work and experiences of T. Reed have been a solid and useful reference to the design, construction and operation of the gasifier. The gasifier

URN:NBN:no-2340

built in our laboratory has, nevertheless, several features that make it different form other similar gasifiers. The next points describe some of these features.

2.2 GASIFICATION AGENT

Air can be supplied at several heights of the cylindrical reactor. A total of seven air supply channels are operative and independent. This means that the air through each air channel is measured and controlled. Such air distribution system allows, for instance, some extra-air addition in the char reduction zone, what could contribute to increase the temperature in this zone and therefore increase the conversion rate.

In the initial design air has been selected as the oxidant agent. It is the easiest to use and is very economical, but it is not the only one possible. There is a pressurized air network (6 bar) in the laboratory and it was only necessary to connect the air supply system to the network and install a pressure reduction valve before the manifold.

Nevertheless, being each air supply channel independent, it is possible to substitute air by steam or product gas or another gas of interest and study its influence on the process. Adding steam, for instance, could increase the hydrogen content of the product gas. In addition, the presence of steam could promote tar cracking reactions. However, steam gasification is a very endothermic process and therefore air should be also added for combustion and heat production. Tar cracking reactions also require heat.

2.3 BIOMASS FEEDING SYSTEM

The feeding system has been specially designed for pellets. The most appreciated characteristics of pellets are their well defined shape, their mechanical strength and improved heating value in comparison to loose materials. Pellets are homogeneous regarding composition and form a bed with homogeneous void fraction or heat transfer properties. Given the small size of the reactor, any other fuel but pellets would create large irregularities in the fuel bed, complicating the reactor operation.

The feeding system for other fuels is commonly based on screw feeders, but such device destroys the pellets producing a thin powder. To avoid pellet's destruction, the feeding system consists of two sliding valves that open in a defined sequence.

URN:NBN:no-2340

A system formed by the two sliding valves, as ours, guarantees that the biomass inlet is sealed and allows for semi-continuous feeding. It would not be correct to say continuous feeding because small batches of pellets (ca. 340 g) are sent to the bed every time the lower sliding valve opens. As presented in Paper I, if the pyrolysis zone is located at the top of the bed, the semi-continuous feeding creates an important disturbance. But if the pyrolysis zone is covered with pellets, as it is the case in Paper II, the semi-continuous feeding does not interfere with the stable operation of the reactor.

Although limited to pellets or other uniform fuel form, there are possibilities of fuel variation. Suitable fuels are for instance wood pellets, lignite pellets, pellets of waste or mixture of them.

2.4 REACTOR SIZE AND DESIGN

The gasifier has a capacity of 4 to 6 kg/h of wood pellets, equivalent to about 30 kW of thermal input. This is a very small size, only suitable for laboratory research. One of the advantages of having a reactor with 100 mm internal diameter though, is that the radial air supply is in principle capable of creating an uniform high temperature zone. As the reactor diameter increases, the probability for low temperature zones also increases. It is because of this that the scale-up capability of downdraft gasifiers is limited.

The ash collecting system consists of a glass bottle attached to the bottom of the reactor. At the time of the design, it was thought to be large enough in relation to the size of the reactor. However, experience with the operation of the reactor has proven the ash collecting system not to be sufficient for long experiments. Even for small scale systems, the ash collecting system should be preferably a continuous removal system or have a larger capacity.

Finally, in a plant of such reduced size, the thermal losses are usually quite relevant compared to the energy output. The air inlet system is insulated so the heat provided by the pre-heater is not lost. The reactor is also insulated.
A modular design has proven to be very useful in this case. It allowed close evaluation of the reactor core after an experiment and also easy access and replacement of the grid when necessary.

URN:NBN:no-2340

2.5 OPERATION PRESSURE

Working at a pressure that is slightly above atmospheric is a consequence of measuring the amount of air supplied to the gasifier. Quantifying the amount of air and biomass supplied to the reactor and also the product gas composition makes possible to calculate the amount of gas produced without measuring it. This last measurement is quite demanding because of the product gas high temperature and particle and tar content that could damage any volumetric flowmeter. However, working above atmospheric pressure can be dangerous because of the increased risk of leakage. A suitable grid design is absolutely necessary to avoid overpressure inside the reactor.

It is also important to notice that the pressure in the reactor depends on the flow resistance downstream. If there is, for example, no pump after the gasifier but only a condenser and a filter a blockage in the filter would increase the pressure in the gasifier. On the other hand, the suction effect of the motor might decrease favourably the gasifier pressure.

2.6 THE CHP PLANT

As mentioned previously, the gasifier is the first element in the CHP plant. The other important element is the engine. It was originally a Diesel motor, modified for its use with natural gas and LCV gas. A more exhaustive description of the engine and the modifications can be found in Paper I and Paper III.

An interesting feature of this CHP plant is that the fuel inlet of the engine is connected in such a way that the engine can run on product gas from the gasifier, on natural gas from a gas bottle battery or on a gas mixture of gasses from bottles selected by the user. This feature has shown to be extremely useful. From an operation point of view, it is more comfortable to start the engine with natural gas until it reaches its operational temperature and then switch to product gas or the desired mixture. It has also allowed the study of mixtures of natural gas and LCV gasses regarding engine behaviour and emissions (Paper III).

It is important to mention that the size of the gas engine, 34 kW, does not match the size of the gasifier and therefore the gas engine only operates at partial load when connected to the gasifier. It is possible, though, to run the engine with mixtures of LCV gas and natural gas, as explained in Paper III, reaching then its nominal capacity.

URN:NBN:no-2340

2.7 WORK PROGRESS

Table 2.1 shows the work progression both for the gasifier and the motor as they were initially developed in parallel and later together, once the upgrading system was constructed.

Date	Achievement
March 1999	Assembly of the reactor core
August 1999	First experiment with the gasifier
August 2000	Stable operation of the gasifier
August 2000	Stable operation of the modified Diesel motor with methane
October 2000	First high temperature filtration experiment
January 2001	Stable operation of the motor with synthesis gas from bottles
January 2001	First tar analysis of the product gas
April 2001	**The motor operates with product gas from the gasifier**

Table 2.1: Work progress at the demonstration CHP plant.

Appendix A contains pictures from the different stages of construction.

2.8 FILTRATION AND OTHER UPGRADING PROCESSES

Two strategies have been developed regarding gas upgrading:

a) Condenser and filter. The system is able to cool down all the gas produced by the gasifier in order to condense moisture and tar and then filtrate it in a fixed bed of charcoal. Figure 2.3 shows a diagram of the installation, the condenser and the filter. The objective of this system is to obtain a clean and cold product gas, using an inexpensive filtration system, for gas engine operation. Although cooling the product gas in the condenser represents a considerable heat loss it is an advantage regarding engine operation. Since the calorific value of the product gas is about ten times lower than natural gas, it is recommendable to increase its density as much as possible in order to compensate for the low energy volumetric content.

URN:NBN:no-2340

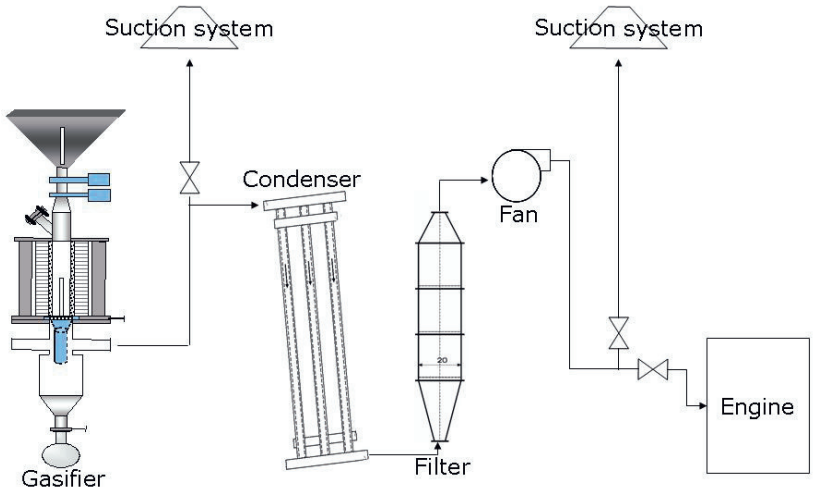

Figure 2.3: Diagram of the installation with condenser and filter.

b) High temperature vertical bed filter. The objective of this system is to retain tar and particles in a sand bed maintaining the gas at high temperature. This upgrading system is far more advanced and complex than the previous one, as it can be observed in Figure 2.4. A detailed description and the results obtained have been recently presented by Risnes (2001).

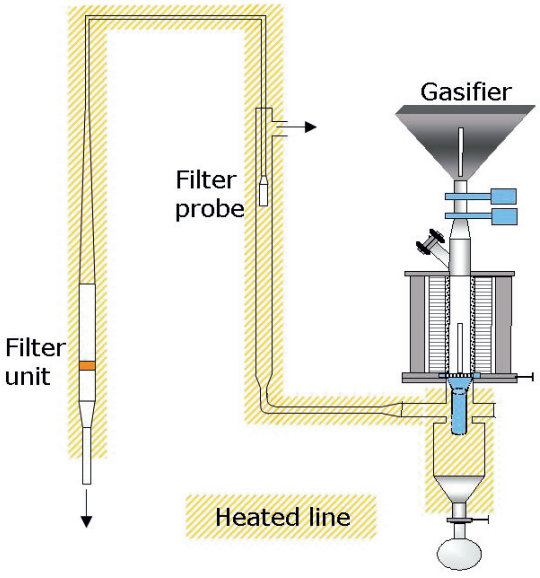

Figure 2.4: High temperature vertical bed filter.

URN:NBN:no-2340

2.9 SAFETY CONSIDERATIONS

The operation of the plant involves certain risk because of the following circumstances:

- High temperatures (max.1000 °C),
- Extremely toxic and moderately flammable gases (CO, H_2),
- Carcinogenic compounds (tar),
- Gasses under pressure (N_2, air).

Several safety measures have been taken to reduce both the risk for accidents and its consequences:

- The gasifier is located inside a 3x3 m room in the basement of the laboratory. The production of toxic gases is confined to the room and the gases are suctioned by a powerful exhaust system.
- Two CO detectors have been used. One of them was left inside the gasifier room and the other was carried by any person entering the room.
- It has been always a priority to have control over the system from outside the room. The biomass feeding system control, the air supply control, the N_2 purge gas and all the data acquisition equipment and control is outside the gasifier room. It is only compulsory to enter the room to:
    - Light the reactor
    - Shake the grid
    - Open the gas analysis line
    - Take a gas sample
- Usage of a gas mask when entering the room if the CO concentration was above 10 ppm.
- There are written protocols for every gasifier operation: start and stop procedure, use of gas mask, use of GC, use of CO detector and emergency stop (see Appendix B). Following procedures also guarantees that the gasifier operation is always started the same way, eliminating – as far as experimental work allows - possible influences on the results.

URN:NBN:no-2340

2.10 GASIFIER CALCULATIONS

This section presents some relevant calculations regarding the operation of the gasifier like mass and energy balances and the evaluation of stable operation. Other calculations of minor relevance (Pellets density and bulk density, biomass feeding rate and calculation error, air excess ratio and air feeding rate) are included in Appendix C. Some information about gas chromatography is also included in this section.

2.10.1 MASS AND ENERGY BALANCES

Table 2.2 to Table 2.6 present the mass and energy balances of the gasifier operation for each experiment. The amount of water at the outlet of the reactor has not been measured. Instead, it has been calculated from the atomic balance of Oxygen. The calculated percentage of water in the outlet products varies between 9 and 14%.

Exp. Number	#8a	#8b	#9	#12	#13a	#13b	#13c	#14
DATA								
Wet Biomass feeding rate (kg/h)*	6,5	6,9	5,8	5,7	4,7	7,5	6,6	6,0
Dry biomass feeding rate (kg/h)	6,0	6,4	5,4	5,2	4,3	6,9	6,0	5,5
Water feeding in the biomass (kg/h) [1]	0,5	0,5	0,4	0,4	0,3	0,6	0,5	0,4
Air feeding rate (Nm3/h)*	7,0	8,2	7,6	7,4	6,0	8,8	7,4	7,6
Air feeding rate (kg/h)	9,0	10,6	9,9	9,6	7,8	11,4	9,6	9,8
Ash rejected (kg/h)*	0,02	0,02	0,06	0,06	0,10	0,10	0,10	n.a.
Product gas rate (Nm3/h) [2]	11,7	14,0	12,8	12,4	9,9	14,7	12,4	12,6
Product gas density (kg/Nm3) [3]	1,15	1,14	1,14	1,15	1,16	1,13	1,15	1,15
Product gas rate (kg/h)	13,4	15,9	14,6	14,3	11,5	16,6	14,2	14,5
GAS COMPOSITION [4]								
N2(%vol)	47,9	46,8	47,3	47,5	48,7	46,3	47,5	47,4
CO(%vol)	24,7	25,8	25,3	25,2	23,9	26,4	25,2	25,3
CO2(%vol)	9,7	9,1	9,3	9,4	10,1	8,8	9,4	9,4
H2(%vol)	16,1	16,8	16,5	16,4	15,6	17,2	16,4	16,4
CH4(%vol)	1,6	1,5	1,5	1,5	1,7	1,4	1,5	1,5
LHV(MJ/Nm3)	5,4	5,6	5,5	5,5	5,3	5,7	5,5	5,5
LHV(MJ/kg)	4,7	4,9	4,8	4,8	4,6	5,0	4,8	4,8
Tar content (g/Nm3)*	3	3	3	3	3	3	3	3
Tar content (kg/h)	0,03	0,04	0,04	0,04	0,03	0,04	0,04	0,04
Particulate (g/Nm3)*	10,5	10,5	10,5	10,5	10,5	10,5	10,5	10,5
Particulate mass rate (kg/h)	0,12	0,15	0,13	0,13	0,10	0,15	0,13	0,13

* Experimental data.
1 Measured pellets moisture of 7,5%.
2 Calculated from the air feeding rate and the N2 content of the product gas.
3 Calculated from gas composition and each component density.
4 Linear regression based on experimental data (See Figure 4, Paper II).

Table 2.2: Mass balance of the gasifier operation (part I)

URN:NBN:no-2340

The energy balance shows cold gas efficiencies between 52 and 64%. The heat losses of the reactor have been estimated assuming that the product gas and the steam produced in the process leave the reactor at 750 °C. The heat losses account for 20 to 30% of the thermal input. Although high, these heat losses are not unexpected, given the small size of the reactor.

Exp. Number	#8a	#8b	#9	#12	#13a	#13b	#13c	#14
CALCULATION								
Mol C in in dry biomass (kmol/h)	2,52E-01	2,69E-01	2,28E-01	2,21E-01	1,83E-01	2,92E-01	2,56E-01	2,33E-01
Mol H in in dry biomass	4,12E-01	4,39E-01	3,73E-01	3,61E-01	3,00E-01	4,78E-01	4,18E-01	3,81E-01
Mol O in in dry biomass	1,58E-01	1,69E-01	1,43E-01	1,39E-01	1,15E-01	1,83E-01	1,61E-01	1,46E-01
Mol H in in water (moisture)	5,38E-02	5,73E-02	4,86E-02	4,72E-02	3,91E-02	6,24E-02	5,46E-02	4,97E-02
Mol O in in water (moisture)	2,69E-02	2,86E-02	2,43E-02	2,36E-02	1,96E-02	3,12E-02	2,73E-02	2,49E-02
Mol O in in air	1,31E-01	1,54E-01	1,44E-01	1,40E-01	1,14E-01	1,66E-01	1,40E-01	1,42E-01
Mol N in in air	4,94E-01	5,79E-01	5,41E-01	5,27E-01	4,28E-01	6,26E-01	5,28E-01	5,36E-01
Mol N out in N2	4,98E-01	5,85E-01	5,39E-01	5,27E-01	4,33E-01	6,06E-01	5,26E-01	5,34E-01
Mol C out in CO+CO2+CH4	1,87E-01	2,27E-01	2,06E-01	2,01E-01	1,59E-01	2,39E-01	2,00E-01	2,04E-01
Mol O out in CO and CO2	2,29E-01	2,75E-01	2,51E-01	2,44E-01	1,96E-01	2,88E-01	2,44E-01	2,48E-01
Mol H out in H2 and Ch4	2,01E-01	2,46E-01	2,22E-01	2,16E-01	1,68E-01	2,61E-01	2,16E-01	2,20E-01
Mol C in - mol C out	6,50E-02	4,16E-02	2,18E-02	2,07E-02	2,48E-02	5,30E-02	5,56E-02	2,93E-02
Mol O in -mol O out	8,72E-02	7,65E-02	6,04E-02	5,81E-02	5,22E-02	9,33E-02	8,41E-02	6,52E-02
Mol N in - mol N out	-4,41E-03	-5,74E-03	1,90E-03	-7,10E-05	-4,82E-03	2,01E-02	1,63E-03	1,10E-03
Mol H in - mol H out	2,65E-01	2,50E-01	1,99E-01	1,93E-01	1,70E-01	2,79E-01	2,57E-01	2,11E-01
Calculated water amount								
mol O in water (kmol/h) [5]	8,72E-02	7,65E-02	6,04E-02	5,81E-02	5,22E-02	9,33E-02	8,41E-02	6,52E-02
mol H in water out (from mol O in water)	1,74E-01	1,53E-01	1,21E-01	1,16E-01	1,04E-01	1,87E-01	1,68E-01	1,30E-01
water out (kg/h)	1,57	1,38	1,09	1,05	0,94	1,68	1,51	1,17
mass in - mass out (incl tar and particles)	0,30	-0,08	-0,21	-0,24	-0,22	0,32	0,17	-0,07
output mass/input mass (%)	**98%**	**100%**	**101%**	**102%**	**102%**	**98%**	**99%**	**100%**
Steam density	0,803571	kg/Nm3						
Water content (Nm3/h)	1,95	1,71	1,35	1,30	1,17	2,09	1,88	1,46
Water percentage in outlet products(%)	14 %	11 %	9 %	9 %	10 %	12 %	13 %	10 %
5 The mass balance is closed by assuming that all mol O out are in water. Excess mol of H could be out as tar.								

Table 2.3: Mass balance of the gasifier operation (part II)

URN:NBN:no-2340

Exp. Number	#8a	#8b	#9	#12	#13a	#13b	#13c	#14
DATA								
Wet Biomass feeding rate (kg/h)	6,5	6,9	5,8	5,7	4,7	7,5	6,6	6,0
Air feeding rate (Nm3/h)	7,0	8,2	7,6	7,4	6,0	8,8	7,4	7,6
Air feeding rate (kg/h)	9,0	10,6	9,9	9,6	7,8	11,4	9,6	9,8
Energy content of pellets (MJ/kg wet)	18,859	18,859	18,859	18,859	18,859	18,859	18,859	18,859
Product gas rate (Nm3/h)	11,7	14,0	12,8	12,4	9,9	14,7	12,4	12,6
Product gas density (kg/Nm3)	1,15	1,14	1,14	1,15	1,16	1,13	1,15	1,15
Product gas rate (kg/h)	13,4	15,9	14,6	14,3	11,5	16,6	14,2	14,5
GAS COMPOSITION								
N2(%vol)	47,9	46,8	47,3	47,5	48,7	46,3	47,5	47,4
CO(%vol)	24,7	25,8	25,3	25,2	23,9	26,4	25,2	25,3
CO2(%vol)	9,7	9,1	9,3	9,4	10,1	8,8	9,4	9,4
H2(%vol)	16,1	16,8	16,5	16,4	15,6	17,2	16,4	16,4
CH4(%vol)	1,6	1,5	1,5	1,5	1,7	1,4	1,5	1,5
LHV(MJ/Nm3)	5,4	5,6	5,5	5,5	5,3	5,7	5,5	5,5
LHV(MJ/kg)	4,7	4,9	4,8	4,8	4,6	5,0	4,8	4,8
Tar content (g/Nm3)	3	3	3	3	3	3	3	3
Tar content (kg/h)	0,03	0,04	0,04	0,04	0,03	0,04	0,04	0,04
Energy content of tar (MJ/kg) [1]	25	25	25	25	25	25	25	25
Particulate (g/Nm3)	10,5	10,5	10,5	10,5	10,5	10,5	10,5	10,5
Particulate mass rate (kg/h)	0,12	0,15	0,13	0,13	0,10	0,15	0,13	0,13

1 Assumed value.

Table 2.4: Energy balance of the gasifier operation (part I)

The ultimate analysis of the pellets is presented in Table 2.5 together with other relevant information regarding the pellets.

Ultimate analysis	
C (% wt, mf)	50.7
O (% wt, mf)	42.4
N (% wt, mf)	<0.3
H (% wt, mf) by diff.	6.9
Other data	
Moisture content (% wt)	7.5
Ash content (%wt, mf)	0.39
Calorific value (MJ/kg raw pellets)	18.86
Bulk density (kg/m^3)	668
Pellet diameter (mm)	6
Pellet length (mm)	6-15

Table 2.5: Ultimate analysis of the pellets and other relevant pellet's data.

URN:NBN:no-2340

Exp. Number	#8a	#8b	#9	#12	#13a	#13b	#13c	#14
Energy balance								
Energy in biomass in (kW)	33,84	36,02	30,58	29,67	24,59	39,20	34,30	31,27
Energy in hot air (220°C) (kW)	0,58	0,68	0,63	0,62	0,50	0,73	0,62	0,63
Energy in gas out (dry) (kW), room temp.	17,60	21,75	19,59	18,98	14,67	23,17	18,95	19,34
Energy in tar (kW)	0,24	0,29	0,27	0,26	0,21	0,31	0,26	0,26
Energy in particles (kW)[2]	1,22	1,47	1,34	1,31	1,04	1,54	1,30	1,33
Cold gas efficiency	**52%**	**60%**	**64%**	**64%**	**60%**	**59%**	**55%**	**62%**
Mol of CO out (kmol/h)	1,29E-01	1,61E-01	1,44E-01	1,40E-01	1,06E-01	1,73E-01	1,39E-01	1,42E-01
Mol of CO2 out (kmol/h)	5,03E-02	5,67E-02	5,33E-02	5,24E-02	4,50E-02	5,74E-02	5,23E-02	5,29E-02
Mol of H2 out (kmol/h)	8,38E-02	1,05E-01	9,39E-02	9,08E-02	6,91E-02	1,12E-01	9,07E-02	9,27E-02
Mol of CH4 out (kmol/h)	8,30E-03	9,12E-03	8,67E-03	8,56E-03	7,54E-03	9,09E-03	8,54E-03	8,62E-03
mol water out (kmol/h)	8,72E-02	7,65E-02	6,04E-02	5,81E-02	5,22E-02	9,33E-02	8,41E-02	6,52E-02
Sensible heat in N2 out (750 °C) (kW)	1,48E+00	1,74E+00	1,61E+00	1,57E+00	1,29E+00	1,81E+00	1,57E+00	1,59E+00
Sensible heat in CO out (750 °C)	7,75E-01	9,71E-01	8,69E-01	8,40E-01	6,39E-01	1,04E+00	8,39E-01	8,58E-01
Sensible heat in CO2 out (750 °C)	4,66E-01	5,26E-01	4,94E-01	4,86E-01	4,17E-01	5,32E-01	4,85E-01	4,91E-01
Sensible heat in H2 out (750)	4,81E-01	6,02E-01	5,39E-01	5,21E-01	3,97E-01	6,45E-01	5,20E-01	5,32E-01
Sensible heat in CH4 out (750)	8,83E-02	9,71E-02	9,22E-02	9,11E-02	8,02E-02	9,67E-02	9,09E-02	9,18E-02
Total sensible heat (kW)	3,30E+00	3,94E+00	3,60E+00	3,51E+00	2,82E+00	4,12E+00	3,50E+00	3,56E+00
Sensible heat in water out (kW), 750 °C	6,31E-01	5,54E-01	4,37E-01	4,21E-01	3,78E-01	6,76E-01	6,09E-01	4,72E-01
Heat Losses (kW)								
energy in -energy out incl. sensible heat out	11,42	8,69	5,98	5,81	5,97	10,12	10,29	6,93
Heat losses as a % of thermal input	**34%**	**24%**	**20%**	**20%**	**24%**	**26%**	**30%**	**22%**
2 Assume LHV as 36MJ/kg, as for coal.								

Table 2.6: Energy balance of the gasifier operation (part II)

2.10.2 EVALUATION OF STABLE OPERATION

The following figures (Figure 2.5) show the temperature variation inside the gasifier during the gasification experiments.

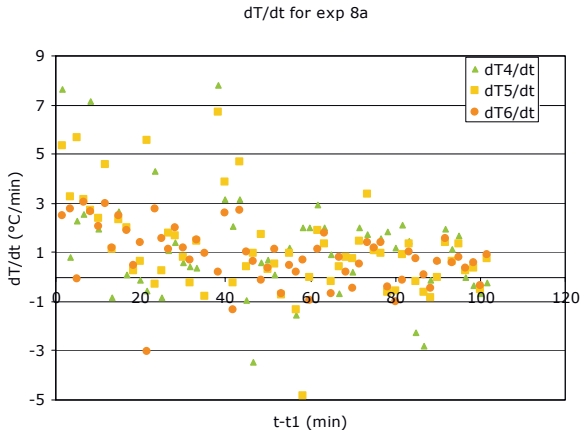

URN:NBN:no-2340

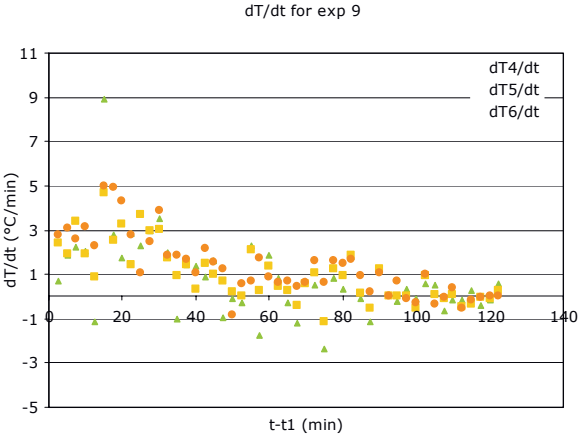

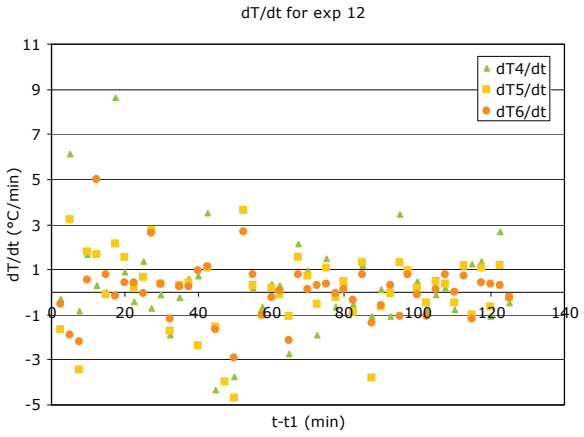

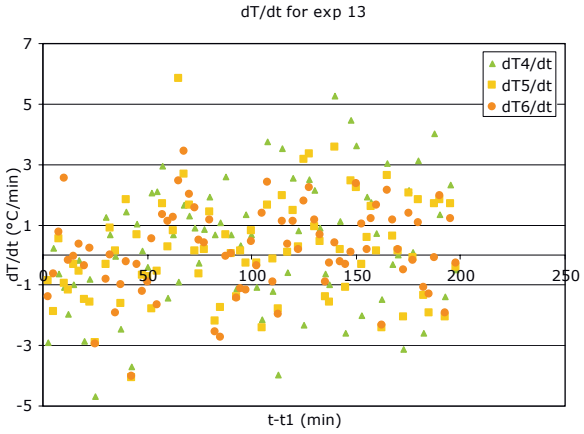

URN:NBN:no-2340

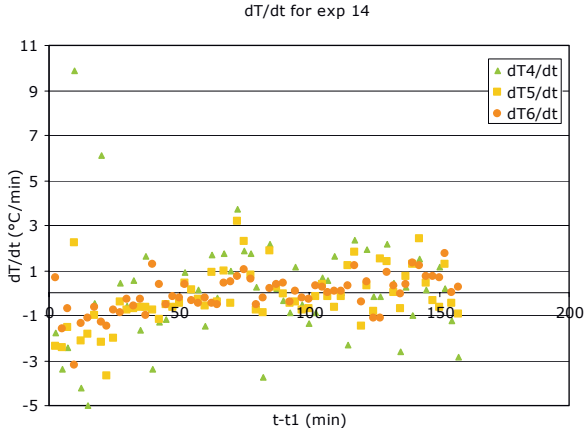

Figure 2.5: Temperature variation as a function of time in the gasification experiments.

The time axis represents the experimental time after the pyrolysis front has past the thermocouple T3. A larger variation in temperature can be observed during the first 20-30 minutes but in most cases it tends to zero as the experiment progresses. The reactor temperature at the beginning of the experiment is about 200 °C due to air preheating and therefore its temperature has to increase up to the operational temperatures, demanding some extra-heat. Thereafter, the operation of the gasifier is stable.

Appendix D includes the temperature record for all the experiments.

2.10.3 GAS CHROMATOGRAPHY

Gas chromatography is used in this investigation to measure the concentration of H_2, CO, CO_2, N_2 and CH_4 in the product gas.

Figure 2.6 shows the principle of operation of the gas chromatograph. The instrument consists basically of two elements:

- An adsorption column
- A detector (in this case, a thermal conductivity detector (TCD)).

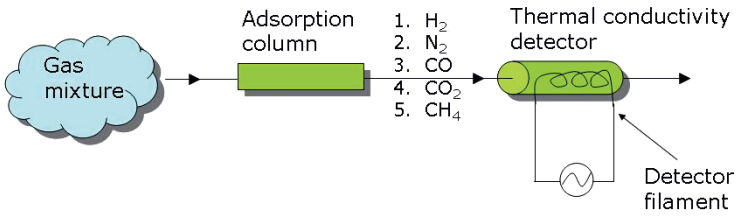

Figure 2.6: Simplified diagram of the Gas Chromatography principle.

URN:NBN:no-2340

Each gas component has a different adsorption time into the column. This means that each gas component of a gas mixture entering the column will take different time to leave the column and therefore the gas components will come out in a defined sequence, separated from each other. The adsorption properties of the column depend on the column material and temperature.

Thereafter, the different gas components enter the detector. The thermal conductivity detector consists basically of a filament whose temperature is held constant by an electrical circuit. As each gas component flows around the filament, the latter will tend to cool down, depending on the thermal conductivity of the gas surrounding the filament and depending linearly on its concentration. The electrical current necessary to maintain the filament at constant temperature is a measure of the gas concentration.

The gas chromatograph (GC) used in this investigation is a 8610C from *SRI Instruments*, equipped with a packed column 60/80 Carboxen-1000 from *Supelco*. The temperature of the TCD was held to 100 °C and the column temperature was varied as follows:

- 5 min. at 50 °C after injection,
- ramp at 10 °C/min until 210 °C
- cool down to 50 °C.

The total time for each gas analysis was 21 minutes. It was necessary to wait about 5 minutes before the column temperature stabilized at 50 °C.

One of the main problems of using gas chromatography with synthesis gases is the measurement of H_2 concentrations. The operation of the GC requires a constant flow of a carrier gas, usually Helium. However, the thermal conductivity of Helium is very similar to H_2 and therefore the filament of the TCD does not register the passage of H_2. To avoid this problem, Argon is used in this investigation as the carrier gas. Argon could interfere with CO_2 because they have similar thermal conductivity, but no conflict was observed during the measurements.

Figure 2.7 shows the analysis result for one of the gas samples during one gasification experiment. The sample volume is 0.5 ml. The column used for these experiments can also detect O_2, but no oxygen was detected unless there was a leakage in the gas sampling line. It can be observed that the baseline is not a

URN:NBN:no-2340

straight line as it could be expected. This is a consequence of using Argon as the carrier gas instead of Helium, since Argon conductivity is not totally insensitive to temperature changes in the column.

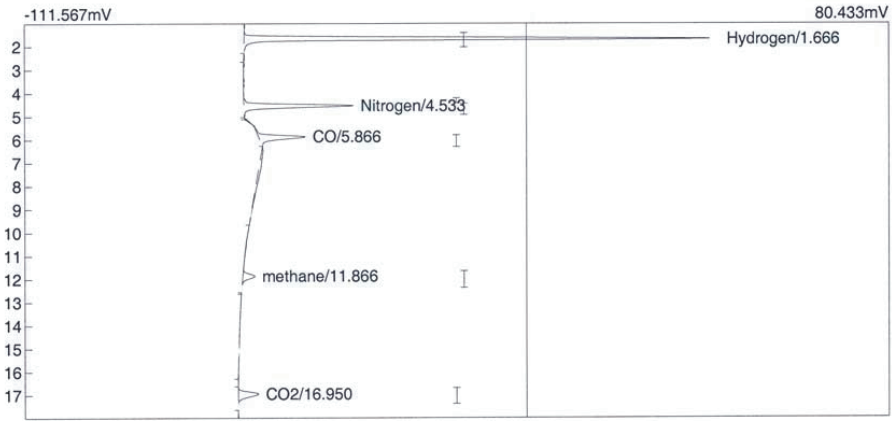

Figure 2.7: Data file from a gas chromatograph analysis

The areas between the detector signal and the baseline are linearly proportional to each gas concentration. To quantify these concentrations calibration is required for each gas. The calibration gases used are shown in Table 2.7; each gas component is calibrated independently. Although in principle only one calibration point is required for each gas, the accuracy of the analysis improves if several calibration points are used. It is also recommended that the calibration gases have similar gas concentrations than the samples.

Gas composition	N_2(%vol.)	CO_2 (%vol.)	CO(%vol.)	H_2 (%vol.)	CH_4(%vol.)
Calibration gas #1	48,5	0,51	16,61	33,85	0,53
Calibration gas #2	77,88	17,7	4,42	0	0

Table 2.7: Calibration gases for gas chromatography

During the calibration runs and during all the experiments the temperature program has to be the same so the areas between the detector signal and the baseline are comparable. The temperature program used in this investigation is quite simple. It could have been more complex in order to reduce the analysis time by increasing the heating rate and making several ramps, for instance. However, if the column temperature is too high, some components might not separate from each other.

URN:NBN:no-2340

Finally, it is important to comment on the sample injection. This instrument is quite simple and the injection is done manually with a syringe into the column. Such injection introduces error due to a human operator (exact amount of sample injected, speed of injection, etc.). More sophisticated GC's have automated injection systems.

2.11 SUMMARY OF PAPERS I, II AND III

Each paper is almost a continuation of the previous, both in time and content. Paper I and Paper II refer to the gasifier while Paper III focuses on the gas engine.

PAPER I

This paper contains a detailed description of the gasifier, including the air and biomass supply systems. The paper describes the experimental experiences until stable operation was reached. The movement of the zones is analysed, showing that the pyrolysis rate is much higher than the char gasification rate resulting in a pyrolysis front moving upwards. The speed of the pyrolysis front depends on the temperature of the char gasification zone.

The main finding is that the gasifier tends to top stabilisation because of the very dry pellets and the difference in the reaction rate between pyrolysis and gasification. However, top stabilisation is not possible because the semi-continuous feeding disturbs this mode of operation. Some tests are conducted varying the air supply location. The results are promising although this air location has not been studied as a parameter during this Ph. D..

A stable mode of operation is reached, called "near top stabilisation" where the air is supplied below the top of the bed and the pyrolysis front cannot climb up from this point. A first gas composition is presented.

PAPER II

This paper presents stable operation experiments. The operation of the gasifier has been characterised by the gas composition and the product gas tar and particle content. Other relevant parameters like the air-excess ratio, the air to fuel ratio and gas to fuel ratio have been calculated for each experiment to allow for comparison with other investigations (processes). It has been observed that the above parameters are independent of load. The temperature profile is obtained and compared with literature.

URN:NBN:no-2340

In addition to this, the article presents a comparison between the design parameters and the operational ones. The main differences are due to an air excess ratio (design) of 0,2 to 0,7 when the experience shows that the air excess ratio is rather constant (0,25-0,3). The design feeding rate was 5-6 kg/h of pellets, but the gasifier can actually work with higher fuel feeding rates (4,3-6,9 kg/h).
Finally, mass balances and evaluation of the operation are included.

The main conclusions presented in this paper are:

- Higher CO content in the product gas than similar gasifiers
- High tar content in the product gas in comparison with similar gasifiers
- The stabilisation of the zones is difficult, being this the major drawback of stratified downdraft gasifiers.

PAPER III
This paper contains a description of the gas engine system, including the condenser unit, filter unit, gas engine and water break.

It presents experiments conducted with the gas engine using mixtures of CH_4, CO, H_2, CO_2 and N_2 as a fuel. Emissions of NO_x and CO in the exhaust gases have been measured. As the content of methane in the mixture increases, NO_x emissions increase. For a gas mixture similar to a LCV gas, the NO_x emissions are low (42 mg/Nm^3). However, a gas mixture equivalent to a LCV gas results in very high CO emissions (3500mg/Nm^3) and decrease as CH_4 is added to the fuel mixture. It was observed that variations in air excess ratio, rotational speed and engine load also affect emissions.

The ignition timing was fixed in these experiments to 20 degrees before top dead centre. This angle might not be the optimal for operation with LCV gas, given the combustion properties of H_2 and CO compared to methane.

2.12 REFERENCES

1. Reed, T.B. & Das, A. (1988). Handbook of biomass downdraft gasifier engine systems. The Biomass Energy Foundation Press, 1810 Smith Rd., Golden, CO. 80401.
2. Risnes, H. High temperature filtration in biomass combustion and gasification processes. Ph. D. Thesis, Norwegian University of Science and Technology.

URN:NBN:no-2340

PAPER I

A SMALL-SCALE STRATIFIED DOWNDRAFT
GASIFIER COUPLED TO A GAS ENGINE
FOR COMBINED HEAT AND POWER
PRODUCTION.

Published in:
Progress in Thermochemical Biomass Conversion
Volume 1
2001
Edited by A. V. Bridgwater
Blackwell Science

URN:NBN:no-2340

URN:NBN:no-2340

A small-scale stratified downdraft gasifier coupled to a gas engine for combined heat and power production.

M. Barrio, M. Fossum[#], J.E. Hustad
Norwegian University of Science and Technology, Department of Thermal Energy and Hydro Power, 7491 Trondheim, Norway
[#]Sintef Energy Research, Department of Thermal Energy, 7465 Trondheim, Norway

ABSTRACT: A small scale (30 kW thermal input) stratified downdraft gasifier is erected in the laboratory at the Norwegian University of Science and Technology (NTNU). The gasifier will be coupled to a gas engine to produce heat and power from biomass fuels. The paper describes the gasifier in detail (500 mm height and 100 mm diameter). One of the singularities of the gasifier design is that it allows for variation of the point of air injection and that air preheating is also possible. The gas engine was originally a diesel engine but it has been modified for producer gas and/or natural gas operation. These changes mainly affect the compression ratio and the fuel injection system. The paper describes the gas engine and explains the modifications.

Experiments have been performed of gasification of wood pellets. The feeding rate was about 5 kg/h, giving an effect of 30 kW. The amount of air supplied to the reactor has been varied in the experiments, in addition to the location of the supply. The fuel gas composition has been measured with a GC. The amount of product gas obtained is about 12.5 Nm^3/h and has a heating value of 4.9 MJ/Nm^3. From these data, the power produced by the gas engine is expected to be about 5 kW_e.

The gas engine will be operated with mixtures of synthesis gas and natural gas and detailed measurements of cylinder pressure, compression ratio and heat released by the engine are planned in addition to emission measurements of CO, unburned hydrocarbons and NO_x. The dependency of the results on the ratio of synthesis gas/natural gas will further be evaluated.

INTRODUCTION

The objective of this project is to produce heat and power at small scale from biomass fuels. Biomass gasification represents a competitive alternative to direct combustion for optimisation of the electricity production. Fixed bed gasifiers are known to produce a gas with low tar and particulate content, and therefore suited for small scale power production[1,2].

The possibility of combining producer gas and natural gas is also of particular interest and specially for Norway with large resources of natural gas.

The plant consists of a stratified downdraft gasifier, a cleaning system and a gas engine. The thermal input to the gasifier is 30 kW, supplied by 5 kg/h of wood pellets. The design of the gasifier is particularly flexible. It allows the use of different gasification agents, different location of the gasification agent supply and almost every

URN:NBN:no-2340

part can be replaced. At the first phase of the project, the gasification agent will be air. This small scale reactor is suitable for laboratory work but one of its drawbacks is that the heat losses are very high compared to the amount of energy involved in the process.

As a first approach, a deep bed filter will be used for gas cleaning, with sand as the filter media. Later, a more advanced high temperature filtration method will be employed[3].

The gas engine was originally a diesel engine that has been modified for synthesis gas or/and natural gas. A relevant feature of this project is the measurement system that has been implemented in the engine. It will allow measurement of the cylinder pressure and the crank angle, providing thus relevant information for the understanding of engine operation with producer gas.

This paper describes the gasifier and the engine. The first experiences with the gasifier are also presented as well as the modifications required by the diesel engine in order to operate with producer gas and/or natural gas.

SMALL SCALE STRATIFIED DOWNDRAFT GASIFICATION

Downdraft gasification generally produces a low particulate and low tar gas and is therefore suited for power generation in small scale applications. There exist mainly two designs for downdraft gasifiers: the Imbert gasifier and the stratified downdraft gasifier (or open core gasifier).

The Imbert gasifier is usually a cylindrical reactor with a constriction near the bottom. The gasification agent is injected just above the constriction, creating a high temperature zone. The stratified downdraft gasifier has no constriction and both feedstock and gasification agent are fed from the top of the gasifier. The air flows through the fuel bed supported by the grate at the bottom of the gasifier. Although much more popular, the Imbert gasifier presents certain disadvantages like the fuel limitations due to the constriction and the difficulties at scale up due to the radial air supply. The stratified downdraft gasifier is easier to construct and the different zones are easier to access. This gasifier has in principle better scale-up properties than Imbert gasifiers[4,5,6].

In the stratified downdraft gasifier four zones can be distinguished. At the top of the bed the pellets are heated and dried. Below this zone the temperatures start to be higher and the pellets release their volatile matter (devolatilization, or pyrolysis). The gaseous products from devolatilization are partially burnt with the existing air. This phenomena is called flaming pyrolysis[5] and it is the source of heat for the drying and pyrolysis already mentioned as well as for the subsequent char gasification. The temperature in this zone can reach 1000-1100 °C and since it is a thin zone it has been called the "pyrolysis front" in this investigation. In the third zone, the char reduction zone, the hot gases formed in the flaming pyrolysis zone (mainly CO_2, H_2O) react with the remaining char in absence of oxygen at around 800-900 °C. The char is converted into the product gas mainly by the following endothermic reactions:

Boudouard reaction:	$C + CO_2 \leftrightarrow 2CO$	$\Delta H_R = + 160{,}9$ kJ/mol
Water gas reaction	$C + H_2O \leftrightarrow H_2 + CO$	$\Delta H_R = + 118{,}4$ kJ/mol

The hot gases and the char coming from the flaming pyrolysis zone provide the energy required. As these reactions proceed the temperature sinks progressively until it becomes so low (700 °C) that the reaction rates are insignificant. This means that the

URN:NBN:no-2340

extent of the char reduction zone is dependent on the amount of energy entering the reduction zone and consequently also on the heat losses from the reactor[7].

The bottom zone, or inert char zone, consists then of char that has not reacted - because the temperatures are too low- and ash. This zone is nevertheless very important since it acts as a reservoir of charcoal that can absorb heat when conditions of operation will change and moreover acts as a particle filter.

The length and position of the zones described above depend on numerous parameters that interact with each other: pyrolysis rate, gasification rate, rate of ash/inert char removal, temperature profile, heat available for reaction, fuel feeding rate, air feeding rate, heat losses, etc.

It is still a challenge to understand how the zone's distribution inside a gasifier affects the quality of the product gas: gas amount, composition, tar content and particle content. This challenge has been faced through experimental work and through modelling[8]. Di Blasi[9] has recently presented a dynamic model for stratified downdraft gasifier where finite rate kinetics for the chemical reactions are included: pyrolysis, gas-phase combustion, gas-phase water shift and heterogeneous char reactions.

Another important matter is the stability of the gasifier operation; the zones can move, as observed by several researchers[1,7]. This fact might affect the product gas quality and this is unwanted while operating the engine.

The raw pellets travel downwards inside the reactor at a rate that can be obtained from the feeding rate, assuming a constant bed height:

$$v_{pellets} = \frac{feeding\ rate(kg/h) * pellets\ bulk\ density(m^3/kg)}{reactor\ diameter(m^2)} \quad (1)$$

Once the pellets have crossed the pyrolysis zone, they continue to travel downwards at the same speed ($v_{pellets}$) if one assumes that the bulk density of the pyrolised pellets is the same than the one of the raw pellets[1]:

$$v_{pellets} = v_{char\ consumed} \quad (2)$$

The mechanical strength of the fuel is relevant to maintain certain porosity of the bed to prevent plugging[6].

In the char reduction zone, the pyrolysed pellets are partially transformed to gases through the gasification reactions. The remaining pellets (inert char) and the ashes leave the bed through the grate. This can be expressed as:

$$char_{consumed} = char_{gasified} + char_{removed} \quad (3)$$

The pyrolysis front moves towards the raw pellets, as a flame front, as already suggested by Reed et al.[10]. Flaming pyrolysis is a fast reaction at around 1000 °C and the length of this zone is relatively small and constant. Therefore, the zones will not move if the speed of this pyrolysis front matches the velocity of the bed moving down, in other words, if the pyrolysis rate is equal to the char consumption rate.

[1] The dimensions of the pyrolysed pellets are approximately 90% of those of the raw pellets.

URN:NBN:no-2340

$$v_{front} = v_{pyrolysis} - v_{char\ consumed}$$

where v_{front} absolute velocity of the pyrolysis front
$v_{pyrolysis}$ velocity of the pyrolysis front relative to the moving bed

If the pyrolysis rate is higher than the char consumption, then the pyrolysis front moves up ($v_{front}>0$) and the length of the char reduction zone increases[7]. If this is the case, the flaming pyrolysis front will climb indefinitely until it reaches the top of the bed and the drying zone almost disappears. Although such operation mode is stable, the radiation from the top of such bed is a significant heat loss[1]. This operation mode is called "Top stabilisation mode" and has been modelled by Di Blasi[9].

DESCRIPTION OF THE STRATIFIED DOWNDRAFT GASIFIER

The gasifier and the surrounding systems are illustrated in Fig. 1 and Fig. 2. This section gives a detailed description of each element.

FEEDING SYSTEM

The feeding system consists of a hopper and of two pneumatic sliding valves. This system provides a pseudo-continuous operation of the reactor. Since the two valves never open simultaneously it is a tight system. A screw feeder was tested earlier but it crutched the pellets. The feeding can be done manually or automatically. Several tests have been conducted to calibrate the feeding system, so both the weight and bulk volume of each charge of pellets is estimated. Pellets have quite uniform properties regarding size, composition and mechanical strength and are therefore better suited for small scale applications.

AIR SUPPLY

The pressurized air network at the Department's workshop (6 bar) supplies the air for the installation. A filter removes the eventual dust and moisture from the air and thereafter the air pressure is reduced to 3 bar. The air is then stored in a manifold that distributes it to 7 independent channels. The amount of air through each channel is measured with a rotameter and controlled with a valve. In addition, an air preheater has been installed before the manifold. Each air channel supplies air to a circular distributor around the gasifier. From each circular distributor five pipes evenly distributed supply air to the reactor. Such system guarantees an even air distribution, for any combination of channels in use. The location of the air levels is shown in Fig. 3, together with the position of temperature and pressure measurements.

Contrary to the usual design where the gasifier works under atmospheric pressure, the air pressure at the reactor is slightly above atmospheric pressure, depending on the pressure losses downstream the reactor. With this design, the amount of air entering the gasifier is well controlled although there is an increased risk for leakages.

URN:NBN:no-2340

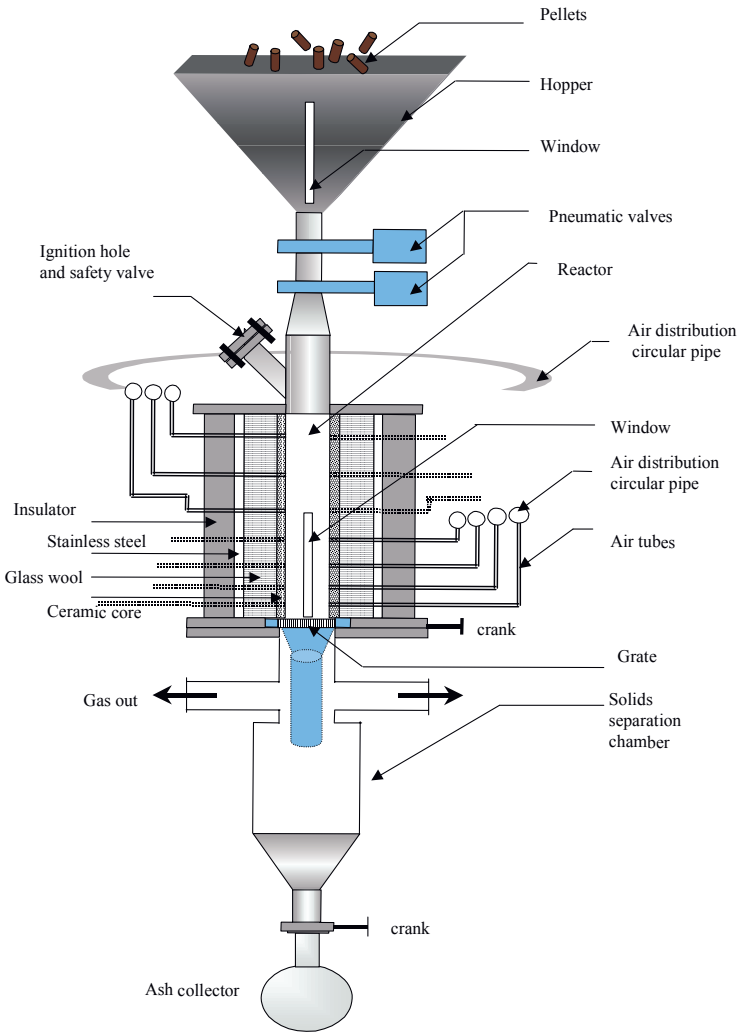

Fig. 1 Sketch of the stratified downdraft gasifier

URN:NBN:no-2340

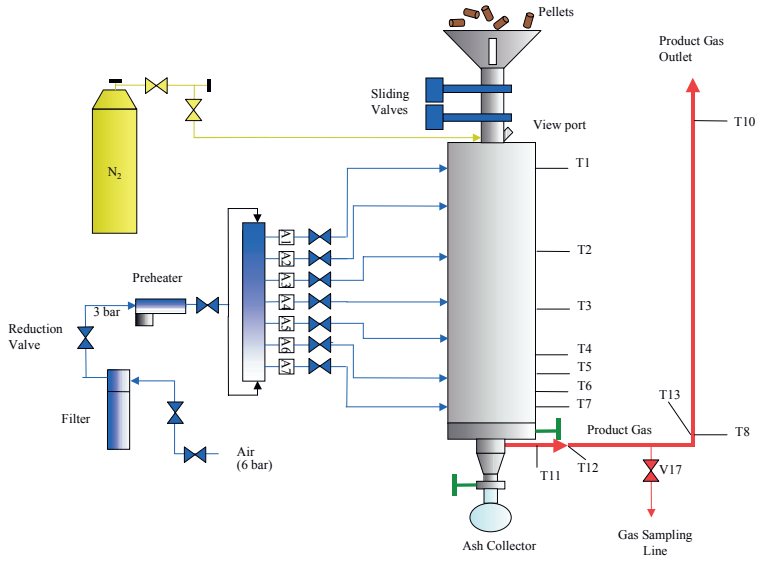

Fig. 2 Sketch of the gasification unit

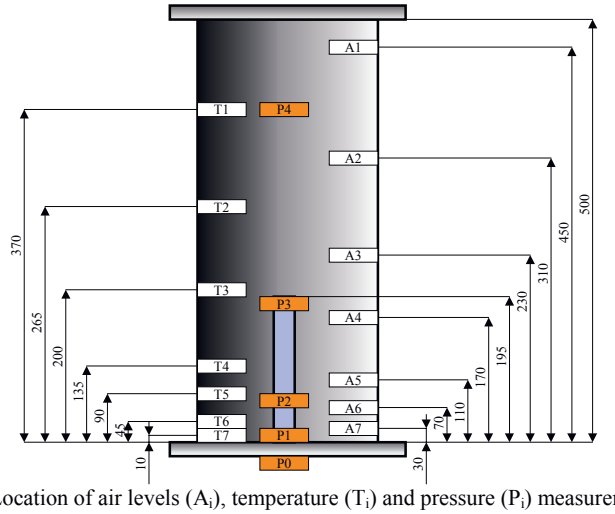

Fig. 3 Location of air levels (A_i), temperature (T_i) and pressure (P_i) measurements.

URN:NBN:no-2340

REACTOR

The reactor itself is a cylinder of 100 mm diameter and 500 mm height, made of refractory ceramic. It has 35 holes for air supply, 7 for temperature measurement and 4 for pressure measurement. The reactor was originally designed with a glass window, so the zones could be observed. It was possible to observe the zones through the window but it was necessary to permanently cover it due to leakages. A steel cylinder of 250 mm surrounds the reactor, with glass wool filling the space between both cylinders as insulator. The steel cylinder is also covered with approx. 7 cm of insulation.

Between the feeding system and the reactor there is a view port that is used to ignite the bed and acts as well as a safety pressure release valve.

The small dimensions of the reactor pose problems like for example that there is no agitator to avoid bridging, that a bed height indicator could be a disturbance and the same with the thermocouples. But on the other hand, such small diameter almost guarantees radial uniform temperatures, and uniform air distribution.

The bottom section of the gasifier accelerates the gas flow so that the char and ash particles will more likely deposit at the ash collector while the gas exits the reactor.
The grate is placed between the reactor and the bottom section. It is a perforated plate of 10 mm thickness, with a crank so it can be shaken manually. As experienced by other researchers, the grate is problematic. Its design has been changed several times either because the char losses were too high or because it blocked and it has been the most challenging element of the installation. Its correct operation and a controlled ash removal is vital for the stable operation of the gasifier[11]. When the grate blocks, the amount of char removed is zero and this also affects the velocity of the pyrolysis front, as shown earlier.

MEASUREMENT EQUIPMENT

The temperature inside the reactor is measured with seven thermocouples (Type K). To avoid channelling, the thermocouples are placed only 5 mm into the bed. The temperature inside the manifold is also measured, as well as at several points at the outlet pipe. The pressure in the manifold and inside the reactor is also measured with the help of pressure transducers. In order to take gas samples, a sample line has been built (Fig. 4). It consists of a steel condenser and three glass bottles in an ice bath, a moisture filter (silica gel), a pump and a gas flowmeter. A sample of 0.5 ml is taken from the gas sample line with a syringe and inserted into a gas chromatograph from *SRI Instruments* equipped with a TCD detector and a Supelco column (Carboxen 1000).

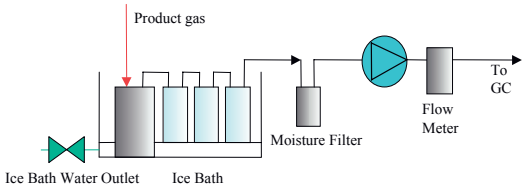

Fig. 4 Gas sampling line.

URN:NBN:no-2340

SAFETY CONSIDERATIONS

To allow an emergency stop, an independent pipe supplies nitrogen to the reactor. If necessary, the air flow can be rapidly stopped and substituted by nitrogen.

Since there is a moderate risk for leakage, the gasifier is placed inside a room with suction system and all the control and measurement equipment is placed outside the room. CO detectors are also installed.

THE ENGINE

In general both diesel and Otto engines can be converted to operate on gaseous fuels. To ensure high efficiency and low emissions it is recommended that the engine is modified according to the specific combustion properties of the actual gaseous fuel, which may be very different compared to both diesel and gasoline.

The diesel engine is more attractive for conversion to producer gas as the reduction in power and efficiency is less compared to an Otto engine. This is due to the higher compression ratio of the diesel cycle and also the operation conditions with high excess air ratios which reduce the difference in the volumetric energy content of diesel/air mixtures and producer gas/air mixtures.

The major engine modifications for a diesel engine include reduction of the compression ratio and installation of an ignition system. The ignition system can either be a spark plug system or a system using diesel fuel in a prechamber as an ignition source for the gas. Direct injection diesel engines are more suited for producer conversion than prechamber engines due to the less heat loss to the cylinder walls, which affect the ignition of the lean producer gas.

Diesel engines fuelled on producer gas are normally operated at a self aspirated mode. Contaminants in the producer gas, especially particles, can cause damages to a turbocharger. The producer gas is mixed with the intake combustion air and distributed to each cylinder by the intake manifold. For small scale integrated gasification and gas engine system the suction from the gas engine is used to feed air into the gasifier.

Overheated exhaust manifolds have been reported from installations running on producer gas[12]. This is most likely due to the low burning velocity of producer gas/air mixtures compared to diesel or natural gas and thus a complete burnout of the gas mixture may occur in the exhaust gas channel and into the exhaust manifold. The high temperature problem can be solved by cooling of the exhaust manifold.

The engine used in this project is a 3-cylinder naturally aspirated direct injected diesel engine (Zetor Z4901). The table below shows the original specifications of the diesel engine:

Table 1 Original engine specifications.

Concept	
Number of cylinders	3
Displaced volume (dm3)	2.7
Bore (mm)	102
Stroke(mm)	110
Compression ratio	17
Power @ 2200 rpm (kW)	34.2
Torque @ 1500 rpm (Nm)	150
Specific fuel consumption (g/kWh)	245 + 10%

URN:NBN:no-2340

The engine was built in 1980, and was originally design for standby stationary power production so instead of an airblown radiator for cooling it is equipped with a water jacket heat exchanger, common in marine applications. The heat exchanger is cooled with cold water being then possible to quantify the amount of heat rejected from the engine. The engine's exhaust manifold is also cooled to avoid problems with overheating, as mentioned before.

The initial phase of experiments will include a mapping of the engine characteristics using natural gas as a fuel. These data will be the basis for comparison and discussion of the results for different gas mixtures. The next step will be to use synthetic producer gas as a fuel as the most extreme low value gaseous fuel. Further experiments will include mixtures of synthetic producer gas and natural gas.

COMPRESSION RATIO, IGNITION SYSTEM AND FUELLING SYSTEM

The original compression ratio is too high for producer gas operation. Our intention is to operate the engine with a variety of gases, from natural gas to producer gas and thus the compression ratio is reduced down to 11:1.[13]

The engine has separate cylinder heads, what makes the modifications easier. The fuel injectors are replaced by spark plugs of the type used in small motorcycle engines. The small spark plugs are used to minimise the thermal mass of the spark plug, thus reducing the cooling effect and the possibility of flame quenching in the ignition zone. Each spark plug is connected to a high voltage coil that provides sufficient ignition energy.

The diesel pump is removed, and an optical pickup for the electronic ignition system is mounted in its shaft. The rotational speed of this shaft is ½ of the engine speed, which is needed for the ignition system. The ignition timing can be accurately set with this system.

A standard fuel feeding system is mounted and modified in order to be able to operate natural gas, producer gas and mixtures of gases.

MEASUREMENT EQUIPMENT

A pressure sensor from Optrand Inc. specially designed for cylinder pressure measurements has been installed in one of the cylinders. In addition, a crank angle decoder has been installed which gives a step signal twice per degree. These pulses trigger the pressure measurements and with this system the cylinder pressure versus the crank angle is recorded 720 times per revolution. The decoder also generates a one step signal for every other revolution in order to identify the compression stroke of the 4-stroke cycle of the engine. The time dependent volume of the cylinder is given explicit from the crank angle and the geometry of the cylinder, connecting rod length and crank radius. Thus, indicated values for power, efficiency, mean effective pressure and rate of heat release can be found.

The air flow to the engine is calculated from the pressure drop over a "honeycomb" viscous duct meter.

The heat balance for the engine is calculated from measurements of the flow of water through the heat exchanger and the according inlet and exit water temperatures. In addition the temperature of the fuel gas/air mixture and the exhaust gas temperatures are measured using thermocouples.

Standard operation will include measurements of the oxygen concentration in the exhaust gas which combined with the measured inlet air flow can be used to estimate

URN:NBN:no-2340

the excess air ratio. More detailed analysis of the exhaust gas will include measurements of CO, CO_2, UHC and NO_x concentrations.

All output signals from temperature sensors and flow controllers are sampled with a commercial acquisition system connected to a PC and data are presented on the screen using a LabView set-up. For the measurements of the cylinder pressure a high speed data acquisition system is installed which also is connected to the PC.

To measure the power generated by the engine, a hydraulic brake has been installed. A load cell attached to the brake measures the torque.

GAS CLEANING

As a first approach deep bed filtration in planned, using sand as the filtration media. The pressure loss across the filter will be observed and when necessary, the sand will be renewed. Eventually, a pump will be installed after the filter to avoid high overpressure inside the gasifier. The engine will have a suction effect later on.

Later, a more complex filtration system at high temperature will be introduced[3].

PRELIMINARY GASIFICATION EXPERIMENTS

Several experiments have been conducted varying the amount of air supplied and its distribution and varying the preheating conditions. These parameters affect:

(1) Fuel/air ratio
(2) Temperature profile inside the gasifier
(3) Position of the zones
(4) Stability of the gasification process
(5) Product gas quality
(6) Product gas composition
(7) Amount of product gas.

It has been found through the experiments that the reactor needs considerable preheating. If the reactor is cold, it absorbs a large amount of the heat produced and the gasification process can hardly be established. All experiments include thus approx. 12 hours of preheating at around 200 °C.

After preheating, a small amount of charcoal (small pieces) was sent through the ignition port and thereafter some pieces glowing charcoal. When the temperature starts to rise, the ignition port is closed and the reactor is filled with pellets. The air flow is adjusted to the desired amount and the experiment starts. The pellets have a diameter of 8 mm and a length that varies between 5 and 15 mm.

The reactor does not have a bed height indicator. Nevertheless, an alternative simple method has been found to measure and control the fuel level. The bed height is controlled by observing the temperature at the top of the gasifier (T1). When the gasifier is filled with pellets, a new charge of pellets only affects T1, that decreases suddenly below 100 °C. When the temperature T1 stabilises at around 180 °C - depending on the preheating temperature-, the level is below T1 and a new charge is fed. If other temperatures are affected by the new charge of pellets, then the bed height is lower. In most experiments, the reactor has been kept filled with pellets. In this way, one possible parameter, bed height, is eliminated and also the heat produced in the pyrolysis zone can be absorbed by the raw pellets as well as by the char bed and not radiated to the top of the reactor.

URN:NBN:no-2340

Fig. 5 shows the temperature record from one of the experiments. The bed height has been kept around T1. The figure shows how the pyrolysis front moves up. This has been observed in all the experiments although the speed of the front has varied. It has been found that several operational parameters like the velocity of the front, the feeding rate and the air excess ratio depend on the temperature of the char reduction zone (Fig. *6*).

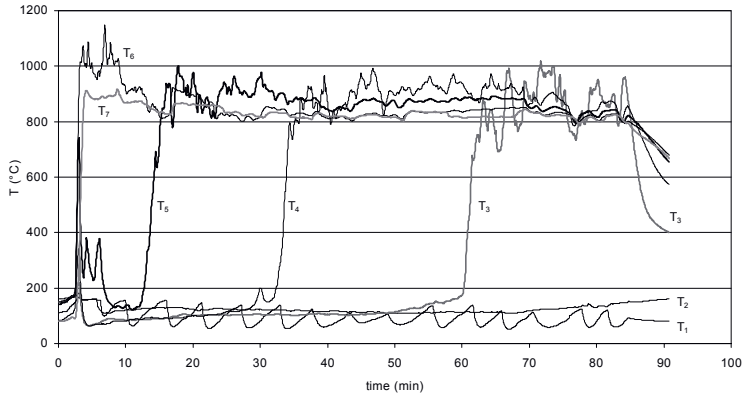

Fig. 5 Temperature record of one experiment.

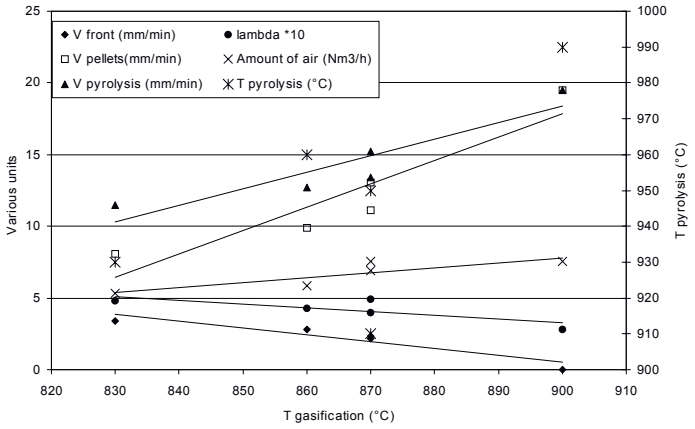

Fig. 6 Influence of the temperature of the char reduction zone on the gasifier operation.

The fuel/air ratio is not considered a parameter in this discussion. The pellets were supplied so the bed height was constant. This means that the fuel/air ratio is not a parameter since it is not the operator who has control over it but the gasifier, as already shown by other authors[14].

URN:NBN:no-2340

The gasifier has been operated with several air distributions:

(1) 100% supply from level A1 ("traditional" open core gasifier)
(2) 80% supply from level A1 and 20% supply from level A4
(3) 20% supply from level A1 and 80% supply from level A4.

The air excess ratio obtained for distributions (1) and (2) is about 0.4-0.45 while the distribution (3) has given a lower ratio (0.3). Distribution (3) also shows some differences on temperature profile like higher char gasification temperature. Fig. 7 shows the temperature profiles during two experiments: one with distribution (1) and another with distribution (3) but both with approximately the same amount of air supplied. Profiles 1a, 1b and 1c correspond to the same experiment, but with the pyrolysis front at different locations. The figure shows that the heat created during the flaming pyrolysis is used in a more efficient way with air distribution (3).

The temperature profiles also show that the temperature below the pyrolysis front is always above 800 °C, i.e. there is no inert char zone. This can mean that the length of the char reduction zone is too short and therefore the gasification reaction is uncompleted.

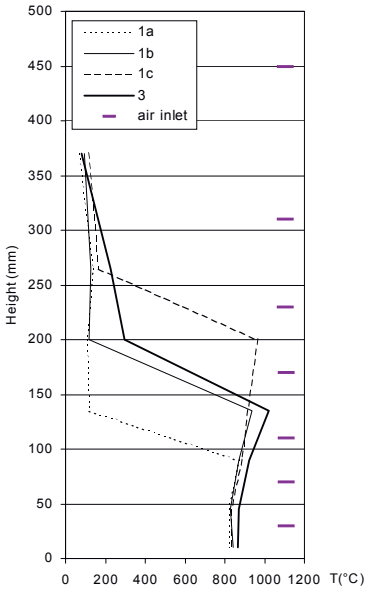

Fig. 7 Temperature profile inside the reactor.

The behaviour of the gasifier suggests that the reactor will operate satisfactory in "Top stabilisation mode", partially because of the low moisture content of the pellets. This mode of operation was tested in one of the experiments, as shown in Fig. 8. Top stabilisation mode was reached after 200 minutes of operation.

One can observe the large variations in the temperature at the top of the bed, as a result from the semi-continuous feeding. Pyrolysis of fresh pellets alternates with char

URN:NBN:no-2340

combustion at the top of the bed and this periodic behaviour affects the temperatures along the reactor, disturbing therefore the stable gas production. The height of the bed is extremely difficult to control with this mode of operation. In addition, the large and frequent temperature variations can damage the thermocouples.

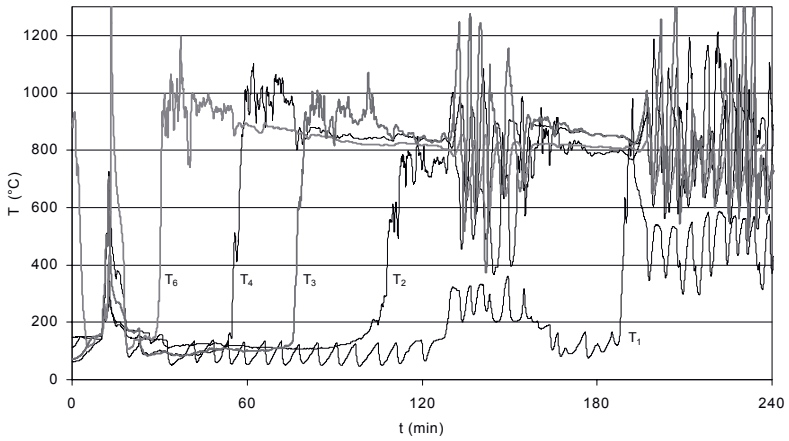

Fig. 8 Top stabilisation mode. Temperature record.

Therefore, the conclusion from this experiment is that top-stabilisation mode, although feasible, is not suitable for our reactor. Under this mode of operation, the semi-continuous feeding becomes an inconvenience.

Further tests have been conducted having the height of the pellet's bed above the point where the air is injected. This mode of operation has shown to be stable and more experiments will be conducted soon.

The approximate gas composition of the product gas is shown in Table 2. The amount of gas produced is calculated from the N_2 content of the product gas and the amount of air provided.

Table 2 Product gas composition, heating value and amount produced.

Product gas composition	
N_2 (% vol.)	46.8
CO (% vol.)	20.6
CO_2 (% vol.)	10.2
O_2 (% vol.)	1.5
CH_4 (% vol.)	0.0
H_2 (by difference) (% vol.)	20.9
Heating value (MJ/Nm^3)	4.9
Amount of product gas (Nm^3/h)	12.6

CONCLUSIONS

(1) A small scale stratified downdraft gasifier is erected at our laboratory. The thermal input is 30 kW, supplied by 5 kg/h of wood pellets.

URN:NBN:no-2340

(2) A gas engine is modified so it can operate with the product gas and with mixtures of product gas and natural gas. The modifications affect the compression ratio, the ignition system and the fuelling system.
(3) The preliminary experiments show that the pyrolysis front moves up; the velocity of the front depends on the char reduction zone temperature. In order to achieve stability, this temperature should be as high as possible. The air distribution can be altered so the air supplied is more efficiently use for heat production. The amount of char removed also affects the stability of the process.
(4) Top-stabilisation mode, although feasible, is not suitable for our reactor. Under this mode of operation, the semi-continuous feeding becomes a problem. It is nevertheless possible to reach stable operation by keeping the bed height above the air injection point.
(5) The air distribution seems to affect the air excess ratio.
(6) Based on the preliminary experiments, the gasifier produces about 12 Nm^3/h of product gas. This gas has a calorific value of approx. 5 MJ/Nm^3 and contains approx. 20 %vol. CO and 20 %vol. H_2.

ACKNOWLEDMENTS

This project is financed by the Norwegian Research Council. The authors want to thank the enthusiastic cooperation of Ole Birger Svendsgaard, Torsten Goehler and Uk Chantaka.

REFERENCES

1. Reed, T.B. & Gaur, S. (1999). A survey of biomass gasification 2000. The Biomass Energy Foundation, Inc., 1810 Smith Rd., Golden, CO. 80401.
2. García-Bacaicoa, P., Bilbao, R. & Usón, C. (1995). Air gasification of lignocellulosic biomass for power generation in Spain: Commercial plants, Proceedings of the 2nd Biomass Conference of the Americas, USA, pp. 676-694.
3. Risnes, H. & Sønju, O.K. Evaluation of granular bed filtration for high temperature applications. *This conference*.
4. Xu, M., Gu, Z.Z., Sun, L., Guo, D.Y. & Han, T. (1997). Research on straw waste gasification and application in straw pulp mill, Developments in Thermochemical Biomass Conversion, Blackie Academic & Professional, 1997, pp 892-899.
5. Reed, T.B. & Das, A. (1988). Handbook of biomass downdraft gasifier engine systems, The Biomass Energy Foundation Press, 1810 Smith Rd., Golden, CO. 80401.
6. Schenk, E.P. , van Doorn, J. & Kiel, J.H.A. (1997). Biomass gasification research in fixed bed and fluidised bed reactors, Gasification and Pyrolysis of Biomass, Stuttgart, April 1997.
7. Milligan, J.B. , Evans, G.D. & Bridgwater, A.V. (1993). Results from a transparent open-core downdraft gasifier, Advances in Thermochemical Biomass Conversion, Blackie Academic & Professional, 1993, pp. 175-185.
8. Reed, T.B. & Levie, B. (1984). A simplified model of the stratified downdraft gasifier, International Bio-Energy Directory and Handbook, 1984, pp.379-390.
9. Di Blasi, C. (2000). Dynamic behaviour of stratified downdraft gasifiers, Chemical Engineering Science, Vol. 55, No. 15, pp. 2931-2947.
10. Reed, T.B. & Markson, M. (1985). Biomass gasification reaction velocities, Proceedings of FPRS industrial wood energy forum '83, No.7, Vol. 2, pp. 355-365.

URN:NBN:no-2340

11. Gabroski, M.S. & Brogan, T.R. (1985). Development of a downdraft modular skid mounted biomass/waste gasification system.
12. Hansen, U. et al. (1996). Heat and power from small scale biomass plants in rural regions. A: typical application case study in Mecklenburg-Vorpommern. Proceedings of the 9th European Bioenergy Conference, pp. 1318-1323.
13. ImechE (1996). Using Natural gas in engines, Seminar Publication.
14. García-Bacaicoa, P., Bilbao, R., Arauzo, J. & Salvador, M.L. (1994). Scale-up of downdraft moving bed gasifiers(25-300 kg/h) - design, experimental aspects and results, Bioresource Technology 48 (1994), pp. 229-235.

URN:NBN:no-2340

URN:NBN:no-2340

PAPER II

OPERATIONAL CHARACTERISTICS OF A SMALL-SCALE STRATIFIED DOWNDRAFT GASIFIER

Published in:
Technologies and combustion for a clean environment
Sixth International Conference
9-12 July, 2001
Porto, Portugal
Volume III

URN:NBN:no-2340

URN:NBN:no-2340

Operational Characteristics of a Small-Scale Stratified Downdraft Gasifier

M. BARRIO, M. FOSSUM[#] AND J.E. HUSTAD
Norwegian University of Science and Technology, Department of Thermal Energy and Hydro Power, 7491-Trondheim, Norway
[#]Sintef Energy Research, Department of Thermal Energy, 7465-Trondheim, Norway

ABSTRACT
A small-scale stratified downdraft gasifier has been operated under stable conditions at the Norwegian University of Science and Technology (NTNU). The thermal input is about 30 kW_{th} supplied by 5-7 kg/h of wood pellets. The air supply has been varied between 6-8 Nm^3/h and resulted in an air excess ratio for the gasification process of 0.25-0.3. The gasifier is coupled to a gas engine for production of heat and power from biomass fuels. Variations in product gas composition have been observed as a function of the air feeding rate and hydrogen contents between 14 and 18 % have been measured. The gasifier produces between 10 and 14 Nm^3/h of product gas, with a heating value of about 5.5 MJ/Nm^3. The tar content of the product gas has been analysed by cold trapping and by solid phase adsorption (SPA) method. Preliminary results indicate a particle content of 10.5 g/Nm^3 and a tar content of 3 g/Nm^3. The paper also includes temperature profiles measured inside the reactor, a comparison between design and operation parameters and mass and energy balances.
Key Words: biomass, gasification, stratified downdraft, product gas.

INTRODUCTION
The traditional design of a fixed bed downdraft gasifier consists of a cylindrical reactor with a constriction near the bottom. The gasification agent is injected just above the constriction, creating a high temperature zone. Because of this constriction the flow is highly turbulent, favouring good mixing (Di Blasi, 2000). This type of gasifier is also known as the Imbert gasifier (Groeneveld, 1980; Garcia-Bacaicoa et al. 1994; Wang and Kinoshita, 1993).

A more recent design is the stratified downdraft gasifier (Reed and Das, 1988; Mukunda et al., Milligan et al., 1993; Manurung and Beenackers, 1993; Walawender et al., 1985; Di Blasi, 2000). The stratified downdraft gasifier has no constriction and both the feedstock and the gasification agent are fed from the top of the gasifier. The air flows through the fuel bed supported by the grate at the bottom of the gasifier. The stratified downdraft gasifier is easier to construct, is able to work with loose materials and its different zones are easier to access. This gasifier has in principle better scale-up properties than the Imbert gasifier. In addition, the oxygen distribution is more uniform and some of the ash melting problems are solved (Di Blasi, 2000).

In the stratified downdraft gasifier four zones can be distinguished. At the top of the bed the pellets are heated and dried. Below this zone the temperatures start to be higher and the pellets release their volatile matter. The gaseous products from devolatilization are partially burnt with the existing air. This phenomena is called flaming pyrolysis and it is the heat source for the drying and devolatilization already mentioned as well as for the subsequent char gasification. The temperature in this zone can reach 1000-1100 °C. In the third zone, the char reduction zone, the hot gases formed in the flaming pyrolysis zone react with the remaining char in absence of oxygen at around 800-900 °C. As these reactions proceed, the temperature decreases progressively until it becomes so low (700 °C) that the reaction rates are insignificant. The bottom zone, or inert char zone, consists then of char that has not reacted –because the temperatures are too low- and ash. The length and position of the zones described above depend on numerous parameters that interact with each other: pyrolysis rate, gasification rate, rate of ash/inert char removal, temperature profile, heat available for reaction, fuel feeding rate, air feeding rate, heat losses, etc.

The construction of the stratified downdraft gasifier at the Norwegian University of Science and Technology started in 1997 and the first experiences, together with a thorough description of the installation, have been previously reported (Barrio et al., 2000). Those first experiments showed that the gasifier tends to stabilize at the top of the reactor, but this mode is not feasible to maintain due to the pseudo-continuous pellets feeding. Graboski and Brogan (1988) refer to the need to install a pilot flame to stabilize the firezone on top of the fuel bed. Reed and Markson (1985) also refer to the difficulties for the pyrolysis zone to reach a stable position inside a stratified downdraft gasifier, since small changes in any parameter can cause the zones to drift. As ways to stabilise the zones they suggest reducing insulation, agitation of the bed, or introducing some of the air at the desired level. A climbing pyrolysis front was also experienced with the Buck Rogers gasifier (Reed, 2000) when using very dry wood. Their solution to localize the start of the flaming pyrolysis zone and prevent it from climbing up was to distribute a fraction of the air at the desired height above the grate. Continuous operation has been reached in this investigation with a so-called near-top stabilisation mode where the air is supplied below the bed freeboard. The bed level is approximately 130 mm above the air supply.

The quality of the product gas is described by its gas composition, tar and particle content. The tar problem is accepted as one of the most important technical barriers for the penetration of biomass gasification in the power markets (Maniatis and Beenackers, 2000). A common interest among research groups working with gasification is to find tar analysis methods that are simple, reliable and that allow for comparison. This investigation presents and compares tar analysis results obtained by two methods: cold trapping with further gravimetric determination and solid adsorption method (SPA), developed at the Royal Institute of Technology (KTH).

The objective of this paper is to report the experimental results from stable operation of the gasifier and compare them with results reported in literature for similar gasifiers. Other researchers can use the experimental data presented here to validate their reactors and computational models. The design parameters for the gasifier are compared with the operational ones. The operational experience reported can orientate others in their work with small-scale gasifiers.

EXPERIMENTAL SETUP AND PROCEDURE
The gasifier is illustrated in Figure 1. The feeding system consists of a hopper and two pneumatic sliding valves and is therefore a pseudo-continuous system. The gasification agent is air, supplied from a pressurized system, dry and

URN:NBN:no-2340

clean from dust. There are 7 independent channels for air supply to the gasifier. Each air channel supplies air to a circular distributor around the gasifier. From each circular distributor five nozzles evenly distributed supply air to the reactor. The amount of air through each channel is measured with a rotameter and controlled with a valve. In addition, an air preheater has been installed before the manifold, allowing an air inlet temperature of about 225 °C at the nozzles.

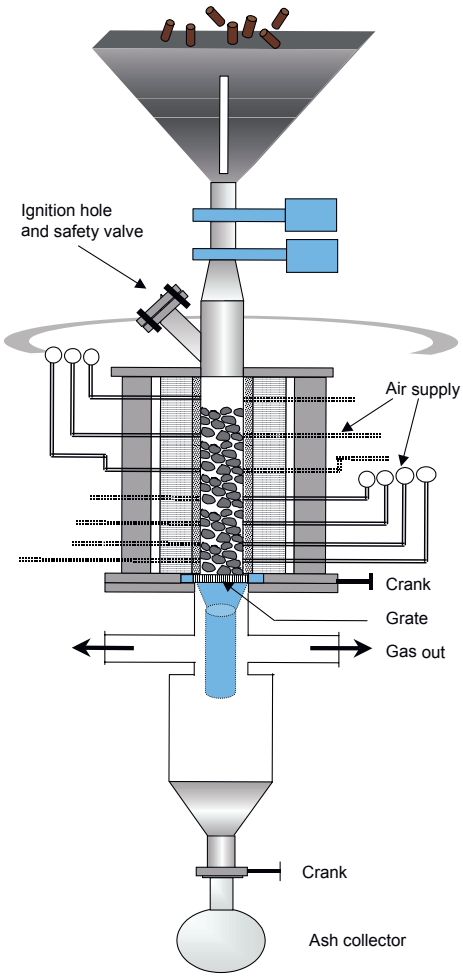

Figure 1- Stratified downdraft gasifier design.

The location of the air levels is shown in Figure 2, together with the position of the temperature measurements. The experiments reported here have been conducted using only one of the levels, situated at 310 mm above the grate (marked A2 in Figure 2).

The air pressure at the reactor is slightly above atmospheric pressure, depending on the pressure losses downstream the reactor. With this design, the amount of air entering the gasifier is well controlled although there is an increased risk of leakage.

The reactor itself is a cylinder of 100 mm diameter and 500 mm height, made of refractory ceramic. A steel cylinder of 250 mm surrounds the reactor, with glass wool filling the space between both cylinders as insulator. The steel cylinder is also covered with approx. 7 cm of insulation.

Between the feeding system and the reactor there is a view port that is used to ignite the bed and acts as well as a safety pressure release valve. The bed level has been maintained above the first temperature measurement (T1). The grate is placed between the reactor and the bottom section. Its design has been changed after the preliminary experiments. It consists now of a net made of steel of 5 mm diameter, forming square openings of 15x15mm, connected to a crank so it can be shaken manually.

The temperature inside the reactor is measured with seven thermocouples (Type K), placed only 5 mm into the bed. The temperature inside the manifold is also measured, as well as at several points at the outlet pipe. The pressure at the manifold and inside the reactor is measured with the help of pressure transducers.

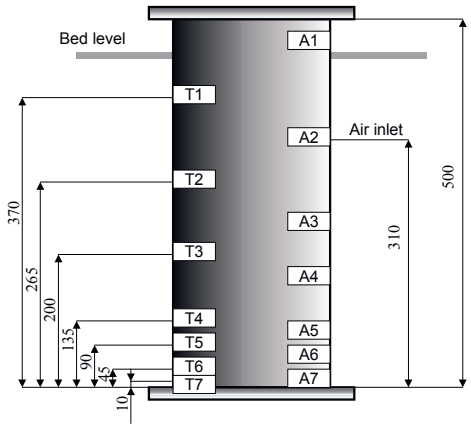

Figure 2 – Location of air nozzles and thermocouples.

Two sampling lines have been installed in order to analyse the gas quality (i.e. gas composition, tar and particle content). One of them has been built following as close as possible the “Guideline for tar analysis” produced by the working group of the Biomass Gasification Task of the IEA Bioenergy Agreement (Neeft et al., 2000; Abatzoglou et al., 2000). This sampling line was used for gravimetric tar and particle analysis and also for gas composition analysis. It is illustrated in Figure 3.

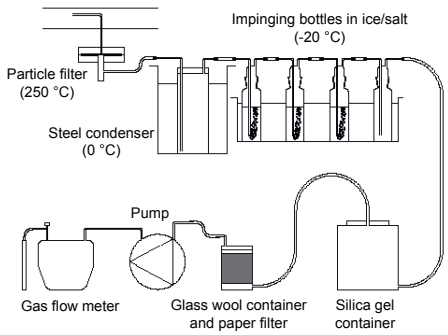

Figure 3 – Gravimetric tar sampling line (Rudberg, 2000).

A sample of 0.1 Nm^3 of product gas was extracted through the sampling line and the sampling period was of about 90 min. The condensate was then distilled using a rotavapor. Most of the acetone was first removed at a temperature of

URN:NBN:no-2340

36 °C and 10 mm Hg of vacuum. For further distillation, the temperature was increased to 41 °C, at the same pressure. The distillation process was considered finished when the weight of the condensate was nearly constant.

The solvent for the cold trap method (gravimetric tar analysis) has been acetone. Although dichlormethane presents great advantages as a solvent for tar analysis, its toxicity remains a major drawback. Acetone is widely available and inexpensive but it could form compounds with the tars and make the distillation process difficult. The selection of an adequate solvent in the "Guidelines for tar analysis" is still unclear and therefore there remains a certain lack of information and agreement regarding the distillation process of the condensate.

Some of the disadvantages of the cold trap methods are the long sampling time, the laborious tar recovery, the sample losses and the analyte segregation resulting from aerosol formation (Brague et al. 1997). It is therefore very unpractical to use gravimetric tar analysis to study the influence of operational parameters in tar formation.

The additional sampling line is dedicated for tar analysis according to the Solid-Phase Adsorption (SPA) method developed at the Royal Institute of Technology (KTH, Sweden)(Brague et al., 1997 and 2000). The SPA method is faster and easy to conduct. In addition, it provides information about the distribution of the tar components although the analysis is limited to the components for which the GC is calibrated. This sampling line consists of a T connection for the tar sampling, a steel condenser, a moisture absorber (silica gel), a filter and a pump. The gas leaving this sampling line has been used for gas composition analysis as well. The samples were collected during experiments #13a, #13b and #13c and sent to the Royal Institute of Technology (KTH), Sweden, for further analysis. In some of the samples, the syringe blocked during the sampling. This can be due to the presence of particles in the gas and could be avoided by placing a high temperature filter before the tar sampling point.

The gas composition is obtained by gas chromatography. A sample of 0.5 ml is taken from the gas sample line with a syringe and manually injected into a gas chromatograph from SRI Instruments equipped with a TCD detector and a Supelco column (Carboxen 1000). The instrument has been calibrated for H_2, N_2, CO, CH_4 and CO_2.

The experimental procedure has been similar in all the experiments. The gasifier is first preheated with air at 250 °C during approx. 16 hours. It is then filled with small pieces of charcoal until one fifth of its height. Thereafter, some few pieces of glowing charcoal are sent to allow ignition. Once the view port is closed and ignition has been observed from the temperature readings, the reactor is filled with raw pellets. Air being supplied from level A_2, the pyrolysis front climbs up through the reactor until it reaches its final position, close to air level A_2. The bed level is maintained above T_1 but its exact location is unknown because it cannot be measured. It takes approximately two hours to reach stable operation from ignition.

The fuel for this investigation is wood pellets. Pellets have quite uniform properties regarding size, composition and mechanical strength and are therefore better suited for small-scale applications. The ultimate analysis and other relevant information about the pellets are presented in Table 1.

Ultimate analysis	
C (% wt, mf)	50.7
O (% wt, mf)	42.4
N (% wt, mf)	<0.3
H (% wt, mf) by diff.	6.9
Moisture content (% wt)	7.5
Ash content (%wt, mf)	0.39
Calorific value (MJ/kg raw pellets)	18.86
Bulk density (kg/m^3)	668
Pellet diameter (mm)	6
Pellet length (mm)	6-15

Table 1 – Ultimate analysis and other fuel data.

RESULTS AND DISCUSSION

The results reported have been obtained from 8 experiments, with a total time of stable operation over 8 hours. The main results are summarized in Table 2.

Product Gas Composition

The product gas composition is presented in Table 3. The first values indicate each gas component concentration based on separate calibration. Assuming there are no other components present, the sum of volumetric concentrations should be 100%. However, this is not true for all cases. A possible reason is that the amount of sample injected into the GC column is not exactly 5ml when injecting manually (due to operator error). Variations in total sample volume have large influence on the results. The second set of gas compositions is obtained by referring the volumetric concentrations to 100%.

The error in gas concentration measurement is estimated to be 12%. This error is rather high and it is due partially to the fact that the injection of the gas sample into the chromatograph is done manually. The reduced amount of calibration points also accounts for part of the inaccuracy.

Although the composition of the product gas is quite stable, there exists some dependency on the amount of air supply, as shown in Figure 4.

Exp. Num.	#8a	#8b	#9	#12	#13a	#13b	#13c	#14	average
Amount of air (Nm^3/h)	6.98	8.18	7.64	7.44	6.04	8.84	7.45	7.56	
Feeding rate (kg/h)	6.46	6.88	5.84	5.66	4.69	7.48	6.55	5.97	
Air excess ratio	0.25	0.27	0.30	0.30	0.29	0.27	0.26	0.29	0.28
Air to fuel ratio (kg air/kg fuel)	1.40	1.54	1.69	1.70	1.66	1.53	1.47	1.64	1.58
Product gas (Nm^3/h)	11.7	14.0	12.8	12.4	10.0	14.7	12.4	12.6	
Specific gas production (Nm^3/s)/(m^2)	0.41	0.50	0.45	0.44	0.35	0.52	0.44	0.45	
Ash removal rate (kg/h)	0.02	0.02	0.06	0.06	0.10	0.10	0.10	n.a.	
Product gas/air supply ratio (Nm^3/h/Nm^3/h)	1.67	1.71	n.a.	n.a.	1.65	1.66	1.67	n.a.	1.67
Gas to fuel ratio (kg gas/kg fuel)	2.08	2.34	n.a.	n.a.	2.44	2.25	2.18	n.a.	2.26
Product gas/biomass feeding (Nm^3/kg)	1.80	2.03	n.a.	n.a.	2.12	1.96	1.90	n.a.	1.96
Specific feeding rate (kg/hm^2)	822.9	875.9	743.7	721.4	598.1	953.2	834.2	760.4	
Percentage of ash removal (%, kg ash/kg fuel)	0.36	0.33	0.96	1.00	2.10	1.32	1.50	n.a.	

Note: Exp. #9 had only preheating during 4 hours.

Table 2 – Summary of results.

URN:NBN:no-2340

Gas composition directly from GC (% vol.)						
Exp. Num.	H_2	N_2	CO	CH_4	CO_2	TOTAL
exp #8a_1	15.30	43.62	23.21	1.45	8.80	92.38
exp #8a_2	17.61	50.28	27.53	1.76	9.09	106.26
exp #8b	16.60	45.77	26.38	1.56	8.79	99.10
exp #13a_1	12.33	42.63	19.98	1.58	9.76	86.28
exp #13a_2	14.48	46.60	24.45	1.61	9.37	96.51
exp #13a_3	17.20	50.77	26.91	1.71	10.09	106.68
exp #13b	14.11	40.86	21.61	1.10	8.13	85.80
exp #13c	15.32	44.43	24.02	1.49	8.43	93.69
Gas composition adjusted to 100% (% vol.)						
Exp. Num.	H_2	N_2	CO	CH_4	CO_2	TOTAL
exp #8a_1	16.57	47.22	25.13	1.57	9.52	100.00
exp #8a_2	16.57	47.32	25.91	1.65	8.55	100.00
exp #8b	16.75	46.18	26.62	1.58	8.87	100.00
exp #13a_1	14.29	49.41	23.16	1.84	11.31	100.00
exp #13a_2	15.01	48.29	25.33	1.67	9.71	100.00
exp #13a_3	16.12	47.59	25.22	1.60	9.46	100.00
exp #13b	16.44	47.62	25.19	1.28	9.48	100.00
exp #13c	16.35	47.42	25.64	1.59	8.99	100.00

Table 3 - Product gas composition from GC analysis.

Table 4 compares the composition of the dry product gas obtained in this work with values found in literature. The carbon monoxide content of the product gas from this investigation is very high compared with other researcher's findings and the nitrogen content is relatively lower. The heating value of the product gas from this work is somewhat high compared with other references, although within the same range.

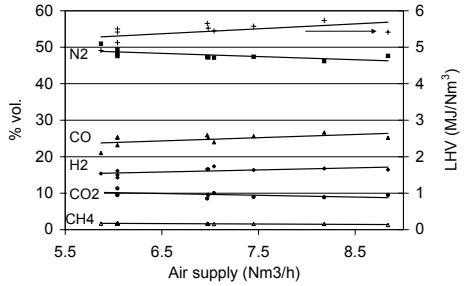

Figure 4 – Gas composition as a function of air supply.

Tar Content

The product gas was sampled for gravimetric tar analysis during experiments #12 and #13a, giving a tar content of 3 g/Nm^3. The SPA method was used during experiments #13a, #13b and #13c.

The tar content according to SPA analysis varies between 3 and 5 g/Nm^3, being the main components: benzene (55%wt. of total tar), toluene (21%), naphthalene (15%), indan (12%), phenol (11%) and o-xylene (8%). A quantitative analysis of the tar composition is beyond the scope of this work.

The two tar analysis methods agree quite well although the SPA method predicts a higher content. This tar content is quite high, compared with other gasifiers, specially stratified downdraft gasifiers. A comparison of tar analysis of several gasifiers is provided in Table 5.

Reference	CO (% vol.)	H_2 (% vol.)	CH_4 (% vol.)	CO_2(% vol.)	N_2 (% vol.)	Heating value (MJ/Nm^3)
This work	23.2-26.6	14.3-16.7	1.3-1.8	8.6-11.3	46.2-49.4	5.3-5.7
Mukunda et al.[1]	15.5-19.6	18.6-20.6	1.1-1.5	12.4-14.9	47.4-49.5	4.8-5.2[2]
Manurung and Beenackers (1993)	12-18	10-12	n.a.	12	55-58	3-5.3
Reed and Gaur (2000)	22.1	15.2	1.7	9.7	50.8	5.8
Milligan et al. (1993)	14.2-17.4	9.2-13.2	1-1.5	12.4-13.7	55.5-61.8	3.2-4.25
Walawender et al. (1985)	18-20	12-16	2.5	14-16	45-53	
Xu et al. (1997)	11.5-12.7	14.4-16.2	1.6-1.7	13.4-14.2	54.5-55.7	3.7-3.8
Schenk et al. (1997)	17-18.1	18.2-20.0	2.4	15.3-16.7	44.0-46.0	5.7-5.8
Groeneveld[3] (1980)*	18.5	17.4	1.1	12.0	51.1	
Wang and Kinoshita (1994)*	17.9-21.1	10.8-12.3	2.5-4.8	9.6-11.3	52.3-54	4.8-5.3
García-Bacaicoa et al. (1994)*	13.0-24.1	15.1-19.2	0.6-1.9	10.0-16.1	48.3-55.7	3.9-5.4

* Imbert gasifier.
[1] Dry gas composition calculated from reported Wet gas composition with 3% vol. H_2O.
[2] Calculated from Q (MJ/kg) assuming a product gas density of 1.15 kg/Nm^3.
[3] Dry gas composition calculated from reported Wet gas composition with 8% vol. H_2O.

Table 4 – Comparison of product gas composition.

Reference	Type	Tar content (g/Nm^3)	Comments
This work	Stratified	3-5	Small scale
Milligan et al. (1993)	Stratified	0.5-0.75	
Knoef (2000)	Open core	3.6-13.8	Rice husk
Schenk et al. (1997)	Stratified	0.1-1.14	
Reed (1997), ref. in Milne et al. (1998)	Stratified	0.1-1	Typical range
Mukunda et al. (1994), ref. in Milne et al. (1998)	Open core	0.04-0.1	100kW
Stassen (1995), ref. in Milne et al. (1998)		0.1-3	Typical small
Reed and Gaur (1998), ref. in Milne et al. (1998)	Stratified	0.8	Buck Rogers

Table 5 – Comparison of tar content in product gas.

URN:NBN:no-2340

In most cases, the tar content of the product gas is below 1 g/Nm^3 but higher tar contents have been reported occasionally. One of the reasons for such high content could be the very small size of the reactor and also the fact that the air is supplied to the gasifier through air nozzles and directly into the bed in order to avoid instabilities of the pyrolysis front, as already mentioned. The air distribution through nozzles might not maintain a uniformly high temperature cross-section (Graboski and Brogan, 1988). The presence of channels within the bed could also result in higher tar content of the gas (Milligan et al., 1993).

Particle Content

The particle content of the product gas has been measured to be 10.5 g/Nm^3. However, the sampling velocity was only about 20-25% of the velocity required for isokinetic sampling and this could affect the measurement considerably. The reason for lower sampling velocity was that a large amount of the solvent was carried out of the impinging bottles when sampling at the required velocity for isokinetic sampling. Some large particles (1mm) were found in the filter, probably due to the rather large openings of the grate. Although such grate design could result in a higher char loss (not observed in this investigation), it favours a low pressure drop through the grate.

The lack of continuous ash removal system will become a problem for long duration experiments, since the ashes not deposited at the ash bottle could entrain the gas flow and increase the particle content of the product gas.

Temperature Profile

The temperature profile inside the gasifier has been obtained from all the experiments, as presented in Figure 5.

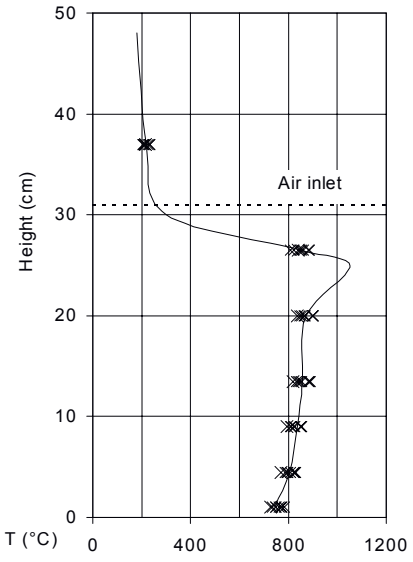

Figure 5 – Temperature profile inside the gasifier.

The pyrolysis temperature is unknown as well as its exact location. The solid line in Figure 5 represents only a possible location of the flaming pyrolysis zone based on the temperature history. It is believed that the flaming pyrolysis zone is located near T_2 because of the high instability of this temperature measurement, typical of the flaming pyrolysis zone where the temperature difference between the solid particles and the gas can be of 500 °C (Reed et al, 1983). Furthermore, being T_2 lower than T_3 in most experiments could indicate that the flaming pyrolysis is below T_2. The temperature profiles are very similar in shape and the maximum temperature difference between experiments is of about 70 °C. This temperature difference can be explained partially by the differences in air supply and partially by differences in operating time before stable operation is reached.

The comparison of temperature profiles among researchers is difficult because of the differences in geometry and the uncertainty regarding the position of the pyrolysis front in this investigation. Nevertheless, it is interesting to compare the temperature profiles reported in literature with the results from this investigation, assuming the location of the pyrolysis zone 255 mm above the grate (Figure 6). All references report higher temperatures at the char reduction zone. The results from Manurung et al. (1993) correspond to a bed height of 0.5 m and a specific feeding rate of 296.23 kg/hm^2 and those from Milligan et al. (1993) refer to the insulated reactor.

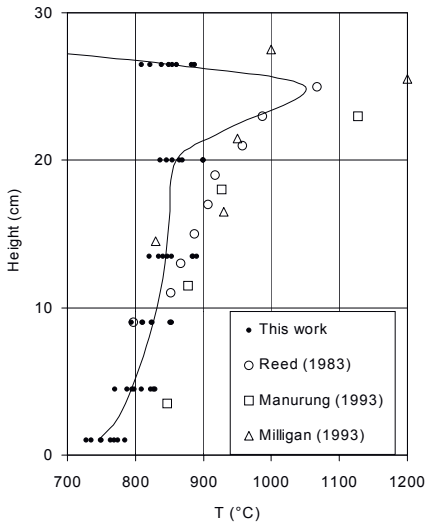

Figure 6 – Comparison of gasification temperatures.

Operational parameters

As previously reported by other researchers (Reed et al. 1983), (Garcia-Bacaicoa, 1994), the air excess ratio does not depend on the air supply to the reactor. This investigation also proves this assertion although the accuracy of the measurement is very low because of the high uncertainty of the bed level. Figure 7 shows the air excess ratio and the biomass feeding rate as a function of air supply. The air excess ratio varies between 0.25 and 0.3, independent of the air supply. The biomass feeding rate increases linearly with air supply, as it should be expected if the air excess ratio is constant.

The amount of product gas is calculated from the air supply and the N_2 content of the product gas, assuming for the calculation that all N_2 in air goes through the reactor without transformation. This might not be true if one considers the formation of NO_x, but it is a reasonable approximation. The gas-to-fuel ratio is an important operational parameter as well as the air-to-fuel ratio. Both

URN:NBN:no-2340

ratios have been calculated and show a rather constant value, independent of gasifier load. (Figure 8).

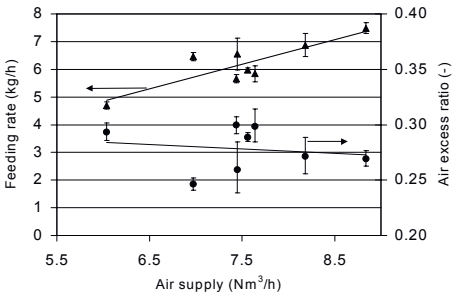

Figure 7 – Feeding rate and air excess ratio as a function of air supply.

Table 6 presents a comparison of operational parameters found in literature. It is remarkable the variation in specific feeding rate and, on the contrary, the close values for the air to fuel ratio (most values lie between 1.5 and 2.0). The specific feeding rate for this investigation is clearly higher than most of the reported values.

The gas yield and the gas to fuel ratio are also relevant design and operation parameters. The table below (Table 7) compares values found in literature with the present work. The gas to fuel ratio varies between 2 and 3 Nm^3/kg and the value from this work is among the lowest values.

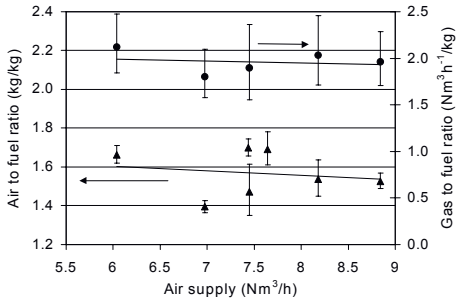

Figure 8 – Air to fuel and gas to fuel ratio as a function of air supply.

Design versus Operational Parameters

The design parameters used for the construction of the gasifier are presented in Table 8 together with the operational parameters.

The main design parameters were the thermal input (or the fuel feeding rate), the gas to fuel ratio, the air excess ratio and the gas velocity at gasifier temperatures. The gas to fuel ratio was selected according to the recommendations of Reed and Das (1988). It was also desired to test for variations in air excess ratio. The rest of the design parameters as well as the gasifier diameter are a consequence of the main design parameters.

A preliminary calculation of the length of the pyrolysis and the char reduction zone was done (Reed and Levie, 1984), giving values of 30-60 mm for each zone.

Reference	Gasifier diameter (mm)	Fuel	Feeding rate (kg/h)	Specific feeding rate (kg/m^2h)	Air supply (Nm^3/h)	Air to fuel ratio (kg/kg)	Air excess ratio
This work	100	Wood pellets	4.7-7.5	600-950	6-8.8	1.4-1.7	0.25-0.30
Manurung et al. (1993)	450	Rice husk	8-54	50-300 optimal: 25-175	7.9-79.5[a]	1.6-2.2[a]	n.a.
Graboski and Brogan (1988)[b]	762	Wood chips	530-665	1160-1459[a]	820-1010	2.0[a]	n.a.
Reed and Gaur (2000)[c]	1000	Wood chips	96.2	123[a]	140.3	1.5[a]	n.a.
Milligan et al. (1993)	75	Wood chips	1.2-1.4[a]	276-320.5	n.a.	n.a.	0.36-0.39
Schenk et al. (1997)	400	Willow	41.2-56.9	328-453	45.8-68.6	1.4-1.6	n.a.
García-Bacaicoa et al. (1994)[d]	500	Wood chips	25-50	1019 (at throat)	40-70	1.8-2.2	0.25-0.32
Wang (1994)[d]	n.a.	Wood chips	23-30	n.a.	38.3-40.5	1.6-2.1[a]	0.24-0.31

[a] Values calculated from information available in the reference.
[b] Syngas gasifier.
[c] Buck Rogers gasifier.
[d] Imbert gasifier.

Table 6 – Comparison of operational parameters.

Reference	Gas yield (Nm^3/h)	Gas to fuel ratio (Nm^3 gas/kg fuel)	Specific gas production (Nm^3/m^2s) (or superficial velocity)
This work	9.9-14.7	1.8-2.1	0.35-0.52
Graboski and Brogan (1988)[b]	1416-1710	2.6-2.7[a]	1.71 (Reed and Gaur, 2000)
Reed and Gaur (2000)[c]			0.28
Reed and Gaur (2000)[d]	1113-1396[a]	2.1[a]	0.13-0.23 (Reed and Das, 1988)
Milligan et al. (1993)	3.5-4.2[a]	2.94-2.98	0.14-0.16[a]
Xu et al. (1997)	470	1.8	
Schenk et al. (1997)	99.9-137.9	2.4[a]	0.22-0.30[a]
Garcia-Bacaicoa et al. (1994)[e]	65-117	2.6[a]	0.48 (at throat)
Groeneveld (1980)[e]		2.98	
Wang and Kinoshita (1994)[e]		1.9-2.5	

[a] Values calculated from information available in the reference.
[b] Syngas gasifier.
[c] SERI gasifier.
[d] Buck Rogers gasifier.
[e] Imbert gasifier.

Table 7 – Comparison of gas yield and gas to fuel ratio.

URN:NBN:no-2340

The operational gas to fuel ratio is slightly lower than expected and the variation in air excess ratio is not possible, as already explained.

Parameters	Design	Operation
Thermal input (kW_{th})	25-30	24.5-39.2
Fuel feeding rate (kg/h)	5-6	4.3-6.9
Expected gas production (kg/kg)	2.50	2.08-2.44 (aver. 2.26)
Expected gas production (kg/h)	12-15	11.5-16.6
Expected gas production (Nm^3/h)	9-11	10.0-14.7
Specific gas production (Nm^3/m^2s)	0.3-0.4	0.35-0.52
Gas velocity at gasifier temp(m^3/m^2s)*	3.3-4.6	3.4-6.0
Air excess ratio	0.2-0.7	0.25-0.3
Expected air consumption (Nm^3/h)	5-16	6-8.8
Specific feeding rate (kg/m^2h)	600-750	600-950
Air to fuel ratio (kg air/kg fuel)	1.3-4.5	1.4-1.7(aver. 1.6)

* Gasifier temp. 700-900 °C, air void fraction: 36.9%

Table 8 – Design vs. operation parameters.

The gasifier has been operated successfully at higher fuel feeding rates than initially designed. However, high gas velocities inside the gasifier produced a higher pressure drop through the reactor and leakage and should be avoided. The performance of the gasifier could have been improved by increasing the reactor diameter.

Mass and Energy Balances

The mass flow input and output rates are summarized in the table below (Table 9). The ash was collected from the glass bottle at the end of each experiment. Although most of the ash left the char bed when shaking the grid, it has been approximated as a constant output rate. The water content of the product gas has been obtained from the molar balance of Oxygen.

Operation of the Reactor

- It has been found very difficult to operate the gasifier without bed level measurement. In addition, the calculation of the feeding rate is rather inaccurate, unless the experiments are very long. Nevertheless, the variation in bed level does not affect the gasification process as far as the raw pellets cover the flaming pyrolysis zone (i.e. the bed level is above the air supply).
- Long experiments are limited because of not having a continuous removal of ash.
- Radial air supply below the bed freeboard is necessary for stabilization reasons. This gasifier cannot operate in top-stabilisation mode because of the pseudo-continuous biomass feeding. This can lead to higher tar production and uneven pyrolysis temperature.
- The difficult stabilization of the zones is a clear drawback for stratified downdraft gasifiers.

Exp. Number	#8a	#8b	#9	#12	#13a	#13b	#13c	#14
Dry biomass feeding rate (kg/h)	5.97	6.36	5.40	5.24	4.34	6.92	6.06	5.52
Water feeding in the biomass (kg/h)	0.48	0.52	0.44	0.42	0.35	0.56	0.49	0.45
Air feeding rate (kg/h)	9.02	10.58	9.88	9.62	7.81	11.43	9.63	9.78
Ash rejected (kg/h)	0.02	0.02	0.06	0.06	0.10	0.10	0.10	n.a.
Product gas rate (Nm^3/h)	11.66	13.99	12.77	12.43	9.95	14.67	12.41	12.63
Product gas rate (kg/h)	13.42	15.94	14.62	14.26	11.55	16.62	14.23	14.47
LHV(MJ/Nm^3)	5.43	5.60	5.52	5.50	5.31	5.69	5.50	5.51
Tar content (g/Nm^3)	3.00	3.00	3.00	3.00	3.00	3.00	3.00	3.00
Tar content (kg/h)	0.03	0.04	0.04	0.04	0.03	0.04	0.04	0.04
Particulate (g/Nm^3)	10.50	10.50	10.50	10.50	10.50	10.50	10.50	10.50
Particulate mass rate (kg/h)	0.12	0.15	0.13	0.13	0.10	0.15	0.13	0.13
Water out (kg/h)	1.57	1.38	1.09	1.05	0.94	1.68	1.51	1.17
Output mass/input mass (%)	**98.0 %**	**100.4 %**	**101.4 %**	**101.6 %**	**101.7 %**	**98.3 %**	**98.9 %**	**100.5 %**
Cold gas efficiency(%)	**52.0 %**	**60.4 %**	**64.0 %**	**64.0 %**	**59.7 %**	**59.1 %**	**55.3 %**	**61.9 %**

Table 9 – Mass and energy balance of the gasifier.

CONCLUSIONS

- The stratified downdraft gasifier at the Norwegian University of Science and Technology has been operated under stable conditions using wood pellets as fuel.
- The product gas contains in average 16% vol. H_2, 25.3% CO, 1.6% CH_4, 9.5% CO_2 and 47.6% N_2 and has a low heating value of 5.3-5.7 MJ/Nm^3. The CO content is especially high compared with other investigations.
- The tar content of the product gas is 3 g/Nm^3 and the particle content of about 10.5 g/Nm^3. Similar gasifiers present in general lower tar content.
- The temperature measured at the char reduction zone of the gasifier varies between 750 °C and 900 °C. The temperature and location of the flaming pyrolysis zone is unknown but has been predicted.
- The air excess ratio varies between 0.25 and 0.3 and it is independent of the gasifier load. The air to fuel ratio and the gas to fuel ratio are about 1.6 kg air/kg fuel and 2.3 kg gas/kg fuel respectively, also independent of load.

SUGGESTIONS FOR FURTHER WORK

- The design of the gasifier allows for variation of the air supply location. Using air at several levels simultaneously could increase the performance of the reactor and lower the tar production.
- Partially replacing the air by steam would increase of H_2 content of the product gas and compensate for the low moisture of the pellets.

ACKNOWLEDGMENTS

This project is financed by the Norwegian Research Council. The authors want to thank the valuable help of José M. Granados, Mathias Olschar and Øyvind Rudberg.

REFERENCES

Abatzoglou, N. et al. (2000). The development of a draft protocol for the sampling and analysis of particulate and organic contaminants in the gas from small biomass gasifiers, *Biomass and Bioenergy*, Vol. 18, pp. 5-17.

Barrio, M. et al. (2000). A small-scale stratified downdraft gasifier coupled to a gas engine for combined heat

URN:NBN:no-2340

and power production, *Progress in Thermochemical Biomass Conversion*, Tyrol, Austria, 17-22 September 2000.

Brague, C. et al. (1997). Use of amino phase adsorbent for biomass tar sampling and separation, *Fuel*, Vol. 76, No. 2, pp. 137-142.

Brague, C. et al. (2000). Tar evolution profiles obtained from gasification of biomass and coal*, Biomass and Bioenergy*, Vol. 18, pp. 87-91.

Di Blasi, C. (2000). Dynamic behaviour of stratified downdraft gasifiers, *Chemical Engineering Science*, Vol. 55, No. 15, pp. 2931-2947.

Gabroski, M.S. and Brogan, T.R. (1988). Development of a downdraft modular skid mounted biomass/waste gasification system, *Energy from Biomass and Wastes XI*, Institute of Gas Technology, Orlando March 16, 1987. Edited by Klass, D.L.

García-Bacaicoa, P. et al. (1994). Scale-up of downdraft moving bed gasifiers(25-300 kg/h) - design, experimental aspects and results, *Bioresource Technology*, Vol. 48, pp. 229-235.

Groeneveld, M.J. (1980). *The co-current moving bed gasifier*, Ph. D. thesis, Twente University of Technology, Enschede, Netherlands.

Knoef, H.A.M. (2000). The UNDP/World Bank monitoring program on small scale biomass gasifers (BTG's experience on tar measurements), *Biomass and Bioenergy*, Vol. 18, pp. 39-54.

Maniatis, K. and Beenackers, A.A.C.M. (2000). Introduction. Tar protocols. IEA Bioenergy Gasification Task, *Biomass and Bioenergy*, Vol. 18, pp. 1-4.

Manurung, R.K. and Beenackers, A.A.C.M. (1993). Modeling and simulation of an open core down-draft moving bed rice husk gasifier, *Advances in Thermochemical Biomass Conversion*, Ed. A.V. Bridgwater, UK, pp. 288-309.

Milligan, J.B. et al. (1993). Results from a transparent open-core downdraft gasifier, *Advances in Thermochemical Biomass Conversion*, Ed. A.V. Bridgwater, UK, pp. 175-185.

Milne, T.A. et al. (1998). *Biomass gasifier "Tars": Their nature, formation, and conversion*. NREL/TP-570-25357, ISBN 1-890607-15-6.

Mukunda, H.S. et al. Results of an Indo-Swiss programme for qualification, testing of an 300 kW IISc-Dasag gasifier, Indian Institute of Science, Bangalore, Department of Aerospace Engineering, *http://144.16.65.129/~cgplhome/new_papers.html.*

Neeft, J.P.A. et al. (2000). Guideline for sampling and analysis of "tars" and particles in biomass producer gases, *Progress in Thermochemical Biomass Conversion*, Tyrol, Austria, 17-22 September 2000.

Reed, T.B. et al. (1983). A mathematical model for stratified downdraft gasifiers*, American Chemical Society, Preprints of papers, Division of fuel chemistry*, Vol. 28, No. 5, pp. 410-420.

Reed, T.B. and Levie, B. (1984). A simplified model of the stratified downdraft gasifier, *International Bio-Energy Directory and Handbook*, pp.379-390.

Reed, T.B. and Markson, M. (1985). Biomass gasification reaction velocities, *Proc. of FPRS industrial wood energy forum '83*, No.7, Vol. 2, pp. 355-365.

Reed, T.B. and Das, A. (1988). *Handbook of biomass downdraft gasifier engine systems*, The Biomass Energy Foundation Press, 1810 Smith Rd., Golden, CO. 80401.

Reed, T.B. and Gaur, S. (2000*). A survey of biomass gasification 2000*, The Biomass Energy Foundation, Inc., 1810 Smith Rd., Golden, CO. 80401.

Rudberg, Ø. (2000). *Theoretical and experimental investigation of a granular filter coupled to a biomass gasifier*, Diploma report, Institute of Thermal Energy and HydroPower, Norwegian University of Science and Technology (NTNU), Norway.

Schenk, E.P. et al. (1997). Biomass gasification research in fixed bed and fluidised bed reactors*, Gasification and Pyrolysis of Biomass*, ECNRX97011, Stuttgart, April 1997.

Walawender, W.P. et al. (1985). Wood chip gasification in a commercial downdraft gasifier, *Fundamentals of Thermochemical Biomass Conversion*, pp. 911-921. Eds. R.P. Overend, T.A. Milne and L.K. Mudge. Elsevier, Amsterdam.

Wang, Y. and Kinoshita, C.M. (1993). Temperature fields in downdraft biomass gasification, *Advances in Thermochemical Biomass Conversion*, Ed. A.V. Bridgwater, UK, pp. 280-287.

Xu, M. et al. (1997). Research on straw waste gasification and application in straw pulp mill, *Developments in Thermochemical Biomass Conversion*, Eds. A.V. Bridgwater and D.G.B. Boocock, UK, pp 892-899.

URN:NBN:no-2340

PAPER III

OPERATIONAL EXPERIENCES FROM A SMALL-SCALE
BIOMASS GASIFIER COUPLED TO A GAS ENGINE

Presented at:

First Biennial Meeting
Organized by:
The Scandinavian-Nordic Section of the Combustion Institute
18-20 April 2001
Chalmers University of Technology,
Göteborg, Sweden

URN:NBN:no-2340

URN:NBN:no-2340

Operational Experiences from a Small-scale Biomass Gasifier coupled to a Gas Engine.

Morten Fossum[#], Maria Barrio and Johan.E. Hustad
Norwegian University of Science and Technology, Department of Thermal Energy and Hydro Power, 7491 Trondheim, Norway
[#]Sintef Energy Research, Department of Thermal Energy, 7465 Trondheim, Norway

ABSTRACT.

A small scale (30 kW thermal input) stratified downdraft gasifier is erected in the laboratory at the Norwegian University of Science and Technology (NTNU). The gasifier is coupled to a gas engine for production of heat and power from biomass fuels. The paper describes the gasifier in detail (500 mm height and 100 mm diameter). One of the singularities of the gasifier design is that it allows for variation of the point of air injection and that air preheating is also possible. The gas engine was originally a diesel engine but it has been modified for producer gas and/or natural gas operation. These changes mainly affect the compression ratio and the fuel injection system. The paper describes the gas engine and explains the modifications.

Experiments have been performed of gasification of wood pellets. The feeding rate was about 5 kg/h, giving an effect of 30 kW. The amount of air supplied to the reactor has been varied in the experiments, in addition to the location of the supply. Temperatures are measured inside the reactor to identify the reaction front and a temperature distribution at stable operation. Mass and energy balances are performed for the reactor. The fuel gas composition has been measured with a GC. The amount of product gas obtained is about 12.5 Nm^3/h and has a heating value of 4.9 MJ/Nm^3. The gas composition as a function of air amount and equivalent ratio is further documented.

The gas engine operates on the synthesis gas and further with mixtures of synthesis gas and natural gas and detailed measurements of cylinder pressure, compression ratio and heat released by the engine are performed. Energy balances show shaft efficiencies varying from 18 % to 25 %. Emission measurements of CO and NO_x are performed and show values from 6 to 18 g/kWh for CO and 0.2 to 16 g/kWh for the NOx emissions dependent of the ratio of synthesis gas/natural gas.

SYSTEM DESCRIPTION

The integrated biomass gasifier and gas engine system that has been build at SINTEF/NTNU includes a downdraft biomass gasifier, gas condenser and filter unit and a gas engine as depicted in Figure 1.

The gasification unit is a down draft reactor design with an inner diameter of 100 mm and a height of 500 mm. Gasification agent can be supplied at 7 vertical levels and each level includes 5 nozzles. Temperatures in the reactor are measured at seven vertical positions and also in the gas exit of the reactor. Static pressure is measured at four vertical levels in the reactor and also in the gas exit chamber. A more detailed description if the gasifier is given in previous publications [1].

URN:NBN:no-2340

The condenser unit includes 3 parallel concentric tubes with producer gas flowing in the inner tube and cooling water in the outer part. The inner diameter of the gas tube is 50 mm and the height is 2000 mm.

The filter unit consists of conical inlet and exit parts with a cylindrical section in the middle with an inner diameter of 200 mm and a height of 900 mm. In the filter unit the gas is led through a bed of charcoal with a height of 250 mm and a 50 mm layer of low density insulation material.

The gas engine is a three cylinder Zetor diesel engine modified for the use of gaseous fuels. The modifications include a reduction of the compression ratio down to 11:1. In addition an ignition system is installed which include replacement of the diesel injection nozzles with spark plugs and separate high voltage supply for each spark plug. Instrumentation of the engine includes temperature measurements of the exit and outlet cooling water, gas inlet and exhaust outlet temperatures and cooling water volume flow. A sensor system for detecting the crank angle and rotation speed is also installed.

The gas engine is connected to a gas supply system, which allows supply of natural gas and mixtures of natural gas, and major gas components found in producer gas (CO, H_2, CH_4, N_2 and CO_2).

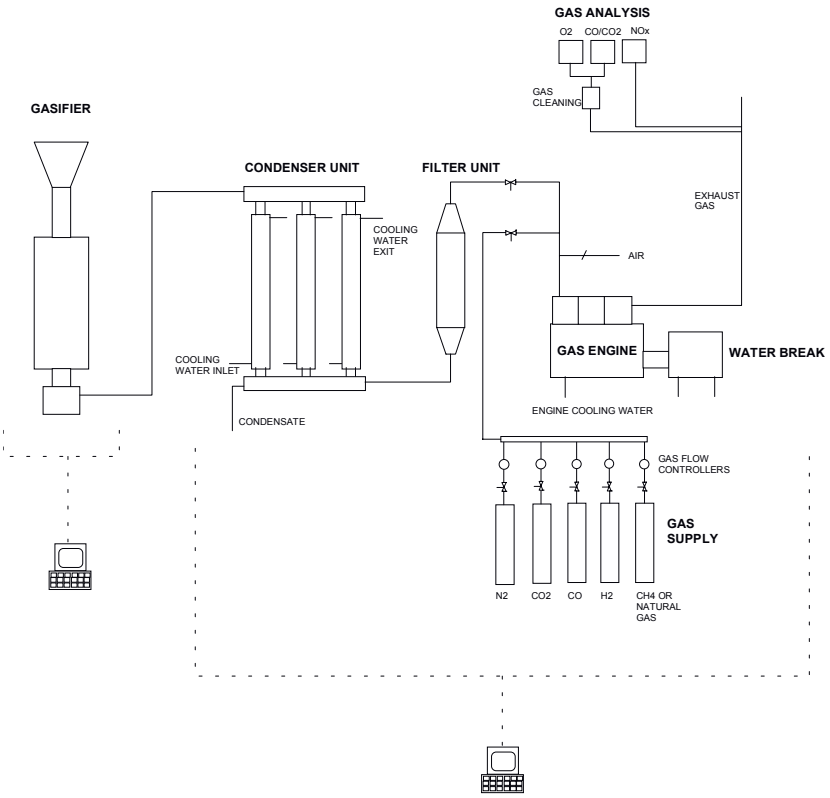

Figure 1. Schematic description of the gasifier and gas engine system.

URN:NBN:no-2340

EXPERIMENTAL RESULTS

The integrated system as depicted in Figure 1 is at the moment in the final stage of construction. The experimental work so far has been aimed at operation of the gasifier and performances of the gas engine operated with different gas mixtures. The presentation of the experimental results is thus dived in two sections.

Operation of the gasifier

The gasifier has been operated with biomass pellets with a diameter of 8 mm and length in the range of 5-15 mm. The pellets are relatively dry with a moisture content of about 8%.

The gasifier is operated with preheated air at about 250 ^{0}C and has so far been operated at the following conditions with respect to air supply:

- 100% air supply at the uppermost nozzles (nozzle row 1).
- 80% air supply at the top and 20% at the nozzle row number 4.
- 20% air supply at nozzle row number 1 and 80% at nozzle row 4.
- 100% air supply at second upper nozzles (nozzle row number 2).

In stratified downdraft gasifiers the fuel bed can be divided in several zones, a preheating and drying zone at the top, a pyrolysis zone or flaming pyrolysis zone followed by a charcoal reduction zone and finally a non-reacting charcoal zone above the grate. The position of the different zones can be approximated from the temperature measurements. If the pyrolysis rate is equal to the char consumption rate the position of the zones will be fixed. However, with dry fuel the pyrolysis zone tends to move upwards and finally the flaming pyrolysis zone will be at the top of the fuel bed. This operation is stable, but the radiation from the top increases the heat losses from the reactor and also the feeding system can be affected by the radiation. This phenomenon was observed for the three first operation conditions. By moving the air supply to nozzle row number 2 the flaming pyrolysis zone could be stabilised under the top of the fuel bed and the gasifier could be operated for hours in continuos and stable conditions.

A typical temperature profile inside the reactor is shown in Figure 2. Temperature T1 is at the top of the gasifier and temperature T7 is just above the grate.

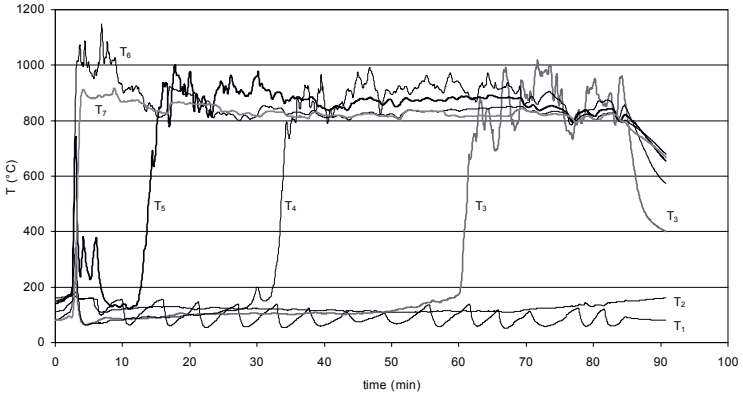

Figure 2. Temperature profile in the gasification reactor.

URN:NBN:no-2340

The composition of the product gas from the gasifier is analysed on a GC. Before sampling the gas is cooled down to separate condensables and filtrated for separation of tars and particles. An approximate gas composition is shown in Table 1.

Table 1. Approximate product gas composition.

Component	Volume fraction (%)
Hydrogen (by difference)	20.9
Carbon monoxide	20.6
Methane	0.0
Nitrogen	46.8
Carbon dioxide	10.2
Oxygen	1.5

Operation of the gas engine

The purpose of this first series of experiments was to observe the performance of the engine for different gas mixtures and gas qualities. The experimental matrix includes gas mixtures as shown in Table 2.

Table 2. Gas mixtures included in the gas engine experiments (vol. %)

Component	Gas 1	Gas 2	Gas 3	Gas 4	Gas 5
CO	19.5	18	12	6	0
CH_4	0.0	27	49	72	100
H_2	19.0	11	7	6	0
CO_2	15.0	8	7	4	0
N_2	46.5	36	25	12	0

Gas 1 represents a gas quality and composition comparable to what is expected from downdraft gasifiers as the unit described above. Gas 2, 3 and 4 represents mixtures of natural gas and LCV gases and Gas 5 is100% methane. As methane is the major component in natural gas the term natural gas is related to methane. It should be mention however, that some experiments were conducted with natural gas with a sale gas quality and composition and the results were similar to the results using methane.

The results clearly show the dependency of the methane content in the gas mixture with respect to the NO_x emission. For the LCV gas quality, Gas 1, the NO_x emission was found to be 42 mg/Nm^3 or 0.2 g/kWh while the NO_x emission for methane was found to be in the range of 650-2300 mg/Nm^3 or 7-16 g/kWh as shown in Figure 2.

The similar dependency for the emission of CO was observed. The emission of CO was found to be very high for the LCV gas, 3500 mg/Nm^3 or 18.7 mg/kWh, while the CO emission for methane was found to be about 570 mg/Nm^3 or 7 mg/kWh as can be seen from Figure 3.

URN:NBN:no-2340

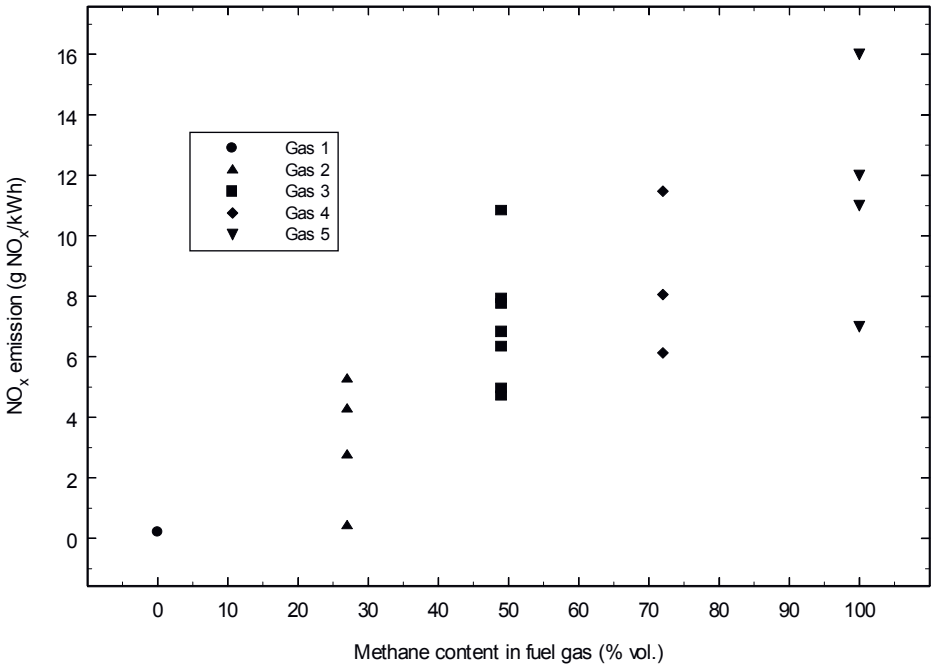

Figure 2. NO_x emission as a function of the methane concentration in the fuel gas.

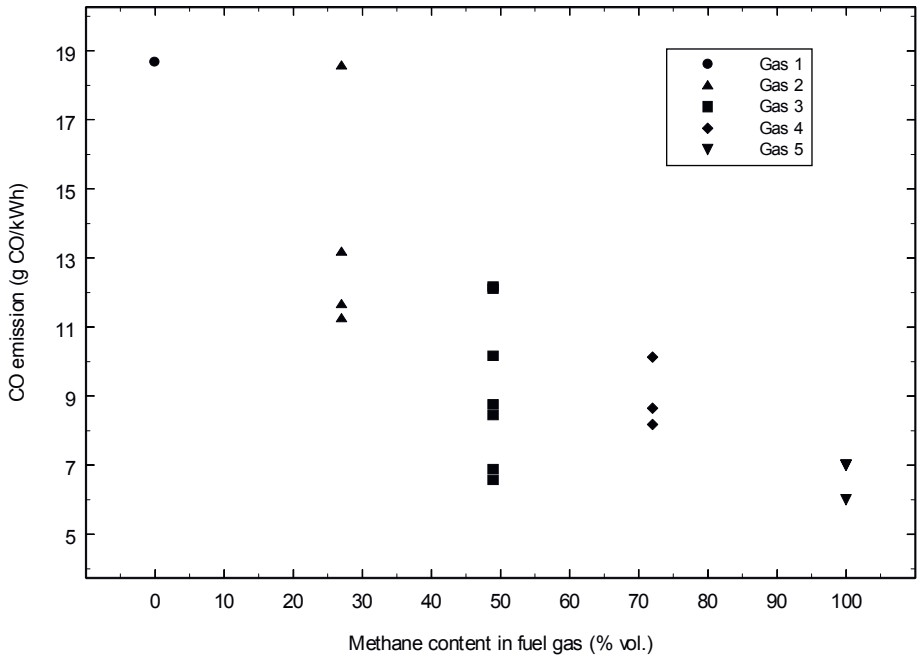

Figure 3. CO emission as a function of the methane concentration in the fuel gas.

URN:NBN:no-2340

The variations in emissions of NO_x and CO are due to variations in excess air ratios, rotation speed and engine load. The experiments with Gas 2 are conducted with 1500 rpm ± 3% and a load of 56 Nm ± 5.5% and a excess air ratio in the range of 1.05 to 1.53. The results show that the emission of CO increases from 11.24 g/kWh at an excess air ratio of 1.05 to 18.56 g/kWh at the highest excess air ratio. At the same time the emission of NOx decreases from 5.27 g/kWh to 0.42 g/kWh. The similar trend in emission of CO and NOx is also noticed for the experiments wit Gas 3, 4 and 5.

The break thermal efficiency fir these experiments was found to vary in the range of 18 to 25% as shown in Figure 4. As the thermal input for the different experiments varies, these efficiencies should be regarded as indicative and should not be compared directly. The thermal input for Gas 1 was 13.6 kW, for Gas 2 44.2 kW, Gas 3 69.2 to 82.0 kW, Gas 4 112.8 to 114.5 kW and for Gas 5 85.9 to 125.6 kW.

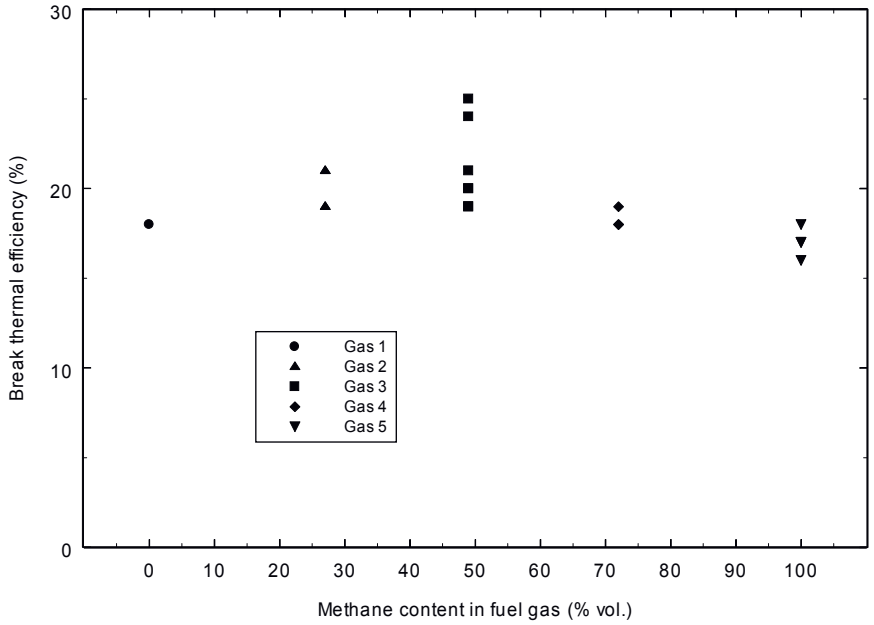

Figure 4. Break thermal efficiency as a function of the methane concentration in the fuel gas.

All the reported experiments are conducted with fixed ignition timing at 20 deg. before top dead centre (BTDC). Further work is planned to optimise also the ignition timing for the given gas quality and gas composition. Especially for LCV gas qualities the engine should be operated with a more advanced timing for improving the combustion efficiency.

References

1. Barrio, M., Fossum, M., Hustad, J., E. A small-scale stratified downdraft gasifier coupled to a gas engine for combined heat and power production. Presented at PITCH 2000, To be published in the PITCH conference proceedings.

URN:NBN:no-2340

3. REACTIVITY STUDIES

3.1 INTRODUCTION

This chapter contains all the experimental work related to the chemical reactions that take place in the char gasification zone. In order to study the chemical reactions only, it is important to use an experimental technique where no heat or mass diffusion are present and where both temperature and atmosphere are controlled. This experimental technique is called Thermogravimetry and consists basically of analysing the weight loss of a small char sample placed inside an oven at controlled temperature, surrounded by a gas whose composition is also controlled by the user. The rate of mass loss depends on temperature, gas composition, degree of conversion and on the intrinsic kinetic parameters of the chemical reaction taking place.

As already mentioned in Chapter 1, several reactions take place simultaneously during char gasification. This Ph. D. study has concentrated on the most relevant heterogeneous reactions:

- Steam gasification $C(s) + H_2O \rightarrow CO + H_2$
- CO_2 gasification $C(s) + CO_2 \rightarrow 2CO$

The above expressions are the overall reactions. Each of them consists of several reaction steps where surface complexes are formed. In addition, each reaction is affected by the presence of other gases in the surrounding atmosphere. For instance, H_2 and CO are known to inhibit the char gasification reactions.
The existing literature about these reactions is not abundant and it is rather scarce regarding inhibition effects or reaction mechanisms.

Finally, it was considered of interest to study not only each char gasification reaction by itself (Paper IV and Paper V) but also the simultaneous gasification in steam and carbon dioxide (Paper VI) in order to study the interaction between both reactions.

URN:NBN:no-2340

3.1.1 OBJECTIVES

The main objectives of these reactivity studies have been:

1. Identify the reaction mechanisms that explain best the experimental results, including the inhibition effect of CO and H_2, but with a fundament in theory.
2. Find a model that relates the mass loss rate to the temperature, gas composition and degree of conversion for each reaction.
3. Supply the experimental information related to chemical reactions necessary for the modelling of a gasification process.

3.2 EXPERIMENTAL INFORMATION

3.2.1 EXPERIMENTAL APPARATUS

Two instruments have been used during this work: a SDT 2960 Simultaneous Thermogravimetric Analyser –Differential Thermal Analyser (TGA-DTA) at our laboratory (Paper V) and a Pressurised Thermogravimetric Analyser (PTGA) at Reatech (Denmark) (Paper IV and Paper VI). A description of each instrument is presented at the respective papers and further references are given there. The following comments refer to the comparison between both apparatus. The main difference between the two is that the PTGA at Reatech admits steam as a gasification agent while the SDT at NTNU does not. The use of steam imposes serious requirements to the equipment, like heated gas lines to avoid steam condensation. In addition, the weighting system has to be especially isolated to avoid the steam.

The PTGA was modified from its original configuration in order to admit steam. It also admits H_2, CO_2, N_2, CO and mixtures of these gases. The following picture (Figure 3.1) shows the experimental setup of the PTGA at Reatech (Denmark).

The operation of the PTGA is complex mainly because of the presence of steam but also because of a rather unfriendly and limited interface between the user and the PTGA control system.

URN:NBN:no-2340

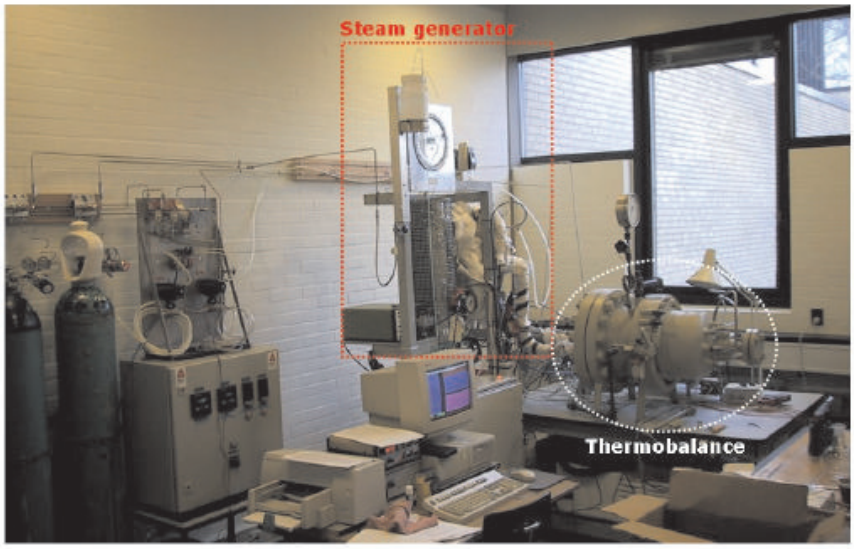

Figure 3.1: PTGA experimental installation

The SDT is a more modern equipment that can operate with N_2, CO_2, CO, O_2 and mixtures. The unit is more compact and the control system is very user friendly. The software of the SDT is far more advanced, what eases for example the calibration process. The SDT at our laboratory is shown in Figure 3.2.

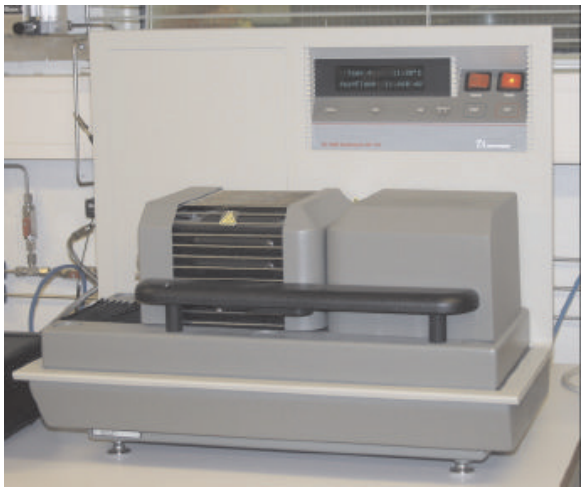

Figure 3.2: SDT experimental installation

URN:NBN:no-2340

Other differences between the equipments are:

- The SDT has two arms: one for the reference and one for the sample. The PTGA only has one arm.
- The two thermocouples are located one under each crucible in the SDT. The PTGA also has two thermocouples, one in the near vicinity of the sample, but not in touch, and the other just some millimetres apart.
- The SDT-TGA uses cups of alumina or platinum. Alumina has been preferred for the CO_2/CO experiments. The PTGA uses one crucible of platinum. The material of the cup or crucible might have had some minor influence in the results.

Figure 3.3 and Figure 3.4 show the location of the thermocouples in each system.

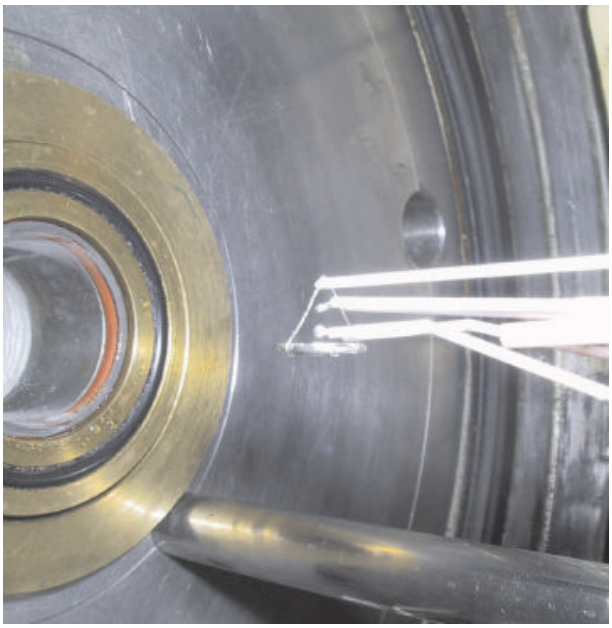

Figure 3.3: Location of crucible and thermocouples in the PTGA

URN:NBN:no-2340

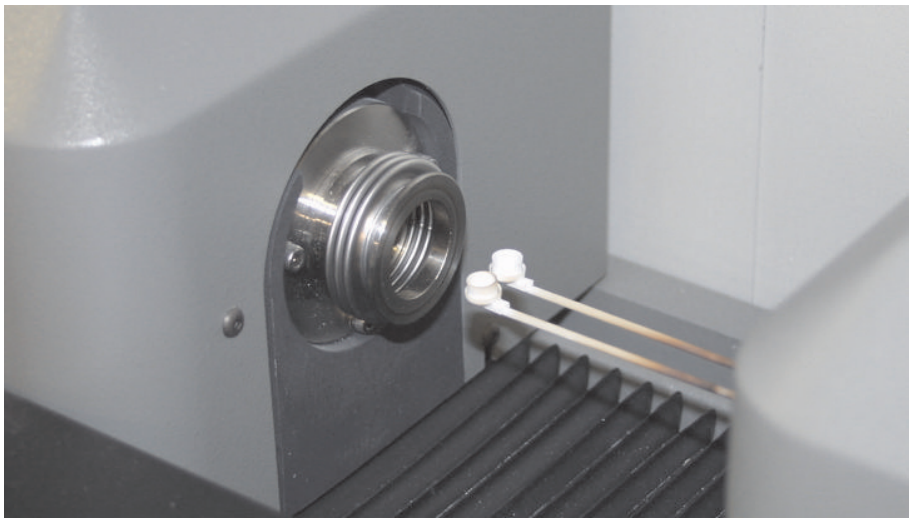

Figure 3.4: Location of crucible and thermocouples in the SDT

3.2.2 CALIBRATION PROCEDURES

This section describes the calibration of the apparatus used for the investigation: the SDT 2960 at NTNU and the PTGA at Reatech (Denmark). The calibration should cover the temperature range of the experiments and should be conducted at the same heating rates than the experiments. Ideally, the calibration should also use the same gases as during the experiments. However, it was considered that using N_2 (99.999 %) was accurate enough.

3.2.2.1 SDT 2690

As already mentioned, the interface between the user and the apparatus is user friendly and very developed. The software assist during the calibration and the calibration results are automatically integrated into the control system.

The calibration of the SDT 2690 consists of a weight calibration and a temperature calibration. When the SDT is to be operated as a Differential Scanning Calorimeter (DSC), an additional DSC heat flow calibration is required.

BASELINE CALIBRATION

The apparatus is heated in a ramp at the heating rate of the experiments through the temperature range of interest (700 °C-1000 °C). All the reactivity experiments conducted in this Ph.D. study are performed at isothermal conditions. However, the heating rate used for calibration is 5 °C/min. This is, according to the manufacturer, sufficiently slow for a correct calibration of isothermal experiments.

URN:NBN:no-2340

For baseline calibration, the apparatus is heated without any sample or any cup. Once the method is finished, the user only has to decide the temperature limits for the calibration within the temperature range of interest and the computer integrates the calibration results into the control system.

The following figure (Figure 3.5) shows the baseline calibration.

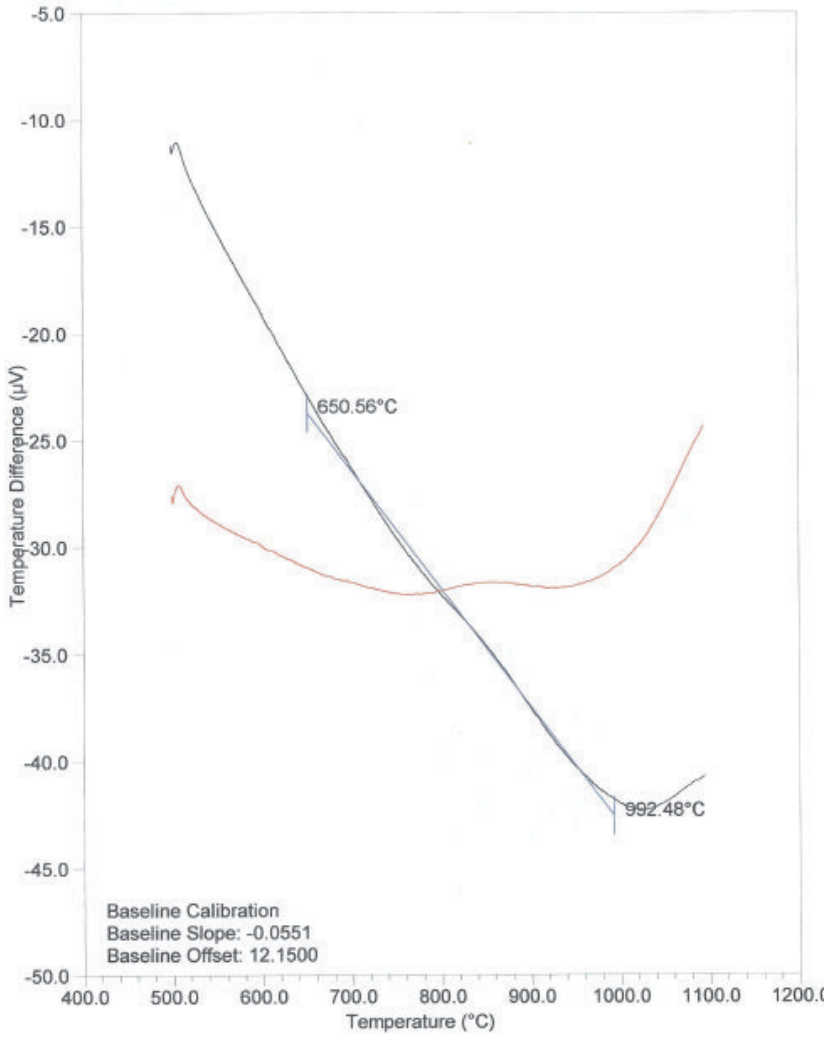

Figure 3.5: Baseline calibration for the SDT

URN:NBN:no-2340

WEIGHT CALIBRATION

The calibration is conducted in two steps. The first one is to run the heating ramp removing the cups, i.e. baseline calibration data file, and the second run uses the same temperature method but having a calibrated weight in each arm.

Once both steps are finished, the user only has to decide the temperature limits for the calibration as for the baseline calibration and the computer integrates the results. The next figure (Figure 3.6) shows the weight calibration results as they appear in the computer screen.

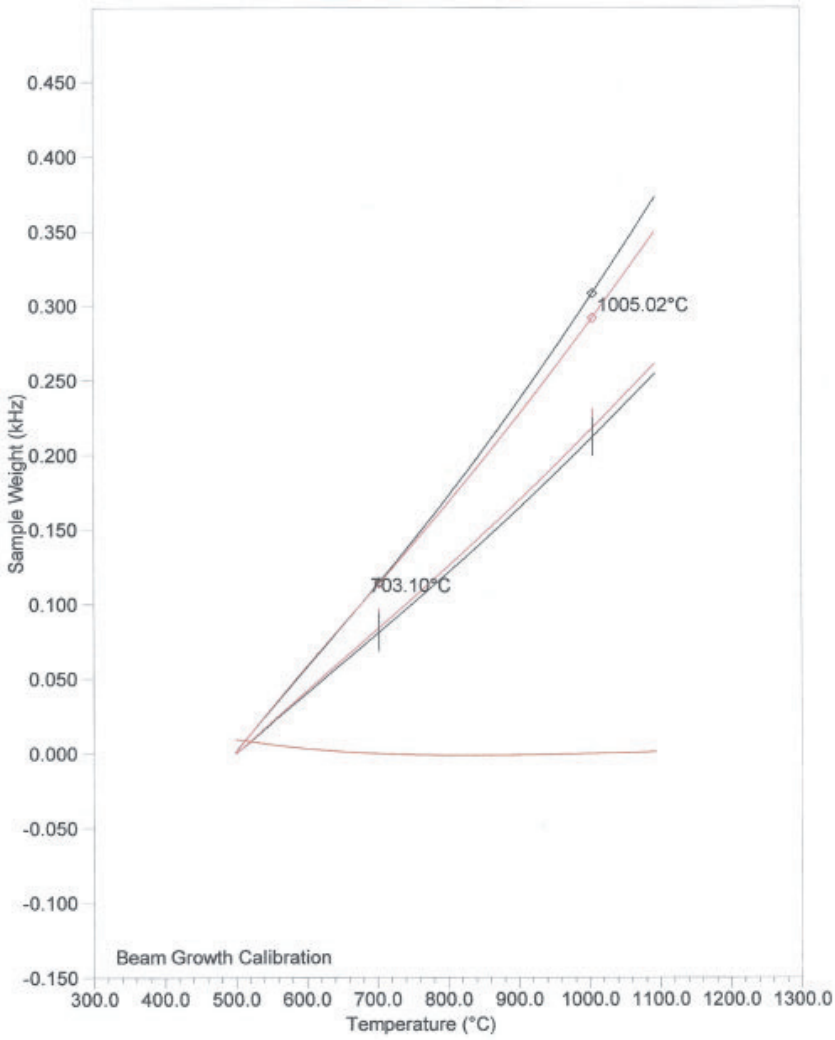

Figure 3.6: Weight calibration for the SDT

URN:NBN:no-2340

TEMPERATURE CALIBRATION

The SDT temperature calibration is based on identifying the melting points of several metals. Since the temperature range of interest is 700 °C to 1000 °C, the following metals have been selected:

Metal	Melting point (°C)
Aluminium	660,33
Silver	961,78
Gold	1064,43

It is also recommended by the manufacturer to use the second melting of each metal as the reference. Therefore, the method for each metal consists of:

a) Fast heating up to 200 °C above the melting point,

b) Cooling until 200 °C below melting point, and

c) Heating at 10 °C/min until 100 °C above the melting point.

The data from step "c" is the one used for temperature calibration. The software helps the user to find the correct melting point, based on this data. The calibration results for Silver are shown in Figure 3.7.

As in the weight calibration, the computer incorporates the calibration results automatically.

3.2.2.2 PTGA

This apparatus is not equipped with the calibration facilities of the SDT 2690. The software does not assist during calibration and the calibration files cannot be easily integrated into the control system.

WEIGHT CALIBRATION

The weight signal is not calibrated. It is a voltage signal whose variation is proportional to the weight by means of an optical system. It was known however that 1 mg of sample will result in a voltage change of 20 mV approximately. Nevertheless, not having a calibrated weight signal is not crucial to the reactivity experiments conducted here because the mass loss rate is measured as a proportion to the total mass loss during the gasification period. Furthermore, the gasification takes place at a constant temperature, so all weight signals –or rather, voltage signals- are received at the same temperature.

URN:NBN:no-2340

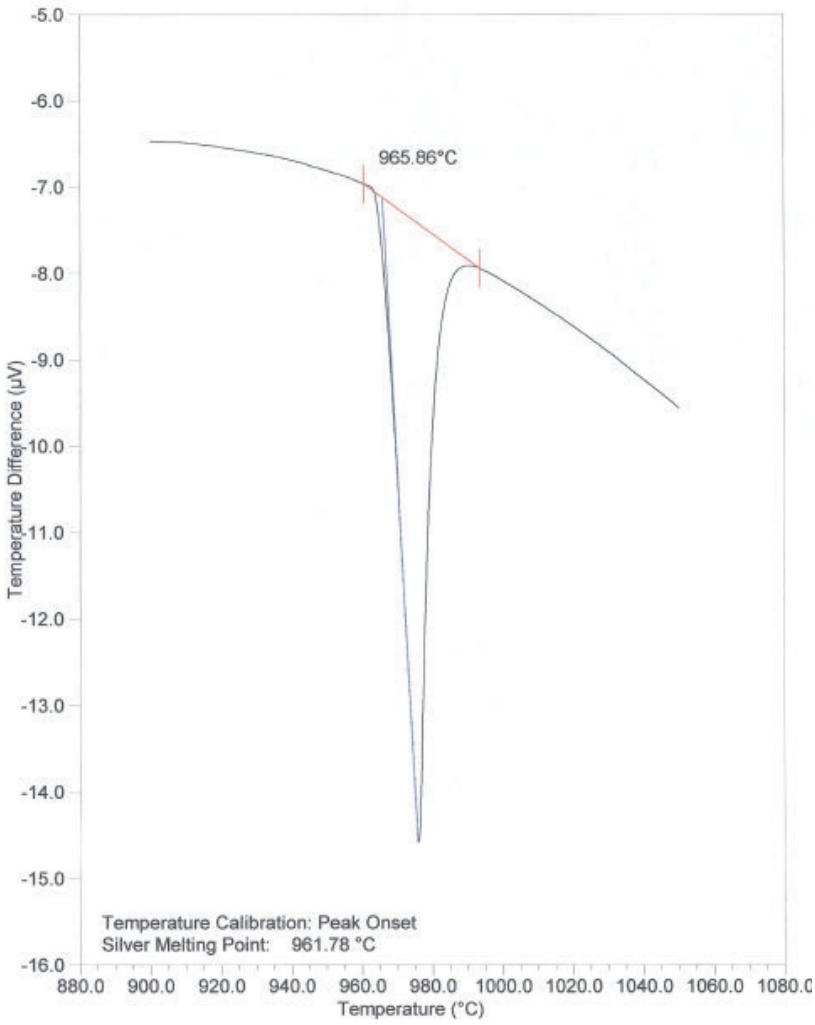

Figure 3.7: Temperature calibration for the SDT (melting point of Silver).

TEMPERATURE CALIBRATION

The same calibration procedure as for the SDT 2690 was conducted at the PTGA. However, the calibration results could not be integrated into the control system but were used later during data processing.

The temperature calibration was also difficult due to some apparatus limitations: Platinum should be avoided for silver and gold temperature calibration because of possible interaction. However, the platinum crucible was used for these calibrations since there was the only possibility.

URN:NBN:no-2340

Having a crucible instead of a cup makes the gold temperature calibration difficult because gold will become liquid and can pour out of the crucible.

Finding the melting point from the calibration results is also done later by the user. Several melting curves for each metal are therefore desired in order to improve the accuracy of the calibration. Processing the calibration results was difficult for silver and gold.

Figure 3.8 shows the calibration results for silver.

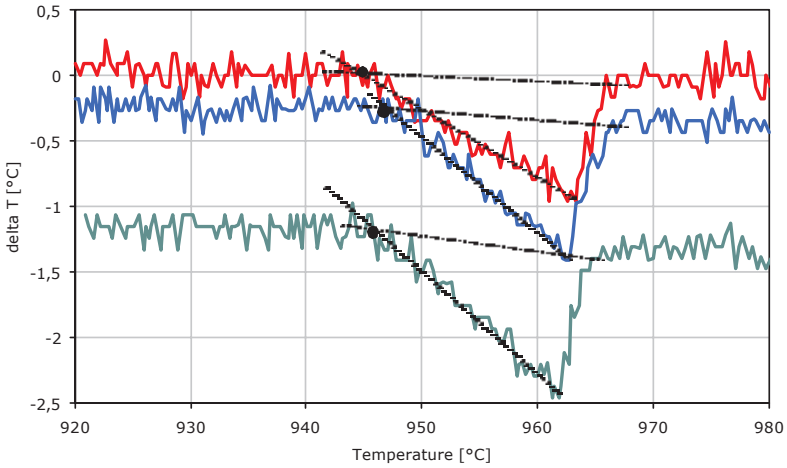

Figure 3.8: Temperature calibration for the PTGA (Silver)

A calibration curve is obtained as shown in Figure 3.9. The curve shows that for instance, when the PTGA indicates a temperature of 800 °C, the real temperature is actually higher (815,48 °C).

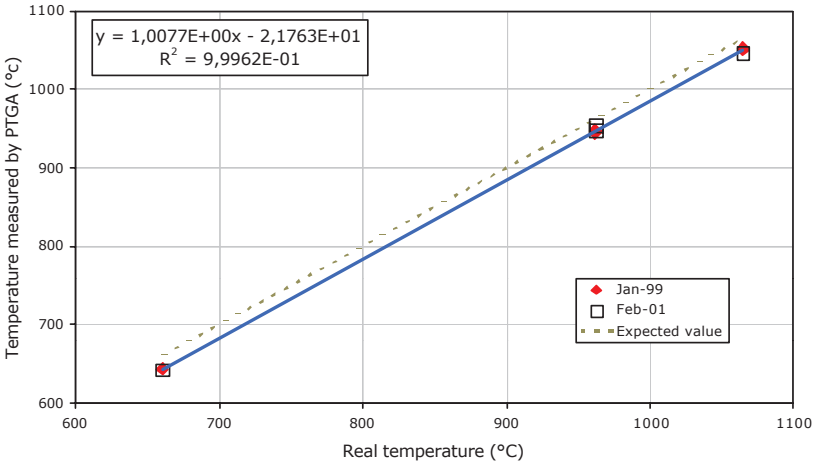

Figure 3.9: Temperature calibration for the PTGA

URN:NBN:no-2340

3.3 RELEVANT REACTIVITY ASPECTS

3.3.1 PYROLYSIS CONDITIONS

The pyrolysis conditions under which the char has been obtained are of primary importance for reactivity. The heating rate, the final pyrolysis temperature and the duration of the final heating period dictate many of the structural characteristics of the char.

Being most of the char gasification reactions surface reactions, it is clear that the porosity of the char and characteristics of the char surface inside the pores are extremely relevant. As already referred by Laurendeau (1978), it is the active surface what counts for reactivity and not the total surface. Whether the accessible sites are active or not will also depend on the pyrolysis heating rate.

To avoid the influence of pyrolysis conditions in this investigation, the char for all the experiments has been obtained exactly under the same conditions and in the same equipment (Macro-TGA). Moreover, the pyrolysis conditions for the char are the same that in the two-stage downdraft gasifier built and in operation at the Denmark University of Technology (Bentzen et al., 1999).

In the recent work of Gøbel (2000), the reactivity information obtained from Thermogravimetric Analysis has been successfully integrated in a model of the two-stage gasifier. The char –beech char, whose reactivity is presented in Paper IV- was obtained, once again, under the same pyrolysis conditions.

3.3.2 THE EFFECT OF THE DEGREE OF CONVERSION

It is well known among reactivity researchers that the char reactivity varies as the reaction proceeds. As observed by Liliedahl and Sjöström (1997) and many others, for most chars of coal, lignite and peat, the reactivity decreases as conversion/time goes, where usually for biomass reactivity increases. There are two possible explanations for this fact. One is the changes in char porosity and structure and the other is related to the catalytic activity of metals and other impurities in the ash. It is out of the scope of this work to prove or reject these explanations.

Nevertheless, it is very important to take into consideration this variation in reactivity. Since the intrinsic kinetic parameters of the reaction do not accept a dependency on degree of conversion, the reaction rate should be expressed as a function of at least two factors: chemical kinetics and pore structural change as a function of the degree of conversion.

$$R=r_c(T, p_{xi}) * f(X)$$

URN:NBN:no-2340

3.3.3 INFLUENCE OF ASH COMPONENTS

3.3.3.1 INTRODUCTION

Biomass has in general a low percentage of ash, but even if the percentage is small, it can be enough to provoke for instance corrosion problems in biomass combustion equipment. Other common problems associated to ash are sintering and agglomeration due to ash melting.

Walker (1985) refers that all carbons contain at least traces of inorganic impurities. Whether these impurities result in significant catalysis of carbon gasification depends upon their concentration, extent of dispersion and specific catalytic activity.

There are however some differences among types of carbons. Steenari (1998) comments that there is a fundamental difference between the ash-forming species of wood and herbaceous biomass and those from coal and peat. In biomass, the inorganic components are integrated in the organic matrix, where in coal the inorganic matter appears as well-defined crystalline minerals. The ash characteristics, she adds, depend not only on the fuel type –and ash composition- but also on the combustion method and combustion parameters.

On the other hand, being ash composed of metals and minerals, it has influence on the reactivity of biomass and biomass chars.

A simple experimental investigation has been conducted in order to understand the influence of ash in reactivity. The number of experiments is rather small and therefore the results are only qualitative.

It is well known that the alkali metals catalyse the gasification reactions (K, P, Ca, etc.) while other ash compounds like silicon will rather inhibit the reaction and form agglomerates. The alkali metals and other ash components that enhance reactivity are usually water soluble compounds while the inhibitors are in general non soluble in water but can be removed by acid washing.

The investigation has consisted of evaluating the reactivity in CO_2 of a acid washed char, i.e. all ash components removed, and studying the effect of alkali metals addition and the effect of non water soluble compounds addition.

Not only reactivity but also the reactivity profile has been examined. If the catalytic activity of ash play a crucial role in gasification, it would be ideally possible to find an expression for the reactivity as (Sørensen, 1999):

URN:NBN:no-2340

R = R(washed char) * F(catalysts) * f(ash)

Where:

- R(washed char) depends on the number of active sites
- F(catalysts) >>> 1, either catalysts from the ash itself (alkali metals, for instance) or added catalyst
- f(ash) <1, depending on the ash analysis and referring to the non soluble components of ash that inhibit the reaction

The catalyst and the ash will interact, becoming F(catalysts) * f(ash) a function of the chemical compounds formed.

3.3.3.2 EXPERIMENTAL SETUP

The experiments have been conducted at an SDT 2690 Simultaneous DTA-TGA from *TA Instruments* at Reatech (Denmark). The straw char sample has been obtained after pyrolysis at 800 °C and then washed in hydrofluoric acid in order to remove all ash compounds. Thereafter the sample was crashed but not sieved.
The alkali metals have been supplied as K_2CO_3 and K_3PO_4, from Merck.
Finally, the silicon containing ash has been obtained after combustion of a straw sample and subsequent water washing in order to remove the water soluble compounds of the ash.

Table 3.1 shows the mixtures that have been tested:

Sample number	Sample name	% wt. washed char	% wt. alkali containing salt	% wt. Si containing ash
1	Char only	100	0	0
2	K_2CO_3 only	0	100 (K_2CO_3)	0
3	K_3PO_4 only	0	100 (K_3PO_4)	0
4	Ash only	0	0	100
5	CC#1	46	54 (K_2CO_3)	0
6	CC#2	78	23 (")	0
7	CC#3	84	16 (")	0
8	CC#4	66	13 (")	21
9	CC#5	55	11 (")	34
10	PC#1	77	23 (K_3PO_4)	0
11	PC#2	60	16 (")	24
12	Ash with K_2CO_3	0	48 (K_2CO_3)	52
13	Ash with K_3PO_4	0	45 (K_3PO_4)	55

Table 3.1: Ash samples

URN:NBN:no-2340

The experimental procedure for most of the experiments has consisted of drying at 110 °C, heating at a heating rate of 24 °C/min in N_2, isothermal period at 750 °C in N_2 and then switch to CO_2 (100 %), also at 750 °C. The duration of the isothermal period both in N_2 and CO_2 has varied between experiments.

The experiments with ash compounds only (samples 4, 12 and 13) have been conducted differently. This last method has consisted of drying at 110 °C and a heating ramp in N_2 between 110 °C and 900 °C at 24 °C/min.

3.3.3.3 RESULTS AND DISCUSSION

WASHED CHAR ONLY (SAMPLE 1)

The reactivity of the washed char at 750 °C in pure CO_2 is very low. The experiment has only been conducted for very low degree of conversion (< 2%) and shows a reactivity of 1,7 e^{-5} s^{-1}. The washed char reactivity might probably increase slightly as the reaction proceeds. Despite this a dramatic increase in reactivity is not expected.

K_2CO_3 ONLY AND K_3PO_4 ONLY (SAMPLES 2 AND 3)

Both compounds show no mass loss during gasification at 750 °C and are very stable at that temperature. K_2CO_3 looses approx. 1,5% weight during the drying, ca. 0,3% during pyrolysis while K_3PO_4 looses ca. 5% during drying and a further mass loss of 9% while the temperature increases until 750°C.

K_2CO_3 ADDITION (SAMPLES 5, 6 AND 7)

Figures 3.10 show the reactivity profile for different percentages of K_2CO_3 addition. In this case, the reaction is considered as both pyrolysis and gasification. This means that the degree of conversion is 0 before pyrolysis is started at 750 °C and X=1 at the end of the gasification.

URN:NBN:no-2340

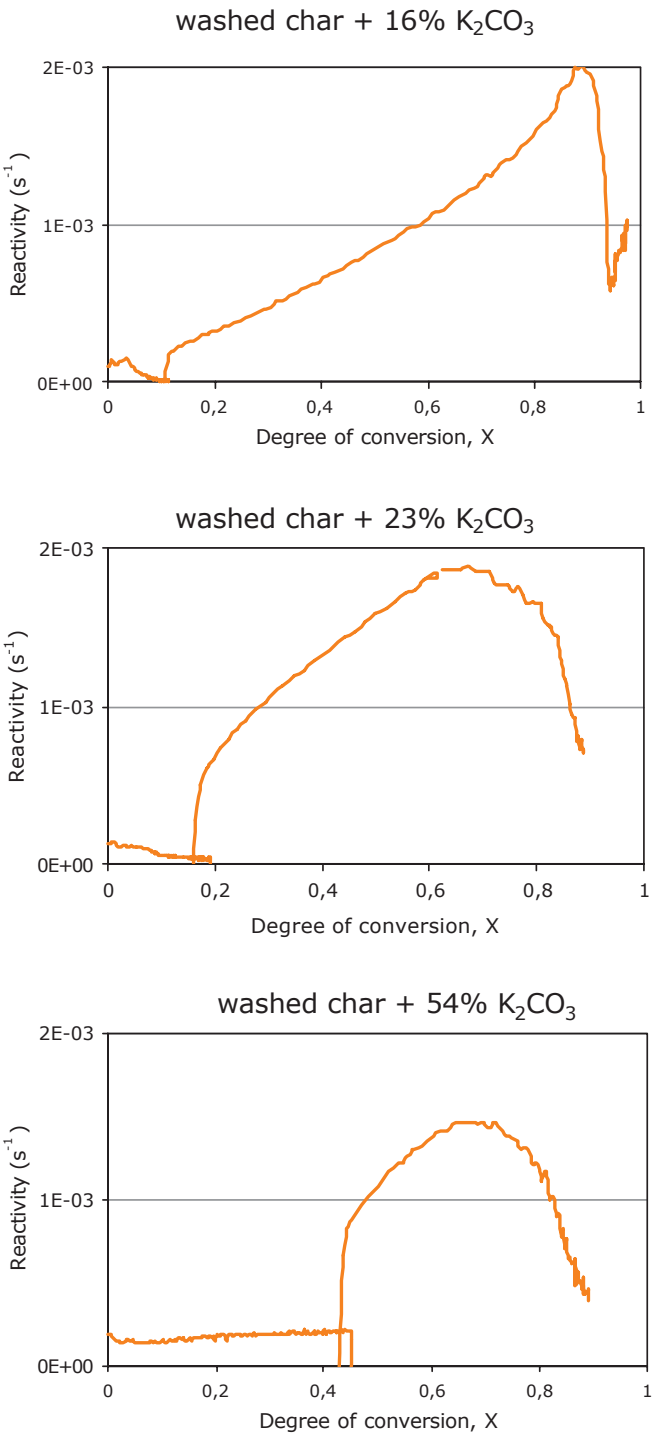

Figures 3.10: Effect of K_2CO_3 addition in char reactivity.

URN:NBN:no-2340

It is clear that K_2CO_3 addition increases the reactivity of the sample. The largest increase in reactivity corresponds to a K_2CO_3 addition of 16% where R= 1.94 e-3.

As the addition of K_2CO_3 increases further, reactivity actually decreases. As the percentage of K_2CO_3 increases, more sample is consumed during pyrolysis. The shape of the reactivity profile during gasification also changes radically with % K_2CO_3.

K_2CO_3 AND ASH ADDITION (SAMPLES 8 AND 9)

As shown in figure Figure 3.11, ash addition decreases reactivity, especially when the addition is above 30% wt. The shape of the reactivity profile also changes remarkably.

In the first case, reactivity increases exponentially at the end of conversion, as it usually does with biomass char. In the other case with higher ash addition, reactivity is almost constant and about the same value as for washed char only.

K_3PO_4 ADDITION AND ASH ADDITION (SAMPLES 10 AND 11)

Figure 3.12 shows the results for the experiments with K_3PO_4 addition and ash addition. It is clear from the figure that ash addition does not influence the reactivity of the sample.

K_3PO_4 addition increases the reactivity of the washed char sample but not as much as K_2CO_3. Reactivity increases almost linearly as the reaction proceeds.

ASH COMPOUNDS ONLY (SAMPLES 4, 12 AND 13)

The experiments with the ash compounds only (Si containing ash and K_2CO_3/ K_3PO_4) were conducted in order to asses their stability and possible changes with temperature.

The results are shown in Figure 3.13.

URN:NBN:no-2340

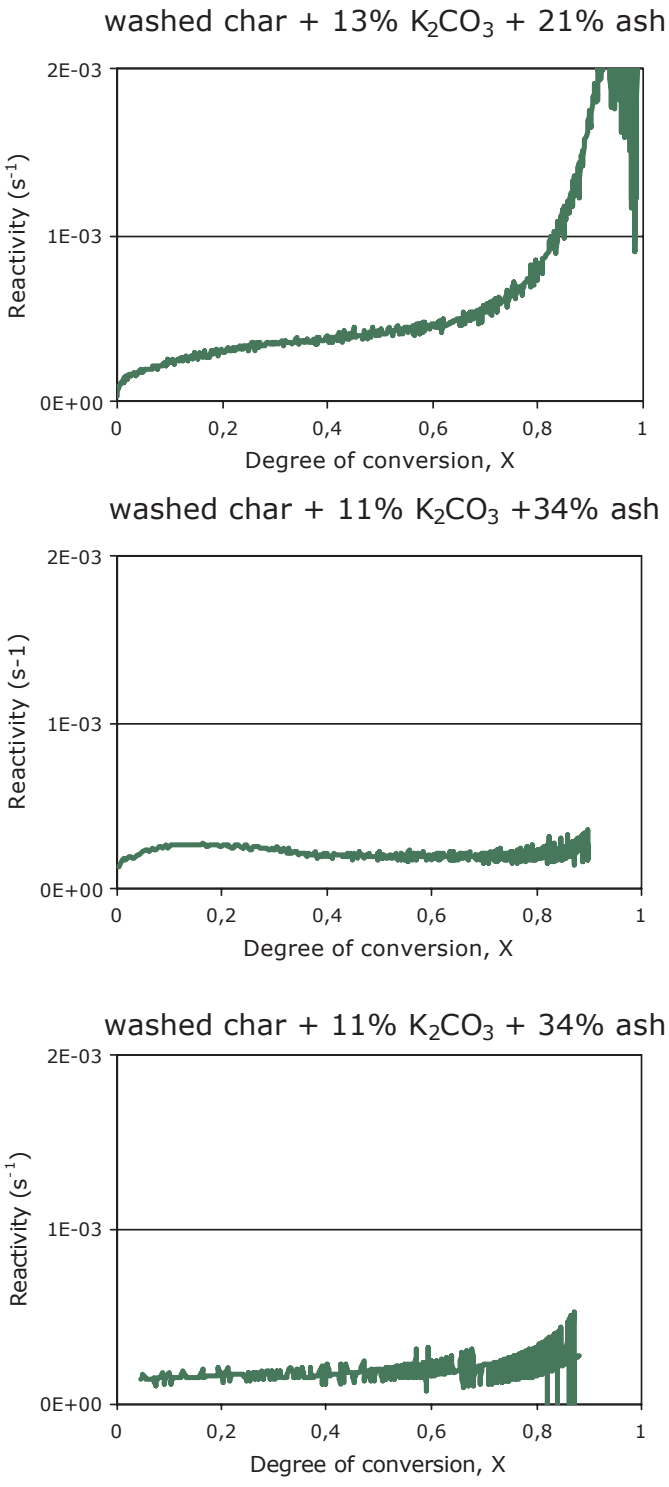

Figure 3.11: Effect of K_2CO_3 and ash addition in char reactivity

URN:NBN:no-2340

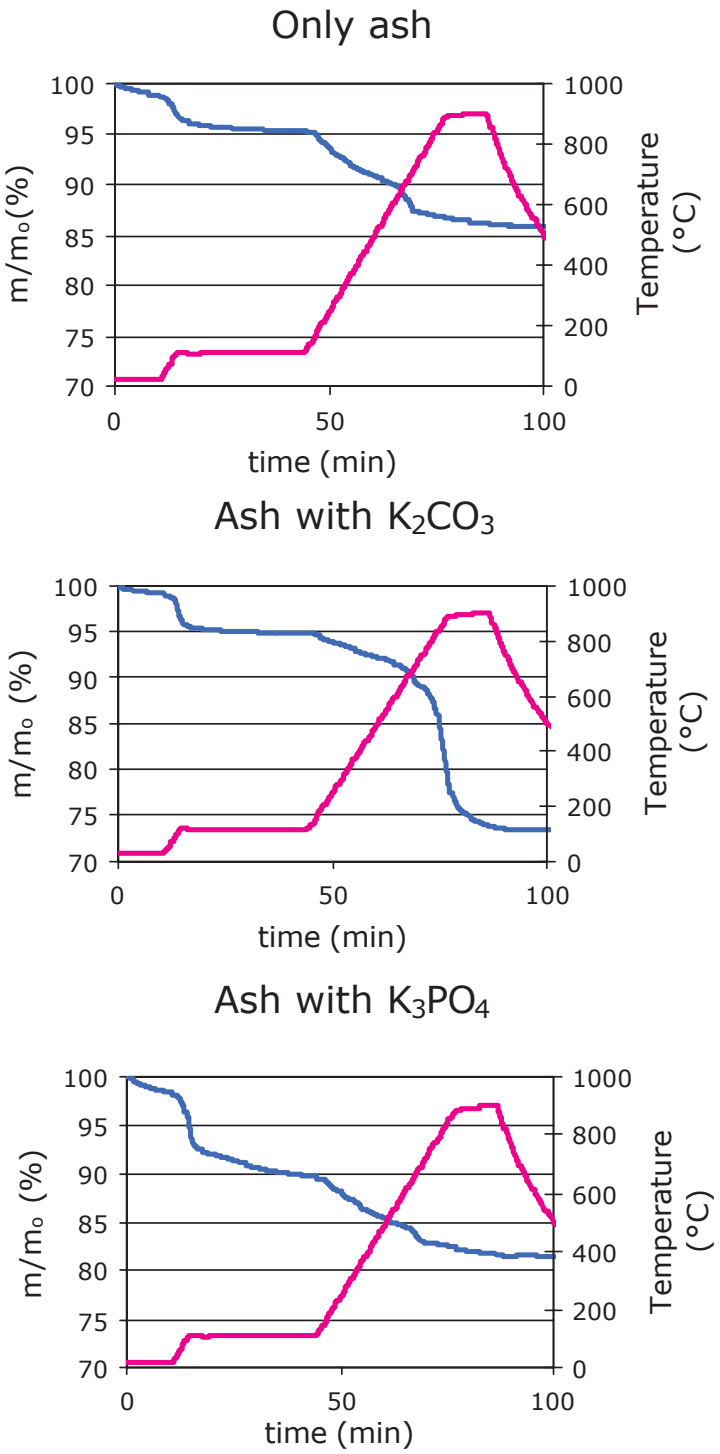

Figure 3.12: Effect of K_3PO_4 and ash addition in char reactivity

URN:NBN:no-2340

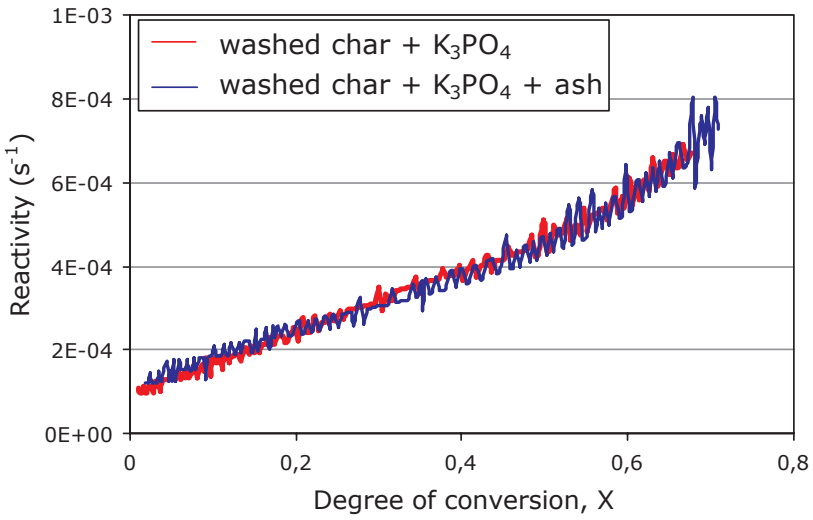

Figure 3.13: Behaviour of ash compounds at gasification conditions

The ash looses about 5% of its weight during drying and about 10% during the pyrolysis. It is not known to this investigator the reason for this mass loss during pyrolysis. Agglomerate was formed during the experiment.

The mixture of ash and K_2CO_3 shows a similar weight loss during drying but a larger weight loss during pyrolysis (22%). K_2CO_3 did also produce a large weight loss during pyrolysis when mixed with the washed char even if the alkali compound is stable at these temperatures. Agglomerate was also formed during the experiment.

Finally, the mixture of ash and K_3PO_4 shows a larger weight loss during drying (10%) but about the same mass loss during the pyrolysis as for ash only. The ash and the potassium phosphate did not form agglomerate.

3.3.3.4 CONCLUSIONS

The conclusions from this short series of experiments can give some idea about the influence of ash components in char reactivity:

- The char by itself has a very low reactivity
- From the few reactivity points obtained, K_2CO_3 addition improves the reactivity of the char sample. The shape of the reactivity profile depends on the amount of K_2CO_3 added.
- The addition of the water non soluble ash compounds diminishes char reactivity when added to the K_2CO_3/char mixture. Moreover, it changes the reactivity profile and forms agglomerate.

URN:NBN:no-2340

- K_3PO_4 also increases the washed char reactivity but not that remarkably. Ash addition does not affect reactivity and does not form agglomerate. There are very few points for any further conclusion.

3.3.4 THE PRESENCE OF O_2

Although in most cases the oxygen added to a gasification process is used for the combustion of the volatile matter, it could eventually also react with the char. The char oxidation by O_2, i.e. combustion, is a much faster reaction compared to CO_2 or H_2O gasification.

Since the combustion reaction is extremely exothermic, it was considered of interest to study the combined effect of O_2 and CO_2 regarding the heat balance between the exothermic O_2 combustion and the endothermic CO_2 gasification. Using Thermogravimetric Analysis and especially Differential Scanning Calorimeter (DSC) techniques was considered as a suitable experimental technique. However, the investigation was rejected after several discussions.

At temperatures above 300 °C or slightly higher, the combustion becomes mass transfer limited and it is therefore difficult to isolate the chemical reaction. On the other hand, the CO_2 gasification reaction does not begin to occur rapidly until the temperature is above 800 °C. At these temperatures, oxidation by O_2 is fully mass transfer limited and therefore, as suggested by Antal (2000), a study of the two reactions together is extremely complicated.

Furthermore, in the opinion of Várhegyi (1986), DSC and DTA are not suitable to study the energy release of the char oxidation processes. The reason for this conclusion is that at moderate heating rates, biomass chars burns off below 600 °C. At this temperature the combustion is "imperfect", forming large amounts of CO. This influences very much the heat evolved, since the formation of CO releases only a fraction of the energy released in the formation of CO_2. In addition, the CO/CO_2 ratio is not constant but depends on a long list of parameters: the temperature, the amount of catalysts in the sample (in form of ash) and its vicinity (sample holder), the contact time of the gases on these surfaces, the heating rate and the gas flow rate.

URN:NBN:no-2340

3.3.5 HEAT OF REACTION FOR GASIFICATION REACTIONS

This section presents a discussion regarding the heat required for the endothermic gasification of wood char by CO_2 under a chemical controlled conditions (zone I) and its experimental determination.

The motivation for this discussion is that it is commonly accepted that the heat of reaction for CO_2 gasification of wood char is equal to the theoretical heat of reaction for graphite. In addition, it was of interest to explore the capabilities of the Thermogravimetric Analyzer working as a Differential Scanning Calorimeter (DSC-TGA).

Apart from registering the weight and time, the DSC-TGA measures the differential heat flow to the sample and reference. The heat flow is proportional to the temperature difference signal, calibrated according to the DSC calibration to take into consideration the effect of temperature.

Based on the scarce literature available, a simple model was elaborated where it was possible to obtain the heat of reaction, ΔH, as a function of:

- the heat flow signal of the experiment (HF),
- the heat flow signal of the background test (HF background),
- the mass and heat capacity of crucible and char sample,
- heating rate,
- initial mass and
- degree of conversion.

The final expression is shown in the following equation:

$$HF - HF_{background} = (m_c c_{pc} + m_{char} c_{ps}) \frac{dT_s}{dt} + m_0 \frac{dX}{dt} \Delta H$$

The difficulty of these experiments lies on the background test. A good background test would imply that all the conditions are equal, but that there is no reaction taking place. Apart from the heat necessary for the reaction, the sample will also absorb the heat necessary to keep the sample at the desired temperature. Ideally, a background test should be conducted with a sample that is inert but that at the same time has the same heat capacity of the sample. In addition, the thermal properties of the char are difficult to predict in general

URN:NBN:no-2340

terms given the high influence of the pyrolysis conditions in the porosity and pore size of the char.

Nevertheless, some experiments were conducted. The experimental heat of reaction obtained was about three times the theoretical value, what indicated that either some of the assumptions for the model are wrong or that the heat absorbed by the char sample is used for other purposes in addition to the CO_2 gasification reaction.

Summarising, the experimental determination of the heat of reaction is complex because:

- Not only CO_2 gasification but probably also rest pyrolysis is taking place.
- DSC calculations need a stable and reliable baseline. The baseline from a background test might not be satisfactory for this determination.
- The fact that most of the char disappears as the reaction takes place (both pyrolysis and gasification) complicates the experiments and subsequent calculations.

3.3.6 THE INFLUENCE OF THE EXPERIMENTAL APPARATUS

The influence of the experimental apparatus in the results deserves some comments. Ideally, the results from Thermogravimetric Analysis depend only on the char sample characteristics and if the correct particle size, sample size and temperature range are chosen, the results will only depend on chemical kinetics.

Grønli et al. (1999) conducted a Round-Robin study of cellulose pyrolysis where eight laboratories participated. Good agreement was observed between the participants although the scatter in temperature measurement was about 17 °C. They suggest that systematic errors in temperature measurement can explain the disagreement between researchers regarding kinetics.

A variation in the results due to the experimental apparatus has been observed in this investigation. Figure 3.14 shows reactivity values obtained for the same char both from CO_2 experiments at the SDT and at the PTGA.

URN:NBN:no-2340

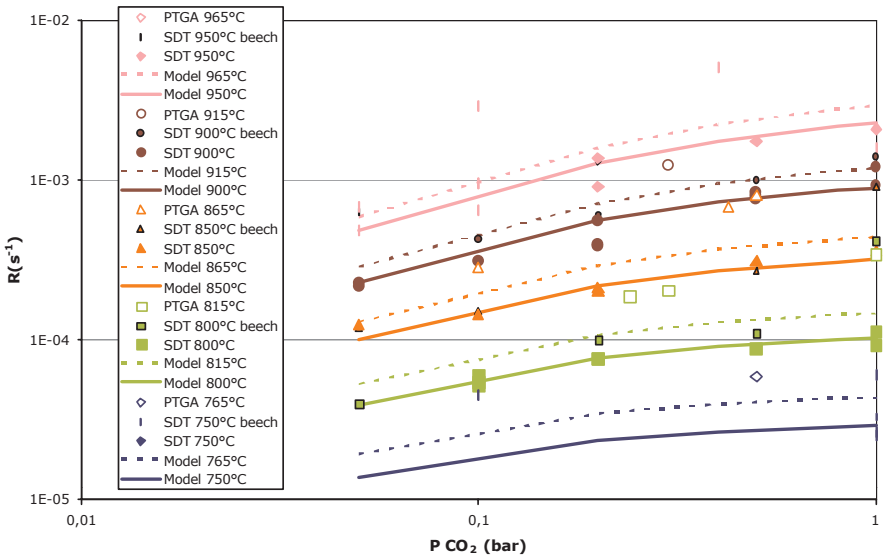

Figure 3.14: Comparison of experimental apparatus for CO_2 gasification

The comparison is difficult since the experiments are not conducted at exactly the same temperature. The continuous and dashed lines represent the expected reactivity based on data obtained from SDT experiments for different temperatures. The experimental data from the PTGA should be fitted by the dashed lines. The figure shows that the experiments at the PTGA show higher reactivity than expected.

Figure 3.15 shows the kinetic constants obtained from each equipment according to n^{th} order kinetics. The reaction kinetic constant for CO_2 at the PTGA is higher than at the SDT, mostly due to a change in the frequency factor. The figure also shows that steam gasification has been found to be 3,8 times faster than CO_2 gasification, independent of temperature.

URN:NBN:no-2340

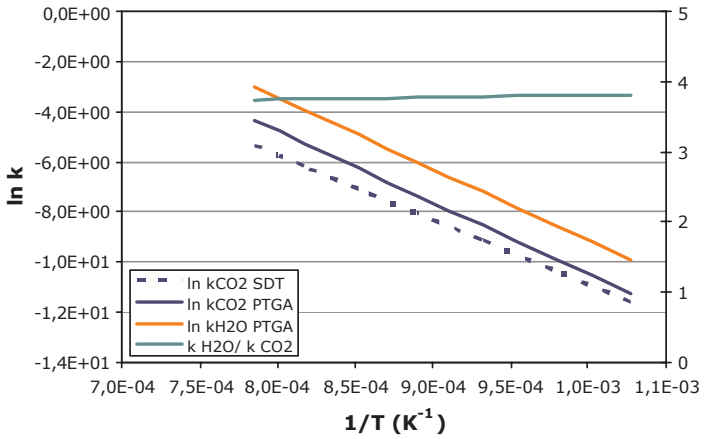

Figure 3.15: Arrehnius diagram for CO_2 gasification at the PTGA and SDT.

There are several possible explanations for this fact. A possible reason is connected to the crucible material. The cups at the SDT are made of alumina while the crucible at the PTGA is made of platinum. Platinum could have acted as a catalyst for the gasification reactions. Also the construction of the apparatus: flow distribution or heat transfer from the oven surrounding the sample, for instance, could have influenced the results.

The fact that there are variations from one apparatus to another does not invalidate all experimental findings but the researcher should be aware of such variations when comparing results from different apparatus. Referring to pyrolysis, Grønli et al. (1999) also reflect about this point and conclude that biomass pyrolysis kinetics are inherently difficult to study by any technique and that they are not aware of other experimental techniques that are more reliable.

3.4 SUMMARY OF PAPERS IV, V AND VI

PAPER IV

This paper reports the reactivity experiments with beech and birch char in mixtures of H_2O, H_2 and N_2. The results are explained according to nth order kinetics and Langmuir-Hinshelwood kinetics, so the inhibition effect of H_2 can be accounted for. The calculation procedure itself has been analysed. Finally, the changes in reactivity as a function of the degree of conversion, also called reactivity profiles, are presented.

URN:NBN:no-2340

The conclusions from this investigation are, first of all, the kinetic parameters found according to each kinetic model. Langmuir-Hinshelwood kinetics model well the inhibition effect of hydrogen.
Birch and beech present very similar kinetic parameters, although they differ in the reactivity profiles. Both wood types are quite similar regarding composition and ash content. However, they might have some structure differences what could explain the differences in reactivity profiles.

Regarding the calculation procedure, it has been observed that it mainly affects the frequency factor and not the activation energy nor the reaction order.

PAPER V

This paper is in some ways similar to Paper IV but referring to birch char reactivity in mixtures of CO_2, CO and N_2.
N^{th} order kinetics and Langmuir-Hinshelwood kinetics have been used to fit the data, both giving very satisfactory results. The parameters obtained have been compared with literature, showing a quite large variation among the referred literature.

The paper gives a detailed explanation about how a representative reactivity data point is obtained from each experiment.
The ratio CO/CO_2 has been found to be a relevant parameter for reactivity.

Finally, the reactivity profiles are discussed. The temperature seems to have a small effect on the shape of the profile while the reactant's partial pressure and the ratio CO/CO_2 have no influence.

PAPER VI

This last paper presents the reactivity experiments conducted in mixtures of CO_2, H_2O and N_2. The char is also obtained from birch under the same pyrolysis conditions as in previous investigations.

The objective of this investigation is to examine if the gasification of birch char in mixtures of H_2O and CO_2 can be predicted from the gasification behaviour in H_2O and CO_2 separately, as in Papers IV and V. An overall kinetic model is of interest, where the reactivity is a function of P_{H2O} and P_{CO2}.

The results suggest that the reaction mechanisms might vary according to the surrounding atmosphere. The kinetic model presented which correctly predicts

URN:NBN:no-2340

gasification in H_2O and CO_2 separately underpredicts the reactivity of the char in mixtures of H_2O and CO_2.

If only kinetic parameters from separate experiments are available, a certain set of kinetic parameters is recommended to predict reactivity in mixtures.

Finally, it is suggested that the best model for combined gasification in mixtures of CO_2 and H_2O would be obtained from experimental data from combined gasification experiments only.

3.5 REFERENCES

1. Antal, M.J. (2000). Personal communication.
2. Bentzen, J.D., Henriksen, U. & Hansen, C.H. (1999). Investigations of a two-stage gasifier, 2nd Olle Lindström Symposium on Renewable Energy, Royal Institute of Technology, Stockholm, Sweden, June 1999, pp. 117-120.
3. Grønli, M., Antal, M.J. & Várhegyi, G. (1999). A Round-Robin study of cellulose pyrolysis kinetics by thermogravimetry, Industrial & Engineering Chemistry Research, Vol. 38, No. 6, pp. 2238-2244.
4. Gøbel, B. (2000). Dynamisk modellering af forgasning i fixed koksbed, Ph. D. Thesis, ET-PHD-99-04, The Technical University of Denmark.
5. Laurendeau, N.M. (1978). Heterogeneous kinetics of coal char gasification and combustion, Prog. Energy Combust. Sci., Vol. 4, pp. 221-270.
6. Liliedahl, T. & Sjöström, K. (1997). Modelling of char-gas reaction kinetics, Fuel, Vol. 76, No. 1, pp. 29-37.
7. Steenari, B.M. (1998). Chemical properties of FBC ashes, Ph. D. Thesis, Chalmers Tekniska Högskola, Göteborg.
8. Sørensen, L.H. (1999). Personal communication.
9. Várhegyi, G., Szabó, P. & Till, F. (1986). Problems in the DSC and DTA study of the burning properties of fuels and other organic materials, Thermochimica Acta, Vol. 106, pp. 191-199.
10. Walker, P.L. (1985). Char properties and gasification, Fundamentals of Thermochemical Biomass Conversion, pp. 485-509. Elsevier Applied Science Publishers.

URN:NBN:no-2340

PAPER IV

STEAM GASIFICATION OF WOOD CHAR AND THE EFFECT OF HYDROGEN INHIBITION ON THE CHEMICAL KINETICS

Published in:
Progress in Thermochemical Biomass Conversion
Volume 1
2001
Edited by A. V. Bridgwater
Blackwell Science

URN:NBN:no-2340

URN:NBN:no-2340

Steam gasification of wood char and the effect of hydrogen inhibition on the chemical kinetics

M. Barrio, B. Gøbel[+], H. Risnes, U. Henriksen[+], J.E. Hustad and L.H. Sørensen[*]
Norwegian University of Science and Technology, Department of Thermal Energy and Hydro Power, 7491 Trondheim, Norway
[+]Technical University of Denmark, Department of Energy Engineering, Nils Koppel Allé, DTU-Building 403, DK-2800 Kongens Lyngby
**ReaTech c/o Centre for Advanced Technology (CAT), Postbox 30, DK-4000 Roskilde*

ABSTRACT: Gasification kinetics parameters have been derived for birch and beech char samples (45μm<d<60μm) pyrolysed under identical conditions. Reactivity experiments were made in steam-hydrogen-nitrogen mixtures at atmospheric pressure. Reactivity profiles have been obtained in the temperature range from 750 °C to 950 °C, for H_2O partial pressures of 0.05, 0.1, 0.2, 0.5 and 1.0 bar and H_2 partial pressures of 0.1, 0.2 and 0.3 bar. Assuming n^{th} order kinetics for pure steam experiments, the activation energy and the reaction order are E=211 kJ/mol and n=0.51 for beech and E=237 kJ/mol and n=0.57 for birch. A kinetic expression based on Langmuir-Hinshelwood kinetics fairly describes the observed hydrogen inhibition effect on the steam-carbon reaction. The differences between the kinetics determined for the two fuels are relatively small and partly due to the origin and quality of the raw wood. The kinetic parameters obtained are presented using a kinetic compensation diagram; they are compared with literature data and discussed. The influence of the calculation procedure on the results is also discussed. It is found that the data evaluation procedure mostly influences the pre-exponential factor and less the activation energy and reaction order.

INTRODUCTION

The gasification process requires an oxidising agent that provides oxygen for the formation of CO from solid fuel. The oxidising, or gasifying, agents are air, oxygen, steam and CO_2. CO_2 is produced during the pyrolysis and early oxidation processes and generally not externally added. The most common agent is air because of its availability at zero cost. Air, though cheap, is not a perfect agent because of its nitrogen content. The product gas from air gasification has generally a low heating value of 4-7 MJ/Nm^3. Oxygen gasification produces a higher heating value (10-18 MJ/Nm^3) but has a drawback due to the high production cost of oxygen.

Steam is another alternative. It also generates a medium calorific value gas (10-14 MJ/Nm^3) and moreover increases the hydrogen content of the product gas. The presence of steam is important in case of further catalytic upgrading of the product gas[1]. Steam gasification is however a highly endothermic reaction and requires a temperature above 800 °C to take place[2] if no catalyst is present[3,4]. The heat required for the reaction has to be transferred either by partial char combustion in the same reactor –mixing H_2O with oxygen/air[1,5]- or by indirect heating[6,7].

URN:NBN:no-2340

Because of biomass moisture, and steam from pyrolysis in downdraft gasification, steam will always be present in gasification whether it is used or not as a gasification agent. Hydrogen is one of the products of steam gasification and its effect on the reaction is also relevant. Some kinetic data for steam gasification of biomass have been published[2,8,9,10,11,12,13,14,15,16,17,18], but very few considering the effect of H_2 inhibition[19,20,21,41].

The diversity in evaluation of the results from char reactivity experiments is large. The definition of gasification rate varies among researchers and so does the criteria to select the reactivity values from the experiments. Few authors[16,22] have concerns regarding this.

This study presents the kinetic parameters and reactivity profiles for steam gasification of birch and beech char. The inhibition effect of hydrogen is also studied using Langmuir-Hinshelwood kinetics. In addition, the influence of the treatment of the experimental results is analysed by comparing the kinetic parameters differently obtained from the same experiments.

The same birch char has been used for CO_2/CO gasification[23]. The kinetic study of char gasification in $H_2O/H_2/CO_2/CO$ mixtures will be a continuation of the work presented.

THEORETICAL BACKGROUND

H_2O/H_2 REACTION MECHANISMS

The overall steam gasification reaction can be represented by:

$$C_f + H_2O \rightleftharpoons CO + H_2 \quad (1)$$

However, the reaction is much more complex and involves several steps. Numerous studies have been conducted in order to understand the mechanisms of the steam gasification reaction. The catalytic activity of the ash plays an important role in this discussion[24,19,25]. H_2O gasification is more complex than CO_2 gasification because not only H_2O is involved but also H_2, CO_2 and CO due to the equilibrium of the water gas shift reaction[19,25].

Hüttinger and Merdes[26] give a comprehensive description of the models proposed in the literature for the carbon-steam reaction. Basically, there are two models of the reaction mechanism: the oxygen exchange model and the hydrogen inhibition model. The equations involved are:

$$C_f + H_2O \underset{k_{1b}}{\overset{k_{1f}}{\rightleftharpoons}} C(O) + H_2 \quad (2)$$

$$C(O) \xrightarrow{k_3} CO + C_f \quad (3)$$

$$C_f + H_2 \underset{k_{4b}}{\overset{k_{4f}}{\rightleftharpoons}} C(H)_2 \quad (4)$$

$$C_f + \frac{1}{2}H_2 \underset{k_{5b}}{\overset{k_{5f}}{\rightleftharpoons}} C(H) \quad (5)$$

The oxygen exchange model is based on equations 2 (reversible -k_{1f} and k_{1b}-) and 3, the traditional hydrogen inhibition model is based on equations 2 (irreversible -only k_{1f}-), 3

URN:NBN:no-2340

and 4 and a different version of the hydrogen inhibition model substitutes equation 4 by equation 5. Each model has a different explanation of the inhibition effect of hydrogen. According to the oxygen exchange model, it is due to the equilibrium of the dissociation reaction (Eq. 2). For the traditional hydrogen inhibition model, the formation of the $C(H)_2$ complex is the reason for inhibition. Finally, the second version of the hydrogen inhibition model involves a dissociative chemisorption of hydrogen on the active sites[27,28], blocking them for the oxygen transfer reaction with steam.

The reaction rate for the models presented is similar, with the exception of dependency on hydrogen partial pressure:

$$r_c = \frac{k_{1f}\, p_{H2O}}{1 + \frac{k_{1f}}{k_3}\, p_{H2O} + f(p_{H2})} \tag{6}$$

where $f(p_{H2}) = \frac{k_{1b}}{k_3}\, p_{H2}$, oxygen exchange model (6.1.)

$f(p_{H2}) = \frac{k_{4f}}{k_{4b}}\, p_{H2}$, hydrogen inhibition model (traditional) (6.2.)

$f(p_{H2}) = \frac{k_{5f}}{k_{5b}}\, {p_{H2}}^{0.5}$, hydrogen inhibition model (second version) (6.3.)

According to Hüttinger and Merdes[26], it is not possible to determine which is the dominating hydrogen inhibiting mechanism by looking at the reaction rate because the equations are identical, with exception of the second version of the hydrogen inhibition model.

It is quite common to reduce equation 6 to the following expression[20,24]:

$$r = \frac{K_1 p_{H2O}}{1 + K_2 p_{H2O} + K_3 p_{H2}} \tag{7}$$

where K_2 and K_3 represent a ratio between rate constants but are not rate constants themselves.

Other authors[19,29] rather use empirical equations to model the chemical kinetics. In this work, the kinetic parameters have been obtained according to the oxygen exchange model, equations 2 and 3, and also according to n^{th} order kinetics.

INFLUENCE OF FUEL TYPE

Several studies have focused on the influence of wood type on CO_2 gasification[30,31,32] and steam gasification[2,14,17,20,33,34,35]. A general conclusion is that the ash content, composition and its catalytic properties explain the differences among the fuels. In particular, Hansen et al.[20] refer to the potassium content of the ashes as being especially relevant.

Moilanen et al.[14] present their results from steam atmospheric gasification of chars from different origins: wood, black liquor, cellulose fibres, peat and coal. All chars, apart from peat, present an increasing reaction rate with conversion, especially wood.

URN:NBN:no-2340

Stoltze et al.[17] find that the gasification of hardwood is 2-3 times slower than straw, probably due to the different char structure and composition. However, since the density of the hardwood char is 5 times higher than the one of straw, in a volume basis the reactivity of wood char is double than of straw. The direct consequence of this fact is that the gasifiers for wood char only require half the volume of a straw gasifier.

Finally, it is important to mention that the pyrolysis conditions also have influence on the char reactivity, as several investigations have proved.

TREATMENT OF THE EXPERIMENTAL RESULTS

There are two definitions of the reactivity commonly used:

$$r = -\frac{1}{(m(t)-m_f)} * \frac{d(m(t)-m_f)}{dt} \tag{8}$$

$$r_w = -\frac{1}{(m_0-m_f)} * \frac{d(m(t)-m_f)}{dt} \tag{9}$$

where m_o is the char mass at the beginning of the gasification and m_f is either negligible, or represents the mass of ash, or – as in this work- the residual mass after gasification. The degree of conversion is obtained as:

$$X(t) = 1 - \frac{m(t)-m_f}{m_0-m_f} \tag{10}$$

Therefore, the relation between the two definitions of reactivity presented above is:

$$r_w = r*(1-X) \tag{11}$$

It is widely accepted that the reactivity depends on the degree of conversion but there is no agreement about how to define one representative value of reactivity for each experiment.

The representative value of reactivity from an experiment is most frequently obtained as the average reactivity between two degrees of conversion: 0-50%[36], 0-70%[16], 0-75%[10], 40-60%[20], 10-50%[37], 60-80%[30].

Bandyopadhyay et al.[38] selects the representative value of reactivity as the reactivity at 5% conversion. Using an earlier value might introduce error because of the gas changing, but a later value would not correspond to a known condition of the sample inside the sample cup holder (depth, mainly).

Stoltze et al.[16] propose a mass-weighed mean reactivity in order to give less importance to the latest stages of conversion.

Finally, other researchers consider the reactivity as a function of the chemical reactivity, dependent of temperature and reactants partial pressure but independent of conversion, and of a structural factor, solely dependent on the degree of conversion[13,39].

Still, it is possible to find other methods to obtain reactivity[11,19].

URN:NBN:no-2340

EXPERIMENTAL SECTION

Kinetics for a Norwegian birch and a Danish beech have been determined. Apart from their origin there are also other differences between the woods. The beech sample is first received as wood chips whose surface has been exposed to the ambient and that partially contains bark. The birch sample comes from a wood log that has been cut into small cubes of 1x1x1cm, removing the bark. The proximate and ultimate analysis is shown in Table 1 and the ash analysis in Table 2.

Table 1 Proximate and ultimate analysis of birch and beech wood.

Proximate analysis	Moisture	Volatile matter*	Fixed carbon	Ash
Birch wood	11.13%	78.7%, mf	20.9%, mf	0.37%, mf
Beech wood	14.16%	75.2%, mf	24.2%, mf	0.56%, mf
Ultimate analysis	C	H	N	O (by diff.)
Birch wood (wt%, mf)	48.7	6.4	0.078	44.45
Beech wood (wt%,mf)	48.1	6.4	0.081	44.82

* Pyrolysis conditions: Heating at 24 °C/min until 600 °C, held for 30 min, natural cooling.

Table 2 Ash analysis of birch and beech wood (%).

Species	Si	Al	Fe	Ca	Mg	K	Na	Ti	S
Beech	1.2	0.14	1.8	25	7.1	28	2	0.029	0.75
Birch	0.03	0.01	0.17	30	4.8	28	0.08	0.007	0.64
Species	P	Cl	Cu	Zn	Ni	Pb	Cd	Hg	
Beech	2	0.29	0.03	0.2	0.02	0.01	<0.001	<0.001	
Birch	3.4	0.03	0.06	0.06	0.01	0.02	<0.001	<0.001	

Both woods have been pyrolysed at the Technical University of Denmark, Department of Energy Engineering (DTU, ET), in a macro-TGA, heated at 24 °C/min to 600 °C, held at that temperature for 30 min and then cooled down to room temperature naturally. Both chars were thereafter crushed and sieved to 45-63 μm.

The instrument used for the reactivity study is a Pressurised Thermogravimetric Analyser (PTGA) at ReaTech, a modified Du Pont Thermogravimetric Analyser. The sample (~5 mg) is placed on a small platinum tray, hanging on a horizontal balance arm. The sample temperature is measured with the help of two thermocouples, near to, but not in contact, with the sample. This investigation is limited to atmospheric pressure although the instrument is prepared for high pressure operation. Rathmann et al.[40] and Sørensen[35] give a detailed description of the PTGA and Hansen et al.[20] describe the modifications required for the instrument to tolerate steam.

Once the char sample is introduced into the PTGA, it is first dried in N_2 during 10 min at 200 °C, then is heated at 24 °C/min to 1000 °C and held at this temperature for 30 min. After this the sample is cooled to the gasification temperature and when conditions are stable, the steam is allowed into the reaction chamber. The sample is hold isothermal until the gasification reaction is complete and then the temperature is raised to 1000 °C to complete the reaction. The sample size is ca. 10 mg and the gas flow 1000 ml/min.

The objective of increasing the temperature up to 1000 °C previous to gasification is to simulate the history of the particle in the two-stage gasifier at DTU, ET. This is also the reason for the heating rate of 24 °C/min. During the 30 min. period at 1000 °C

URN:NBN:no-2340

in the nitrogen atmosphere some fraction of the catalytic species K and Na devolatilise and are carried away from the sample and therefore the char could be less reactive.

The experimental matrix for this investigation is shown in Table 3.

Table 3 Experimental matrix for H_2O gasification experiments

	T(°C)							
P_{H2O} (bar)	750	800		850		900		950
			With H_2		with H_2		with H_2	with H_2
0.1	○●	○●●	①	○○●	①❶❸	○●	①❶❸	③❸
0.3	○○●●	○●	❷❷❸	○●	❸	●	②❸	
0.5	○●	○○●	①❶	○●	①❶		③	③

(○,①,②,③) Birch char; (●,❶,❷,❸) Beech char. The numbered symbols indicate the partial pressure of hydrogen (x10 bar).

The design of the installation is described in Fig. 1.

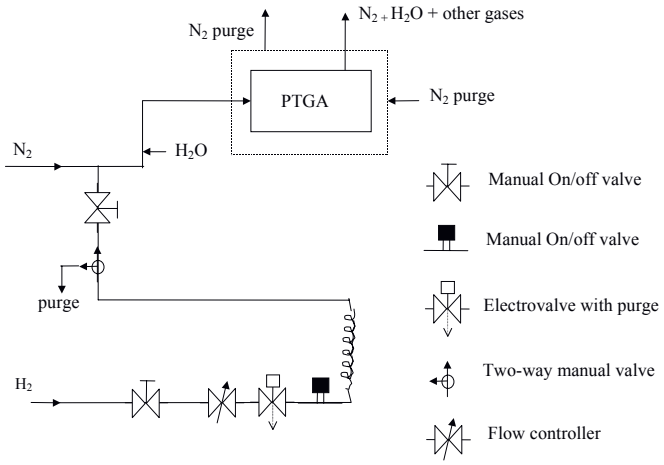

Fig. 1 Schematic drawing of the installation set-up.

RESULTS AND DISCUSSION

GASIFICATION RATE

Fig. 2 shows the mass loss curve for one of the experiments. The initial and final weights for the gasification reaction are also indicated. Fig. 3 shows the reactivity as a function of the degree of conversion, i.e. the reactivity profile, for the same experiment according to equations 8 and 9. In addition, the figure shows the average reactivity (from eq. 8) between 20 and 80% conversion.

URN:NBN:no-2340

It is important to notice that the shape of the reactivity profile is very dependent on the reactivity definition. For the following discussion, the reactivity has been obtained according to equation 8.

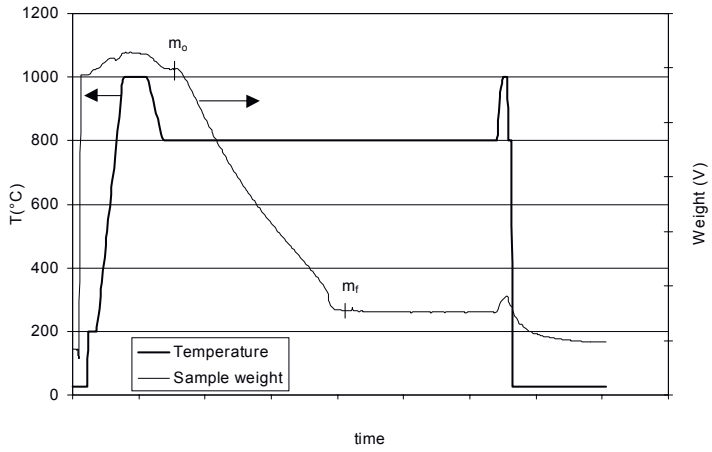

Fig. 2 Temperature and weight signal as a function of time. Experimental data.

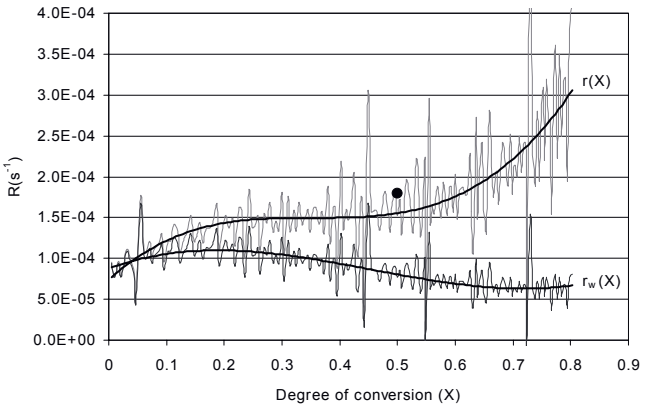

Fig. 3 Reactivity as a function of conversion.
(●: Average reactivity between 20 and 80% conversion).

PURE STEAM EXPERIMENTS

Fig. 4 shows the reactivity of the pure steam experiments as a function of temperature and steam partial pressure. The representative reactivity value has been obtained as the reactivity at 50% conversion. The continuous line shows the n^{th} order reaction model for the birch experiments. The figure shows that beech is more reactive than birch at

URN:NBN:no-2340

low temperatures (750-800 °C). The kinetic parameters obtained according to n^{th} order kinetics are shown in Table 4 together with results from other references.

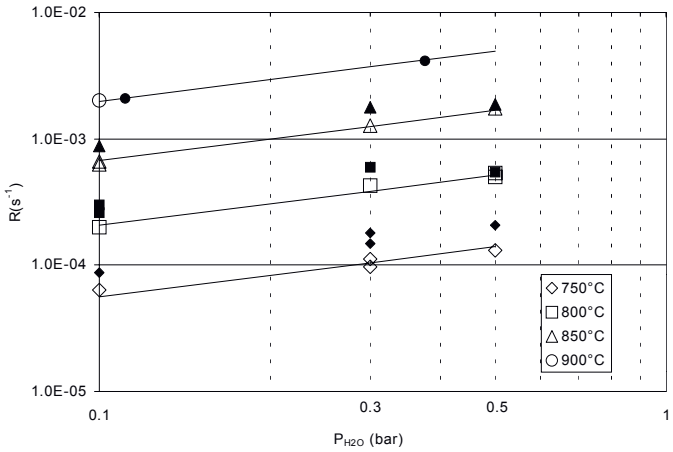

Fig. 4 Reactivity as a function of steam partial pressure and temperature.
(Filled symbols: beech, hollow symbols: birch).

Table 4 Kinetic parameters comparison for steam gasification experiments.

		N^{th} order kinetics		
Reference	Char origin	E(kJ/mol)	k_o	n
This work*	Birch	237± 0.4	$2.62\cdot10^{8}\pm5\cdot10^{6}$ $s^{-1}bar^{-n}$	0.57± 0.03
This work+	Beech	211± 6.1	$1.71\cdot10^{7}\pm1\cdot10^{7}$ $s^{-1}bar^{-n}$	0.51±0.05
Capart et al.[12]	Woodchar	138	$1.79\cdot10^{3}$ $s^{-1}atm^{-n}$	1.00
Hemati et al.[13]	Woodchar	198	$1.23\cdot10^{7}$ $s^{-1}atm^{-n}$	0.75
Richard et al.[8]	Fir wood	104.5±8		
Li et al.[9]	Black liquor	210±10		
Whitty[19]	Black liquor	230		0.56
Timpe et al.[10]	Poplar	271		
	Cattails	262		
Moilanen et al.[14,15]	Wood	196, 217		
	Black liquor	226		
Stoltze et al.[16,17]	Straw	151	$4.77\cdot10^{7}$ %/min	~0.5
(Large TGA)	Wood chips	119	$1.76\cdot10^{6}$ %/min	~0.5
Rensfelt et al.[2]	Poplar wood	182	$1.2\cdot10^{8}$ min^{-1}	
	Straw	182	$5.9\cdot10^{7}$ min^{-1}	
Groeneveld [18]	Wood char	217	$10^{6} – 10^{7}$ $s^{-1}m^{2.1}mol^{-0.7}$	0.7

* $R_{sqr} = 0.9919$, + $R_{sqr} = 0.9784$

From the above comparison one can see that the activation energy varies between 105 and 270 kJ/mol. Most values for E lie between 180 and 270 kJ/mol and the parameters obtained in this investigation are well within this range. The reaction order obtained is

URN:NBN:no-2340

also similar to the values found in literature, eventually among the lower values. These data will be further discussed in Fig. 7.

H_2 INHIBITION EFFECT

The experiments show that the presence of hydrogen inhibits the steam gasification reaction, as presented in Fig. 5.

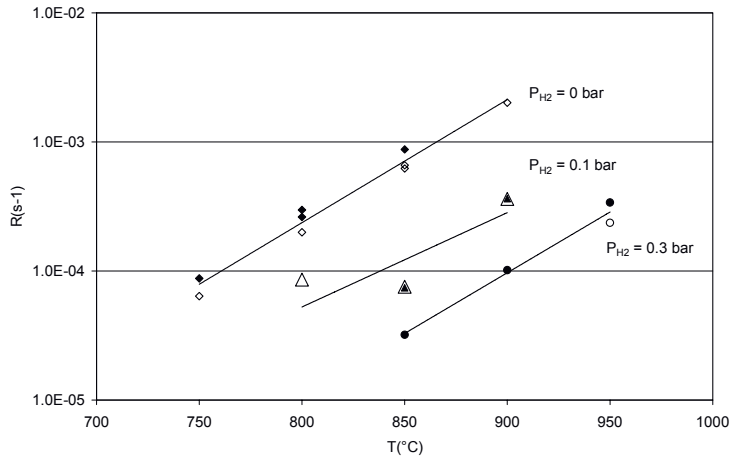

Fig. 5 Inhibition effect of H_2 as a function of temperature and H_2 partial pressure. (P_{H2O}= 0.1 bar, filled symbols: beech, hollow symbols: birch)

The equations 6 and 6.1 have been used to model the reaction. Table 5 shows the kinetic parameters obtained in this investigation. In spite of the high uncertainty of the model parameter calculation, the model fits well the experimental results (See Fig. 6).

Table 5 Kinetic constants for H_2O/H_2 gasification of birch and beech char.

Wood species	E_{1f} (kJ/mol)	k_{o1f} ($s^{-1}bar^{-1}$)	E_{1b} (kJ/mol)	k_{o1b} ($s^{-1}bar^{-1}$)	E_3 (kJ/mol)	k_{o3} (s^{-1})
Beech	199	$2.0 \cdot 10^7$	146	$1.8 \cdot 10^6$	225	$8.4 \cdot 10^7$
Birch	214	$7.6 \cdot 10^7$	284	$2.1 \cdot 10^{12}$	273	$1.6 \cdot 10^{10}$

Table 6 compares these results with the few kinetic parameters found in the literature. Although there is a certain agreement in the value of E_3, the other values are somewhat different. This could be explained by the high uncertainty of the calculation, as also mentioned by Hansen et al.[20] or by the differences in char origin.

URN:NBN:no-2340

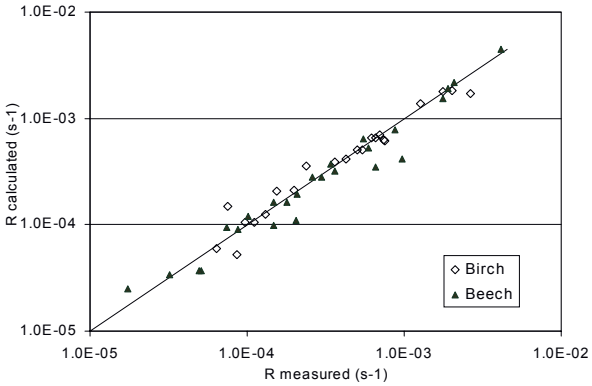

Fig. 6 Calculated reactivity values versus experimental values.

Table 6 Comparison of kinetic parameters for H_2O/H_2 gasification.

		Langmuir-Hinshelwood kinetics				
Reference	Char origin	E_{1f} (kJ/mol)	E_{1b} (kJ/mol)	E_3 (kJ/mol)	E_{1f}-E_3 (kJ/mol)	E_{1b}-E_3 (kJ/mol)
This work	Birch	214	284	273	-59	11
This work	Beech	199	146	225	-26	-79
Hansen et al. [20]	Wheat straw	149	140*	257*	-108	-117
Sørensen et al.[41+]	Wheat straw	158	126	269	-111	-143

* Calculated values, implied in the kinetic model.
+ Recalculation from Hansen et al.[20] experiments.

Fig. 7 compares all the kinetic parameters obtained with those found in literature, with and without hydrogen inhibition, by means of a kinetic compensation diagram. A solid line has been drawn for each of the Langmuir-Hinshelwood constant. Most of the values lie within the same line what might be a sign of consistency in spite of the disparity in activation energies. The kinetic parameters according to n^{th} order kinetics are somewhat more scattered although still aligned. The differences between kinetic parameters can be also due to parameters not studied in this investigation like the number of active sites or the effect of temperature on the active sites behaviour. The three sets of kinetic parameters for birch (Langmuir-Hinshelwood kinetics) represent three valid numerical solutions in the model fitting.

URN:NBN:no-2340

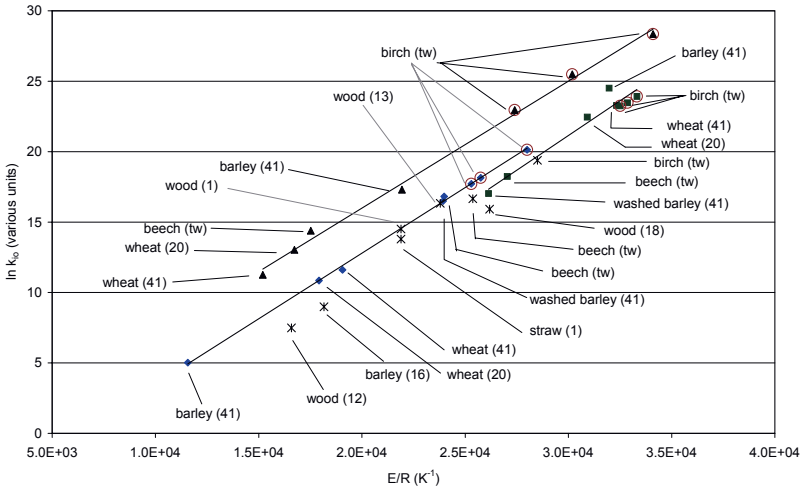

Fig. 7 Kinetic compensation diagram for H_2O and H_2O/H_2 gasification.
(✳: n^{th} order, ◆: k_{1f}, ▲: k_{1b}, ■: k_3, tw: this work)

EFFECT OF FUEL TYPE

With respect to reactivity, the results have shown no large differences between birch and beech. There are however certain differences regarding the effect of temperature on the reactivity profile, and the shape of the profile itself. Fig. 8 shows several reactivity profiles, normalised with respect to their reactivity at 20% conversion to allow comparison. The final increase in gasification rate is more drastic for beech than for birch, especially noticeable for beech at lower temperatures.

Moilanen and his co-workers[14,21] also obtain increasing reactivity profiles with conversion, except for peat. They expect such increasing reactivity because of pore development structure, enhanced by the catalytic effect of the ash, since the ratio catalyst/carbon increases with char conversion. Stoltze et al.[16] obtain similar profiles with barley straw. Rensfelt et al.[2] find as well increasing reactivity with conversion, and a characteristic shape of the reactivity profile for each fuel, having each fuel the same curve independent of temperature. However, for washed barley chars, Sørensen et al.[41] find a decreasing reactivity as a function of conversion.

The ash analysis presented in Table 2 shows very similar values for the potassium content of both woods, but there is some variation regarding other ash components. It cannot be known from the experiments whether the differences in the reactivity profiles are due to these other ash components or to a different porosity evolution as the conversion proceeds.

URN:NBN:no-2340

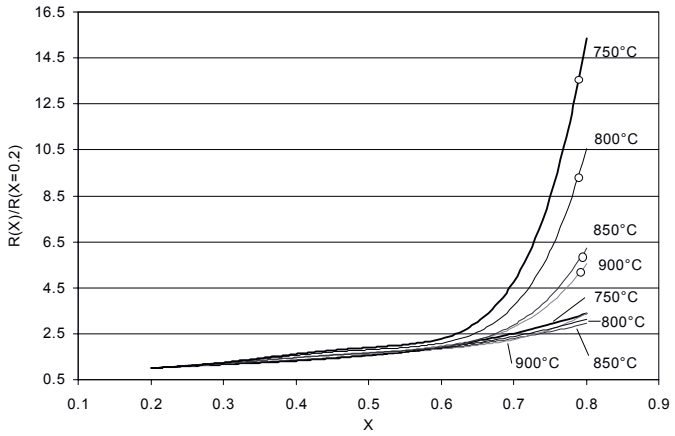

Fig. 8 Reactivity profiles for H_2O experiments. (5: beech experiments).

INFLUENCE OF REACTIVITY DEFINITION

In this section, six different procedures are used to select a representative reactivity value (r_c) from the same experiments, using the reactivity definition (eqn. 8). All the definitions are explained in Table 7.

Table 7 Representative reactivity definitions compared in this section.

	Description	X	Definition of r_c
1	Reactivity at 20% conversion	0.2	$r_c = r\ (X=0.2)$
2	Reactivity at 50% conv.	0.5	$r_c = r\ (X=0.5)$
3	Reactivity at 80% conv.	0.8	$r_c = r\ (X=0.8)$
4	Average reactivity (20-80% conv.)	0.2-0.8	r_c= average r between X=0.2 and 0.8
5	Structural profile f(X) assumed [35,39,42]	0.2-0.8	$r=r_c(T, P_{H2O})*f(X)$
6	Time for 80% conversion	0-0.8	$r_c=1/t(X=0.8)$

The kinetic parameters for the n^{th} order kinetic model have been obtained using these definitions of reactivity for the pure steam gasification experiments of birch. All the activation energies lie between 228-238 kJ/mol and the reaction orders between 0.54 and 0.58, apart from definition 3. The frequency factors are somewhat more scattered, lying between $5 \cdot 10^7$ and $3 \cdot 10^8$. Regarding the uncertainty of the calculation, definitions 2, 5 and 4 seem to give more precise results and it is interesting to notice that the error of the reaction order calculation does not depend on how a representative reactivity value is defined.

It is very important to analyse the influence of the reactivity definition (eqn. 8 and 9) on the kinetic parameters. Since all representative reactivity definitions are related to a fixed degree of conversion (or a fixed interval), the difference between r and r_w will be a multiplying factor, independent of temperature and pressure, and therefore absorbed in the frequency factor. This means that whether equation 8 or 9 is used, the activation energy and the reaction order calculation will give the same result.

URN:NBN:no-2340

CONCLUSIONS

(1) The kinetic parameters according to the n^{th} order reaction model for steam gasification of wood char are E= 237 kJ/mol, k_0= $2.62 \cdot 10^8$ and n= 0.57 for birch, E= 211 kJ/mol, k_0= $1.71 \cdot 10^7$ and n= 0.51 for beech char.

(2) Hydrogen inhibits the steam gasification reaction. The char gasification reaction with steam and hydrogen can be modelled based on Langmuir-Hinshelwood kinetics. The model fits well the results.

(3) The type of wood affects very little the kinetic parameters but shows some influence on the reactivity profile.

(4) The definition of the reactivity will not affect the activation energy or the reaction order calculation.

(5) The method to select a representative reactivity value from one experiment has more influence on the frequency factor than on the activation energy and reaction order. The accuracy of the calculation might also be affected.

ACKNOWLEDGMENTS

The work was supported by the Norwegian Research Council, the Danish Ministry of Energy and EK Energy A.m.b.A. The authors want to thank Torben D. Pedersen, Peter Mørk and Torben Lyngbech for their help during the experimental work.

REFERENCES

1. Gil, J., Aznar, M.P., Caballero, M.A., Francés, E. & Corella, J. (1997). Biomass gasification in fluidized bed at pilot scale with steam-oxygen mixtures. Product distribution for very different operating conditions, Energy and Fuels, Vol. 11, pp. 1109-1118.
2. Rensfelt, E., Blomkuist, G., Ekstrom, S., Espenäs, B.G. & Liinanki, L. (1978). Basic gasification studies for development of biomass medium-btu gasification processes, Energy from Biomass and Wastes, IGT, 14-18 August 1978. Paper No. 27, pp. 466-494.
3. Bilbao, R., García, L., Salvador, M.L. & Arauzo, J. (1998). Steam gasification of biomass in a fluidized bed, effect of a Ni-Al catalyst, Biomass for Energy and Industry. 10th European Conference and Technology Exhibition, 8-11 June 1998, Würzburg, Germany, pp. 1708-1711.
4. Rapagnà, S., Jand, N. & Foscolo, P.U. (1998). Utilisation of suitable catalysts for the gasification of biomasses, Biomass for Energy and Industry. 10th European Conference and Technology Exhibition, 8-11 June 1998, Würzburg, Germany, pp. 1720-1723.
5. Evans, R., Knight, R. A., Onischak, M. & Babu, S.P. (1987). Process performance and environmental assessment of the Renugas process, Energy from Biomass and Wastes X, IGT, pp. 677-696.
6. Paisley, M.A. et al. (1999). Commercial demonstration of the Battelle/FERCO biomass gasification process: Startup and initial operating experience, Proceedings of the 4th Biomass Conference of the Americas, Oakland, CA,USA, pp.1061-1066.
7. Zschetzsche, A., Hofbauer, H. & Schmidt, A. (1998). Biomass gasification in an internal circulating fluidized bed, Proceedings of the 8th EC on Biomass for Agriculture and Industry, Vol. 3, pp. 1771-1777.

URN:NBN:no-2340

8. Richard, J.R. , Cathonnet, M. & Rouan, J.P. (1982). Gasification of charcoal: Influence of water vapor, Fundamentals of Thermochemical Biomass Conversion, pp. 589-599. Elsevier Applied Science Publishers.
9. Li, J. & van Heiningen, A.R.P. (1991). Kinetics of gasification of black liquor char by steam, Industrial & Engineering Chemistry Research, Vol. 30, No, 7, pp. 1594-1601.
10. Timpe, R.C. & Hauserman, W.B. (1993). The catalytic gasification of hybrid poplar and common cattail plant chars, Energy from Biomass and Wastes XVI, Institute of Gas Technology, March 2-6, 1992, pp. 903-919.
11. Kojima, T., Assavadakorn, P. & Furusawa, T. (1993).Measurement and evaluation of gasification kinetics of sawdust char with steam in an experimental fluidized bed, Fuel Processing Technology, Vol. 36, pp. 201-207.
12. Capart, R. & Gélus, M. (1988). A volumetric mathematical model for steam gasification of wood char at atmospheric pressure, Energy from Biomass 4. Proceedings of the 3rd contractors'meeting, Paestum, 25-27 May, pp. 580-583.
13. Hemati, M. & Laguerie, C. (1988). Determination of the kinetics of the wood sawdust Steam-gasification of charcoal in a thermobalance, Entropie, No. 142, pp. 29-40.
14. Moilanen, A., Saviharju, K. & Harju, T. (1993). Steam gasification reactivities of various fuel chars, Advances in Thermochemical Biomass Conversion, Blackie Academic & Professional, 1993, pp. 131-141.
15. Moilanen, A. & Saviharju, K. (1997). Gasification reactivities of biomass fuels in pressurised conditions and product gas mixtures, Developments in Thermochemical Biomass Conversion, Blackie Academic & Professional, 1997, pp 828-837.
16. Stoltze, S., Henriksen, U., Lyngbech, T. & Christensen, O. (1993). Gasification of straw in a large-sample TGA, Nordic Seminar on Solid Fuel Reactivity, Chalmers University of Technology, Gothenburg, Sweden, 24 November 1993.
17. Stoltze, S., Henriksen, U., Lyngbech, T. & Christensen, O. (1994). Gasification of straw in a large-sample TGA, Part II Nordic Seminar on Biomass Gasification and Combustion, NTH, Trondheim, 21 June 1994.
18. Groeneveld, M.J. (1980). The co-current moving bed gasifier, Ph.D.thesis, Twente University of Technology, Enschede, Netherlands.
19. Whitty, K.J. (1997). Pyrolysis and gasification behaviour of black liquor under pressurized conditions, Academic Dissertation, Report 97-3, Åbo Akademi, Department of Chemical Engineering.
20. Hansen, L.K., Rathmann, O., Olsen, A. & Poulsen, K.(1997). Steam gasification of wheat straw, barley straw, willow and giganteus, Risø National Laboratory, Optics and Fluid Dynamics Department, Project No. ENS-1323/95-0010
21. Moilanen, A. & Mühlen, H.J. (1996). Characterization of gasification reactivity of peat char in pressurized conditions. Effect of product gas inhibition and inorganic material, Fuel, Vol. 75, No. 11, pp. 1279-1285.
22. Whitty, K.J. (1993). Gasification of black liquor char with H2O under pressurized conditions, Report 93-4, Department of Chemical Engineering, Combustion Chemistry Research Group.
23. Barrio, M.& Hustad, J.E. CO2 gasification of birch char and the effect of CO inhibition on the calculation of chemical kinetics, *This conference*.
24. Mühlen, H-J., van Heek, K.H. & Jüntgen, H. (1985). Kinetic studies of steam gasification of char in the presence of H2, CO2 and CO, Fuel, Vol.64, July, pp. 944-949.

URN:NBN:no-2340

25. Meijer, R., Kapteijn, F. & Moulijn, J.A.(1994).Kinetics of the alkali-carbonate catalysed gasification of carbon: H_2O gasification, Fuel,Vol.73,No.5, pp.723-730.
26. Hüttinger, K.J. & Merdes, W.F. (1992). The carbon-steam reaction at elevated pressure: formations of product gases and hydrogen inhibitions, Carbon, Vol. 30, No. 6, pp. 883-894.
27. Weeda, M., Abcouwer, H.H., Kapteijn, F. & Moulijn, J.A. (1993). Steam gasification kinetics and burn-off behaviour for a bituminous coal derived char in the presence of H_2, Fuel Processing Technology, Vol. 36, pp. 235-242.
28. Linares-Solano, A., Mahajan, O.P. & Walker, P.L. (1979). Reactivity of heat-treated coals in steam, Fuel, Vol. 58, May, pp. 327-332.
29. Liliedahl, T. & Sjöström, K. (1997). Modelling of char-gas reaction kinetics, Fuel, Vol. 76, No. 1, pp. 29-37.
30. DeGroot, W.F. & Shafizadeh, F.(1984). Kinetics of gasification of Douglas Fir and cottonweed chars by carbon dioxide, Fuel, Vol. 63, February, pp. 210-216.
31. Kannan, M.P. & Richards, G.N.(1990). Gasification of biomass chars in carbon dioxide: dependence of gasification rate on the indigenous metal content. Fuel, Vol. 69, June, pp. 747-753.
32. Illerup, J.B.& Rathmann, O.(1995).CO2 gasification of Wheat straw, barley straw, willow and giganteous, Department of Combustion Research, RISØ National Laboratory, 12th December.
33. Espenäs, B.G. (1993). Reactivity of biomass and peat chars formed and gasified at different conditions, Advances in Thermochemical Biomass Conversion, Blackie Academic & Professional, 1993, pp. 142-159.
34. Moilanen, A. & Kurkela, E. (1995). Gasification reactivities of solid biomass fuels, Preprints of papers, American Chemical Society, Division of Fuel Chemistry, Vol. 40(3), pp. 688-693.
35. Sørensen, L.H. (1994). Fuel reactivity as a function of temperature, pressure and conversion, Ph.D. thesis, Risø National Laboratory, Denmark.
36. Chen, G., Yu, Q. & Sjöström, K.(1997). Reactivity of char from pyrolysis of birch wood, Journal of Analytical and Applied Pyrolysis, Vol. 40-41, pp. 491-499.
37. Zanzi, R., Sjöström, K. & Björnbom, E. (1995). Rapid pyrolysis of agricultural residues at high temperature, Proceedings of the 2nd Biomass Conference of he Americas: Energy, Environment, Agriculture, pp. 630-636.
38. Bandyopadhyay, D., Chakraborti, N. & Ghosh, A.(1991). Heat and mass transfer limitations in gasification of carbon by carbon dioxide, Steel Research, Vol. 62, No. 4, pp. 143-151.
39. Sørensen, L.H., Gjernes, E., Jessen, T. & Fjellerup, J. (1996). Determination of reactivity parameters of model carbons, cokes and flame-chars, Fuel, Vol. 75, No. 1, pp. 31-38.
40. Rathmann, O., Stoholm, P. & Kirkegaard, M. (1995). The pressurized thermogravimetric analyzer at the Department of Combustion Research,, Risø: Technical description of the instrument, Roskilde: Risø National Laboratory, Risø-R-823(EN), Denmark.
41. Sørensen, L.H. et al. (1997). Straw - H2O gasification kinetics. Determination and discussion, Nordic Seminar on Thermochemical Conversion of Solid Fuels, 3rd December, 1997, Chalmers University of Technology, Sweden.
42. Risnes, H., Sørensen, L.H. & Hustad, J.E. CO_2 reactivity of char from Danish wheat, Norwegian spruce and Longyear coke. *This conference*.

URN:NBN:no-2340

URN:NBN:no-2340

PAPER V

CO_2 GASIFICATION OF BIRCH CHAR AND THE EFFECT OF CO INHIBITION ON THE CALCULATION OF CHEMICAL KINETICS

Published in:
Progress in Thermochemical Biomass Conversion
Volume 1
2001
Edited by A. V. Bridgwater
Blackwell Science

URN:NBN:no-2340

URN:NBN:no-2340

CO_2 gasification of birch char and the effect of CO inhibition on the calculation of chemical kinetics.

M. Barrio, J.E. Hustad
Norwegian University of Science and Technology, Department of Thermal Energy and Hydro Power, 7491 Trondheim, Norway

ABSTRACT: Reactivity experiments have been performed in a TGA in the temperature range from 750 °C to 950 °C in steps of 50 °C. The CO_2 partial pressure has been 0.05, 0.1, 0.2, 0.5 and 1.0 bar. Reactivity profiles have been obtained as a function of conversion for all temperatures and partial pressures and kinetic expressions have been calculated. An important feature of this investigation is that it compares the chemical kinetics according to two models: n^{th} order kinetics and Langmuir-Hinshelwood kinetics. The n^{th} order model is widely used and allows comparison among researchers since more results are available. The activation energy obtained according to n^{th} order kinetics is 215 kJ/mol, the frequency factor $3.1 \cdot 10^6$ and the reaction order 0.38. Since the n^{th} order model does not include the effect of CO inhibition, the parameters for Langmuir-Hinshelwood kinetics have also been obtained. In spite of the large discrepancies for these kinetic parameters among researchers, the model fits very well the experimental data presented here. The ratio CO/CO_2 appears to be a relevant factor for reactivity.

INTRODUCTION

Among the thermochemical conversion processes that take place in a gasifier, the gasification reducing reactions are the limiting step. The reactions of CO_2 and H_2O with the char to produce CO and H_2 are considerably slower than the drying, pyrolysis or combustion reactions. A deep knowledge of the chemical reactions involved, as well as the heat and mass transfer mechanisms, would allow an effective enhancement of the gasification process. The residence time and temperature requirements for complete reaction are crucial factors regarding reactor design[1,2]. On the other hand, chemical information is required as part of any gasification model[3,4,5]. Thermogravimetric analysis allows isolation of the chemical information.

The inhibition effect of CO is widely accepted and reasonably well documented for coal char gasification but not for biomass. The lack of extensive literature for wood char CO_2 gasification kinetics including CO has strongly motivated this investigation.

This paper shows the results of birch char gasification experiments with CO_2 and CO. Kinetics for both n^{th} order model and Langmuir-Hinshelwood kinetic model have been obtained. The evolution of reactivity with degree of conversion is also studied, as well as the relevance of the ratio CO/CO_2.

A parallel investigation has been conducted with the same char but gasified in H_2O/H_2 mixtures[6]. Future work is planned to combine these investigations.

URN:NBN:no-2340

REACTION MECHANISMS

It is widely accepted[7,8,9,10,11] that the char gasification reaction with CO_2 can be represented by the following reaction path:

$$C_f + CO_2 \underset{k_{1b}}{\overset{k_{1f}}{\rightleftarrows}} C(O) + CO \tag{1}$$

$$C(O) \xrightarrow{k_3} CO + C_f \tag{2}$$

where C_f represents an available active site and C(O) an occupied site[12] also called a carbon-oxygen complex[10] or a transitional surface oxide[7]. The inhibiting effect of CO consists of lowering the steady-state concentration of C(O) complexes by the backwards reaction 1b[10].
The evolution of the carbon sites and porosity during the char gasification reaction has been subject of several studies[7,13,14,15]. Plante and his co-workers[7] present a summary of the different models used to take into account the changes in reactivity due to the degree of conversion: changes in the carbon structure as the reaction proceeds and variations in the mineral content. In this investigation, as suggested by Sørensen's work[16], the variation of reactivity as a function of the degree of conversion is represented by a function f (*X*), called the structural profile.

$$r(T, P_{CO2}, P_{CO}, X) = r_c(T, P_{CO2}, P_{CO}) * f(X) \tag{3}$$

With such definition, the chemical kinetics, r_c, do not depend on the degree of conversion. The structural function value for 50% conversion is assumed to be 1.

Using Langmuir-Hinshelwood kinetics and the steady state assumption for C(O), the reaction rate will be defined as:

$$r_c = \frac{k_{1f} P_{CO2}}{1 + \frac{k_{1f}}{k_3} P_{CO2} + \frac{k_{1b}}{k_3} P_{CO}} \tag{4}$$

Although some researchers do include dual-site absorption[11], most investigations prefer the above expression[9,17] and a further simplification to nth order kinetics is often adopted[7,18,19]:

$$r_c = k \ P_{CO2}{}^n \tag{5}$$

Ergun[20] reduces however the reaction rate to a different expression in order to show the importance of the ratio CO/CO_2:

URN:NBN:no-2340

$$r_c = \frac{k_3}{1 + \frac{k_{1b}}{k_{1f}} \frac{P_{CO}}{P_{CO2}}} \quad (6)$$

Cerfontain et al.[10] also show that the gasification rate for activated carbon only depends on the ratio P_{CO}/P_{CO2} and not on P_{CO2} or P_{CO}.

EXPERIMENTAL SECTION

The wood used in this investigation is Norwegian birch. The proximate and ultimate analysis of the wood are presented in Table 1. The wood sample was cut in cubes (10x10x10mm) and then pyrolysed in a Macro-TGA at 24 °C/min, up to a temperature of 600 °C. The sample was held at 600 °C during 30 minutes and then cooled naturally. The gasification experiments include a further pyrolysis up to 1000 °C with a heating rate of 30 °C/min. The pyrolysis temperature and heating rate were chosen equal to those used in a previous work for steam gasification of the same char, for the sake of coherence. De Groot et al.[19] also heat the char to 1000 °C to drive off any adsorbed species and desorb any surface oxidation products.

Table 1 Proximate and ultimate analysis of birch.

Proximate analysis	Moisture	Volatile matter*	Fixed carbon	Ash
Birch wood	15.76%	93.3%, mf	6.3%, mf	0.37%, mf
Ultimate analysis	C	H	N	O (by diff.)
Raw wood (%, mf)	48.7	6.4	0.078	44.45

* Pyrolysis conditions: Heating at 24 °C/min until 600 °C, held for 30 min, natural cooling.

More than 50 experiments have been conducted, all of them isothermal and under a total pressure of 1 bar. Since the reactivity not only varies with reactant partial pressure and temperature but also with the degree of conversion (X), it was found more satisfactory to avoid the variation of two parameters simultaneously. Several researches have modelled the dependence of the reactivity on the degree of conversion with a function called structural profile[13], or reactivity factor[21]. It is then possible to run non-isothermal experiments by including the dependency of reactivity on X in the calculations. Also Narayan and Antal[22] contribute to this discussion regarding non-isothermal experiments. During an endothermic reaction (biomass pyrolysis, in their case) the sample will hold a constant temperature due to the heat demand of the reaction and therefore experience a thermal lag. This will lead to an underestimation of the activation energy and the frequency factor.

Once pyrolysed, the char was sieved to 32-45 μm. This particle size was found to avoid heat transfer limitations. Based on previous research on the same equipment[23], a sample of about 5 mg and a gas flow of 200 ml/min during gasification were used for all experiments. The char sample was first dried in N_2 (99,999%) at 110 °C for 30 min, then heated up at 30 °C/min to 1000 °C, kept at 1000 °C for 20 minutes and then brought to the gasification temperature of the experiment. After 10 minutes for

URN:NBN:no-2340

stabilisation of the temperature, the gas was switched to the gasification gas: a defined mixture of N_2 (99,999%), CO_2 (99,2%) and CO (99,5%). The gasification reaction continues until complete char conversion.

The thermogravimetric analyser is a SDT-DTA from *TA Instruments*, supported by an HP PC and software for control and data handling. The system consists of a dual beam horizontal balance. Each arm holds one cup and there is one thermocouple under and in contact with each cup. One cup contains the char sample and the other cup is empty, used as a reference for temperature effects. Detailed description of the instrument can be found somewhere else[23]. Ceramic cups were used for most of the experiments. The apparatus has been recently upgraded and it was possible to operate in a TGA-DSC mode. Therefore, not only the temperature and the weight have been registered but also the heat demand of the process. Table 2 and Table 3 show the experimental matrix for this work.

Table 2 Experimental matrix for CO_2 gasification experiments

	T(°C)				
P_{CO2} (bar)	750	800	850	900	950
0.05			■	■■	■■
0.1		■■■	■	■	■■■
0.2		■■	■■	■■■	■■
0.5		■	■	■■■	■
1	■■	■■	■	■■	■■

Table 3 Experimental matrix for CO_2 gasification with CO inhibition

	T(°C)			
P_{CO} (bar)	850	900	950	1000
0.05	■□	■□□	■□	□
0.1		■■	■	■
0.2		■□	■	□
0.25		□	■■□□	■

(■) PCO_2=0.5 bar; (□) PCO_2=0.2 bar.

It was observed that the mass loss rate during pyrolysis at 1000 °C did not decrease with time, but continued stable and, given enough time, consumed totally the char sample.

This phenomenon is not uncommon. De Groot et al.[19] observed some pyrolytic gasification during the preheating of the chars under flowing nitrogen. They attribute it to the gasification of the oxidised surface species formed during storage and handling of the chars. Also Tancredi et al.[24] encountered a weight loss of about 28% during pyrolysis up to 1000 °C for carbon already pyrolysed at 800 °C. Mackay and Roberts[25] suggest that a prolonged exposure of the char to high temperature in N_2 produces rearrangement and shrinkage of the char structure, hindering the diffusion of gas reactants and products. Rathmann et al.[17] experience the same problem and refers to Whitty[26], who suggests to use a weakly reducing gas, 1-2% CO in N_2 while reaching the gasification temperature to avoid this unwanted reaction.

After an exhaustive maintenance control of the instrument, the mass loss rate decreased but did not disappear. In order to avoid the reactions that consumed the char during pyrolysis it was found necessary to increase the N_2 flow during pyrolysis to

URN:NBN:no-2340

500 ml/min. Under these new conditions, the mass loss during rest pyrolysis was about 20% for all the experiments and mostly while reaching the pyrolysis highest temperature, allowing a better reproducibility of the following gasification experiment.

The original gas line installation for the TGA was modified in order to operate safely with CO (See Fig. 1). The outlet of the TGA, initially open to the room, was connected to a steel tube of 6mm internal diameter for ca. 400 mm, followed by a plastic tube of 10 mm i.d. that conducted the gasses to the suction system. This change in the installation did not seem to affect the results significantly. As a precaution, a CO detector was used during all the CO_2/CO experiments.

During the experiments with high concentrations of CO, small carbon deposition was observed on both arms and cups of the thermobalance.

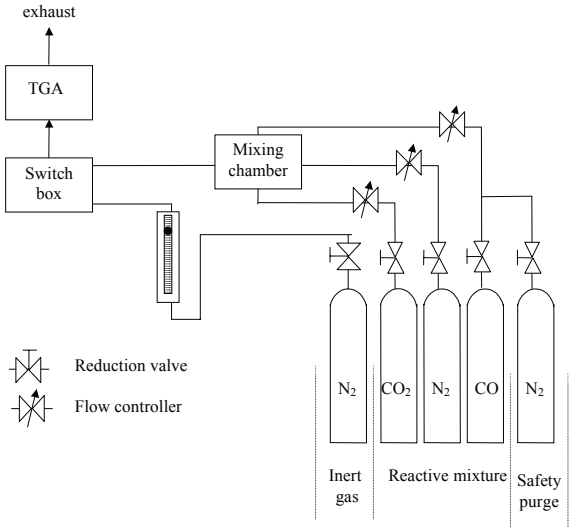

Fig. 1 Schematic drawing of the experimental set-up.

TREATMENT OF THE RESULTS

The reactivity is calculated in this work as:

$$r = -\frac{1}{m(t) - m_f}\frac{d\left(m(t) - m_f\right)}{dt} \tag{7}$$

where r reactivity, (s^{-1})
$m(t)$ mass of char at the time t, (g)
m_f mass of char at the end of the gasification reaction, at the gasification temperature, (g)

URN:NBN:no-2340

Several authors prefer the expression:

$$r = -\frac{1}{m_0 - m_f}\frac{d(m_0 - m_f)}{dt} \tag{8}$$

where m_o represents the mass of char(g) at the beginning of the gasification reaction, at the gasification temperature. This expression, however, implies a continuous decrease in reactivity as the reaction proceeds. The degree of conversion, *X(t)*, is obtained from:

$$X(t) = 1 - \frac{m(t) - m_f}{m_0 - m_f} \tag{9}$$

Defined in this way, *X* will be 0 right before the gasification starts, and 1 when the gasification reaction is finished. This degree of conversion does not include then any pyrolysis reaction but only gasification and is independent of buoyancy effects and changes in flow. Moilanen et al.[27] consider for example m_o as the initial mass of the experiment, previous to drying and pyrolysis. This implies that the gasification reaction takes place at degrees of conversion of 80-100%.

Combining the above expressions for reactivity and degree of conversion one obtains:

$$r = -\frac{1}{(1-X)}\frac{dX}{dt} \tag{10}$$

and this expression, discretised by backwards differencing, gives the reactivity as a function of the degree of conversion, *r(X)*, i.e. the reactivity profile. The profile is then fitted with a 5th order polynomial function, *R*(*X*), and for each experiment, *R*(*X*=0.5) is selected as a representative reactivity value.

$$\begin{aligned} &R(X = 0.5) = R_c * f(X = 0.5) \\ &where \quad f(X = 0.5) = 1 \end{aligned} \tag{11}$$

RESULTS AND DISCUSSION

KINETIC PARAMETERS FOR CO_2 GASIFICATION

Fig. 2 shows the reactivity for all the experiments with CO_2 and the kinetic models used to fit the results: nth order (continuous line) and Langmuir-Hinshelwood (dashed line). The kinetic model based on Langmuir-Hinshelwood kinetics fits better the results, especially at low temperatures.

URN:NBN:no-2340

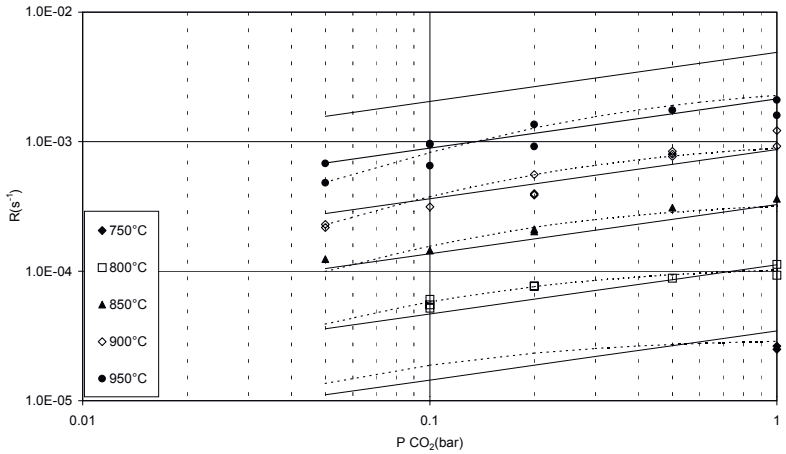

Fig. 2 Influence of CO_2 partial pressure and temperature on char reactivity.

The parameters have been calculated with the statistical program Sigma Plot® and are shown in Table 4, together with results from other references for comparison. The activation energy obtained according to n^{th} order kinetics compares quite well with the other references except Plante et al.[7] and Illerup and Rathmann[28]. Most values lie between 196-250 kJ/mol. The order of reaction comparison shows however larger variation. The reaction order obtained in this investigation is relatively low; only Henrich et al.[30] and Risnes et al.[31] have obtained similar values.

Table 4 Comparison of kinetic parameters for CO_2 gasification of char.

		n^{th} order kinetics		
Reference	Char origin	E(kJ/mol)	k_o	n
This work	Birch	215	$3.1 \cdot 10^6\ s^{-1}bar^{-0.38}$	0.38
Tancredi et al.[24]	Eucalyptus	230-260		
Illerup & Rathmann[28]	Wheat	152		
Bandyopadhyay[29]	Coconut	250		
Plante et al.[7]	Dry poplar	109.5	92112 $Mpa^{-1}min^{-1}$	1.2
De Groot & Shafizadeh[19]	Cotton wood	196	$4.85 \cdot 10^8$	0.6
	Douglas fir	220	$1.97 \cdot 10^9$	0.6
Groeneveld[18]	Wood	217.1	10^6–$10^7\ s^{-1}\ m^{2.1}mol^{-0.7}$	0.7
Henrich et al.[30]	Graphite			0.36
	Municipal w.			0.27
	Soot			0.6
Risnes et al.[31]	Spruce	220	$1.3 \cdot 10^9\ min^{-1}$	0.36

URN:NBN:no-2340

INHIBITION EFFECT OF CO

It is clear from the investigation that the addition of CO inhibits the CO_2 gasification reaction. Two calculation methods to obtain the kinetic constants in the Langmuir-Hinshelwood based model have been compared: the two-steps calculation and the direct calculation. In the two-steps calculation, k_{1f} (k_{1fo} and E_{1f}) and k_3 (k_{3o} and E_3) are first calculated from the CO_2 gasification experiments only, according to Eq. (12), based on Eq. (4):

$$\frac{1}{r_c} = \frac{1}{k_{1f}} P_{CO2}^{-1} + \frac{1}{k_3} \tag{12}$$

and only k_{1b} (k_{1bo} and E_{1b}) are obtained from the CO_2/CO gasification experiments with linear regression analysis, following the equation below:

$$\frac{1}{r_c} = \left[\frac{1}{k_{1f}} P_{CO2}^{-1} + \frac{1}{k_3} \right] + \frac{1}{k_3 k_{1f}} k_{1b} \frac{P_{CO}}{P_{CO2}} \tag{13}$$

The direct calculation obtains the six constants simultaneously from all the experiments, with and without CO. It is worth noting that the second method requires a powerful statistical tool since it is not possible to simplify the equation for linear regression analysis. Furthermore, a considerable number of experiments and reasonable initial values are required to allow a trustful calculation.

Table 5 compares the kinetic constants obtained with these two methods and *Fig. 3* allows further comparison between the calculation methods. The Arrehnius diagram shows very similar values for k_{1b} and k_3 but some discrepancies for k_{1f}. Both methods have a high level of uncertainty in the calculation of k_{1bo} and E_{1b}.

Table 5 Kinetic constants for CO_2/CO gasification of char, this work.

	Langmuir-Hinshelwood kinetics					
Method	E_{1f} (kJ/mol)	k_{o1f} ($s^{-1}bar^{-1}$)	E_{1b} (kJ/mol)	k_{o1b} ($s^{-1}bar^{-1}$)	E_3 (kJ/mol)	k_{o3} (s^{-1})
Two-steps calculation	161	$9.2 \cdot 10^4$	36.4	$1.91 \cdot 10^0$	233	$2.3 \cdot 10^7$
Direct calculation	165	$1.3 \cdot 10^5$	20.8	$3.6 \cdot 10^{-1}$	236	$3.23 \cdot 10^7$

URN:NBN:no-2340

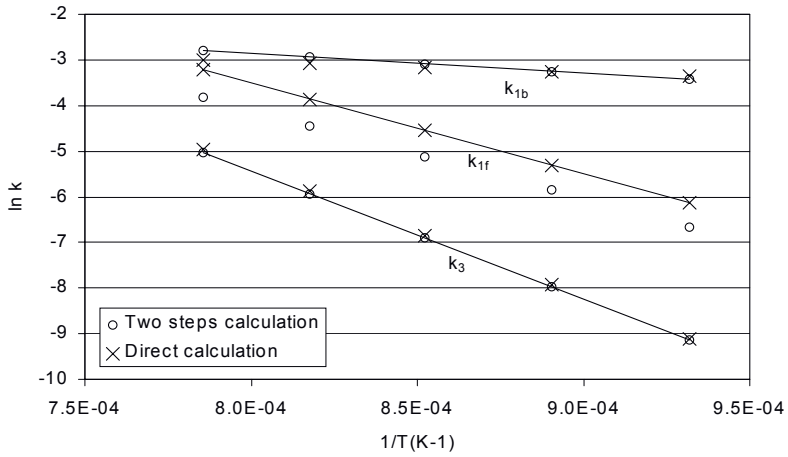

Fig. 3 Arrehnius diagram of the Langmuir-Hinshelwood kinetic constants.

The fitting of the results is very satisfactory, as shown in Fig. 4 and Fig. 5 for the CO_2/CO experiments, in spite of the uncertainty of the kinetic constants calculation –in particular the frequency factor-. This was also observed by Rathmann et al.[17]. The lines in Fig. 4 and Fig. 5 and represent the reactivity according to Langmuir-Hinshelwood kinetics, using the parameters obtained by direct calculation.

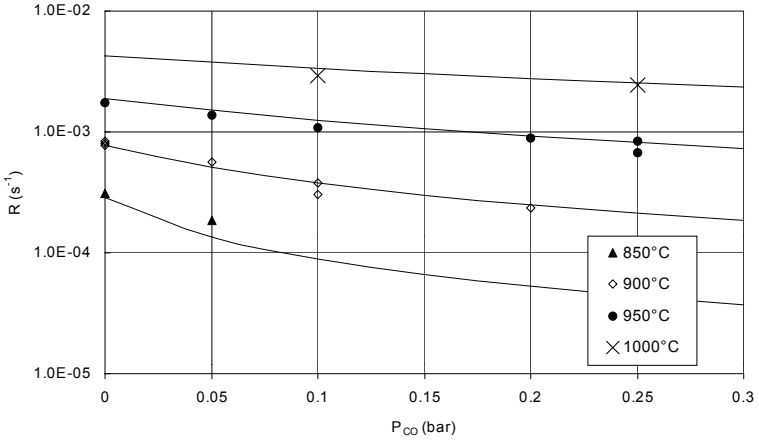

Fig. 4 Reactivity as a function of CO partial pressure for P_{CO2}=0.5 bar.

URN:NBN:no-2340

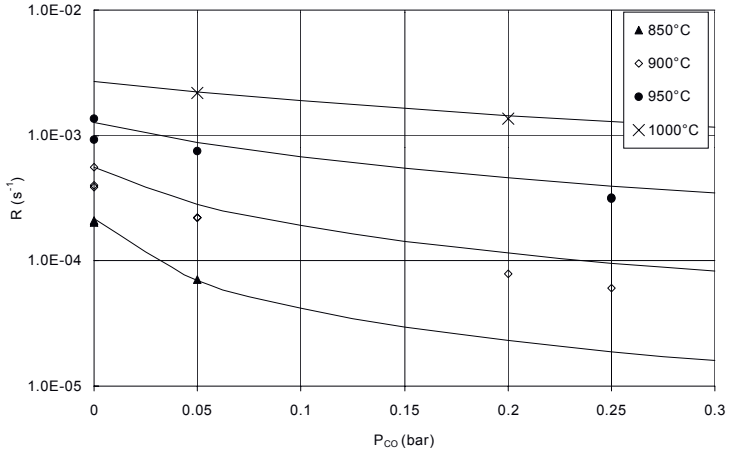

Fig. 5 Reactivity as a function of CO partial pressure for P_{CO2} = 0.2 bar.

Table 6 compares the results with data from other references where CO inhibition has been studied. Although the differences are remarkable, there are some similarities in the values of E_{1f} (between 100 and 165 kJ/mol in most cases). Most authors also agree that E_3 is larger than E_{1f} and therefore that the gasification of the solid carbon –reaction (2)- is the limiting step of the reaction mechanism. Finally, the activation energy E_{1b} is very low for several authors, including this work. This is however not the case for Bandyopadhyay and Gosh[32]. Since the activation energy cannot be negative, the results could be understood as a zero activation energy, i.e. the backward reaction (1) does not depend on temperature.

Table 6 Comparison of kinetic constants for CO_2/CO gasification of char.

		Langmuir-Hinshelwood kinetics				
Reference	Char origin	E_{1f} (kJ/mol)	E_{1b} (kJ/mol)	E_3 (kJ/mol)	E_{1f}-E_3 (kJ/mol)	E_{1b}-E_3 (kJ/mol)
This work	Birch	165	20.8	236	-71	-215.2
Rathmann et al.[17]	Wheat	100	-7*	155*	-55	-162
Illerup et al.[28]	Wheat	151.7	-2.1*	240.6*	-88.9	-242.7
Bandyop. et al.[32]	Coconut	157	260	421	-251	-165
Gadsby et al.+ [32]	Coconut	245	-70.3	120	126	-190.5

***** Calculated values, implied in the kinetic model.
+ Fixed bed reactor.

The ratio CO/CO_2 as a relevant parameter

As already referred by several authors[10,12,20], the ratio P_{CO}/P_{CO2} appears to be an important factor for reactivity. This investigation shows the same fact, as reflected in Fig. 6. This figure is very similar to the one shown by Freund[12] for carbon.

URN:NBN:no-2340

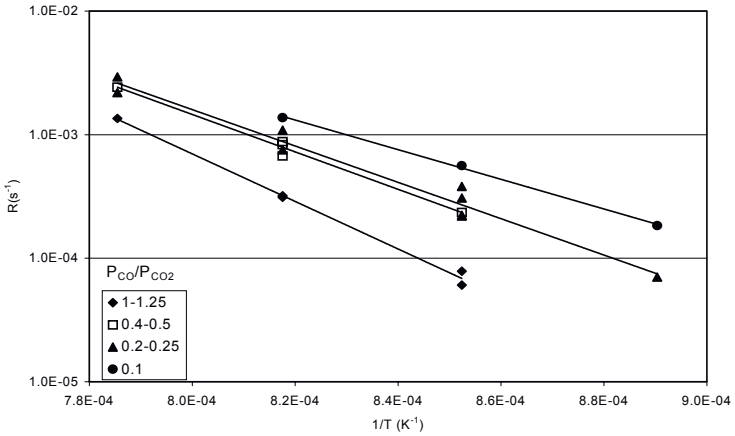

Fig. 6 Influence of the ratio P_{CO}/P_{CO2} on char reactivity.

REACTIVITY PROFILES

Fig. 7 shows the reactivity profile obtained for some of the experiments with CO_2, all of them with a CO_2 partial pressure of 0.2 bar. The reactivity profiles of experiments with CO (0.05 bar), for the same CO_2 partial pressure, are also shown. To allow comparison, reactivity values have been normalised by the function:

$$R_n(X) = \frac{R(X)}{R(X = 0.2)} \tag{14}$$

The reactivity increases always as the char is consumed, especially during the last stages of conversion. All experiments have shown similar profiles. Other researchers[17,24] have also observed this type of profiles.

The slope and shape of the reactivity profile depends to a certain extent on the gasification temperature. This trend has been observed in all the experiments, both with and without CO addition. However, the differences between reactivity profiles at the same temperature are relatively large and therefore do not suggest any further conclusion.

Regarding the concentration of reactants, there seems to be no influence on the shape of the reactivity profiles. The reactivity profiles of the experiments with CO do not show a systematic deviation from the experiments without CO_2 and no conclusions should be extracted to this respect.

Finally, the shape of the reactivity profile does not show any correlation with the ratio CO_2/CO.

URN:NBN:no-2340

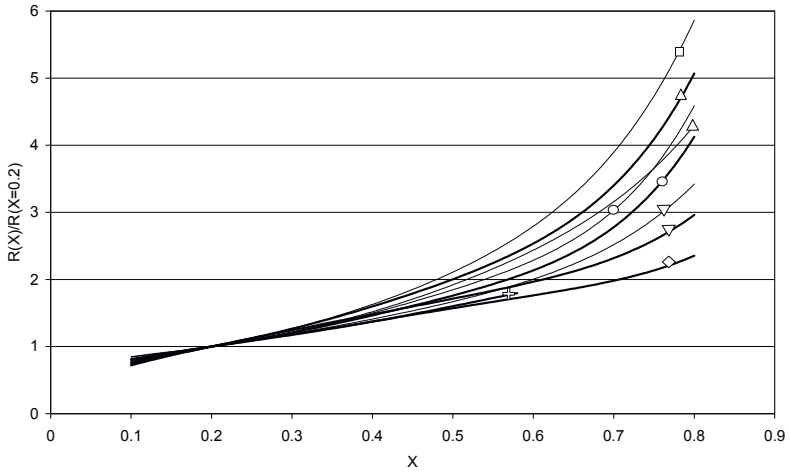

Fig. 7 Reactivity profiles as a function of degree of conversion, temperature and presence of CO. (✙ 750°C, ◆ 800°C, ▼ 850°C, ● 900°C, ▲ 950°C, ■ 1000°C, thick line: CO_2 experiments, thin line: CO_2/CO experiments).

CONCLUSIONS

(1) It has been found that the activation energy is 215 kJ/mol, the frequency factor $3.1 \cdot 10^6$ $s^{-1}bar^{-0.38}$ and the reaction order 0.38 for the CO_2 gasification experiments, according to the n^{th} order reaction model. Langmuir-Hinshelwood kinetics give a better fit to the results.

(2) CO addition has an inhibition effect on the CO_2 gasification reaction. The Langmuir-Hinshelwood kinetics model fits well the results.

(3) The ratio CO/CO_2 appears to be a relevant factor for reactivity.

(4) The char reactivity increases with the degree of conversion in a very similar manner for all experiments. To a certain extent, the reaction temperature affects the shape of the reactivity profile. Neither the gasification agent composition nor the ratio CO/CO_2 seem to affect the shape of the reactivity profile.

ACKNOWLEDGEMENTS

This investigation has been supported by the Norwegian Research Council. The authors want to thank also Silke Hubner and Lena N. Berg for their contribution to the experimental work.

REFERENCES

1. Kojima, T., Assavadakorn, P. & Furusawa, T. (1993). Measurement and evaluation of gasification kinetics of sawdust char with steam in an experimental fluidized bed, Fuel Processing Technology, Vol. 36, pp. 201-207.

URN:NBN:no-2340

2. Mühlen, H-J., van Heek, K.H. & Jüntgen, H. (1985). Kinetic studies of steam gasification of char in the presence of H_2, CO_2 and CO, Fuel, Vol.64, July, pp. 944-949.
3. Koss, L.I. & Walker, L.P. (1988). An iterative kinetic model for the updraft gasification of wood, The 8th Miami International Conference on Alternative Energy Sources.
4. Whitty, K.J., Backman, R. & Hupa, M. (1993). Empirical modeling of black liquor char gasification, Åbo akademi, Report 93-8. Department of Chemical Eng. Combustion Chemistry Research Group, Finland.
5. Gøbel, B. et al. (1999). Dynamic modelling of the two-stage gasification process, Proceedings of the 4th Biomass Conference of the Americas, Oakland, CA, USA, pp. 1025-1032.
6. Barrio, M., Gøbel, B., Risnes, H., Henriksen, U., Hustad, J.E. & Sørensen, L.H. Steam gasification of wood char and the effect of hydrogen inhibition on the chemical kinetics, *This conference*.
7. Plante, P., Roy, C. & Chornet, E. (1988). CO_2 gasification of wook charcoals derived from vacuum and atmospheric pyrolysis, The Canadian Journal of Chemical Engineering, Vol. 66, April, pp. 307-312.
8. Kubiak, H. & Mühlen, H.J. (1998). Gas and electricity production from waste material and biomass via allothermal gasification, Biomass for Energy and Industry, 10th European Conference and Technology Exhibition, 8-11 June 1998, Würzburg, Germany, pp. 1693-1695.
9. Hansen, L.K., Rathmann, O., Olsen, A. & Poulsen, K. (1997). Steam gasification of wheat straw, barley straw, willow and giganteus, Risø National Laboratory, Optics and Fluid Dynamics Department, Project No. ENS-1323/95-0010.
10. Cerfontain, M.B., Meijer, R., Kapteijn, F. & Moulijn, J.A.(1987). Alkali-catalyzed carbon gasification in CO/CO_2 mixtures: An extended model for the oxygen exchange and gasification reaction, Journal of Catalysis, vol. 107, pp. 173-180.
11. Capart, R., Gelus, M., Lesgourgues, M. & Li, Z. (1989). Study of biomass gasification under pressure, Pyrolysis and Gasification, London (UK), Elsevier Applied Science, pp. 593-597.
12. Freund, H. (1985). Kinetics of carbon gasification, Fuel, Vol. 64, May, pp. 657-660.
13. Sørensen, L.H. (1994). Fuel reactivity as a function of temperature, pressure and conversion, Ph. D. thesis, Risø National Laboratory, Denmark.
14. Della Rocca, P.A., Cerrella, E.G., Bonelli, P.R. & Cukierman, A.L. (1999). Pyrolysis of hardwoods residues: on kinetics and char characterization, Biomass and Bioenergy, Vol. 16, pp. 79-88.
15. Ye, D.P., Agnew, J.B. & Zhang, D.K. (1998). Gasification of a Sough Australian low-rank coal with carbon dioxide and steam: kinetics and reactivity studies, Fuel, Vol. 77, No. 11, pp. 1209-1219.
16. Sørensen, L.H., Gjernes, E., Jessen, T. & Fjellerup, J. (1996). Determination of reactivity parameters of model carbons, cokes and flame-chars, Fuel, Vol. 75, No. 1, pp. 31-38.
17. Rathmann, O. et al. (1995). Combustion and gasification of coal and straw under pressurized conditions. Task 2: Determination of kinetic parameters in PTGA, Roskilde: Risø National Laboratory, Risø-R-819 (EN), Denmark.
18. Groeneveld, M.J. (1980). The co-current moving bed gasifier, Ph.D. thesis, Twente University of Technology, Enschede, Netherlands.

URN:NBN:no-2340

19. DeGroot, W.F. & Shafizadeh, F. (1984). Kinetics of gasification of Douglas Fir and cottonweed chars by carbon dioxide, Fuel, Vol. 63, February, pp. 210-216.
20. Ergun, S. (1956). Kinetics of the reaction of carbon dioxide with carbon, Phys. Chem., Vol. 60, pp. 480-485.
21. Gjernes, E. et al. (1995). EFP91. Theoretical and experimental investigation of coal and biomass combustion and gasification properties at high pressure and temperature. Final report, Roskilde: Risø National Laboratory, Risø-R-859(EN), Denmark.
22. Narayan, R. & Antal, M.J. (1996). Thermal lag, fusion and the compensation effect during biomass pyrolysis, Industrial & Engineering Chemistry Research, Vol. 35, No, 5, pp. 1711-1721.
23. Grønli, M. (1996). Theoretical and experimental study of the thermal degradation of biomass, Ph.D. thesis, Norwegian University of Science and Technology, NTNU.
24. Tancredi, N., Cordero, T., Rodríguez-Mirasol, J. & Rodríguez, J.J. (1996). CO2 gasification of eucalyptus wood chars, Fuel, Vol. 75, No. 13, pp. 1505-1508.
25. Mackay, D.M. & Roberts, P.V. (1982). The influence of pyrolysis conditions on the subsequent gasification of lignocellulosic chars, Carbon, Vol. 20, No. 2, pp. 105-111.
26. Whitty, K.J. , Sorvari, V., Backman, R. & Hupa, M. (1993). Pressurized pyrolysis and gasification studies of biomasses, Combustion Chemistry Research Group, Report 93-7, Åbo Akademi.
27. Moilanen, A. & Kurkela, E. (1995). Gasification reactivities of solid biomass fuels, Preprints of papers, American Chemical Society, Division of Fuel Chemistry, Vol. 40(3), pp. 688-693.
28. Illerup, J.B. & Rathmann, O. (1995). CO2 gasification of Wheat straw, barley straw, willow and giganteous, Department of Combustion Research, RISØ National Laboratory, 12th December.
29. Bandyopadhyay, D., Chakraborti, N. & Ghosh, A. (1991). Heat and mass transfer limitations in gasification of carbon by carbon dioxide, Steel research, Vol. 62, No. 4, pp. 143-151.
30. Henrich, E. et al. (1999). Combustion and gasification kinetics of pyrolysis chars from waste and biomass, Journal of Analytical and Applied Pyrolysis, Vol. 49, pp. 221-241.
31. Risnes, H., Sørensen, L.H. & Hustad, J.E. CO_2 reactivity of char from Danish wheat, Norwegian spruce and Longyear coke. *This conference*.
32. Bandyopadhyay, D. & Ghosh, A. (1996). Validity of rate equation based on Langmuir-Hinshelwood mechanism for gasification of carbon - a reappraisal, Steel research, Vol. 67, No. 3, pp. 79-86.

URN:NBN:no-2340

PAPER VI

WOOD CHAR GASIFICATION CHEMICAL KINETICS
IN MIXTURES OF CO2 AND H2O

Submitted for Publication

URN:NBN:no-2340

URN:NBN:no-2340

Wood char gasification chemical kinetics in mixtures of CO2 and H2O

M. Barrio, B. Gøbel[+], U. Henriksen[+], J.E. Hustad and L.H. Sørensen[*]

Norwegian University of Science and Technology, Department of Thermal Energy and Hydro Power, 7491 Trondheim, Norway
[+]Technical University of Denmark, Department of Energy Engineering, Nils Koppel Allé, DTU-Building 403, DK-2800 Kongens Lyngby
**ReaTech c/o Centre for Advanced Technology (CAT), Postbox 30, DK-4000 Roskilde*

Abstract

Wood char gasification experiments have been conducted in mixtures of H_2O/N_2, CO_2/N_2 and $H_2O/CO_2/N_2$ in a temperature range 750 °C – 950 °C. The objective of the investigation is to find a kinetic model that predicts the gasification rate in complex gas mixtures based on Langmuir-Hinshelwood kinetics. It has also been investigated if experiments with H_2O/N_2 and CO_2/N_2 can be used to predict gasification in $H_2O/CO_2/N_2$ mixtures.
The results suggest that the rate of desorption of the C(O) complex varies depending on the gas mixture surrounding the char. They also show that experiments with H_2O/N_2 and CO_2/N_2 could give a fair approximation for gasification in complex mixtures.
Finally, it has been found that kinetic models based on H_2O/N_2, CO_2/N_2 and $H_2O/CO_2/N_2$ experimental data and Langmuir-Hinshelwood kinetics tend to underpredict the gasification rate in H_2O/CO_2 mixtures.

Introduction

Reactivity studies for the gasification of coal and biomass are numerous both in CO_2 and in H_2O. Literature available for CO_2/CO or H_2O/H_2 is somewhat more scarce, especially for biomass. But there are even less references for the gasification of carbon in mixtures of CO_2 and H_2O or mixtures of CO_2, CO, H_2O and H_2. The only available references are the extensive work of Meijer et al. (1991 and 1994) regarding alkali-catalyzed gasification of peat char, Groeneveld (1980) with wood char, Mühlen et al. (1985) with bituminous coal, Liliedahl and Sjöström (1997) with Ptolemais lignite char, Bjerle et al. (1982) with Swedish shale and Whitty et al. (1993) with black liquor.

According to Chen and Yang (1998) and several other researchers the kinetic behaviour of the carbon gasification reaction is very similar in CO_2 and H_2O but very different from the carbon oxidation in O_2, regarding both the activation energy and the rate of reaction. For CO_2 and H_2O char gasification the rate-limiting step is the breaking of the C-C bonds on the edges to release the CO molecule. For the $C+O_2$ reaction, however, due to the high dissociative chemisorption constant of O_2 on carbon, the C-C bonds are significantly weakened, which results in lower activation energy. Recently Hurt and Calo (2001) suggested a three-step semi-global kinetics model, oxygen oxidises the chemisorped oxygen site. Chen et al. (1993) comment that the active surface complexes are crucial in understanding the gas-carbon reactions, especially those involving oxygen-containing gases. They also mention that only surface groups with intermediate stability at high temperatures will contribute to the reactions.

The CO_2 gasification reaction is often described by Langmuir-Hinshelwood kinetics e.g. by the following reaction mechanism:

$$C_f + CO_2 \underset{k_{1bc}}{\overset{k_{1fc}}{\rightleftharpoons}} C(O) + CO \qquad \text{(r. 1)}$$

$$C(O) \xrightarrow{k_{3c}} CO + C_f \qquad \text{(r. 2)}$$

Similarly, for H_2O gasification:

$$C_f + H_2O \underset{k_{1bw}}{\overset{k_{1fw}}{\rightleftharpoons}} C(O) + H_2 \qquad \text{(r. 3)}$$

$$C(O) \xrightarrow{k_{3w}} CO + C_f \qquad \text{(r. 4)}$$

URN:NBN:no-2340

The thee-step semi-global kinetics model proposed by Hurt and Calo (2001) for the oxygen reaction includes the following step:

$$C(O) + O2 \xrightarrow{k_{3O2}} CO2 + C(O) \qquad \text{(r. 5)}$$

There are, however, some differences when comparing both gasification reactions. Regarding the desorption of C(O) (reactions r.2 and r.4), Kapteijn et al. (1991) found two types of CO desorption step: one fast and one slow reaction pathway. They propose that the reaction r. 1 gives semiquinone structures at some edges of the graphitic carbon planes by interaction of the CO_2 with the active sites. The decomposition of this structure yields the slow desorbing CO. Some other sites can also be oxidixed but giving a diketone structure which is more unstable than the semiquinone. The diketone structure breakes easily into two adsorbed CO molecules, carbonylic structures, and represents the faster CO desorption. The diketone structures are only formed continuously if CO_2 is present. According to this explanation, k_{3w} and k_{3c} could represent significantly different pathways and therefore their values might not be equal and might depend on the reactant gas mixture composition.

However, according to Chen et al. (1993) referring Tremblay (1978), if the heterogeneity of the carbon surface is high two distinct decays may not be distinguishable. The fast reaction step is caused, according to Chen et al. (1993), by a surface complex with a certain structure while the slow reaction is attributed to surface complexes containing semiquinone and carbonyl structures. If the heterogeneity of the carbon surface is very high, the same local structures may have different bond energies and thus the activities of the two main groups may have a very large overlap.

There is little reported regarding simultaneous gasification in CO_2 and H_2O. The most comprehensive work has been conducted by Meijer et al. (1991). They studied in detail the oxygen exchange reactions in connection with the catalytic activity of the alkali metals. The sample was an acid washed steam activated peat char enriched with catalyst (K) in steam in the presence of alkali-carbonate. The catalyst was added by pore volume impregnation with a liquid K_2CO_3 solution. Catalyst loading is expressed as K/C ratio. They observe a strong influence of the composition of the reactant gas mixture on the oxygen exchange reactivity. They present experimental proof for the strong interaction of CO_2 with the alkali cluster by chemisorption. They also observe that H_2O is not chemisorbed into the alkali species but is capable of oxidizing the alkali cluster. Their results give reasons to believe that there is a strong competition between CO_2 and H_2O for, respectively, chemisorption or oxidation of the "empty" catalytically active sites. They suggest the following three step model to describe the alkali-catalysed oxygen exchange reactions in mixtures of H_2O, CO_2, H_2 and CO:

$$H_2O + * \rightleftharpoons H_2 + O - * \qquad \text{(r. 6)}$$

$$CO + O - * \rightleftharpoons CO_2 - * \qquad \text{(r. 7)}$$

$$CO_2 - * \rightleftharpoons CO_2 + * \qquad \text{(r. 8)}$$

where *, O-* and CO_2-* represent empty, oxygen containing and CO_2 containing catalytically active sites respectively.

In a later work, Meijer et al. (1994) conducted experiments with the same fuel in pure H_2O, and mixtures including H_2O/CO_2. They observe that with an increasing percentage of CO_2 in the feed, the total rate of gasification decreases. The addition of only 10% CO_2 to the H_2O containing gas mixture strongly decreases the overall rate of gasification by ~40%. This effect is attributed to the chemisorption of CO_2 into the active alkali cluster, making fewer sites available. Without CO_2 in the feed, and at low H_2O conversion levels, the amount of sites with chemisorbed CO_2 (CO_2-*) is fairly small.

On the other hand, Suuberg et al (1993) study the nature of the active sites in "young" lignite chars. They refer that although a correlation between active sites involved in hydrogen gasification and those involved in CO_2 gasification has been demonstrated, there is no direct proof that the same active sites are involved in both reactions.

URN:NBN:no-2340

Mims and Pabst (1987) refer that the predicted relationship between the rates of CO_2 and H_2O gasification reactions is simple when site oxidation (reactions r.1 and r.3) is much faster than the desorption of C(O) (reactions r.2 and r.4), which is generally thought to be the case at moderate pressures. Under these conditions, they affirm, the carbon sites have no memory of whether CO_2 or H_2O is the oxidant, and the predicted difference in reactivity of two gases is due solely to their different oxidizing powers. They refer to Ergun and Mentser (1956) who concluded that the number of sites available for the H_2O-carbon reaction was about 60% higher than that for the CO_2-carbon reaction. Mims and Pabst (1987) suggest nevertheless that the presence of CO_2 in the reactant gas induces changes in the dispersion of the alkali catalyst.

Gasification rates in mixtures of CO_2 and H_2O

The comparison between H_2O and CO_2 gasification rates is often found in literature. For instance, Rensfelt et al. (1978) obtains H_2O to CO_2 gasification rate ratios around two and Rathmann et al. (1995) found this ratio to be larger than three.

Bjerle et al. (1982) conducted experiments with mixtures of H_2O, CO_2, H_2 and CO with Swedish shale with high ash content. They calculated the reaction rate assuming steam and carbon dioxide react in parallel according to the following expression:

$$R = c_c\left[k_1 \frac{k_2 P_{H2O}}{1 + k_2 P_{H2O} + k_3 P_{H2} + k_3' P_{CO}^{0.25}}\right] + \left[k_4 \frac{k_5 P_{CO2}}{1 + k_5 P_{CO2} + k_6 P_{CO}^{0.05} + k_6' P_{H2}}\right] \quad (1)$$

The prediction of the experimental reactivity is shown in Figure 1. The maximal difference between the calculated and the experimental value is smaller than half an order of magnitude.

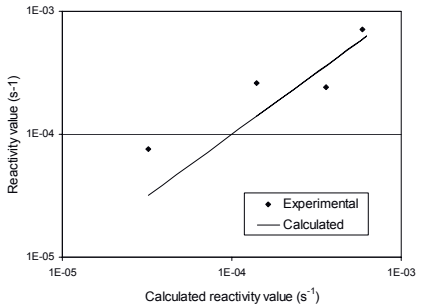

Figure 1: Prediction of reaction rate for Swedish shale (Bjerle et al., 1982).

Groeneveld and Swaaij (1980) assume the same reaction order, activation energy and frequency factor for both reactions, and present the following expression for wood char gasification:

$$-R_A = k\, C_s (C_{CO2} + C_{H2O})^{0.7} \quad (2)$$

where

$$k = A\, e^{-\frac{217100}{RT}}$$

and A varies between 10^6 and 10^7 $s^{-1}m^{2.1}mol^{-0.7}$. They present no information about how does this expression fit the combined gasification experiments.

Liliedahl and Sjöstrom (1997) refer to Van Heek et al. and write the chemical reaction rate term as

$$k = \frac{p_{CO2} k_{CO2} + p_{H2O} k_{H2O}}{1 + p_{CO} K_{CO}} \quad (3)$$

where p_{H2O}, p_{CO2} and p_{CO} are the partial pressures of steam, carbon dioxide and carbon monoxide respectively, k_{H2O} and k_{CO2} are the reaction rate constants for steam and carbon dioxide and K_{CO} is an equilibrium constant for carbon monoxide.

URN:NBN:no-2340

This expression originates from Langmuir-Hinshelwood kinetics, but the retarding effect of carbon dioxide and steam relative to that of carbon monoxide was considered to be minimal at amospheric pressure and therefore, those terms are omitted in the denominator. They do not mention the inhibition effect of H_2. The values of each constant are given for Ptolemais lignite char.

Mühlen et al. (1985) describe the gasification of coal char in complex gas mixtures by the following equation:

$$R = \frac{r_1 P_{CO2} + r_8 P_{CO2}^{\ 2} + r_9 P_{H2O} + r_{11} P_{H2O}^{\ 2} + r_{12} P_{H2O} P_{H2} + r_4 P_{H2}^{\ 2}}{1 + r_2 P_{CO2} + r_3 P_{CO} + r_{10} P_{H2O} + r_5 P_{H2}} \quad (4)$$

As presented by Gøbel (2001), referring to Sørensen and Laurendau, one reactivity expression of char in mixtures of H_2O and CO_2 as a function of the constants for only H_2O and CO_2 gasification is:

$$R = \frac{k_{1fw} P_{H2O} + k_{1fc} P_{CO2}}{1 + \frac{k_{1fw}}{k_{3w}} P_{H2O} + \frac{k_{1fc}}{k_{3c}} P_{CO2}} \quad (5)$$

If k_{3w} and k_{3c} refer to the same reaction, equation (5) could be further simplified to:

$$R = \frac{k_{1fw} P_{H2O} + k_{1fc} P_{CO2}}{1 + \frac{k_{1fw}}{k_3} P_{H2O} + \frac{k_{1fc}}{k_3} P_{CO2}} \quad (6)$$

This work as a continuation of the investigation with H_2O/H_2 and CO_2/CO previously reported (Barrio 2000a, 2000b). The objective of this investigation is to examine the kinetic model represented in equation (5) (or 6) and evaluate is ability to predict reactivity in mixtures of H_2O and CO_2. This investigation also tries to find out whether the experiments with H_2O and CO_2 separately can predict the gasification rate in mixtures of both gasses or not.

Experimental setup

The wood used in this investigation is Norwegian birch, as in previous work (Barrio et al., 2000a and 2000b). The proximate and ultimate analysis of the wood are presented in Table 1. The wood sample has been pyrolysed at the Technical University of Denmark, Department of Energy Engineering (DTU, ET) in a Macro-TGA. The char sample was thereafter crushed and sieved to 45-63 μm. The pyrolysis temperature and heating rate were chosen equal to those used in a previous work for steam and carbon dioxide gasification of the same char.

Proximate analysis	Moisture	Volatile matter*	Fixed carbon	Ash
Birch wood	15.76%	93.3%, mf	6.3%, mf	0.37%, mf
Ultimate analysis	C	H	N	O (by diff.)
Raw wood (%, mf)	48.7	6.4	0.078	44.45

* Pyrolysis conditions: Heating at 24 °C/min until 600 °C, held for 30 min, natural cooling.

Table 1: Proximate and ultimate analysis of birch.

The instrument used for this investigation is a Pressurised Thermogravimetric Analyser (PTGA) at ReaTech, a modified Du Pont Thermogravimetric Analyser that has been described elsewhere (Rathmann et al., 1995; Sørensen, 1994 and Hansen et al., 1997). The experiments are conducted under atmospheric pressure. The sample is placed on a small platinum tray, hanging on a horizontal balance arm. The sample temperature is measured with the help of two thermocouples, near to, but not in contact, with the sample. Temperature calibration was performed using as a reference the melting of aluminium (660.33 °C), silver (961.78 °C) and gold (1064.43 °C). The experimental matrix is presented in Table 2.

URN:NBN:no-2340

		H_2O			
		0 %	10 %	30 %	50 %
CO_2	0 %		♦ ◊◊ ●● oo	♦♦ ◊ ●●	♦ ◊◊◊ ●
	10 %	♦ ● oo ⊗[1]	◊	o	♦ ●
	30 %	◊◊ o	● oo	♦ ◊◊	●●
	50 %	♦ ●● ⊗[2]	◊	●	
	100 %	♦ ◊ o			

Table 2: Experimental matrix (♦: 750 °C, ◊: 800 °C, ●: 850 °C, o: 900 °C, ⊗: 950 °C).

Once the char sample is introduced into the PTGA, it is first dried in N_2 during 10 min at 200 °C, then is heated at 24 °C/min to 1000 °C and held at this temperature for 30 min. After this, the sample is cooled to the gasification temperature and when conditions are stable, both steam and CO_2 are allowed into the reaction chamber. The sample is hold isothermal until the gasification reaction is complete and then the temperature is raised to 1000 °C to complete the reaction. The sample size is approx. 5 mg and the total gas flow 1000 ml/min.

Results and discussion

Kinetic parameters obtained from experiments with H_2O/N_2 and CO_2/N_2 mixtures but without H_2O/CO_2 mixtures

Table 3 presents the kinetic parameters obtained according to Langmuir-Hinshelwood kinetics. k_{1fw} and k_{3w} are obtained from experiments with H_2O/N_2 while k_{1fc} and k_{3c} are obtained from the CO_2/N_2 experiments. The four constants are plotted in figure 2. This figure shows clearly that k_{3w} is not equal to k_{3c}. This means that the rate of desorption for the complex C(O) varies from H_2O to CO_2 gasification. It also supports the assumption suggested in the introduction that there are at least two types of CO desorption step and that the gas composition surrounding the char would affect the reaction path.

Kinetic parameter	K_{oi}	E_i(J/mol)	Kinetic parameter	K_{oi}	E_i(J/mol)
k_{1fw}	2.81e+8 $bar^{-1}s^{-1}$	2.29e+5	k_{1fc}	3.48e+5 $bar^{-1}s^{-1}$	1.64e+5
k_{3w}	1.56e+10 s^{-1}	2.77e+5	k_{3c}	1.70e+8 s^{-1}	2.47e+5

Table 3: Kinetic parameters from experiments with H_2O/N_2 and CO_2/N_2.

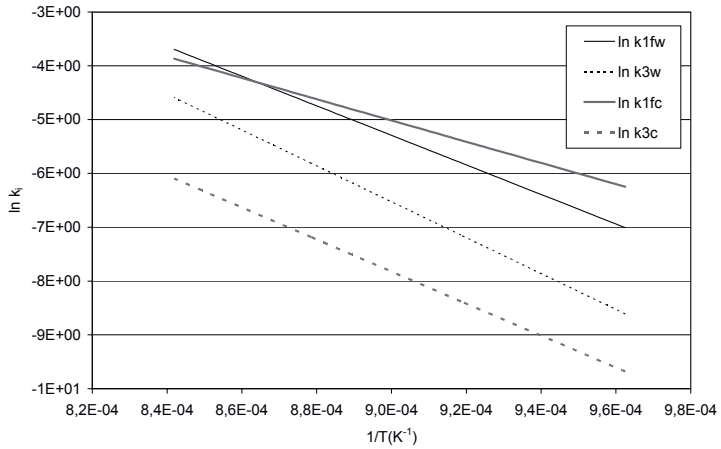

Figure 2: Kinetic constants for H_2O/N_2 and CO_2/N_2 experiments (Case 1 and 2).

[1] The experiments at 900 °C were conducted with 5 % CO_2.

[2] The experiment at 950 °C was conducted with 40 % CO_2.

URN:NBN:no-2340

These constants fit very well the experiments with H_2O/N_2 and CO_2/N_2 as shown in figures 3 and 4 respectively. The maximum deviation between predicted and calculated values is well below half an order of magnitude. Each prediction has been identified with a case number for the sake of clarity. The solid line represents the prediction of reactivity. It the points – experimental values- lay over the solid line it means that the predicted value is smaller than the experimental value. Alternatively, if the points lay under the solid line, the prediction over estimates the experimental results.

In order to predict the reactivity in H_2O/CO_2 mixtures based on H_2O/N_2 and CO_2/N_2 experimental data, there exist three alternatives regarding the value of k_3:

- Case 3: Equation (6), where $k_3=k_{3w}$
- Case 4: Equation (6), where $k_3=k_{3c}$
- Case 5: Equation (5)

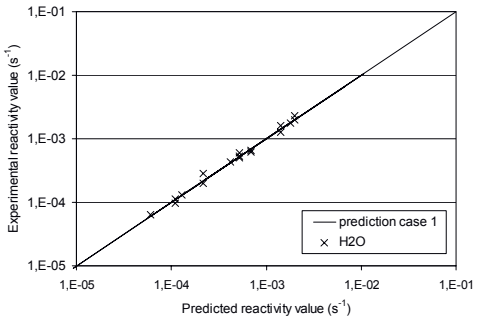

Figure 3: Fitting of experimental values for H_2O/N_2 experiments (Case 1).

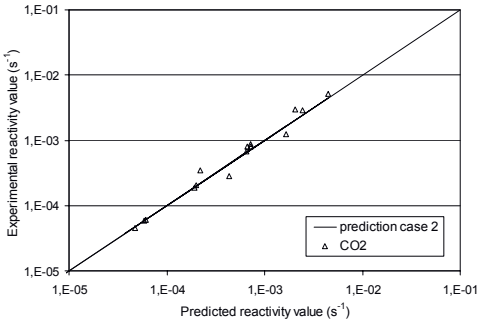

Figure 4: Fitting of experimental values for CO_2/N_2 experiments (Case 2).

The fitting of each set of predicted values to the experimental data is shown in figures 5, 6 and 7. Figure 5 (case 3) shows a good prediction of the H_2O/N_2 experiments, as expected. The prediction of H_2O/CO_2 mixtures is also very good (maximal deviation well below half an order of magnitude) while the reactivity in CO_2/N_2 mixtures is overpredicted by half an order of magnitude in most cases.

URN:NBN:no-2340

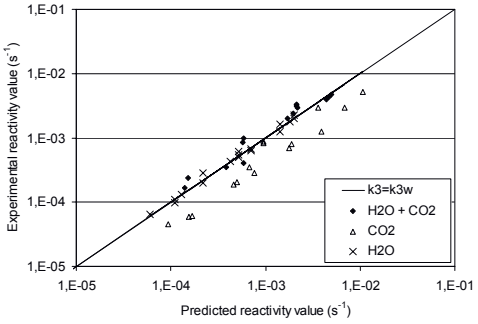

Figure 5: Fitting of experimental values (Case 3).

On the contrary, figure 6 (case 4) shows a good prediction of the CO_2/N_2 mixtures but underpredicts the H_2O/N_2 data (by approx. half an order of magnitude) and underpredicts even more the H_2O/CO_2 data.

Finally, case 5 –shown in figure 7- predicts correctly both H_2O/N_2 and CO_2/N_2 data but underpredicts by ca. half an order of magnitude the H_2O/CO_2 data.

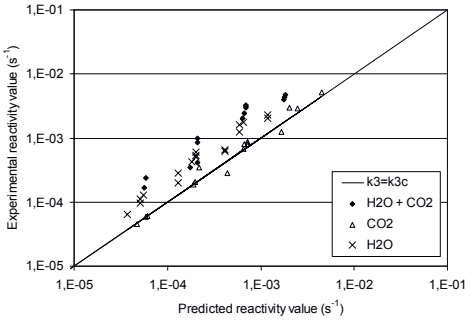

Figure 6: Fitting of experimental values (Case 4).

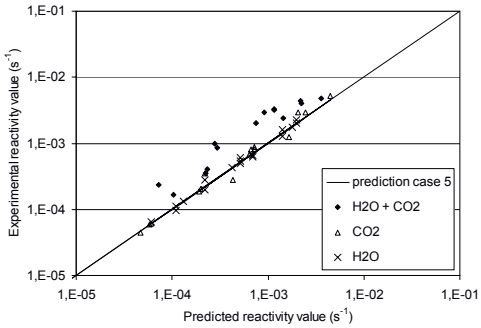

Figure 7: Fitting of experimental values (Case 5).

The results presented so far are somewhat unexpected. Even assuming different reaction rates for CO desorption for H_2O and CO_2 –case 5-, the char reactivity in mixtures of H_2O and CO_2 is underpredicted.

It is important that since $k_{3w} >> k_{3c}$ and k_{1w} is nearly equal to k_{1c} the reactivity in H_2O/CO_2 is fairly well predicted by k_{3w} from the steam reaction only. This result is contradictory to the results of Meijer et al. (1994) and is of practical importance since it indicates that if no kinetic data from mixtures are

URN:NBN:no-2340

available, equation (6) with $k_3=k_{3w}$ is a fair approximation. Case 3 overpredicts, however, the reactivity in CO_2/N_2 indicating that steam accelerates also the CO_2 gasification reaction.

Kinetic parameters obtained from experiments with H_2O/N_2, CO_2/N_2 and H_2O/CO_2 mixtures

Two cases have been analysed corresponding to whether equation (6) (case 6) or equation (5) (case 7) is used. The new kinetic parameters are presented in Table 4.
Figure 8 shows the new set of kinetic parameters for case 6 compared with the previous values. The figure shows that k_{1fw}^* is similar to k_{1fw} and k_3^* is also similar to k_{3w}. However, k_{1fc}^* differs considerably from k_{1fc}.

Case 6			Case 7		
Kinetic parameter	K_{oi}	E_i (J/mol)	Kinetic parameter	K_{oi}	E_i (J/mol)
k_{1fw}^*	2.19e+8 $s^{-1}bar^{-1}$	2.25e+5	k_{1fw}^{**}	8.70e+8 $s^{-1}bar^{-1}$	2.39e+5
k_{1fc}^*	3.50e+8 $s^{-1}bar^{-1}$	2.43e+5	k_{1fc}^{**}	4.78e+6 $s^{-1}bar^{-1}$	1.97e+5
k_3^*	1.55e+10 s^{-1}	2.77e+5	k_{3w}^{**}	1.56e+10 s^{-1}	2.76e+5
			k_{3c}^{**}	2. 70e+9 s^{-1}	2.68e+5

Table 4: Kinetic parameters obtained form experiments with H_2O/N_2, CO_2/N_2 and H_2O/CO_2 mixtures.

Regarding the prediction of experimental data, figure 9, the H_2O/N_2 experiments are very well predicted. The CO_2/N_2 experiments are reasonably predicted in most cases; the deviation between experiments and predicted values is below half an order of magnitude but in some cases the deviation is larger. Finally, the H_2O/CO_2 experiments are underpredicted although the maximal deviation is only half an order of magnitude.

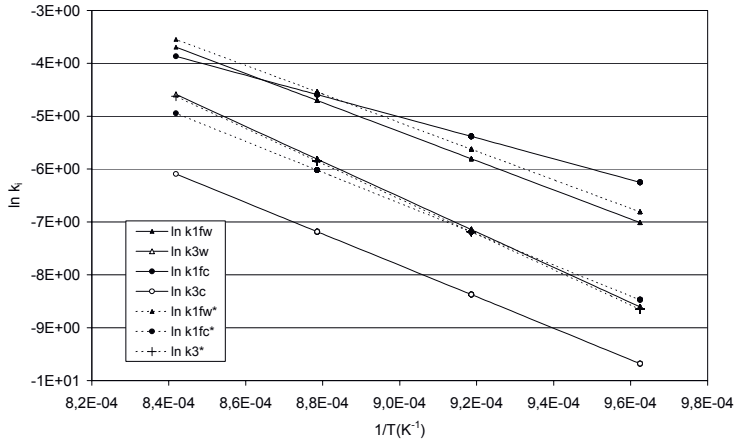

Figure 8: Kinetic constants for H_2O/N_2,CO_2/N_2 and H_2O/CO_2 experiments (Case 6).

URN:NBN:no-2340

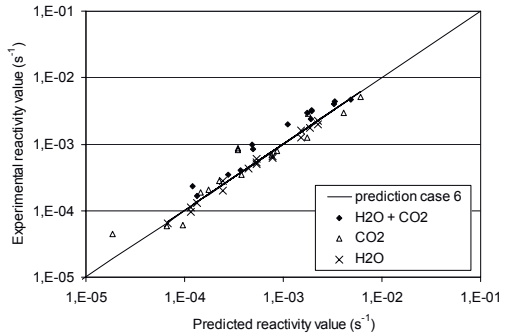

Figure 9: Fitting of experimental values (Case 6).

Although the prediction of CO_2/N_2 is reasonable, it is questionable if the kinetic parameters are correct. Figure 10 compares the fitting of the CO_2/N_2 data for case 2 and case 6. The shape of the curves in case 6 does not show the characteristic shape of Langmuir-Hinshelwood kinetics.

Case 7 uses equation (5). Accepting that k_{3w} is different from k_{3c} will allow for differences in the desorption of CO between H_2O and CO_2 gasification (reactions 2 and 4). Figure 11 shows the new kinetic constants in the Arrehnius diagram. k_{1fw}^{**} and k_3^{**} change little with respect to k_{1fw} and k_{3w} respectively. On the other hand, k_{1fc}^{**} changes considerably from k_{1fc} and also k_{3c}^{**} differs from k_{3c}. The variation is mostly due to changes in the frequency factor (k_{oi}) and less due to changes in activation energy.

The fitting of the experimental values is shown in figure 12. The prediction is good for H_2O/N_2 and CO_2/N_2 – well below half an order of magnitude- but H_2O/CO_2 experimental data are again underpredicted by half an order of magnitude in the worst case.

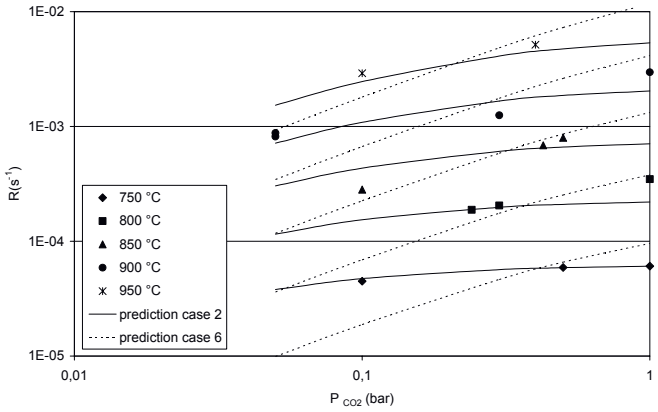

Figure 10: Fitting of experimental CO_2/N_2 data according to case 2 and case 6.

URN:NBN:no-2340

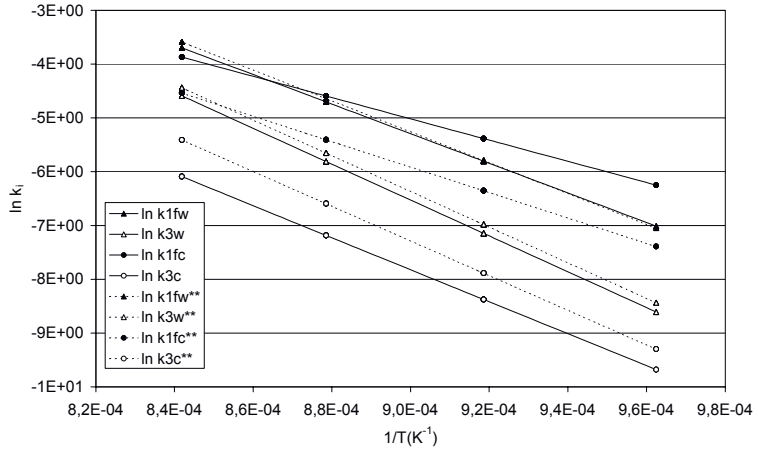

Figure 11: Kinetic constants for H_2O/N_2,CO_2/N_2 and H_2O/CO_2 experiments (Case 7).

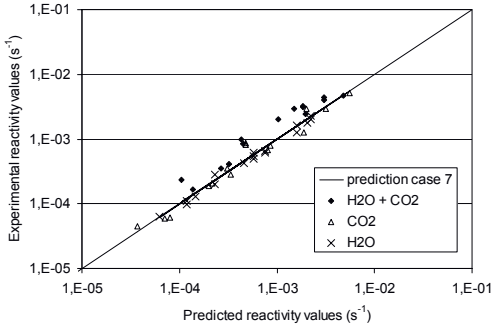

Figure 12: Fitting of experimental values (Case 7).

Case 6 and 7 give very similar predictions. Nevertheless, the fitting of the CO_2/N_2 data looks better in case 7 (Figure 13).

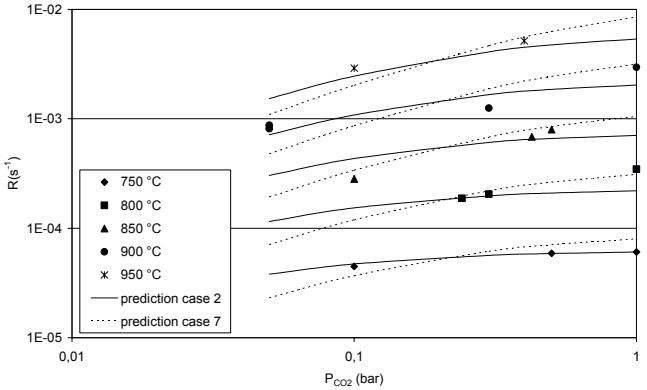

Figure 13: Fitting of experimental CO_2/N_2 data according to case 2 and case 7.

URN:NBN:no-2340

These last two cases do not give totally satisfactory results. Taking into consideration that many other factors affect the conversion of biomass in a reactor (heat transfer, diffusion properties, etc.), maybe the accuracy of the prediction presented here is acceptable. However, the results clearly show a general underprediction of the reactivity in H_2O/CO_2 mixtures (apart from case 3). In addition, the prediction of CO_2/N_2 mixtures using all data (case 6 and 7) shows a trend that has little theoretical explanation even if numerically the results are acceptable.

One explanation for the results is that the surrounding atmosphere has a marked relevance regarding reaction paths for the gasification reactions. If this is true, only data from H_2O/CO_2 experiments should be used to find the kinetic parameters for the simultaneous gasification in H_2O and CO_2. Unfortunately, the amount of experiments with mixtures of H_2O and CO_2 is not large enough to allow for such kinetic calculation.

Finally, there is no experimental evidence from this investigation to reject Langmuir-Hinshelwood kinetics. On the contrary, it looks like they can predict correctly gasification reactivity. The question raised here is that the reaction paths might change depending on the surrounding atmosphere. The presence of both CO_2 and H_2O could result in a faster desorption of C(O). Alternatively, there might be different active sites for the reaction with CO_2 than with H_2O, being the competition between both reactions lower than generally assumed. Table 5 presents a summary of the results.

Case	Experimental data	Constants obtained	Fitting of H_2O/N_2 experiments	Fitting of CO_2/N_2 experiments	Fitting of H_2O/CO_2 experiments
1	H_2O/N_2	k_{1fw}, k_{3w}	Very good d << ½ oom	n.a.	n.a.
2	CO_2/N_2	k_{1fc}, k_{3c}	n.a.	Very good d<< ½ oom	n.a.
3	H_2O/N_2 CO_2/N_2	k_{1fw}, k_{1fc}, $k_3=k_{3w}$ Equation (6)	Very good d<< ½ oom	Overpredicted by ½ oom	Very good d<< ½ oom
4	H_2O/N_2 CO_2/N_2	k_{1fw}, k_{1fc}, $k_3=k_{3c}$ Equation (6)	Underpredicted by ½ oom	Very good d<< ½ oom	Underpredicted by >½ oom
5	H_2O/N_2 CO_2/N_2	k_{1fw}, k_{1fc}, k_{3w}, k_{3c} Equation (5)	Very good d<< ½ oom	Very good d<< ½ oom	Underpredicted by ½ oom
6	H_2O/N_2 CO_2/N_2 H_2O/CO_2	k_{1fw}^*, k_{1fc}^*, k_3^* Equation (6)	Good d<< ½ oom	Reasonable d< ½ oom Very wrong trend	Underpredicted by <= ½ oom
7	H_2O/N_2 CO_2/N_2 H_2O/CO_2	k_{1fw}^{**}, k_{1fc}^{**}, k_{3w}^{**}, k_{3c}^{**}, Equation (5)	Good d<< ½ oom	Reasonable d< ½ oom Wrong trend	Underpredicted by <= ½ oom
8	H_2O/CO_2 only	Not enough experimental data points for this calculation.			

Table 5: Summary of results (d: deviation between experiment and prediction, oom: order of magnitude).

Conclusions

- The rate of desorption for the complex C(O) varies depending on the gas mixture surrounding the char. This explains why k_{3w} is different from k_{3c} and these from k_3^*.

- If the experimental data are obtained from separate H_2O/N_2 and CO_2/N_2 experiments, the reactivity of the char in mixtures of CO_2 and H_2O will be better predicted using equation (6) where $k_3=k_{3w}$.

- The kinetic model based on H_2O/N_2, CO_2/N_2 and H_2O/CO_2 experimental data gives reasonable results for H_2O/N_2 and CO_2/N_2 gasification but underpredicts the reactivity of char in mixtures of H_2O and CO_2.

- The optimum prediction of reactivity for mixtures of H_2O/CO_2 should be obtained from experiments conducted with $H_2O/CO_2/N_2$ mixtures only. Since 8 constants have to be calculated, a larger number of experiments should be conducted to find these constants.

URN:NBN:no-2340

References

1. Barrio, M. & Hustad, J.E. (2000a). CO2 gasification of birch char and the effect of CO inhibition on the calculation of chemical kinetics, Progress in Thermochemical Biomass Conversion, Tyrol, Austria, 17-22 September 2000, pp. 47-60.
2. Barrio, M., Gøbel, B., Risnes, H., Henriksen, U., Hustad, J.E. & Sørensen, L.H. (2000b). Steam gasification of wood char and the effect of hydrogen inhibition on the chemical kinetics, Progress in Thermochemical Biomass Conversion, Tyrol, Austria, 17-22 September 2000, pp. 32-46.
3. Bjerle, I.et al. (1982). Thermogravimetric analysis of Swedish shale char. Kinetics of the steam-carbon and carbon dioxide-carbon reactions, Industrial & Engineering Chemistry Research, Vol. 21, pp. 141-149.
4. Chen, N. & Yang, R.T. (1998). Ab initio molecular orbital study of the unified mechanism and pathways for gas-carbon reactions, Journal of Physical Chemistry A, Vol. 102, No. 31, pp. 6348-6356.
5. Chen, S.G. et al. (1993). A new surface oxygen complex on carbon: Toward a unified mechanism for carbon gasification reactions, Industrial & Engineering Chemistry Research, Vol. 32, No. 11, pp. 2835-2840.
6. Groeneveld, M.J. & Swaaij, W.P.M. (1980). Gasification of char particles with CO2 and H2O, Chemical Engineering Science, Vol. 35, pp. 307-313.
7. Gøbel, B. (2000). Dynamisk modellering af forgasning i fixed koksbed, Ph. D. Thesis, ET-PHD-99-04, The Technical University of Denmark.
8. Hansen, L.K., Rathmann, O., Olsen, A. & Poulsen, K. (1997). Steam gasification of wheat straw, barley straw, willow and giganteus, Risø National Laboratory, Optics and Fluid Dynamics Department, Project No. ENS-1323/95-0010.
9. Hurt R.H. & Calo J.M. (2001). Semi-global intrinsic kinetics for char combustion modelling. Combustion and Flame, Vol. 125, pp. 1138-1149.
10. Kapteijn, F., Meijer, R. & Moulijn, J.A. (1991). A transient kinetic study of the gasification of carbon in CO2, American Chemical Society, Preprints of papers, Division of fuel chemistry, pp. 906-913.
11. Liliedahl, T. & Sjöström, K. (1997). Modelling of char-gas reaction kinetics, Fuel, Vol. 76, No. 1, pp. 29-37.
12. Meijer, R., van der Linden, B., Kapteijn, F. % Moulijn, J.A. (1991). The interaction of H2O, CO2, H2 and CO with the alkali-carbonate/carbon system: a thermogravimetric study, Fuel, Vol. 70, February, pp. 205-214.
13. Meijer, R., Kapteijn, F. & Moulijn, J.A. (1994). Kinetics of the alkali-carbonate catalysed gasification of carbon: H2O gasification, Fuel, Vol. 73, No. 5, pp. 723-730.
14. Mims, C.A. & Pabst, J.K. (1987). Alkali-catalyzed carbon gasification kinetics: Unification of H2O, D2O, and CO2 reactivities, Journal of Catalysis, vol. 107, pp. 209-220.
15. Mühlen, H-J. , van Heek, K.H. & Jüntgen, H. (1985). Kinetic studies of steam gasification of char in the presence of H2, CO2 and CO, Fuel, Vol.64, July, pp. 944-949.
16. Rathmann, O., Stoholm, P. & Kirkegaard, M. (1995). The pressurized thermogravimetric analyzer at the Department of Combustion Research,, Risø: Technical description of the instrument, Roskilde: Risø National Laboratory, Risø-R-823(EN), Denmark.
17. Rensfelt, E., Blomkuist, G., Ekstrom, S., Espenäs, B.G. & Liinanki, L. (1978). Basic gasification studies for development of biomass medium-btu gasification processes, Energy from Biomass and Wastes, IGT, 14-18 August 1978. Paper No. 27, pp. 466-494.
18. Suuberg, E.M., Calo, J.M. & Wojtowicz, M. (1993). Oxygen chemisorption as a tool for characterizing "young" chars, American Chemical Society, Preprings of papers, Division of fuel chemistry, pp. 186-193.
19. Sørensen, L.H. (1994). Fuel reactivity as a function of temperature, pressure and conversion, Dr. techn. avhandling, Risø National Laboratory, Denmark.
20. Whitty, K.J., Backman, R. & Hupa, M. (1993). Empirical modeling of black liquor char gasification, Åbo akademi, Report 93-8. Department of Chemical Eng. Combustion Chemistry Research Group, Finland.

URN:NBN:no-2340

4. CONCLUSIONS AND RECOMMENDATIONS FOR FURTHER WORK

4.1 THE SMALL SCALE DOWNDRAFT GASIFIER

A stratified downdraft gasifier has been built as part of a small scale combined heat and power (CHP) plant. Its design is very flexible allowing for air injection at several locations. The gasifier has a thermal input of about 30 kW_{th} (4-6 kg/h pellets) and produces product gas with a low heating value of 5,3-5,7 MJ/Nm^3.

The first experiments had the objective of reaching stable operation. The movement of the zones has been analysed, showing that the pyrolysis rate is much higher than the char gasification rate resulting in a pyrolysis front moving upwards. The speed of the pyrolysis front depends on the temperature of the char gasification zone. During these first experiments it was observed that the pyrolysis front tends to stabilise at the top of the bed because of the very dry pellets and the difference in reaction rate between pyrolysis and gasification. However, top stabilisation was not possible because the semi-continuous feeding disturbs this mode of operation.

A stable mode of operation is reached, called "near top stabilisation" where the air is supplied below the top of the bed and the pyrolysis front cannot climb up from this point.

The stable operation of the gasifier has been characterised by the gas composition and the product gas tar and particle content. Other relevant parameters like the air-excess ratio, the air to fuel ratio and gas to fuel ratio have been calculated for each experiment to allow for comparison with other investigations (processes). The temperature profile inside the gasifier has also been obtained and compared with literature.

The energy balance shows cold gas efficiencies between 52 and 64%. The heat losses account for 20 to 30% of the thermal input. Although high, these heat losses are not unexpected, given the small size of the reactor.

The main differences between the design and the operational parameters are due to an air excess ratio at design of 0,2 to 0,7 when the experience shows that the air excess ratio is rather constant (0,25-0,3). The design feeding rate was

URN:NBN:no-2340

5-6 kg/h of pellets, but the gasifier can actually work with higher fuel feeding rates (4,3-6,9 kg/h).

The CO content of the product gas is higher than in similar gasifiers. The tar content in the product gas is also quite high in comparison with similar gasifiers.

From the experimental experience it has been concluded that the major drawback of the stratified downdraft gasifier is the difficult stabilisation of the zones.

Experiments have been conducted with a gas engine using mixtures of CH_4, CO, H_2, CO_2 and N_2 as a fuel. For a gas mixture similar to a LCV gas, the NO_x emissions are low (42 mg/Nm^3). As the content of methane in the mixture increases, NO_x emissions increase.

The CO emissions from the engine using LCV gas are very high (3500mg/Nm^3) and decrease as CH_4 is added to the fuel mixture. It was observed that variations in air excess ratio, rotational speed and engine load also affect emissions.

FURTHER WORK

The flexible design allows for changes in the location of the air supply. By adding air at different heights simultaneously the temperature profile could be altered and the gas composition, tar and particle content may vary.

The gas composition, namely the hydrogen content, can also be altered by substituting partially the air by steam as the gasification agent.

Finally, the tar content of the product gas should be reduced. It is expected that a more uniform high temperature at the pyrolysis front will have a positive influence.

4.2 REACTIVITY STUDIES

The main objectives of these reactivity studies have been to identify the reaction mechanisms that explain best the gasification of birch char in CO_2 and H_2O, including the inhibition effect of CO and H_2 and find a model that relates the mass loss rate to the temperature, gas composition and degree of conversion for each reaction.

The pyrolysis conditions under which the char has been obtained are of primary importance for reactivity. To avoid the influence of pyrolysis conditions in this

URN:NBN:no-2340

investigation, the char for all the experiments has been obtained exactly under the same conditions and in the same equipment.

The variation of reactivity with the degree of conversion has also been considered. Each experiment has been conducted until complete gasification of the sample and under isothermal conditions.

The ash components influence reactivity. The alkali compounds enhance reactivity while Si containing species decrease it. It has been observed that the char without any ash compounds has a very low reactivity. A short investigation has shown that K_2CO_3 addition improves the reactivity of the char sample but the addition of the water non soluble ash compounds (Si containing) diminishes char reactivity when added to the K_2CO_3/char mixture. K_3PO_4 also increases the washed char reactivity but not that remarkably. Ash addition in this case does not affect reactivity.

It has been observed that the experimental apparatus has some influence in the results. Possible explanations are connected to the crucible material and to the construction of the apparatus.

Kinetic parameters have been obtained for the steam gasification of birch and beech char. Langmuir-Hinshelwood kinetics predict fairly the inhibition effect of hydrogen. Birch and beech present very similar kinetic parameters, although they differ in the reactivity profiles. It has been observed that the calculation procedure mainly affects the frequency factor and not the activation energy or the reaction order.

The gasification of birch in CO_2 has been studied in a similar manner, also including the inhibition effect of CO. Again, Langmuir-Hinshelwood kinetics predict very well the experimental data. The ratio CO/CO_2 has been found to be a relevant parameter for reactivity. Temperature seems to have a small effect on the shape of the reactivity profile while reactant's partial pressure and the ratio CO/CO_2 show no influence.

The gasification experiments in mixtures of CO_2 and H_2O give reasons to believe that the rate of desorption for the complex C(O) varies depending on the gas mixture surrounding the char.

URN:NBN:no-2340

It has been found that if the experimental data are obtained from separate H_2O/N_2 and CO_2/N_2 experiments, the reactivity of the char in mixtures of CO_2 and H_2O can be fairly predicted. Nevertheless, the optimum prediction of reactivity for mixtures of H_2O/CO_2 should be obtained from experiments conducted with $H_2O/CO_2/N_2$ mixtures only.

FURTHER WORK

The catalytic reactions involving ash components are of great importance and should be studied further. The changes in char structure during gasification deserve also additional attention since the relevant reactions take place at the particle surface. Finally, further experiments with complex gas mixtures should be conducted in order to provide a better basis to a kinetic model.

4.3 CONNECTION BETWEEN THE EXPERIMENTAL WORK WITH THE GASIFIER AND THE REACTIVITY STUDIES

CHAR GASIFICATION AS THE BOTTLE NECK FOR GASIFICATION PROCESSES

Char gasification is a crucial element in a gasification process because it is the slowest part of the process. The movement of the zones observed in the gasifier, as described in Paper I, is directly related to the low char gasification rate compared to the pyrolysis rate. The rate of char gasification is also relevant regarding zone stabilisation. Better knowledge of char gasification will allow improvement in process efficiency.

STRONG INFLUENCE OF PYROLYSIS

The gasification reactivity depends strongly on the properties of the char formed during pyrolysis. Pyrolysis conditions are totally inherent to each reactor: residence time, temperature history, maximal temperature achieved, location of the oxidant supply (and therefore location of the heat source). The composition of the pyrolysis/devolatilization gas is difficult to obtain experimentally but very relevant to model the char gasification zone.

TAR FORMATION

The temperature in the pyrolysis zone is the most important parameter regarding tar formation. A simple model would predict a uniform temperature at the pyrolysis zone, while that might not be the case in the operational reactor. Not only the model should be accurate enough to predict the temperature field especially at the pyrolysis zone but also the experimental work should focus on how to obtain high and uniform temperature fields in this zone. The experimental

URN:NBN:no-2340

work presented here might have suffered from irregular temperature at the pyrolysis zone resulting in higher tar formation than expected.

CHAR REACTIVITY IN COMPLEX GAS MIXTURES

The gas mixture surrounding the char depends on:

- Gasifying agents
- Gas products from pyrolysis
- Combustion of pyrolysis products in air or other oxidant agent
- Heat management inside the reactor (heat properties of the pellets, heat losses of the reactor)

In addition, as char gasification proceeds, the composition of the gas mixture changes, especially the amounts of H_2 and CO. The inhibition effect of these gases in the gasification reactions is therefore important, as it has been shown in this investigation.

Finally, it is common in gasification modelling that each of the gasification reactions is treated rather independently. This investigation has shown, however, that there might be some interaction between both reactions.

CHAR REACTIVITY AND DEGREE OF CONVERSION

Char reactivity depends on the degree of conversion. This fact is usually taken into consideration in modelling but the practical implications have not been given too much attention. Because of the endothermic gasification reaction, the temperature drops fast after the flaming pyrolysis. This implies that the active gasification zone where the temperature is above 800 °C is quite thin. The residence time of the char in this zone would be short, allowing only for lower degrees of conversion. As experienced during the reactivity experiments of this investigation, lower degrees of conversion correspond to lower reactivity. It remains a challenge how to make use of the high char reactivity at high degrees of conversion.

The reactivity profile f(X) can be obtained experimentally but f(X) is difficult to model since it is connected to char structure and presence of catalysts.

It is difficult to reduce all the experimental data to only one reactivity profile as it is desired for modelling purposes.

CHAR REACTIVITY IS ONE OF MANY FACTORS

There are many other factors that influence product gas composition and gasification efficiency. It is questionable how relevant is char reactivity in comparison with other parameters. Among others, the equilibrium of the water

URN:NBN:no-2340

gas shift reaction seems to be a very significant element dictating the product gas composition.
On the other hand, it has been experienced in this investigation that the gas composition changes very little with air addition.

HEAT MANAGEMENT IN THE GASIFICATION PROCESS

There is no experimental evidence from this investigation that an increase in air addition results in an increase of temperature inside the gasifier. Increased air supply has resulted in increased biomass supply with an almost constant air to fuel ratio. Such self-adjusting process still remains unexplained.

MODELLING PARAMETERS VS. EXPERIMENTAL PARAMETERS

The gasification experiments presented in this work have only one experimental parameter: air supply. The biomass feeding rate, air-to-fuel ratio, air excess ratio and gasification temperature are not parameters but consequences of the variation in air supply. However, the air excess ratio is a common modelling parameter.

Modelling is a useful tool to predict the behaviour of the reactor if some experimental parameters change and therefore any model should include experimentally determined parameters. The almost constant air excess ratio represents a challenge to model.

Other possible experimental parameters are the location and temperature of the air supply. Also the substitution of air by other oxidant agents has not been investigated. The effect of reactor geometry is also difficult to observe experimentally. It would be very interesting to obtain some predictions in these directions from a model.

Summarising, char reactivity depends on surrounding atmosphere, temperature and degree of conversion, as obtained experimentally. All three factors vary along the reactor (like temperature, observed experimentally). It might be difficult to integrate such complex environment in a reactor model.

URN:NBN:no-2340

APPENDIX A
Pictures

URN:NBN:no-2340

URN:NBN:no-2340

Figure A.1: Stratified downdraft gasifier. Inner reactor

Figure A.2: Stratified downdraft gasifier. Outer reactor

URN:NBN:no-2340

Figure A.3: Biomass feeding system

Figure A.4: Air feeding system

URN:NBN:no-2340

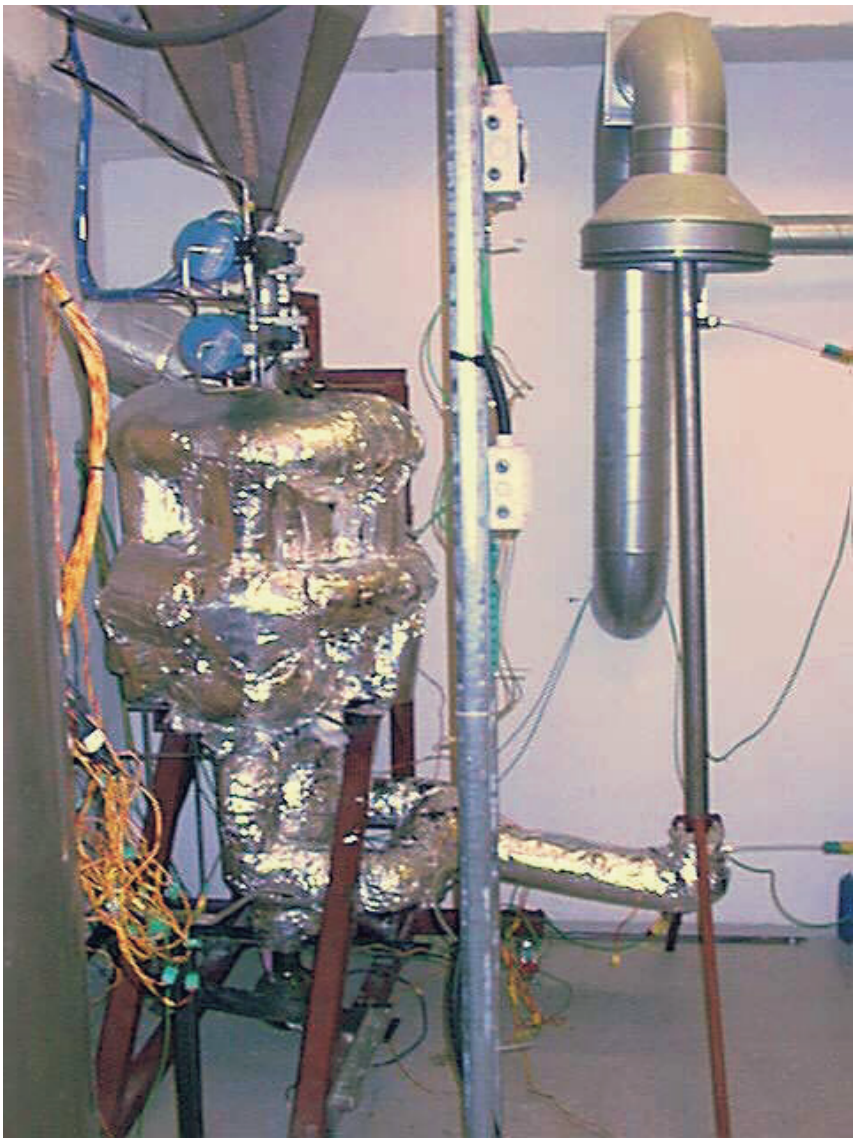

Figure A.5: Stratified downdraft gasifier. Overview

URN:NBN:no-2340

Figure A.6: Flaming pyrolysis inside the gasifier

URN:NBN:no-2340

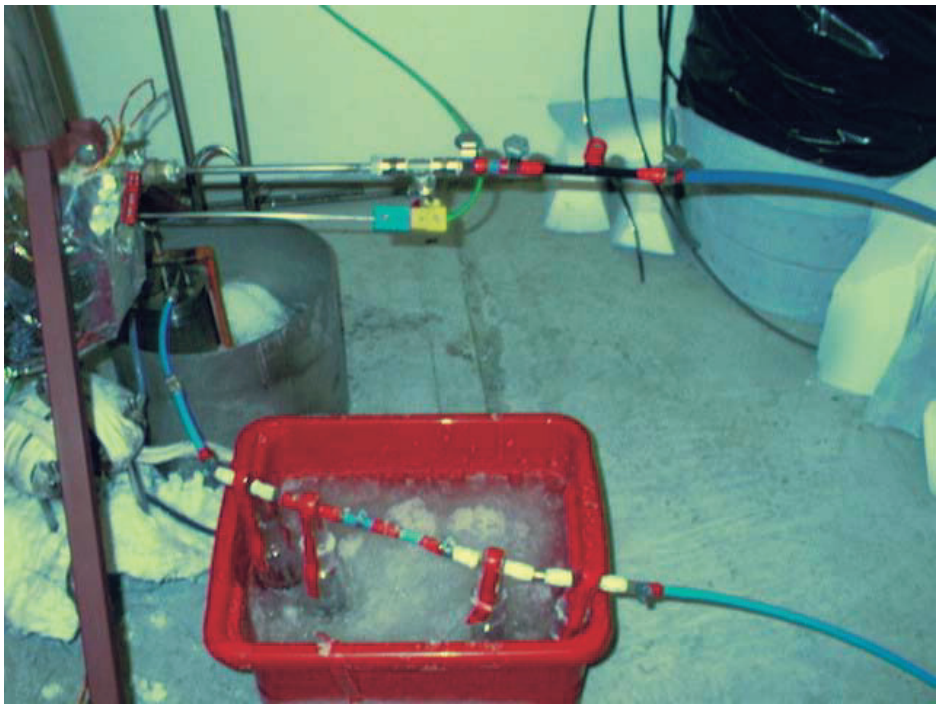

Figure A.7: Gas sampling line.

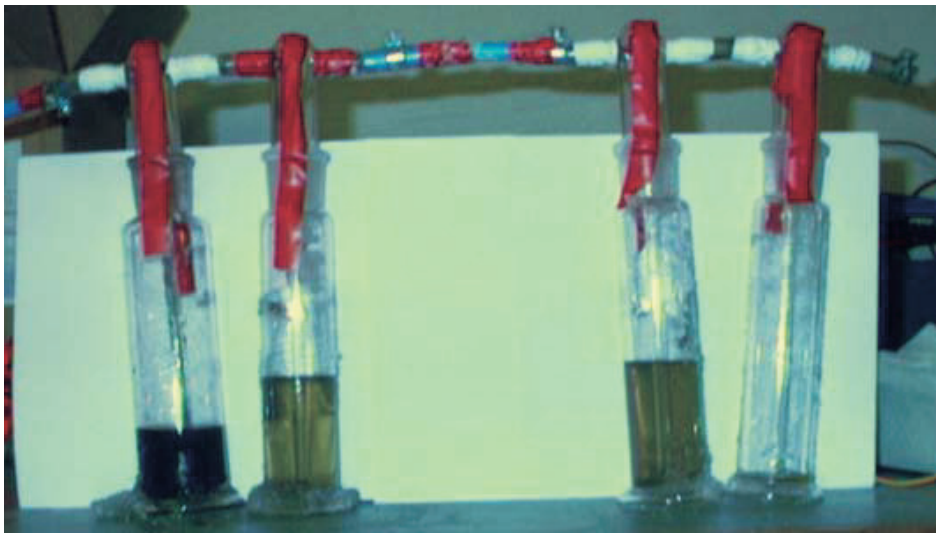

Figure A.8: Impinging bottles after experiment

URN:NBN:no-2340

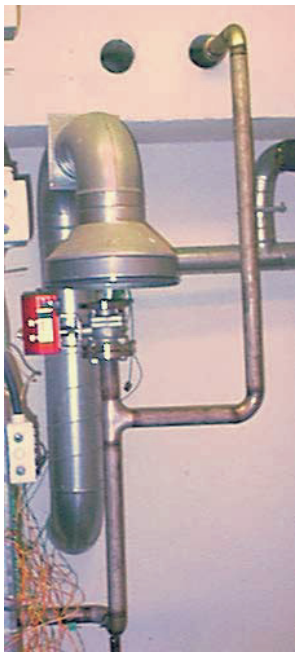

Figure A.9: Connection between the gasifier and the condenser

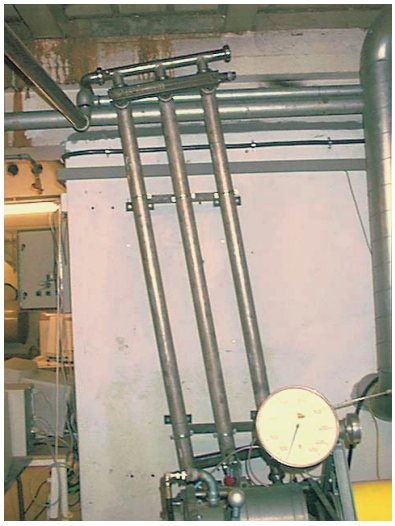

Figure A.10: Condenser and filter

URN:NBN:no-2340

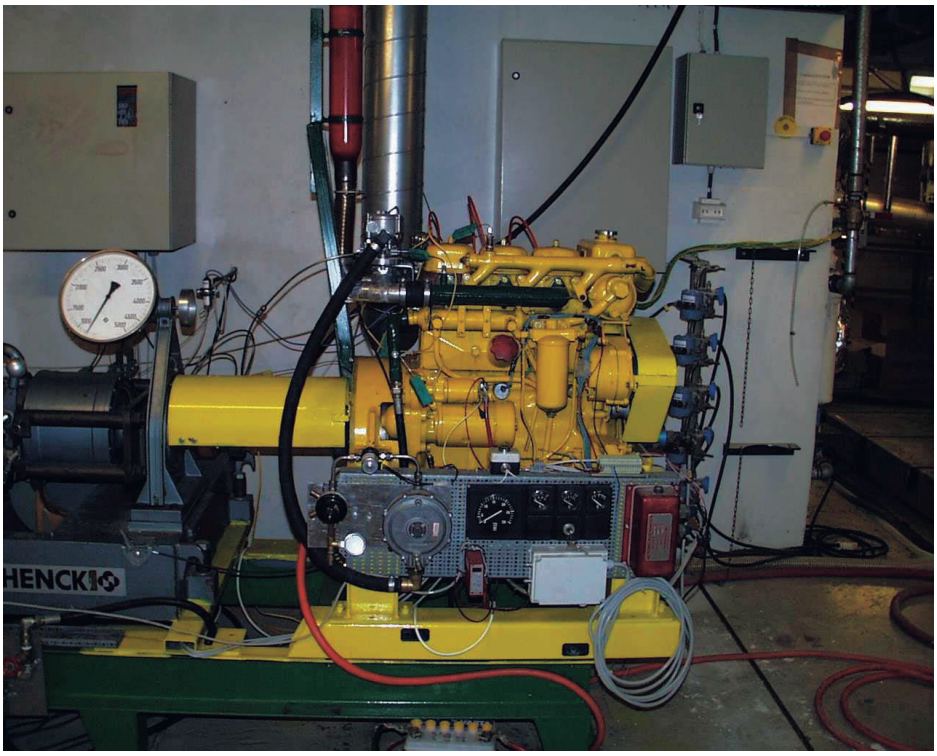

Figure A.11: Modified Diesel engine

URN:NBN:no-2340

URN:NBN:no-2340

APPENDIX B

PROCEDURES

URN:NBN:no-2340

URN:NBN:no-2340

B.1 STARTING AND STOPPING PROCEDURE FOR THE OPERATION OF THE GASIFIER

PREPARATIONS SOME DAYS IN ADVANCE OF THE EXPERIMENT

- If the nitrogen bottle is empty, or the pressure reads less than 100 bar it must be replaced.
- The GC must be switched on 2 days before the experiment (**NB: Follow GC-PROCEDURE**).
- Check that there are pyrolysed pellets available. If not, commercial charcoal has to be cut in small pieces, as similar to the pellets as possible.

CHECKLIST BEFORE PREHEATING

- Check that the pressure in the N_2 bottle is more than 100 bar.
- Check that the emergency stop is not pressed.
- Check that the preheater temperature is set to 0°C.
- Check that the valve for pressurised air to the sliding valves (V3) is closed.
- Make sure the pressure-cells are connected.
- Connect the preheater.
- Start the computer and the Lab View program.
- Check that the feeding system control shows that the sliding valves are closed.
- Check that the pressure connections are fine, no loose ends, that P_0 is connected to the bottom of the gasifier.
- Check that the view port is closed.
- Check that the valve for gas analysis is closed. (**NB: The gas analysis has its own procedure**).
- Check that the glass bottle is in place
- Check that the crank for ash removal is almost closed.
- Check that the hopper is empty.

URN:NBN:no-2340

PREHEATING PROCEDURE (DAY BEFORE EXPERIMENT)

- Open the air supply:
    - Check that V2, the reducing valve (V4) and all air channel valves (V6-V10) are closed.
    - Check that the valve before the manifold (V5) is open.
    - Open 3 or 4 air channels. To do this, rotate the air channel valve approximately 200° anti-clockwise.
    - Open the air supply valve (V2).
    - Open the reducing valve (V4) slowly, looking at the pressure reading at the manifold, and avoiding oscillations in the air channel valves. If oscillation appears in the manometer, open the air channel valve carefully until the oscillation stops. Then, close the air channel valve a little bit.
- Adjust the pressure and airflow for preheating. ($P_{manifold} \simeq$ 1,2 barg, all levels at 30%)
- Check that air is coming out of the last pipe. (Go inside and check that everything is OK).
- Set preheater to 100°C
- Set the warning signs: Warm signs at the rotameters and around the gasifier, and contact in case of problems.
- Check temperature with the computer.
- Check that none of the thermocouple cables are in contact with hot surfaces.
- Write down the preheating conditions in the lab book.
- After some time, increase the temperature in the preheater to 250°C.
- Switch on the current to the filament to the GC. (**NB: Low current, follow GC-PROCEDURE**).

NEXT MORNING

- Check the temperature readings at the computer (T manifold < 400°C), and eventually adjust the temperature of the preheater.
- Other temperatures should be stable.
- Set the biomass feeding control system into "MANUAL" mode.
- Check insulation condition.
- Prepare 1000 ml charcoal by filling up the glass recipient, weight it and note down the weight in the lab book.
- Prepare charcoal in small pieces for ignition.
- Find a tong and a propane burner.

URN:NBN:no-2340

- Get the CO detector.
- Prepare the CO protection mask
- Make sure you have the air flow measurement sheet.
- Remove the hopper cover.
- Fill the hopper with pellets (Done from 1st floor).
- Prepare the N_2 bottle:
    - Check that the main valve (V6), the reduction valve (V7) and the on/off valve (V9) is closed.
    - Open the main valve (V6).
    - Open the on/off valve (V9).
    - Open slowly the reduction valve until a little flow of N2 comes out. (It is possible to hear it).
    - Once the flow is adjusted, close the on/off valve.
- Open the valve for air supply to the sliding valves (V3).
- Start the suction system and put the note: "Do not switch off,"
- Make sure the gas sampling line is ready (**NB: It has its own procedure**).
- Increase the pressure in the manifold to 2 barg.

RIGHT BEFORE STARTING THE EXPERIMENT

- Connect the CO alarm
- Open the file for collecting data.

HOW TO START THE GASIFIER?

- Stop the air supply.
- Open the view port.
- Feed the char (1000ml) through the view port.
- Ignite the charcoal pieces and insert them in the reactor with the tong.
- Close the view port
- Put some air in level 2 (40%) and 4 (10%). (**NB: Be careful NOT to use too much air! Thermocouples could melt!**).
- Look at T4-T7 and see if there is ignition.
- Once the temperatures are going up (very fast up to 1000°C), send 4 charges of pellets.
- Close air level 4 and adjust air level 2 to the right amount (usually 50-60%).
- Now the experiment is started. GOOD LUCK!!
- NB: Remember to note down P manifold, changes in air supply, GC samples and grid shaking.

URN:NBN:no-2340

WHEN THE EXPERIMENT IS FINISHED (BUT STILL WARM)

- Close the valves before the pressure cells. If we're producing tar, the pressure cells could be damaged.
- Close the reducing valve for air supply, and close all levels carefully.
- Shut down the GC. (**NB: Follow the GC-PROCEDURE**).
- Biomass control: OFF mode
- Stop the CO detector, if no danger.
- Write report in the lab book.
- If some reaction is going on, do not turn the fan off neither remove the note. Nevertheless, try to not have the fan on during the night.

WHEN THE REACTOR HAS COOLED DOWN (NEXT MORNING)

- Close the N_2 bottle and remove it if it is empty.
- Remove the warning signs
- Shut down the fan if still on and remove the warning note.
- Open the reactor if necessary. **If opened, then remove the pellets from the hopper**. If there is no need to open the reactor, the pellets inside should be removed using a vacuum cleaner.
- Shut down the computer
- Collect the ash from the ash bottle, eventually char, condensate from the gas line, etc.

URN:NBN:no-2340

B.2 STARTING AND STOPPING PROCEDURE FOR THE GAS CHROMATOGRAPH

BEFORE STARTING THE EXPERIMENT

- Open the Argon bottle. (P=3.0 bar)
- Lift the red cover and check that the detector current is off.
- Switch on the GC.
- Check that there is a green light.
- Actual pressure =30 psi.
- Oven temperature should be ambient temperature.
- Lift the red cover and check that there is Argon coming out of the detector (submerge the orange rubber hose in a small water recipient and see that there are bubbles coming out)
- Switch on the computer.
- When the PC asks for the Network Password, just close the window.
- Start Peak Simple program.
- Check that the oven starts to heat up (new total set point 50°C).
- Select the control file to be used (argon.con).
- Wait for 24 hours for the GC to stabilise.
- Set the warning sign "Do not touch the equipment"
- Lift the red cover and switch on the detector to **LOW CURRENT!**
- Wait for 24 hours for the detector to stabilise. The reading in TCD protect actual value should be ca.423 (411).
- Now the GC is ready for operation.

WHEN THE EXPERIMENT IS FINISHED

- Lift the red cover and switch off the detector current.
- Log out the computer.
- Switch off the GC power.
- Close the Argon line. (Only main valve, to assure equal flow in all experiments.)

URN:NBN:no-2340

URN:NBN:no-2340

APPENDIX C

Technical data

URN:NBN:no-2340

URN:NBN:no-2340

C.1 PELLETS DENSITY

The pellet's density is calculated based on their cylindrical shape.

Nr.	length [mm]	diameter [mm]	mass [g]	density [kg/m3]
1	15,2	6,6	0,513	986
2	15,4	6,3	0,561	1169
3	11,1	6,4	0,406	1137
4	8,2	6,3	0,294	1150
5	7,1	6,5	0,228	968
6	7,3	6,2	0,229	1039
7	6,4	6,1	0,208	1112
8	5,0	6,0	0,156	1103
9	7,6	6,4	0,219	896
10	6,7	6,4	0,220	1021
			average:	**1058**

C.2 PELLETS BULK DENSITY

This measurement has been conducted at the reactor diameter (100mm).

D_i [m]	Height [m]	weight [kg] (sample + vessel)	weight [kg] sample	average weight [kg] sample	bulk density [kg/m^3]
0,1	0,1	0,752	0,5043	**0,5247**	**668**
		0,7848	0,5371		
		0,7804	0,5327		

C.3 INITIAL BED DENSITY

The experiments are always started in the same manner. Once the reactor is hot, a fixed volume of pyrolysed pellets or small charcoal pieces is introduced through the ignition hole. The amount of pellets or charcoal introduced fills a recipient of 100mm diameter and 100mm height. The following table shows the weight of the pyrolysed pellets (or small charcoal pieces). The accuracy of the measurement is very low.

Once ignition is detected by a sudden increase in temperature, the ignition hole is closed and the reactor is filled with raw pellets from the hopper.

URN:NBN:no-2340

Exp number (char origin)	D_i [m]	Height [m]	Weight (s+v) [kg]	Weight vessel [kg]	Weight sample [kg]	Average weight [kg]	bulk density [kg/m^3]
3 (pellets)	0,1	0,1			0,2033	**0,2079**	**265**
4(charcoal)					0,182		
5(pellets)					0,1703		
6 (pellets)			0,501	0,243	0,258		
7(mix)			0,5044	0,243	0,2614		
8(charcoal)			0,499	0,243	0,256		
9(pellets)			0,432	0,242	0,19		
12 (charcoal)			0,4509	0,2431	0,2078		
13(charcoal)			0,4665	0,243	0,2235		
14 (charcoal)			0,3689	0,242	0,1269		

C.4 FEEDING RATE

The pellets are fed semi-continuously by means of two sliding valves. Every time, the sliding valves deliver approximately the same amount of pellets, i.e. a ”charge” of pellets. During the experiment, the number of charges fed is recorded as well as when it took place.

The following table show measurements of the mass of pellets supplied to the gasifier per charge.

Sample number	kg per charge
1	0,3392
2	0,3399
3	0,3446
4	0,3478
5	0,3474
average [kg]:	**0,3438**

C.5 ERROR IN FEEDING RATE

During the experiment, the bed level is maintained at some height between the location of thermocouple T1 (h=310 mm) and the top of the reactor (h=500 mm). The exact location of the bed level is unknown and this results in an error in the feeding rate.

The following table shows the error in feeding rate for each experiment.

URN:NBN:no-2340

kg pellets per charge			0,344					
Gasifier diameter (m)			0,1					
Gasifier cross section (m2)			0,00785					
Pellets bulk density (kg/m3) at ø100mm			668					
Uncertainty bed level (m)			0,095	=(0,500-0,310)/2				
Uncertainty bed volume (m3)			0,0007458					
Uncertainty mass of pellets (kg)			0,498161					
Uncertainty (charges)			1,45					
Exp. Num.	#8a	#8b	#9	#12	#13a	#13b	#13c	#14
Feeding rate (kg/h)	6,46	6,88	5,84	5,66	4,69	7,48	6,55	5,97
t1 for feeding rate (min)	84,1	152,06	126,1	141,15	125,25	229,65	273,65	248,05
t2 for feeding rate (min)	147,966	173,06	161,433	214	226,3	271	289,4	372,45
Charges of pellets during experiment	20	7	10	20	23	15	5	36
Max. biomass feeding rate (kg/h)	6,93	8,30	6,68	6,07	4,99	8,21	8,45	6,21
Min. biomass feeding rate (kg/h)	5,99	5,45	4,99	5,25	4,40	6,76	4,65	5,73
+/- error in feeding rate (kg/h)	0,47	1,42	0,85	0,41	0,30	0,72	1,90	0,24
% error in biomass feeding rate	**7,2%**	**20,7%**	**14,5%**	**7,2%**	**6,3%**	**9,7%**	**29,0%**	**4,0%**

C.6 STOICHIOMETRIC AMOUNT OF AIR REQUIRED FOR COMBUSTION

This calculation is based on the ultimate analysis of the pellets, their moisture and ash content.

PROXIMATE ANALYSIS BASED ON WET FUEL

		VI-TRE Pellets
Volatiles	% wt	**x**
fixed C	% wt	**y**
Moisture	% wt	**7,50**
Ash	% wt	**0,39**

ULTIMATE ANALYSIS

	VI-TRE Pellets	
	with ash + moisture [%]	daf [%]
C	46,70	50,70
O	39,05	42,40
H	6,36	6,90
N	0,00	0,00
S	0,00	0,00
ash	0,39	
moisture	7,50	
S	100,00	100,00

URN:NBN:no-2340

MINIMUM AMOUNT OF OXYGEN REQUIRED FOR COMBUSTION

1,867 x C		
5,600 x H	o_{min} [m^3_{O2}/kg $_{Pellet}$]:	0,9544
0,700 x S	$l_{min,dry}$ [$m^3_{Air,dry}$/kg_{Pellet}]:	4,5448
- 0,700 x O	$l_{min,dry}$ [$kg_{Air,dry}$/kg $_{Pellet}$]:	5,8765
SUM = o_{min}		

C.7 AIR AMOUNT

The air amount is measured by rotameters. The rotameters are initially calibrated for 4 bar absolute pressure and 20 °C. Different temperature and pressure conditions require correction factors. The tables below indicate the corrections and air flow readings.

P correction		
Pabs(bar)	Prel(barg)	P correction
4	3	1
3	2	0,86
2,5	1,5	0,789
2	1	0,706

T correction	
T (°C)	T correction
20	1
50	0,95
100	0,88
150	0,83
200	0,78
250	0,75
300	0,72
350	0,66
400	0,64

Working pressure: 3bar (abs)

Flow (Nm^3/h) = Scale x $Flow_{max}$ x P_{corr} x T_{corr}

$Flow_{max}$ = 24 Nm^3/h

FLOW (Nm3/h)	Temp. (°C)								
Scale	**20**	**50**	**100**	**150**	**200**	**250**	**300**	**350**	**400**
10 %	2,06	1,96	1,82	1,71	1,61	1,55	1,49	1,36	1,32
20 %	4,13	3,92	3,63	3,43	3,22	3,10	2,97	2,72	2,64
30 %	6,19	5,88	5,45	5,14	4,83	4,64	4,46	4,09	3,96
40 %	8,26	7,84	7,27	6,85	6,44	6,19	5,94	5,45	5,28
50 %	10,32	9,80	9,08	8,57	8,05	7,74	7,43	6,81	6,60
60 %	12,38	11,76	10,90	10,28	9,66	9,29	8,92	8,17	7,93
70 %	14,45	13,73	12,71	11,99	11,27	10,84	10,40	9,54	9,25
80 %	16,51	15,69	14,53	13,70	12,88	12,38	11,89	10,90	10,57
90 %	18,58	17,65	16,35	15,42	14,49	13,93	13,37	12,26	11,89
100 %	20,64	19,61	18,16	17,13	16,10	15,48	14,86	13,62	13,21

URN:NBN:no-2340

APPENDIX D

EXPERIMENTAL RECORDS

URN:NBN:no-2340

URN:NBN:no-2340

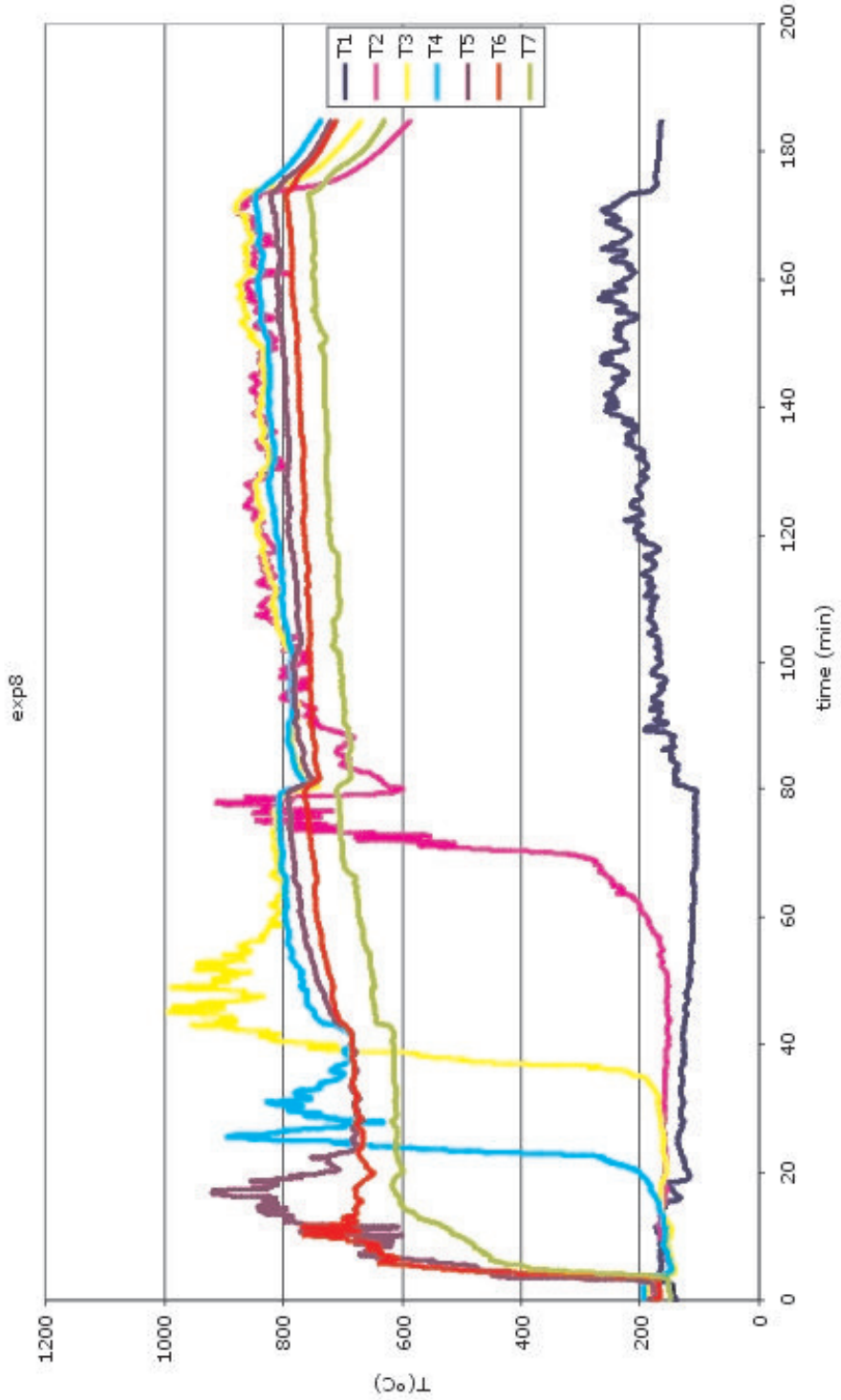

URN:NBN:no-2340

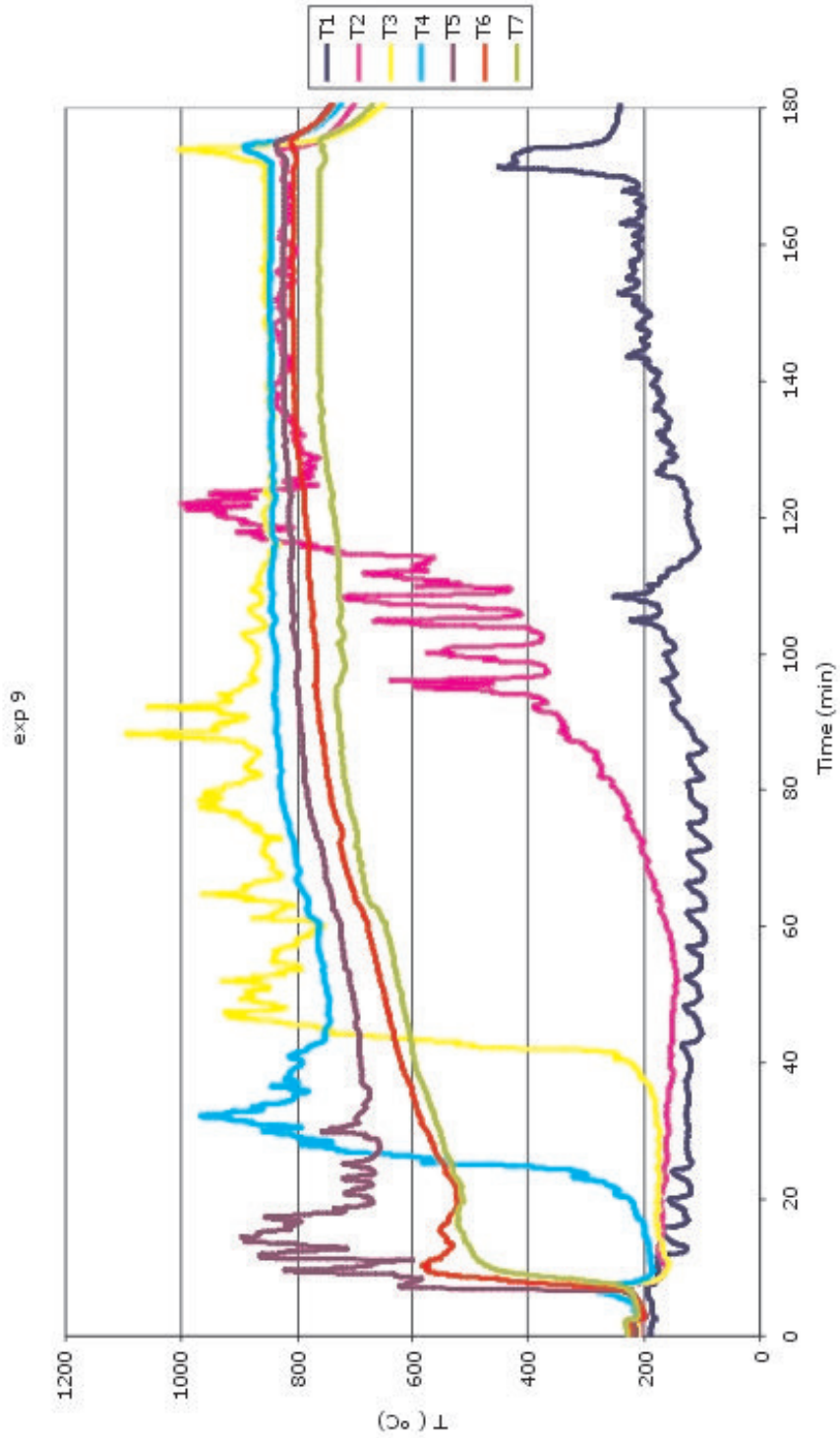

URN:NBN:no-2340

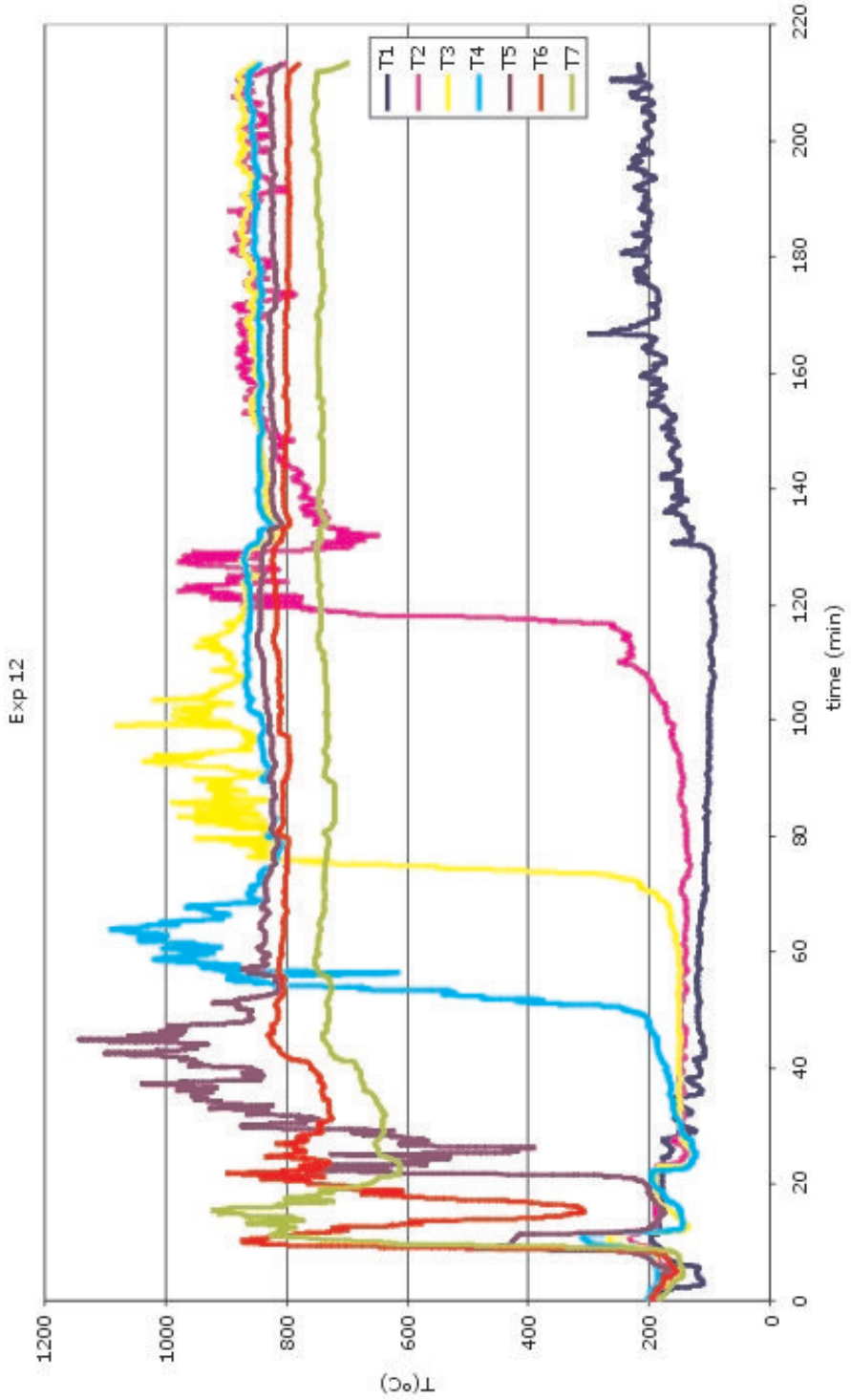

URN:NBN:no-2340

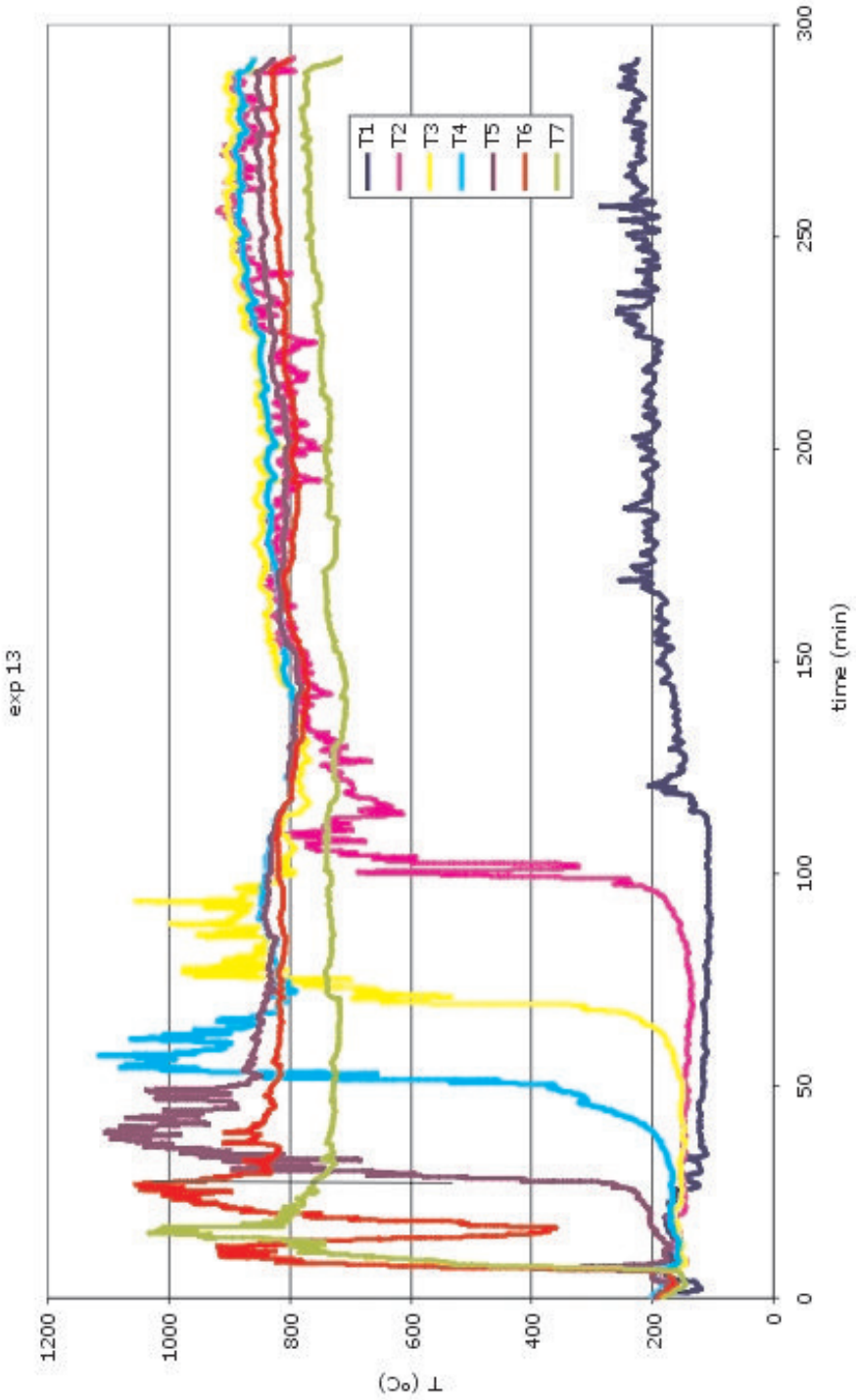

URN:NBN:no-2340

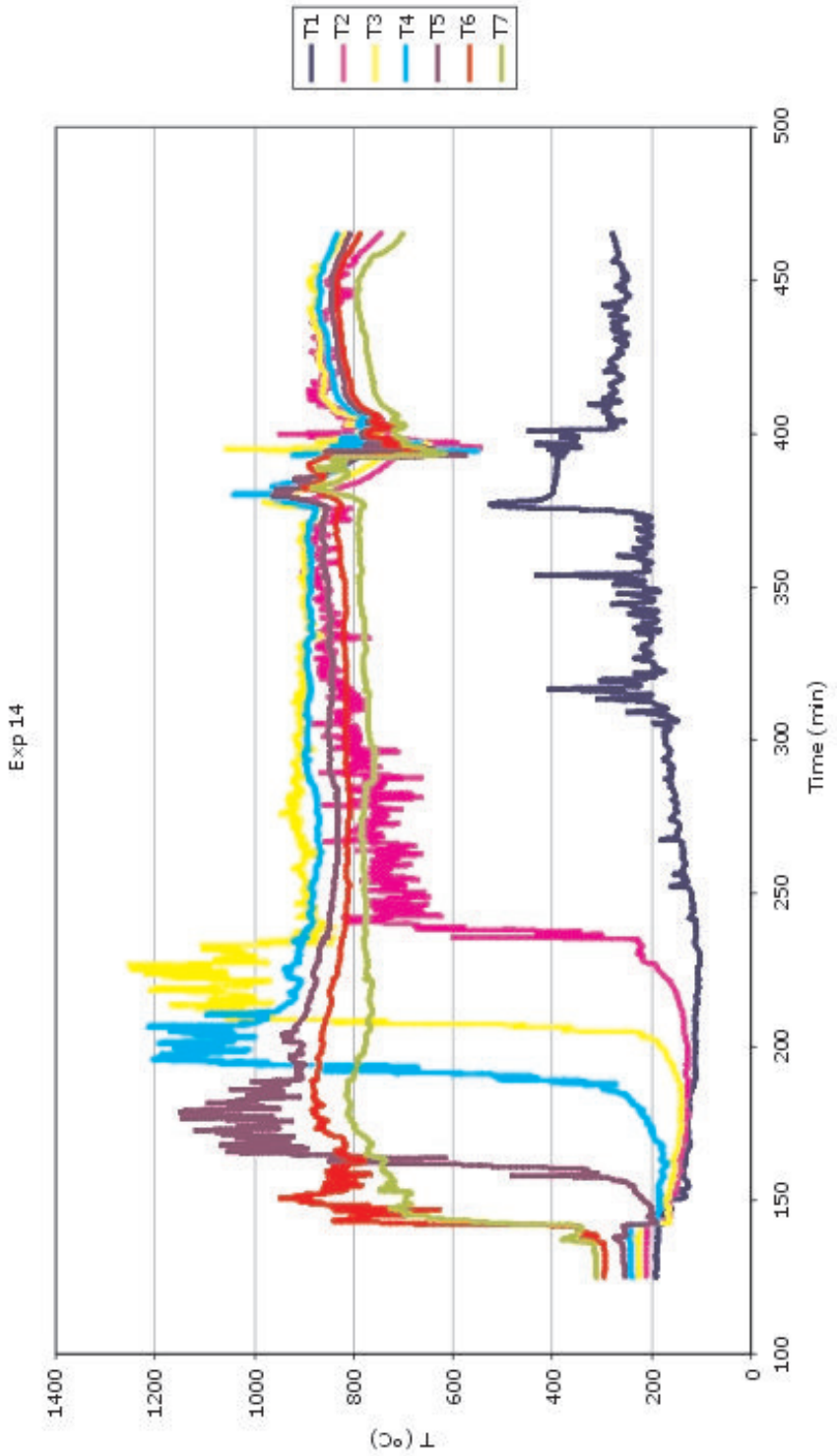

URN:NBN:no-2340

URN:NBN:no-2340